

# The Encoding of Binocular Visual Direction and Stereoscopic Depth Perception in Human Vision

Yalige Ba

Thesis submitted to the University of Nottingham for the  
degree of Doctor of Philosophy

November 2024

# Abstract

The visual brain determines the depth and direction of objects in space relative to the viewer. This thesis investigates fundamental mechanisms of binocular vision, focusing on the computation of visual direction, depth perception, and neural plasticity in the adult visual system. Through a series of ten psychophysical experiments, it explores how the brain integrates visual inputs from both eyes to form a unified percept. The findings reveal that binocular visual direction is computed as a weighted average of monocular inputs, with a strong reliance on coarse-scale spatial information. Two competing models of how visual direction is computed were tested, resulting in one account being rejected. Then the variability in egocentric localization across a large sample of individuals was determined. Our data confirm that the visual egocentre is typically located near the median plane of the head, though significant individual differences exist due to the dynamic integration of monocular and binocular cues. When the egocentre is displaced towards one eye, short-term monocular deprivation induces transient shifts in the egocentre location back towards the median plane of the head. This study highlights that egocentre location remains plastic, even in the adult visual system. Finally, we introduce a novel method using linear polarizing filters to quantify eye dominance and assess plastic changes induced by visual deprivation. This method precisely quantifies eye dominance and its plasticity in response to sensory disruption. These findings have important implications for understanding binocular vision as a dynamic and adaptable system, with potential applications for treating visual disorders such as amblyopia and for developing personalized approaches to vision therapy.

# Acknowledgements

Completing this PhD thesis has been a transformative journey, and it would not have been possible without the support, guidance, and encouragement of many individuals. I am deeply grateful to everyone who has contributed to my academic and personal growth throughout this process.

First and foremost, I would like to express my sincere gratitude to my supervisors, Professor Timothy Ledgeway, Professor Paul McGraw, and Professor Alan Johnston, for their invaluable support, insightful guidance, and constructive feedback throughout the past few years. My transition into vision research began in 2019 when I contacted Tim to express my interest in this field. Under the supervision of Tim and Paul, I pursued my second master's degree, which laid the foundation for my PhD journey. Their encouragement and belief in my potential have been irreplaceable, and I would not have come this far without their support. It has been a privilege to work with all three of my supervisors, and I am profoundly grateful for the opportunity. I would also like to extend my thanks to my internal examiner, Dr. Denis Schluppeck, for his valuable support, particularly with MATLAB coding and feedback during annual reviews.

I also feel happy to be a member of the Nottingham Vision Group, where I was surrounded by a community of friendly and supportive colleagues, including Dr. Dan, Dr. Kirsten, Dr. Richard, Dr. Ryan, and Dr. Elliot. Their assistance with data collection, especially during the demanding sessions requiring participants to wear a patch over one eye, was invaluable. I deeply appreciate their generosity with their time and effort, which was essential for the completion of my work. I also want to extend my special thanks to Dr. Mengxin, who introduced me to vision research and has been a constant source of support throughout my academic journey. Her guidance at the start of my research career and her readiness to assist with academic challenges have been invaluable.

I owe heartfelt thanks to my family for their unconditional love, support, and understanding. My husband, Dr. Zhenyu Wang, has been a constant source of strength and encouragement. His unwavering belief in me has increased my confidence, and his sacrifices—especially in taking care of our son—have allowed me to persevere through the most challenging moments. My son, Harry, has brought immense joy and courage into my life. Balancing my PhD studies and childcare over the past three years has been a rewarding challenge, and Harry's presence has reminded me of my resilience and capabilities. I am also deeply grateful to my parents and parents-in-law for their support in every aspect of my life.

I would like to thank my dear friends, Dr. Dewen, Dr. Jingru, and Dr. Mi for sharing their experiences and offering consistent support throughout my journey. Their advice, companionship, and encouragement made this process more enriching and enjoyable. My officemates, Dr. Sandra, Prerita, and Karen, created many pleasant memories that I will recollect for years to come. Finally, I express my gratitude to the participants who generously contributed their time to my experiments. I am also thankful to the technical staff, Gary and Chris, and the administrative team, Jasmine, Gisela, and Marie, for their essential support. Without their efforts, this research would not have been possible.



# Contents

<b>Abstract</b>	<b>1</b>
<b>Acknowledgements</b>	<b>2</b>
<b>List of Figures</b>	<b>8</b>
<b>List of Tables</b>	<b>13</b>
<b>An overview glossary</b>	<b>15</b>
<b>Chapter 1. General introduction</b>	<b>16</b>
<b>1.1 The fundamentals of binocular vision</b>	<b>16</b>
1.1.1 The lateral geniculate nucleus	18
1.1.2 The primary visual cortex	19
1.1.3 The horopter and stereopsis	22
<b>1.2 The binocular visual direction</b>	<b>30</b>
1.2.1 The frame of references	31
1.2.2 Two strands of visual direction research	32
1.2.3 Basic law of visual direction	35
<b>1.3 The cyclopean view</b>	<b>43</b>
1.3.1 The cyclopean eye (or the visual egocentre)	43
1.3.2 Methods of measuring the location of the cyclopean eye	47
<b>1.4 Individual differences</b>	<b>49</b>
<b>1.5 Eye dominance</b>	<b>52</b>
1.5.1 Different forms of eye dominance	52
1.5.2 Eye dominance and generalized laterality	56
1.5.3 The relationship between the visual egocentre and the dominant eye	58
<b>1.6 Short-term monocular deprivation on sensory eye dominance</b>	<b>60</b>
1.6.1 Short-term plasticity	63
1.6.2 Timescale	66
1.6.3 The mechanisms underpinning shifts in eye dominance	69
1.6.4 Plasticity in Ocular Dominance: Implications for Amblyopia	73
1.6.5 Quantifying neural plastic changes on sensory eye dominance	75
<b>1.7 Overview</b>	<b>79</b>
<b>Chapter 2. General methods</b>	<b>80</b>

<b>2.1 Observers .....</b>	<b>80</b>
<b>2.2 Apparatus &amp; stimuli .....</b>	<b>81</b>
<b>2.3 Luminance calibration .....</b>	<b>87</b>
<b>2.4 Procedure .....</b>	<b>90</b>
2.4.1 Measuring binocular visual direction (Experiments 1-4) .....	90
2.4.2 Measuring the visual egocentre location (Experiments 5-8).....	92
2.4.3 Quantifying sensory eye dominance (Experiments 9-10).....	93
<b>2.5 Curve fitting .....</b>	<b>94</b>
<b><i>Chapter 3. Establish the best fitted model for binocular visual direction</i></b>	<b>96</b>
<b>3.1 Introduction .....</b>	<b>96</b>
<b>3.2 Experiment 1: The effects of contrast on binocular visual direction - a replication of Mansfield and Legge's (1996) study.....</b>	<b>103</b>
3.2.1 Methods .....	103
3.2.2 Results .....	109
<b>3.3 Experiment 2: Egocentric visual direction using one-dimensional correlated noise stimuli.....</b>	<b>112</b>
3.3.1 Methods .....	113
3.3.2 Results .....	115
<b>3.4 Experiment 3: Egocentric visual direction using one-dimensional uncorrelated noise stimuli .....</b>	<b>123</b>
3.4.1 Methods .....	123
3.4.2 Results .....	124
<b>3.5 Experiment 4: Comparison with longer presentation.....</b>	<b>129</b>
3.5.1 Methods .....	129
3.5.2 Results .....	130
<b>3.6 Discussion .....</b>	<b>136</b>
<b><i>Chapter 4. Measurement of the visual egocentre location.</i></b>	<b>142</b>
<b>4.1 Introduction .....</b>	<b>142</b>
<b>4.2 Experiment 5: Variation in the location of the visual egocentre measured using a monocular and binocular sighting task .....</b>	<b>147</b>
4.2.1 Methods .....	147
4.2.2 Results .....	152

4.3 Discussion .....	158
<b>Chapter 5. Short-term monocular deprivation biases the location of the visual egocentre</b>	<b>165</b>
5.1 Introduction .....	165
5.2 Experiment 6: What is the optimum period of monocular visual deprivation?.....	168
5.2.1 Methods .....	168
5.2.2 Results .....	172
5.3 Experiment 7: Can egocentre location be modified by short-term monocular deprivation on the non-dominant eye? .....	176
5.3.1 Methods .....	176
5.3.2 Results .....	178
5.4 Experiment 8: Shifts in egocentre location after patching the dominant eye .....	183
5.4.1 Methods .....	183
5.4.2 Results .....	184
5.5 Discussion .....	192
<b>Chapter 6. The magnitude of plastic changes in eye dominance measured using an alignment task</b>	<b>200</b>
6.1 Introduction .....	200
6.2 Experiment 9: Measuring visual alignment of targets in depth across a range of horizontal eccentricities .....	203
6.2.1 Methods .....	203
6.2.2 Results .....	206
6.3 Experiment 10: The effects of short-term monocular deprivation on visual alignment in depth .....	211
6.3.1 Methods .....	211
6.3.2 Results .....	217
6.4 Discussion .....	229
<b>Chapter 7. General discussion</b>	<b>236</b>
7.1 Summary of Findings .....	236
7.2 A synthesised framework.....	239

7.2.1 The contribution of eye-position and retinal position information in binocular visual direction. ....	241
7.2.2 Factors contributing to individual variations in visual egocentre location	245
7.2.3 Eye dominance and its influence on egocentric visual direction.....	247
7.2.4 The influence of short-term monocular deprivation on eye dominance plasticity .....	250
<b>7.3 Limitations and further directions.....</b>	<b>252</b>
<b>7.4 Conclusion.....</b>	<b>255</b>
<b><i>References</i></b>	<b>256</b>

# List of Figures

Figure 1.1: Binocular visual field. ....	17
Figure 1.2: Schematic illustration of V1 ocular dominance columns.....	20
Figure 1.3: The comparison of classical model and revised model .....	22
Figure 1.4: An illustration of The Vieth-Müller circle, horopter and Panum's fusional area. ....	25
Figure 1.5: examples of binocular rivalry images.....	26
Figure 1.6: Schematic of mirror stereoscope. ....	28
Figure 1.7: A chronology of the major contributors. ....	34
Figure 1.8: A demonstration of Wells's (1792) Propositions .....	37
Figure 1.9: Another demonstration of Wells's (1792) Proposition I, II and III. ....	38
Figure 1.10: An illustration of Wells's (1792) Propositions III.....	39
Figure 1.11: The visual direction of an object. ....	43
Figure 1.12: Position in depth. ....	44
Figure 1.13: The representation of visual stimuli changed from reflecting retinal images to reflecting cyclopean images. ....	46
Figure 1.14: Schematic of four methods of locating the cyclopean eye. ....	47
Figure 1.15: The effect of 90-minute monocular deprivation on mean phase durations. ....	66
Figure 1.16: The timecourse of the patching effect of 150-minute monocular deprivation.....	68
Figure 1.17: The timecourse of the patching effect of 30-minute monocular deprivation.....	68
Figure 1.18: The effect of patching on dichoptic masking strength is depicted in two panels. ....	70
Figure 1.19: Ding-Sperling's (2006) gain control model.....	72
Figure 1.20: The mean point of subjective equality (PSE).....	73
Figure 1.21: Schematic representation in the contrast-balance-point tasks for demonstration.....	77
Figure 2.1: Wheatstone mirror stereoscope.....	82

Figure 2.2: A pair of vertically-separated Gabor patches used in Experiment 1 .....	83
Figure 2.3: An example of noise patterns. ....	84
Figure 2.4: The custom-built apparatus used in the experiment.....	85
Figure 2.5: Apparatus used in Experiment 9-10 .....	86
Figure 2.6:How two polarizer filters work together to attenuate the light intensity.....	87
Figure 2.7: Luminance calibration in Experiment 9-10.....	88
Figure 2.8: The luminance measured without polarizer, only one polarizer and two polarizers.....	90
Figure 2.9: Schematic representation of one trial. ....	92
Figure 2.10: Measurements were made along the horizontal azimuth .	95
Figure 3.1: The geometry of the conventional model.....	99
Figure 3.2: The difference of two models.....	102
Figure 3.3: The apparatus used in the experiment. ....	105
Figure 3.4: Example stereo-Gabor patches used in the experiment...	106
Figure 3.5: A top-down view of this task. ....	107
Figure 3.6: Schematic representation of one trial .....	108
Figure 3.7: Data from three participants. ....	110
Figure 3.8: Two vertically-separated, Gaussian-windowed, 1-d correlated noise patches used in Experiment 2 .....	114
Figure 3.9: The example data of an observer measured in correlate patterns .....	118
Figure 3.10: Data with correlated patterns from one participant is replotted with X and Z converted into physical distances (cm).....	119
Figure 3.11: Binocular visual line fitted to the PPAs between the mixed and equal contrast target .....	120
Figure 3.12: The effect of contrast ratio between the left and right eye (LE:RE) measured with correlated patterns across three disparity conditions.....	123
Figure 3.13: Two vertically-separated, Gaussian-windowed, 1-d uncorrelated noise patches used in Experiment 3 .....	124
Figure 3.14: Group data of six participants in correlated and uncorrelated patterns .....	126

Figure 3.15: The effect of contrast ratio between the left and right eye (LE:RE) measured with uncorrelated patterns across three disparity conditions.....	128
Figure 3.16: Individual data of six observers viewing with correlated and uncorrelated patterns .....	132
Figure 3.17: Data from 6 observers with 1s presentation is replotted with X and Z converted into physical distances diagram.....	133
Figure 3.18: The effect of contrast ratio between the left and right eye (LE:RE) measured with correlated patterns at 0arcmin .....	134
Figure 3.19: The effect of contrast ratio between the left and right eye (LE:RE) measured with uncorrelated patterns at 0arcmin .....	135
Figure 3.20: The prediction of two models.....	138
Figure 4.1: The apparatus used in the experiment. ....	148
Figure 4.2: Schematic representation of the experiment. ....	150
Figure 4.3: Three representative sets of data for both monocular and binocular measures.....	151
Figure 4.4: The comparison between IPD and monocular sighting task distance across 26 participants.....	154
Figure 4.5: Measured egocentre location plotted against averaged egocentre location.....	156
Figure 4.6: The relationship between average absolute deviations from the median plane and stereo classification .....	157
Figure 5.1: Schematic representation of the experiment. ....	170
Figure 5.2: The baseline visual egocentre location of the observer....	171
Figure 5.3: Schematic illustration of the experimental procedure .....	172
Figure 5.4: The visual egocentre for the median plane.....	173
Figure 5.5: The results for the corneal.....	174
Figure 5.6: The baseline visual egocentre location of the three representative observers .....	177
Figure 5.7: The schematic illustration of the procedure .....	178
Figure 5.8: The egocentre location (relative to the median plane) of 10 participants was monitored for 45 minutes after removing the eye patch from the non-dominant eye. plane. ....	180

Figure 5.9: The egocentre location (relative to the corneal plane) of 10 participants was monitored for 45 minutes after removing the eye patch from the non-dominant eye.....	182
Figure 5.10: Comparison of individual egocentre positions relative to the median plane between patching the non-dominant eye (red lines) and the dominant eye (blue lines). ....	187
Figure 5.11: Comparison of individual egocentre positions relative to the corneal plane between patching the non-dominant eye (red lines) and the dominant eye (blue lines).....	188
Figure 5.12: The changes of the egocentre location after the end of monocular treatment for the non-dominant eye compared with the dominant eye averaged across all the participants.....	191
Figure 6.1: Apparatus used in the experiment. ....	205
Figure 6.2: The data of three representative observers measured at 100cm .....	207
Figure 6.3: The data in different absolute distance of one representative participant measured across three viewing distances .....	208
Figure 6.4: The post-deprivation data of one representative participant in different absolute distance measured across three viewing distances .....	210
Figure 6.5: How two polarizer filters work together to attenuate the light intensity.....	213
Figure 6.6: Luminance calibration.....	214
Figure 6.7: The luminance measured without a polarizer, only one polarizer and two polarizers .....	215
Figure 6.8: Balance points for ten participants (S1 to S10) measured at -12° eccentricity.....	219
Figure 6.9: Balance points for ten participants (S1 to S10) measured at 0° eccentricity.....	220
Figure 6.10: Balance points for ten participants (S1 to S10) measured at 12° eccentricity.....	221
Figure 6.11: Average balance points ( $\text{cd/m}^2$ ) for perceiving single and diplopic vision measured at three eccentricities.....	223



Figure 6.12: Inter-ocular luminance differences across three eccentricities. ....	226
Figure 6.13: Balance points across three eccentricities with sequential measurements after deprivation. ....	228
Figure 7.1: The diagram of Ding-Sperling-Klein-Levi (DSKL) model. .	241
Figure 7.2: An integration of binocular retinocentric and eye-movement information. ....	244
Figure 7.3: An enhanced model for incorporating retinal and eye position signals for achieving egocentric perception. ....	248

# List of Tables

Table 3.1: Fit results (Eq. 3.5) of the binocular visual direction from 6 observers when the upper target disparity was fixed at +30arcmin measured with correlated noise patches. ....	121
Table 3.2: Fit results (Eq. 3.5) of the binocular visual direction from 6 observers when the upper target disparity was fixed at 0arcmin measured with correlated noise patches. ....	122
Table 3.3: Fit results (Eq. 3.5) of the binocular visual direction from 6 observers when the upper target disparity was fixed at -30arcmin measured with correlated noise patches. ....	122
Table 3.4: Fit results (Eq. 3.5) of the binocular visual direction from 6 observers when the upper target disparity was fixed at +30arcmin measured with uncorrelated targets.....	127
Table 3.5: Fit results (Eq. 3.5) of the binocular visual direction from 6 observers when the upper target disparity was fixed at 0arcmin measured with uncorrelated targets.....	127
Table 3.6: Fit results (Eq. 3.5) of the binocular visual direction from 6 observers when the upper target disparity was fixed at -30arcmin measured with uncorrelated targets.....	128
Table 3.7: Fit data (Eq. 3.5) of the binocular visual direction from 6 observers when the upper target disparity was fixed at 0 arcmin measured with correlated targets and longer presentation.....	134
Table 3.8: Fit results (Eq. 3.5) of the binocular visual direction from 6 observers when the upper target disparity was fixed at 0 arcmin measured with uncorrelated targets and longer presentation.....	135
Table 5.1: Fits results (Eq. 5.3) of the time course of the egocentre location.....	193
Table 6.1: Mean balance points ( $\text{cd/m}^2$ ) for perceiving single and diplopic vision measured at three eccentricities across ten observers before deprivation. ....	222

Table 6.2: Mean balance points ( $\text{cd/m}^2$ ) for perceiving single and diplopic vision measured at three eccentricities after 60-min monocular deprivation across ten observers. ....	224
Table 6.3: Pre- and post-deprivation inter-ocular luminance differences at three eccentricities for 10 participants. ....	225
Table 6.4: Paired t-test results for changes in balance points induced by monocular deprivation across conditions. ....	227
Table 6.5: Averaged changes in balance points measured at three eccentricities after 60-min monocular deprivation averaged across ten participants with three separate repetitions. ....	229

## An overview glossary

**Binocular vision** - The neural and psychological collaboration between the two eyes, particularly in relation to this shared region of overlap.

**Binocular Disparity** – A small difference in the position of input on the two retinas that provides a cue to depth.

**Horopter** - The set of points in space that stimulate corresponding points in the eyes, resulting in single vision.

**Lateral Geniculate Nucleus (LGN)** - The primary processing centre for visual information received from the retina of the eye.

**The cyclopean eye** - All objects are perceived as if seen from the cyclopean eye, at a reference point, which is located in the midway between the two eyes.

**The visual egocentre** – The location from which visual judgements are made.

**The median plane** - A vertical plane that passes through the midline of the body and bisects the body into two symmetrical halves: right and left.

**The corneal plane** - It is commonly used as a reference plane in ophthalmology, optometry, and corneal topography for measurements and imaging of the eye.

**Stereopsis** - The ability to utilize retinal disparity signals to make extremely fine relative-depth judgments.

**Visual line** - All straight lines, termed visual lines, joining points in the object plane to their corresponding points on the retina pass through the nodal point.

**Visual axis** - The visual line that connects the fixation point and the centre of the fovea.

**Panum's fusional area** - The images from the two eyes falling in this region can be fused into a single percept.

# Chapter 1. General introduction

## 1.1 The fundamentals of binocular vision

In humans and higher mammals with forward-facing eyes, a significant portion of the visual field is commonly observed by both eyes (Boff et al., 1986). The term binocular vision is characterized as the neural and psychological collaboration between the two eyes, particularly in relation to this shared region of overlap. Although a single eye can function effectively on its own, human vision is inherently binocular. It is worth exploring how does brain combine the signals from the two eyes.

The visual experience begins in the eye, where highly complex neural circuits pre-process sensory information and transmit it to other parts of the central nervous system associated with each eye (Grünert & Martin 2020; Roska & Meister 2014). Unlike other parts of the brain, the neural connections between the retina and the thalamus are in one direction, suggesting that there are no feedback connections back to the retina from the primary projection targets of retinal neurons.

Any optical system that produces an image comprises an anterior nodal point and a posterior nodal point, both situated on the optic axis. It is generally considered that the two nodal points of the human eye coincide at a point on the optic axis located 17 mm in front of the retina. All straight lines, termed visual lines, joining points in the object plane to their corresponding points on the retina pass through the nodal point. The fovea, situated in the central region of the retina, exhibits the highest visual acuity. The visual line connecting the fixation point and the centre of the fovea is defined as the visual axis (Howard & Rogers, 1995). The normal monocular visual field for human spans roughly  $107^\circ$  towards the temporal direction (away from nose) and approximately  $60^\circ$  towards the nasal direction (toward the nose) from the vertical meridian, and about  $70^\circ$  above and  $80^\circ$  below the horizontal meridian (Hueck, 1840; Rönne,

1915; Spector, 1990; Traquair, 1938). The visual cortex receives information from a multitude of neurons, each of which selectively responds to particular features of the visual scene. The visual cortex gathers all incoming information and reconstructs a visual representation of the surroundings based on the activated neurons (Figure 1.1).

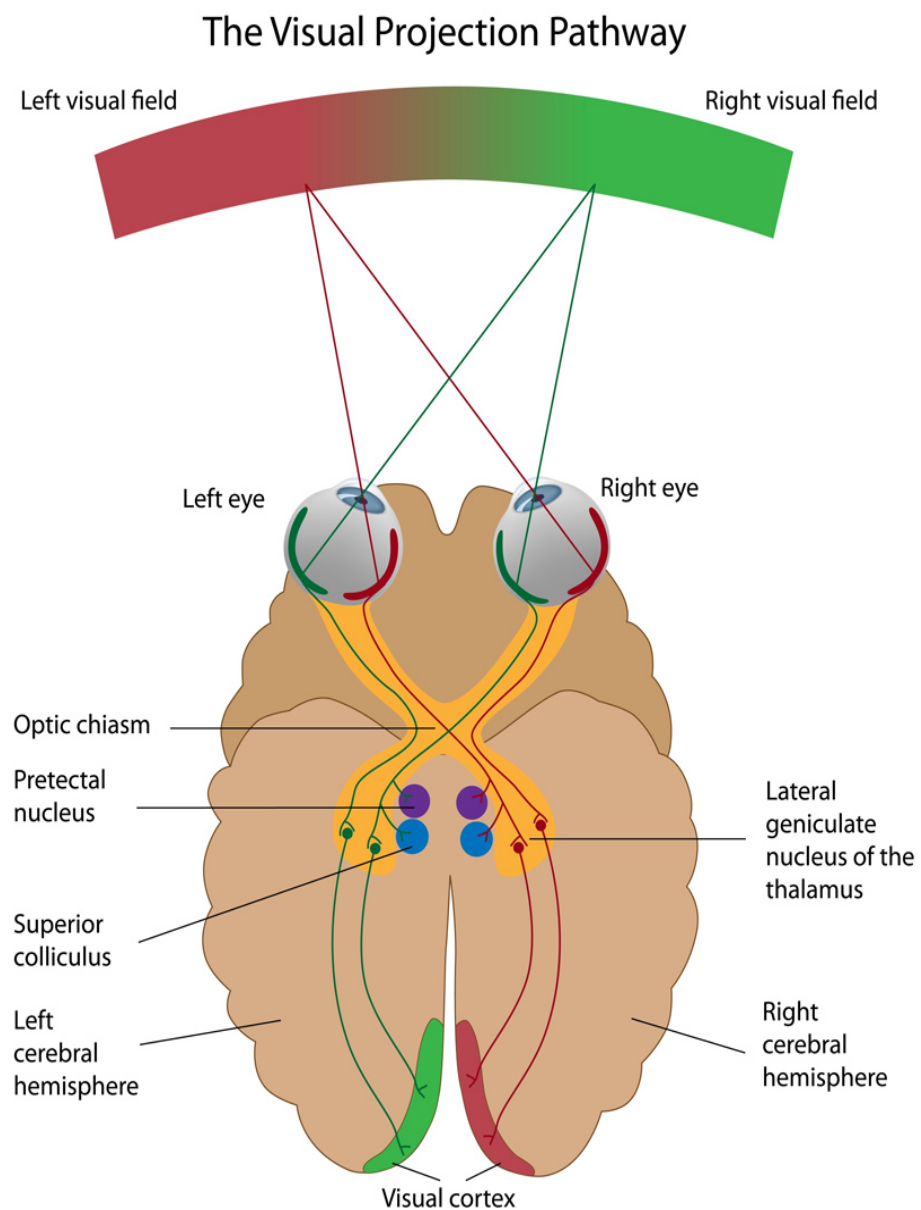


Figure 1.1: Binocular visual field.

The overlapping field in the middle is the binocular visual field. Ipsilateral visual field information crosses over at the optical chiasm to reach the opposite side of the brain, whereas contralateral visual field information projects directly to the ipsilateral side of the brain. Image adapted from: <https://researchoutreach.org/articles/binocular-vision-shaped-early-visual-experience/>.

### 1.1.1 The lateral geniculate nucleus

The primary projection target of the optic nerve is the lateral geniculate nucleus (LGN) in the thalamus. The LGN is organized into several layers, each receiving input from only one eye, with minimal interconnections between the eye-specific layers (Casagrande & Boyd, 1996). This structure suggests that the LGN is an intermediate site for the transmission of visual information from the retina to the primary visual cortex (V1). Electrophysiological studies demonstrated that LGN neurons respond primarily to stimuli from only one eye, a feature that was once thought to indicate that the signals from the two eyes are tightly segregated before they reach V1. Hubel and Wiesel (1959) observed that activated cortical cells of each eye have two receptive fields that are mapped to each eye, each with separate excitatory and inhibitory zones that are similarly shaped and oriented and located in homologous regions within their receptive fields. This has led to the view that the LGN functions monocularly, similar to the retina, primarily serving as a relay for visual information. However, this idea, along with the broader concept of the LGN as a simple relay station, has been questioned by more recent research (e.g., Dougherty et al., 2018). Although LGN neurons respond primarily to stimuli from one single eye, they actually receive information about the other eye as well. This interaction of binocular information affects the responses of LGN neurons, which in natural visual conditions are manifested as different responses to stimuli from the two eyes. The evidence from human neuroimaging studies and neurophysiological study in cats revealed that neurons in different layers of the LGN appear to receive information about the other eye despite responding to only one eye. This information is functionally relevant and effective because it alters or modulates the response under natural viewing conditions in which both eyes receive stimuli (Dougherty et al., 2018). Recent studies showed that roughly one third of LGN neurons in awake behaving primates exhibit binocular influences (Dougherty et al., 2021), and these binocular influences were found across all layers and cell types. Additionally, Zeater et al. (2015) found a small group of LGN neurons

respond binocularly, indicating that LGN plays a larger functional role on visual processing than previously recognized. These findings demonstrate that visual processing is not purely monocular before becoming binocular, but rather the combination of two eyes' signals may occur gradually and hierarchically.

### 1.1.2 The primary visual cortex

Primary visual cortex (V1) is regarded as one of the main sources of binocular feedback to the LGN (see Figure 1.1). In primates and mammals, axons from the temporal half of the left eye combine with decussated axons from the nasal half of the right eye, forming the left optic tract, and vice versa. Subsequently, each optic tract departs from the chiasma, terminating on its respective hemisphere in a section of the thalamus identified as the lateral geniculate nucleus (LGN). Axons from relay cells exit the LGN on both sides and disperse to create the optic radiations, which then extend backward and upward, connecting to the visual cortex within the ipsilateral occipital lobe of the cerebral cortex (Figure 1.2). Due to the reversal of retinal images, the left half of the visual field (left hemifield) is processed in the right cerebral hemisphere, while the right hemisphere is responsible for the representation of the left hemifield.

The pioneering research (Hubel & Wiesel, 1962, 1968) on V1 revealed that two main findings about V1 responses to each eye: First, very few V1 neurons respond exclusively to one eye or equally to both. In contrast, most V1 neurons respond to both eyes, but there is a preference for the response strength. This response preference, termed as ocular dominance, is one hallmark of V1 function though not exclusive to V1. Second, V1 neurons with comparable ocular dominance are organised in columns, termed as ocular dominance columns, which resembles similar column cells in V1, such as orientation, colour and object columns (see Figure 1.2).



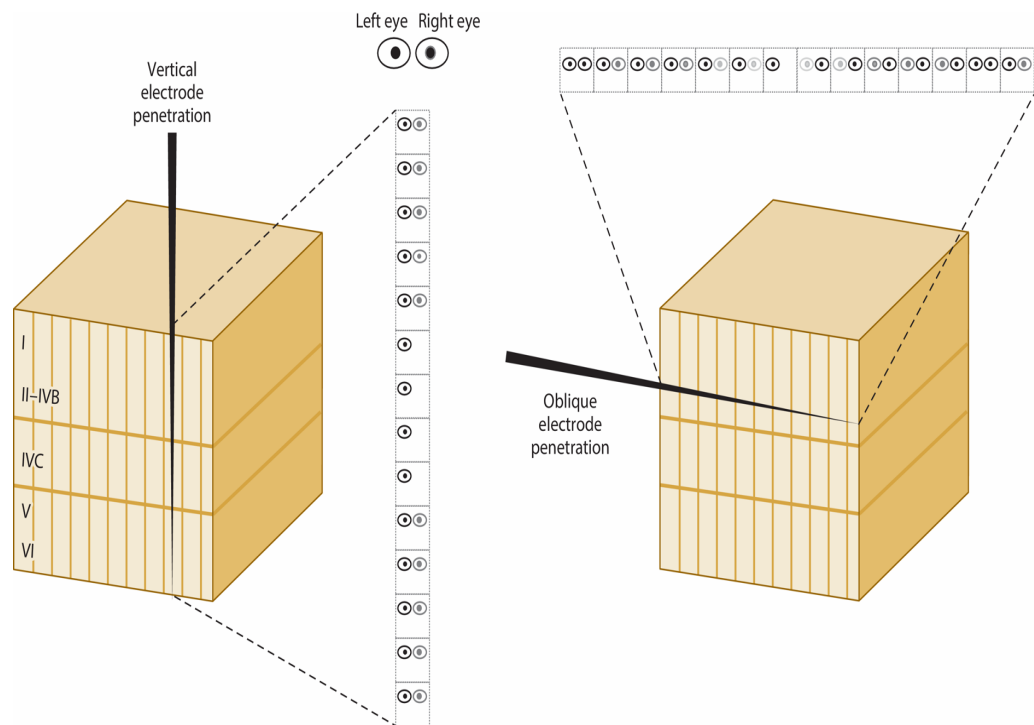


Figure 1.2: Schematic illustration of V1 ocular dominance columns. Measurement of neurons responses arranged across layers I-VI (left side), which reveals a consistent response preference for one eye relative to the other. The middle layers (4C) is the only exception to the shared ocular dominance of neurons within the same V1 column, as many neurons in this layer respond to only one eye (in this case, the left eye), suggesting the existence of a hierarchical structure of columnar processing. Right side measures neuronal response tangentially across columns, indicating a slow transfer of ocular dominance from one eye to the other. V1 columns containing neurons that respond to one eye (monocular columns) and to both eyes (fully binocular columns) are alternated with columns to form a gradient of preference for one eye over the other. Image from Maier et al., 2022.

Hubel and Wiesel (1962) highlighted a segregation of cells based on field complexity, in which simple and complex fields could exhibit distinct characteristics. Their research shed light on binocular interaction in cortical cells, demonstrating the role of eye dominance in modulating responses and the presence of binocular synergy in visual processing. Though their research limited the generalizability of the findings to other species or cortical regions in different animals, including humans, as well as overlooked other aspects of visual processing and cortical functionality, it raised the possibility of ocular dominance in relation to binocular depth.

The current consensus on V1's lamination identifies six main layers, in which layer 4C in primates receives most of the sensory inputs from the LGN (Mitzdorf 1985, Schroeder *et al.*, 1998). Compared with neurons in the supragranular and infragranular layers respond binocularly, neurons in layers 4C primarily respond to one eye. This monocular response pattern is consistent with the observation that the majority of LGN neurons respond to one eye, indicating a low degree of thalamocortical synaptic convergence across the inputs from the two eyes.

The pioneering anatomical and electrophysiological work of Hubel and Wiesel (1972) and others established the classical model of binocular convergence in the early primate visual system that has dominated the field ever since. The model can be summarized as follows: the projections of each retina remain anatomically and functionally separated until monocular neurons located in input layer 4C of V1 converge and activate binocular neurons in the layer above. However, new findings regarding binocular integration challenge this view that the signals from the two eyes remain isolated until they reach V1's input stage and being combined thereafter. In order to perform complex computation (i.e. combine two eyes' views, resolve their difference and compute depths), recent discovery (Verhoef *et al.*, 2015) indicated the early primate visual system appears to be more binocular at early stages and less binocular at later stages (see Figure 1.3).

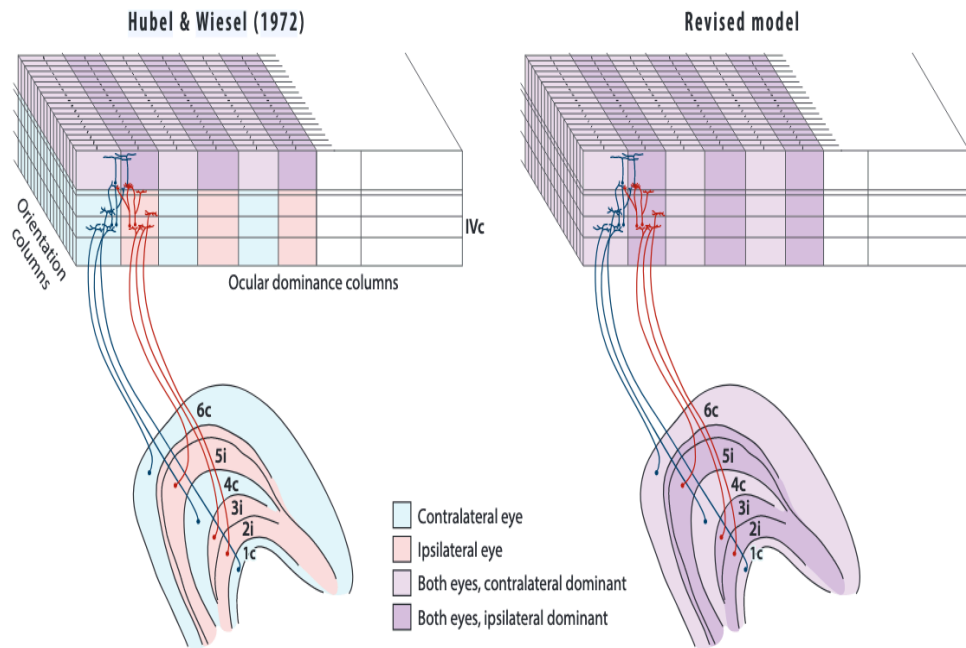


Figure 1.3: The comparison of classical model and revised model for binocular integration within V1 pathway.

Left side: Schematic model of Hubel and Wiesel (1972), which involves two processing phases: an initial monocular phase comprising the lateral geniculate nucleus (LGN) of the thalamus and granular layer 4C of the primary visual cortex (V1), followed by a binocular phase starting from the topmost layer of V1. Only the middle and upper layers are shown for simplicity. Specifically, LGN neurons receive inputs from the ipsilateral eye (red) that project to layer 4C of a set of V1 ocular dominance columns (top). LGN neurons receive inputs from the contralateral eye (green) project to layer 4C of the neighbouring eye dominance column. The model relies on strict isolation of signals from each eye at the 4C level of the LGN and V1 primary input layer and explains the origin of the ocular dominance columns as well as the presence of monocular neurons at the centre of each column. Right side: The revised model shows a greater degree of binocularity from the first postretinal synapse. Specifically, although the primate LGN layer consists almost entirely of neurons activated by only one eye, a large proportion of these neurons significantly change their responses when the other eye is also stimulated (indicating that these neurons receive information about binocularity). Image from Maier et al., 2022.

### 1.1.3 The horopter and stereopsis

Binocular vision is a process engendered by stimuli arising in the two eyes, and is generally distinguished by three levels of processing (Worth, 1921). The first level is simultaneous macular perception, which is the ability of the visual system to perceive and compare the separate stimuli received by the two eyes at the same time. In this level of binocular

processing, a stimulus presented to one eye is not affected by another stimulus presented to the other. The corresponding regions of the two retinæ receive input from virtually the same locations in the environment due to their substantial overlaps in visual fields. The second level refers to the ability to combine these binocular inputs into a single presentation, which requires sensory unification of the two retinal images as well as motor coordination between the two eyes in order to maintain sensory fusion. Since two eyes perceive the external world differently due to their physical horizontal separation in the head, an offset in spatial perception between the views of both eyes is known as binocular disparity (Howard & Rogers, 1995; Julesz, 1971; Wheatstone, 1838). Fusion can only occur when this disparity is within a certain range, where the two retinal images can be merged and perceived as a single object. However, when the disparity of retinal images exceeds a threshold, the images cannot be fused, resulting in the perception of two distinct images originating from different regions of space – a condition referred to as diplopia (Howard & Rogers, 1995). When binocular fusion has been achieved by solving the correspondence problem (i.e. matching the appropriate features of a single object in two eyes), binocular disparity becomes an essential cue for coding depth in stereoscopic images (Fender & Julesz, 1967; Gonzalez & Perez, 1998; Mach & Dvorak, 1872; Mitchell, 1966a; Ogle, 1950; Pulfrich, 1922). As the highest level of binocular vision, stereopsis refers as the ability to perceive depth and three- dimensional structure based on binocular disparity between the images projected to each eye.

The horopter describes the set of points in space that stimulate corresponding points in the eyes, resulting in single vision. Each eye has corresponding points evenly distributed at equal angles relative to the oculocentric primary visual direction. The geometric horopter is called the Vieth-Müller circle (Figure 1.4), which was first proposed by Aguilonius (1613). An object placed near the horopter can produce an image with a crossed disparity in the two eyes as the visual lines from each eye cross inside the horopter (point A in Figure 1.4). On the other hand, an object placed beyond the horopter could produce an image with an uncrossed

disparity (Point B in Figure 1.4). Panum (1858) proposed that a specific retinal point in one eye could correspond to a small group or region of retinal points in the other eye (Mitchell, 1966b; Panum, 1858). This region of correspondence is known as "Panum's fusional area" - where the images from the two eyes falling in this region can be fused into a single percept, and beyond this region diplopia (double vision) is experienced. The distinction between fusion and diplopia is whether the process of combining two monocular views is success or not. nevertheless, even diplopia resembles a single binocular experience from a phenomenological perspective. During diplopia, the images of the two eyes appear superimposed rather than side-by-side without overlap, suggesting that binocular perception is fundamentally singular (Maier, et al., 2022).

Human vision is fundamentally binocular, which involves processes for integrating information from two eyes in the brain to represent the three-dimensional layout of the world by using the extracted disparity (Ogle, 1950). This disparity helps the brain to sense relative depth and causes the retinal images of three-dimensional objects to differ both vertically and horizontally. Horizontal disparities, denoting side-to-side distinctions in the positions of corresponding images between the two eyes, can create a compelling sense of three-dimensionality. Vertical disparities refer to the differences in the vertical positions of corresponding points in the images received by the two eyes (Rogers & Bradshaw, 1993). These differences arise due to the slightly different vantage points of the two eyes when viewing a three-dimensional scene. Because the distance from each eye to an object varies, the visual system uses these disparities to scale depth and size in stereoscopic vision.

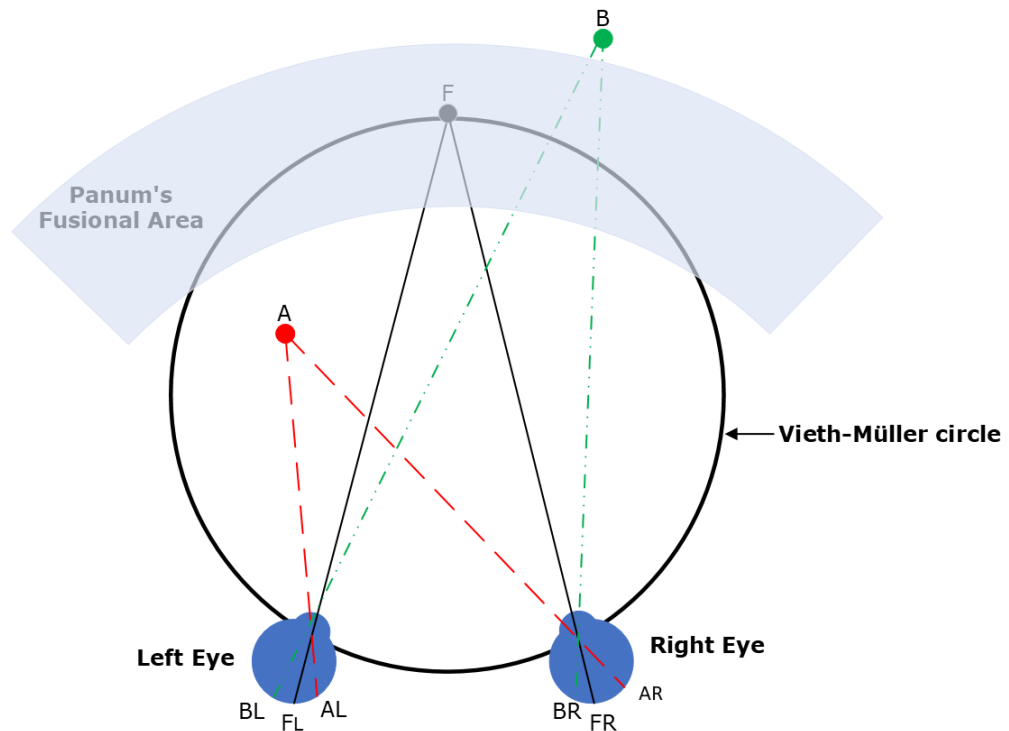


Figure 1.4: An illustration of The Vieth-Müller circle, horopter and Panum's fusional area. It is the top view of the eyes fixating at F (black dot), A (red dot) and B (green dot). This theoretical circle that describes the spatial distribution of points in the visual field that generate corresponding retinal images in both eyes. The curved line on the top is horopter, all points along this curve line have zero disparity with the fixation point F. The region surrounding the horopter corresponds to Panum's fusional area, within which objects exhibit disparities tolerable for a unified percept. However, point A and B generate a disparity beyond the fusional range, resulting in physiological diplopia. Point A is nearer than the Fixation point, the visual lines from each eye cross inside the horopter. The images of point B are uncrossed as it is farther than the Fixation point and the visual lines from each eye cross beyond the horopter.

Barlow et al. (1967) were the first to report the discovery that certain cortical units in cats were optimally excited by objects situated at different distances. In their experiment, electrode was placed in area 17 of adult cats to record the action potentials of single neurons in V1. They found that stimuli under constant convergence could activate distinct neurons, providing a plausible foundation for binocular depth discrimination and stereopsis. Even though there is much to uncover regarding how this depth information is separated among various primary cortical cells as well as how it is further processed and organized by higher-order visual neurons.

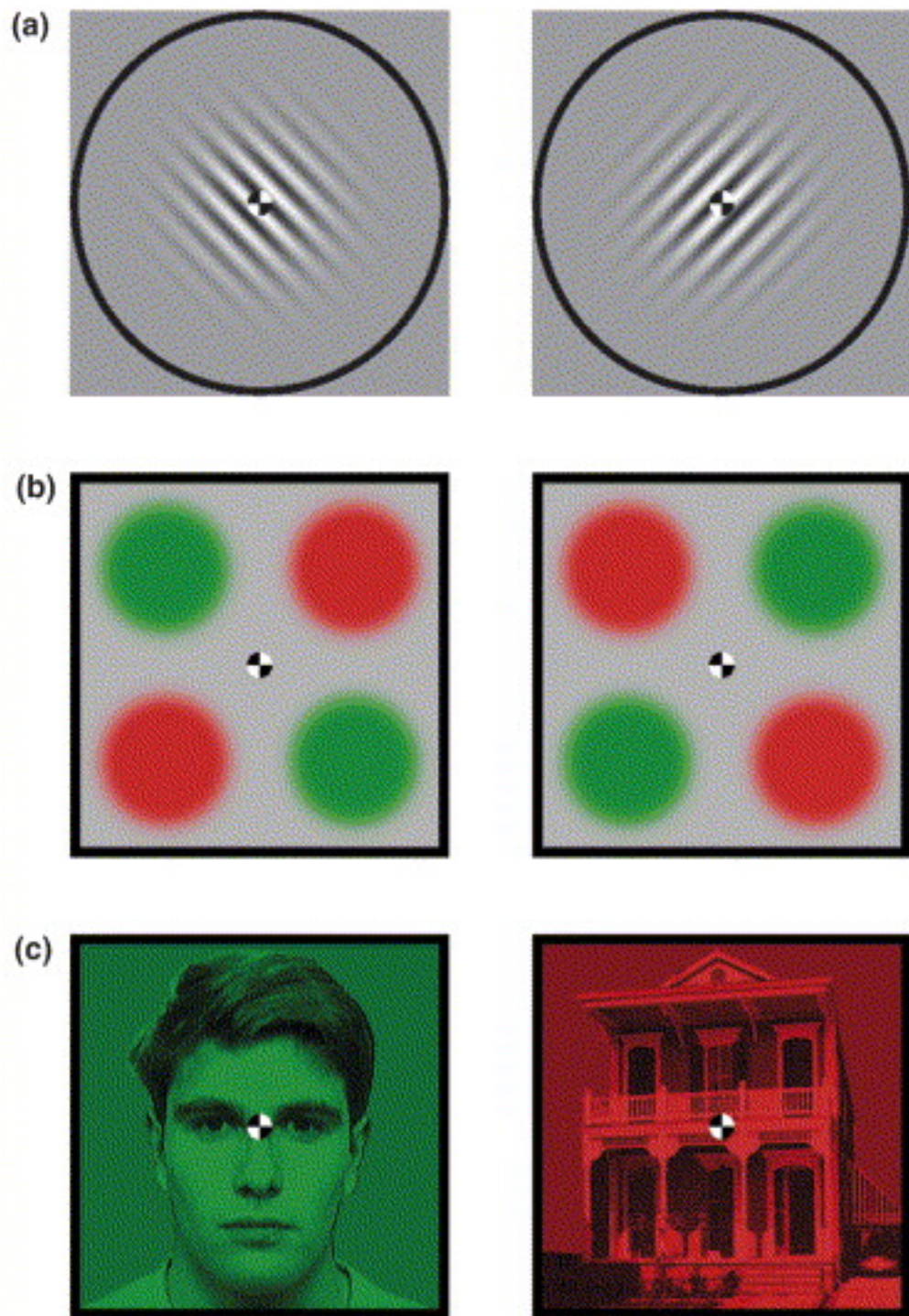


Figure 1.5: examples of binocular rivalry images.  
 (a). Dichoptic orthogonal gratings; (b) Stimuli designed to investigate interocular grouping; (c). Complex stimuli involving presenting a picture of face to one eye and a picture of house to the other eye. Image from Tong et al., 2006.



The ability to utilize retinal disparity signals to make extremely fine relative-depth judgments is a process termed stereopsis. Binocular stereopsis creates the impression of depth from binocular cues, which underlies our ability to discriminate between differences in depth. However, the traditional understanding of stereopsis as a by-product of binocular vision is challenged by empirical observations demonstrating that monocular viewing—particularly when combined with motion cues, such as motion parallax—can also elicit a vivid impression of tangible solid form and immersive space, akin to the qualitative experience of stereopsis. This suggests that stereopsis, as a perceptual phenomenon, is not exclusively tied to binocular disparity but may arise from other depth cues as well (Vishwanath & Hibbard, 2013). An alternative hypothesis posits that stereopsis is fundamentally a qualitative visual experience related to the perception of egocentric spatial scale. Specifically, the primary phenomenal characteristic of stereopsis—the impression of “real” separation in depth—is proposed to be linked to the precision with which egocentrically scaled depth (absolute depth) is derived. This precision in depth perception may play a functional role in guiding motor action, providing a plausible explanation for the secondary phenomenal characteristics associated with stereopsis, such as the impression of interactability and realness. By conceptualizing stereopsis as a generic perceptual attribute rather than a product of specific depth cues, this hypothesis offers a more unified account of the variation in stereopsis across different viewing conditions, including real scenes and pictorial representations. Furthermore, it provides a theoretical basis for understanding how depth perception can be maintained in pictures despite the presence of conflicting visual signals.

Binocular rivalry (BR) occurs when conflicting monocular images are presented to each eye, the two images may compete for exclusive dominance with perceptual awareness alternating between images rather than forming a stable composite (see Figure 1.5). During the phenomenon of binocular rivalry, visual awareness alternates between the images perceived by the two eyes. Typically, only one image is



perceived at a time (i.e., the dominant image), while the other is temporarily invisible to the viewer (Levelt, 1965). In contrast, when the two images are sufficiently similar and their disparities fall within the brain's fusional range, the visual system can achieve fusion, integrating the two images into a coherent three-dimensional percept. This fusion is what gives rise to the vivid impression of depth and solidity characteristic of stereopsis. Importantly, the distinction between rivalry and fusion highlights that stereopsis is not merely a mechanical consequence of binocular disparity but depends on the brain's ability to match and integrate corresponding features from the two retinal images. Sir Charles Wheatstone made a great contribution to studying binocular rivalry, as he was the first to systematically describe the phenomenon of binocular rivalry in his monograph with the invention of the stereoscope (Wheatstone, 1838). This optical device (Figure 1.6) could present images to the same region of the left and right eye separately. With this device, Wheatstone observed that the pair of images appeared as a single image in the median plane beyond the mirrors.

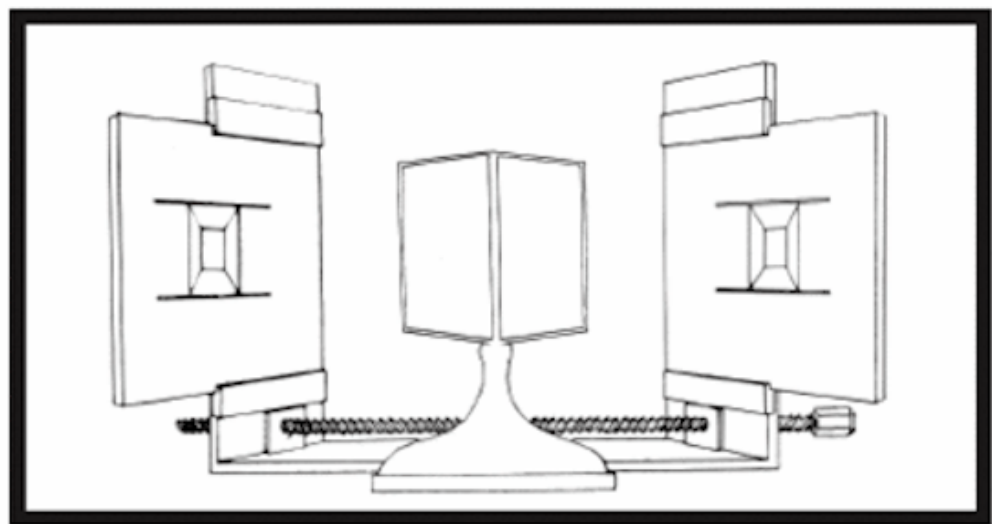


Figure 1.6: Schematic of mirror stereoscope. This equipment can divide the binocular vision into two halves, left eye can only see the image presented in the left screen and vice versa. Image from Wheatstone, 1838.

When observing incompatible objects, the human visual system may first match corresponding features from the two eyes' view (Marr, 1982). An individual with normal eye alignment can find matching features of two images when presenting the two images simultaneously to the two eyes. If left- and right-eye foveas' images cannot match, conflicting information will be provided to the brain, resulting in binocular rivalry. Blake (1989) concluded that rivalry was the default result caused by the failure of stereopsis. Blake, Yang, and Wilson (1991) favoured the proposition that stereopsis took precedence over rivalry by dichoptically presenting two gratings with different spatial frequencies to observers. The study showed that dichoptic gratings with a slight difference in spatial frequency (3%) resulted in stable stereoscopic single vision, while a larger difference in spatial frequency (260%) between two gratings produced binocular rivalry. Constructed in this way, the visual system may continuously search for matching features from rival targets, and when the matching process fails binocular rivalry will result.

Understanding the fundamental bases of visual perception is a central goal of neuroscience and is vital to our understanding of sensory processing in biological systems. To perceive the three-dimensional layout of a scene, both the depths and visual directions of the objects within it need to be determined. A key step and a computational challenge faced by the brain is how to combine the information from the two eyes to achieve a single, unified representation of the world and determine the visual direction of objects in space relative to the viewer. Our everyday visual experience tells us that this is accomplished effortlessly, but nonetheless, the underlying mechanisms are still poorly understood. Understanding these mechanisms is central to the aim of this thesis, which seeks to uncover the neural and computational principles that enable the brain to integrate binocular information and resolve potential conflicts between the two eyes' inputs. This thesis will focus on how humans encode binocular visual direction and attempt to illuminate the mechanisms used to assign a single visual direction to a binocular feature, for which the left and right eyes are signalling different directions.

## 1.2 The binocular visual direction

The left and right eyes perceive different perspectives of the same object, and the differences between these two views are recognized to create convincing stereoscopic perceptions of relative distance or depth (Wheatstone, 1838). Shimono and Wade (2002) explored the alignment of vertical lines at different physical horizontal positions within the same eye and how this alignment varied with perceived depth between them. By conducting two experiments using random-dot stereograms and rectangular stereograms with binocular disparity, they found that visual direction and the perceived depth of monocular stimuli are mediated by different mechanisms. In random-dot stereograms, monocular lines with different visual directions can be perceived in the same visual direction, challenging the notion that the retinal local sign of a monocular stimulus remains fixed when transformed into visual direction. In rectangular stereograms, the comparison monocular line was always to the left of the standard line, but the difference in horizontal positions of aligned lines varied across different disparity conditions. These results suggest that two vertical monocular lines can be regarded as a part of the binocular stereogram when presented in the binocular area, which contracts conventional monocular law of visual direction that the processing mechanism for visual direction of monocular line is determined simply on the basis of retinal position. Thus, the finding indicates that the processing mechanisms for visual direction and depth perception are separate, the visual direction of monocular stimuli may be determined after the depth perception.

Binocular cues allow for estimating actual shape, size, and location of objects in the visual scene, which enables observers to perceive depth and spatial relationships with greater accuracy and detail (e.g. Harris, 2004; Hibbard, Haines, & Hornsey, 2017; McKee, 1983; Stevenson, Cormack, & Schor, 1989). Stereoscopic displays result in a significant enhancement in performance on tasks involving spatial understanding or object manipulation (McIntire et al., 2012). Additionally, they are also

moderately beneficial for tasks requiring the judgment of object position or distance, as well as for tasks involving object finding, identification, or classification (McIntire et al., 2012). As proposed by Palmisano et al. (2010), binocular disparity decreases with the square of the observation distance for the same depth separation. This suggests that binocular disparity for a particular depth is considerably greater when the observation distance is short, leading to the conclusion that stereopsis is primarily valuable in near spaces. Behaviourally, humans are highly sensitive to binocular disparity (McKee et al., 1990) but exhibits individual variation across population (Bosten et al., 2015; Dorman & van Ee, 2017; Hess et al., 2015; Hess et al., 2016; Zaroff, Knutelska, & Frumkes, 2003), human stereoacuity has been found smaller than 5 seconds of arc (McKee, 1983; Stevenson, Cormack, & Schor, 1989).

### 1.2.1 The frame of references

To interact effectively with objects in our environment, we require precise information about their locations. This involves understanding their positions relative to ourselves (an absolute or egocentric direction task) and relative to other objects within the visual field (a relative or exocentric direction task). People can judge the direction of an object in any of the following reference frames, the first three of which are egocentric because they involve some part of the observer's body (Mapp, Ono, & Howard, 2012). Oculocentric judgments only require the image's position on the retina (Moidell & Bedell, 1988). A headcentric judgment requires the observer to register both the position of the images in the eyes (the oculocentric component) and the angular position of the eyes within the head (the eye-position component) (Howard, 1982; Matin, 1986). This combination allows for a comprehensive understanding of the object's position relative to the observer's head. Torsocentric judgments further require information about the position of the head relative to the torso (Longo et al., 2020). In exocentric judgments, the direction of one visual object is assessed with respect to a second object or an external reference frame (Sterken et al., 1999; Wade & Swanston, 1996;

Wertheim, 1994). When making a directional judgment about an object, it is crucial to know which frame of reference the viewer is using. In this thesis we mainly concentrate on headcentric directional judgments (Mapp, Ono, & Howard, 2012).

## 1.2.2 Two strands of visual direction research

The history of research on visual direction reflects an ongoing struggle between two approaches from antiquity to the present. The first relies on observation and phenomenology, initially with little underlying theory. This method results in a summary of observations in the form of propositions, principles, or laws of visual direction. An alternative approach relies on underlying theories (such as geometry or optics), after which observations become subordinate to the theory (Ono & Wade, 2012). The evolution and researchers responsible for these two different strands are shown in Figure 1.7.

The observational approach was promoted by Aristotle (384–322 BC). By making controlled observations of the perceived locations of vertical cylinders, Ptolemy (c. 150) defined single vision and distinguished between crossed and uncrossed directions in diplopic perception in the second century AD (Howard & Wade, 1996; Smith, 1996; Tyler, 1997). Wells (1792) defined the optic axis, visual base and common axis in relation to visual direction. Wells (1792) introduced three propositions, stating that objects on the optic axis appear in the common axis, objects in the common axis appear in the eye's axis, and objects in a line through the intersection of optic axes to the visual base appear in another line towards the left or right (see Figure 1.8). Wells' propositions, although not widely acknowledged, were unique and laid the foundation for understanding visual direction with two eyes. In the second half of the 19<sup>th</sup> century, Towne (1866), Hering (1868/1977, 1879/1942) and LeConte (1871) continued developing Wells' propositions. Above all, Hering (1868/1977, 1879/1942) made great contributions upon rediscovering

Wells' experiments and proposed that the reference point for judging visual direction was a "cyclopean eye", and thus concluded that objects located along an eye's visual axis were perceived as lying along a line that represented the average of the visual axes. In the 20<sup>th</sup> century, the observational strand had accepted the idea of a reference point for visual direction, which was called "central eye" (Towne, 1866), "double eye" (Hering, 1868/1977) and "cyclopean eye" (Hering, 1879).

Euclid (c. 300 BC) developed the optical approach and demonstrated that physical location and perceived visual locations were not necessarily identical. During 17<sup>th</sup> to 18<sup>th</sup> centuries, Johannes Kepler developed the optical tradition by explaining how light was refracted through the eye's structures and focused on the retina. According to his view, the position of an object could be estimated from the direction in which a ray of light originates, regardless of how refraction alters the direction along its path between the eye and the object. Significant disagreement existed around whether the light ray entering the eye was directly responsible for determining visual direction. Subsequently, Porterfield (1737) proposed an explicit theory of visual direction based on the location of the retinal image. In the first half of the 19<sup>th</sup> century, Brewster (1830, 1831) linked the definition of projection in the visual ("visible" in his terminology) direction with retinal anatomy. Additionally, Brewster (1844) found stimulation of the peripheral retina produced visible objects different from their actual positions, he used the term of "ocular parallax" to describe such difference and argued the deviation of the visual direction from the actual direction was very small. With the invention of Wheatstone's stereoscope (1833), he was able to correctly predict the apparent location of a fused image based on disparate stimuli in the stereoscope.





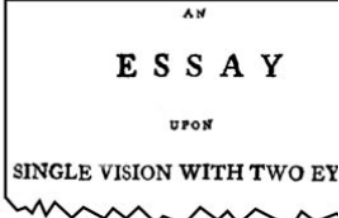

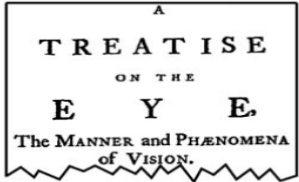





Observation strand		Optics strand	
<p>Aristotle</p>  <p>Ptolemy</p> 		<p>Euclid</p>  <p>Ancient era</p>	
<p>Alhazen</p> 		<p>11<sup>th</sup> Century</p>	
<p>Wells</p> 		<p>Kepler</p>  <p>17<sup>th</sup> &amp; 18<sup>th</sup> Centuries</p> <p>Porterfield</p> 	
<p>Towne</p>  <p>Hering</p>  <p>LeConte</p> 		<p>Brewster</p>  <p>Wheatston</p>  <p>19<sup>th</sup> Century</p>	

Figure 1.7: A chronology of the major contributors. This table includes portraits and the books they wrote on this topic. Image adapted from Ono & Wade, 2012.

Recent studies have accepted the claim that reference point is an important conceptual summary of the experience of visual direction (Erkelens, 2000; Erkelens & van Ee, 2002), though there is a continuous debate about where the reference point for visual direction is located. Some eye dominance studies (Wall, 1951; Robin & Wall, 1969) proposed that the reference point for visual direction is located in one eye, called the “directionalizing eye” (Robin & Wall, 1969, p.368), but experiments conducted with a wider population have failed to confirm this prediction (Barbeito, 1981; Barbeito & Simpson, 1991; Ono & Barbeito, 1982; Ono, Wilkinson, Muter, & Mitson, 1972; Pickwell, 1972). However, they neglected the rules that two objects aligned with an eye would appear to be on the common axis. Therefore, Mapp and others (2003) proposed that one cannot simply conclude reference point is located in one eye, as the location of the reference point should be inferred from the physical location of the objects rather than from a line passing through the perceived and apparent locations of the objects. These two strands of historical research on visual direction have been competing for dominance. However, these two strands need not be in opposition, people like Ptolemy and Wells made significant advances because they combined optical knowledge with observational experiences.

### 1.2.3 Basic law of visual direction

The perceived retinal image location can be used to determine both distance and direction in binocular vision. In terms of visual direction, an object fixated binocularly appears to have only one direction in space, despite the eyes pointing in different directions relative to the head's median plane. The two eyes somehow combine directional information to form a unitary visual property or qualia. The question then arises as to where in the head direction judgment originates? There is a possibility that it originated from the dominant eye, but it's widely acknowledged that directional judgments are referenced to a point located midway between the two eyes - known as the visual egocentre (or the cyclopean eye) (Mapp & Ono, 1999; Mapp, Ono, & Barbeito, 2003; Ono, 1991).



Therefore, information from each eye must be integrated into a cyclopean representation. This section explores the mechanisms of this integration, both when the images from the two eyes correspond and when directional information is obtained from disparate images.

#### 1.2.3.1 Wells's (1792) Propositions of the visual direction

The analysis of visual direction starts with the visual line, which is the basic unit of all directional judgments. A visual line is any line passing through the pupil of an eye and the nodal point (the area where all visual lines intersect). Among all the visual lines, the one through the centre of the fovea is termed the visual axis. It is also possible to specify a visual line according to its eccentricity and meridional angle, each fixed point in space has only one physical and apparent direction for a particular eye position. Wells (1792) defined some terms he employed in his experiments. For example, the optic axis is determined as a line passing through an object placed in a position where is more visible than in any other situation and a point between such object and the eye by a visual alignment task. The visual base is defined as the distance between the cornea points where the axes enter the eye. The common axis is represented by the line from the centre of the visual base through the intersection of the axes. There followed three propositions were made to better perceive visual direction:

Proposition I: Objects in the optic axis are perceived in the common axis (see Figure 1.8(b)).

Proposition II: Objects that lie on the common axis do not appear to be on that line, but on the axis of the eye that cannot see them (Figure 1.8 (c)).

Proposition III: Objects lie along any lines passing through the intersection of optic axes to the visual base do not appear to be in that line. Instead, it appears to be in another line passing through the same intersection but shifts to a point, which is displaced by half the distance

of the visual base. It describes the perceived displacement of visual objects in relation to the eyes' alignment (see Figure 1.8(d)).

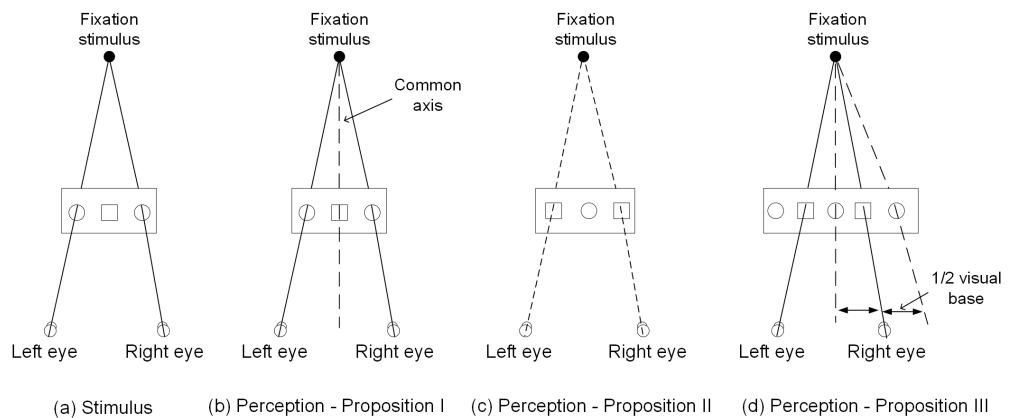


Figure 1.8: A demonstration of Wells's (1792) Proposition I, II and III, shown with (a): Stimulus. (b)- (d) Perception in Proposition I, II and III

A card with two circular holes placed 3 cm apart, positioned in the middle between two eyes and fixation stimulus. The left eye views the stimulus through the left hole, while right eye views the stimulus from the right hole. According to Proposition I and II, when fixation on the stimulus, they may perceive square in the common axis from each optic axis, also the circular holes in the optic axes are seen as one square in the common axis. Two outside circular holes are predicted by Proposition III, which is used to determine the apparent location of diplopic images,

Wells' propositions are clearly stated and empirically supported. Proposition I emphasize the role of both eyes acting as a single organ when perceiving objects. Proposition II highlights the unified perception of visual stimuli by the two eyes. Proposition III, the most comprehensive of the three, logically encompasses the first two propositions and serves as the fundamental principle of Wells' theory. It involves determining the apparent locations of diplopic images based on the point of fixation and the stimulus position.

During the experiment, Wells placed a card with two circular holes (one in each optic axis) in front of the eyes and observed a circular hole along the common axis (Figure 1.8) in accordance with Proposition I. In this situation, an imaginary hole appears in the median plane, and through this hole, the fixated object is seen. In Figure 1.8(a), there is a square-shaped stimulus in the median plane. Figure 1.8(b), according to Proposition I, describes that the object is perceived from the common

axis. Figure 1.8(c) illustrates that, according to Proposition II, the square-shaped stimulus occurs in two places, specifically at the location of the visual axes. The two outer circular holes shown in Figure 1.8(d) can be explained by Proposition III.

Figure 1.9 shows another demonstration of Wells' proposition. Solid red and dashed green lines represent the perceptual outcomes of the distinct inputs received by each eye. For the majority of the observers, a line alternated in colour between red and green can be seen pointing to the base of the nose. Two other lines are also visible, they appear to point to the outside of the eyes instead of being directed towards the eyes.

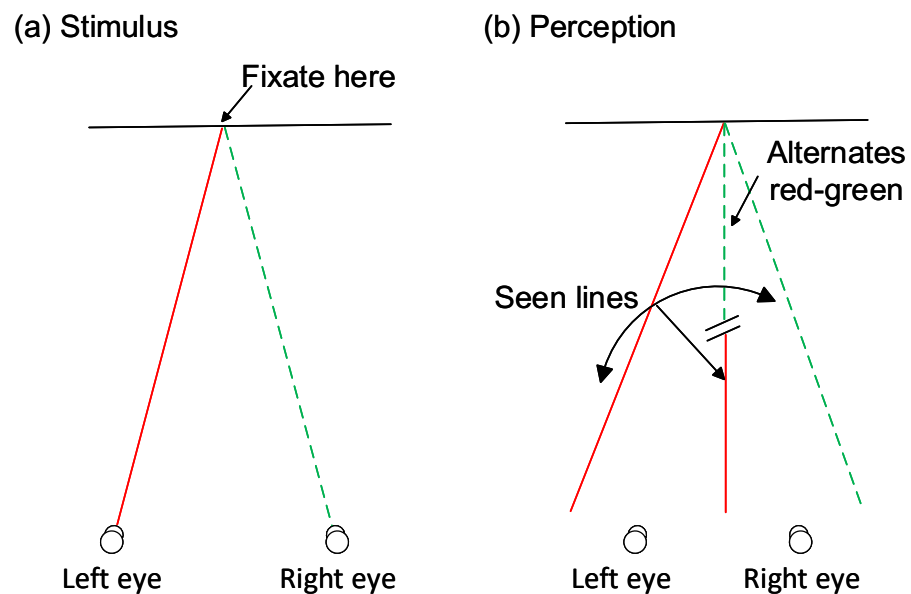


Figure 1.9: Another demonstration of Wells's (1792) Proposition I, II and III. When the stimulus in (a) is viewed binocularly and fixed on the intersection of the red and green lines, illustrated in (b) in which the alternating red and green lines appear to point to the nose is predicted by Proposition III. Image created on the basis of the illustrations by Ono (1991).

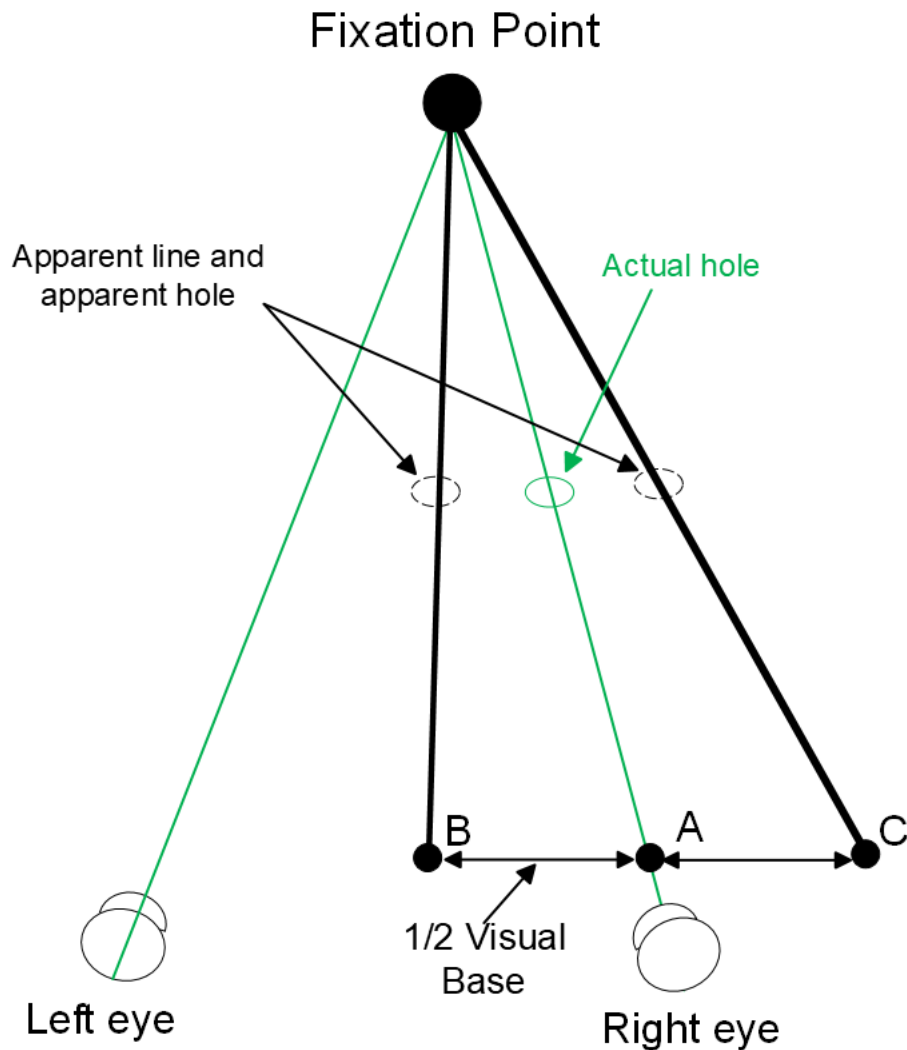


Figure 1.10: An illustration of Wells's (1792) Propositions III, determining the apparent location of the diplopic images. Two thick lines link the fixation point with the location of the stimulus (black circle), called the line of the apparent location by Wells. The green lines with green circle on are the real line of the stimulus, passing through the intersection of two visual axes and the real stimulus. Point B and C are determined as the half the distance of the visual base from point A. The diplopic image will be seen on the line passing through this point (e.g. point B to fixation point) on the visual base to the fixation point. Imaged reproduced from Ono, 1991.

Wells's (1792) first two propositions, as the special cases of Proposition III, can be derived from the Proposition III. Figure 1.10 explains how Proposition III can be used to determine where the outer holes appear in Figure 1.8(b), as well as the lines that appear to point toward the ear and nose in Figure 1.9 (b). Figure 1.10 demonstrates how Wells's Proposition

III can be used to determine the apparent locations of the illusory images. The first step in applying Proposition III is to draw a line through the intersection of the two visual axes and the actual position of the object, for example, the green line that coincides with the right axis here. The second step is to determine the intersection of the actual position line with the visual base (point A). Point B and C are determined as the half the distance of the visual base from point A. The line passing through the fixation point to each of these two points as the apparent line. One of the lines passes through point B to the fixation point refers as common axis here, and along it lies the apparent hole through which the target lies on one of the green lines is seen. The other line connects point C to fixation point, passing through an outer apparent circular hole and another green line points towards the right ear. According to Proposition III, when the stimulus is viewed binocularly, it will be seen as a single image if it is positioned at the intersection of the visual axes; it appears double when not at the intersection, one is on the common axis, and the other is shifted to the outward.

In contrast, other theoretical concepts like the cyclopean eye, horopter, corresponding points, and identical visual direction are incorporated into the laws of visual direction that developed subsequent to Wells' research. Utilizing these constructs, Hering (1879/1942) demonstrated the law of identical visual direction. Hering's (1879/1942) principle introduces the cyclopean eye as the reference point to combine visual inputs, predicting that objects seen separately by each eye will be perceived at different locations on their respective optic axes unless the images are perfectly aligned. Modern mathematical translations of these rules reveal that Hering's formulations (are discussed below) are more accurate in predicting binocular visual directions (van de Grind et al., 1995).

### 1.2.3.2 Hering's (1879/1942) law of visual direction

There are several different restatements of Hering's (1879/1942) psychophysical law, in which is the most comprehensive one is provided by Howard (1982). The following describes Howard's restatements.

#### *1.2.3.2.1 The laws of oculocentric direction*

A visual line is an imaginary line connecting an object to the nodal point of the eye. Each eye may perceive the object differently due to their physical separation. When objects are perceived to be aligned or superimposed, they share the same oculocentric direction, resulting in a unified perceptual experience. In contrast, non-over-lapping objects creates a disparity between the images seen by both eyes, resulting in a cue for depth perception.

#### *1.2.3.2.2 The law of cyclopean eye*

All objects are perceived as if seen from the cyclopean eye, at a reference point, which is located in the midway between the two eyes. With symmetrical convergence, any objects located on either of the corresponding visual lines will appear spatially superimposed. Assuming that the horopter conforms to the Vieth-Müller circle, the cyclopean eye lies on this circle, midway between the eyes.

#### *1.2.3.2.3 The law of monocular visual direction*

When viewing the object monocularly, those aligned along the same visual lines are perceived have the same visual direction, all visual lines point to the cyclopean eye.

#### *1.2.3.2.4 The law of cyclopean projection*

First, objects fall on the visual axes of both eyes are perceived as lying on the common axis, defined as the line passing through the cyclopean eye and the intersection of two visual axes. Second, an object located on a visual line is perceived to deviate from this common axis by an angle, which is equal to the angle between the visual axis and the visual line

containing that object (as an addition law supplemented by Howard (1982), this law does not apply to the fused images discussed in the law of binocular visual direction, but it highlights how perception is affected by angular relationship within the visual field). As shown in Figure 1.11(a), The object is perceived as a single image as if seen from the cyclopean eye in a direction that corresponds to its angle of entry relative to each visual axis (angle  $\alpha$  and  $\beta$  represent the equal angle between visual line and visual axis for the two eyes). The angle between the direction seen from the cyclopean eye and the common axis matches the angle between the visual line and visual axis.

#### *1.2.3.2.5 The laws of binocular visual directions*

(a) Each visual line in one eye corresponds to a visual line in the other eye, with the same apparent visual direction, known as the law of identical visual direction. In Figure 1.11(a), an object does not occur on either axis, but on two corresponding visual lines, which means that the stimulus stimulates corresponding points on both retinae.

(b) The perceived visual direction of slightly disparate different images is the average of the visual directions of the individual monocular images. As shown in Figure 1.11(b), when an object is outside the horopter, it produces an uncrossed disparity. The angle subtended by the visual line and visual axis are different for the two eyes.

If the disparity is minimal, the perceived visual direction is the average of the monocular images' visual directions.

(c) In the presence of competing images, the visual direction is determined by the dominant image, resulting in a suppression of the rivaling image. As the disparity in Figure 1.11(b) is large, one of the two possible apparent locations outside the horopter is perceived, resulting in a non-veridical visual direction. In this case, the perceived location does not correspond accurately to the object's actual location.

(d) Widely disparate images are perceived in two distinct visual directions. If the disparity in Figure 1.11(b) is even larger, two separate objects are seen.

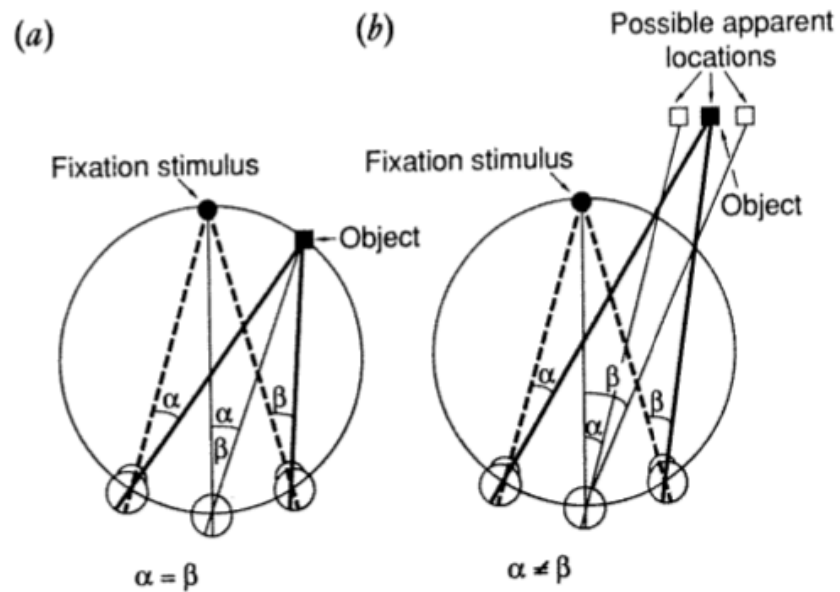


Figure 1.11: The visual direction of an object.

Fixation is on a point in the median plane of the head, so the eyes are in primary gaze position; the visual axes are represented by thick lines. An object is shown along with its corresponding visual lines (thick lines).  $\beta$  is the binocular visual direction of the target and is equal to the angle between the head's median plane and a line from the midpoint of the interocular axis to the target. The thin line from the cyclopean eye through the apparent position of the target is the binocular direction. In (a), the angles  $\alpha$  subtended by the visual line and the visual axis for the two eyes are equal. In (b), the angle subtended by the visual line and the visual axis of the left eye is smaller than that of the right eye. Image from Ono (1991).

## 1.3 The cyclopean view

### 1.3.1 The cyclopean eye (or the visual egocentre)

The cyclopean eye was described by Hering and Helmholtz as a hypothetical single 'eye' or "the mind's eye", based on a single stereoscopic image given appropriate stimuli in the two eyes. Julesz (1971) used the term "cyclopean" to describe the central processing of visual stimuli, he proposed that the essence of a cyclopean stimulus



occurs at some central location in the human brain. With random-dot stereograms, it is possible to portray information on the “mind’s retina”—a place where the left and right visual pathways combine in the visual cortex.

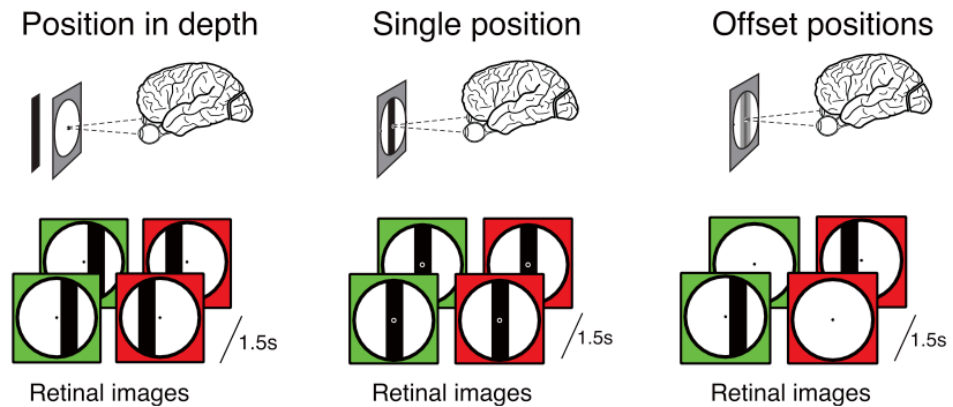


Figure 1.12: Position in depth.

Each eye is shown two horizontally offset bars simultaneously. In this case, the retinal locations stimulated differ from the perceived visual location of the bar, and therefore its depth is perceptually perceived. “Single position” stimulus: a bar is presented in the same position in both eyes and repositioned every 1.5s (1 TR) to determine the population receptive field of each cortical area. “Offset positions” stimulus: a bar is alternatively presented between the two eyes, and the bar is presented in the same retinal location as the “position in depth” stimulus. Image from Barendregt et al., (2015).

A computational challenge faced by the brain is how to combine the information from the two eyes to achieve the cyclopean view and determine the visual direction of objects in space relative to the viewer. Recent evidence from a functional magnetic resonance imaging (fMRI) study suggested the transformation from a retinotopic to cyclopean representation takes place between the striate (V1) and extra-striate (V2) human visual cortex (Barendregt *et al.*, 2015). This study presented two contrast bars with slight opposite horizontal offsets in front of each eye, so that it could produce depth perception (“position in depth” in Figure 1.12). Two types of control stimulus were based on stimulus position either in the two retinal images or in the cyclopean image were measured in this study. One of the control stimuli was the contrast bars presented with identical position in each retinal image without binocular disparity (“Single position” in Figure 1.12. The other was presented alternately in

front of the two eyes, as the stimuli stimulated the same retinal position of both eyes, but was not integrated into a single image due to temporal alternation (“offset positions” in Figure 1.12). The blood-oxygen-level dependent (BOLD) response was used to estimate the population receptive field (pRF), that is, the area of visual space that optimally stimulated the group of neurons at each recoding site. Through comparing the BOLD responses in V1, V2 and V3 for two control models, there was a reliable distinguish evoked by these two conditions in V1 and V2, but the differences in responses predictions were insufficient to identify the stimulus presentation in V3 though all inclusive recording sites were considered (see Figure 1.13(a)). The pRF models based on either retinal images or the cyclopean images were compared to investigate the responses evoked by viewing “position in depth” stimulus. The left panel in Figure 1.13(b) demonstrates V1 represents the stimuli based on retinal positions while V2 represents stimuli based on cyclopean image, it is confirmed by the significant differences in how well retinal and cyclopean models best predict neural responses in each area, highlighting a transition from retinal to cyclopean representation between V1 and V2. Subsequent BOLD responses in extrastriate cortex (such as V2, V3, V3A, LO1 and LO2 in Figure 1.13(b)) reflects the position of binocular stimuli in the cyclopean image rather than in the retinal images. Taken together, Barendregt and others (2015) provided the evidence that V1 undergoes a transformation from two separate retinotopic maps to a single cyclopean map. In extrastriate cortex (starting from V2), the neural response become less dependent of retinal position and more aligned with the position in the cyclopean image. These human fMRI findings are consistent with earlier research on other primates, which show that neurons in V1 mainly respond to input from one eye or the other, whereas V2 onwards, neurons are mostly binocular, responding to inputs from either eye (Chen, Lu, & Roe, 2008).

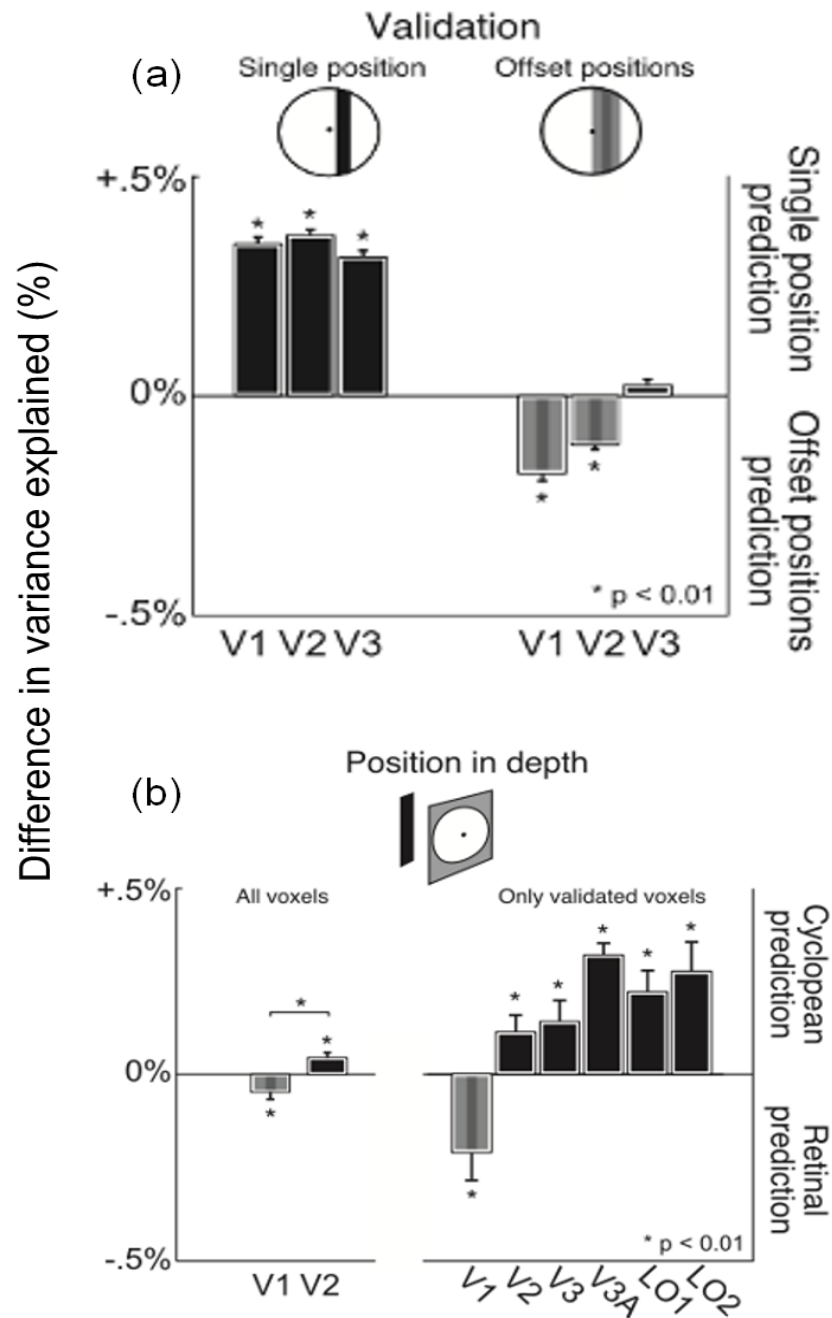


Figure 1.13: The representation of visual stimuli changed from reflecting retinal images to reflecting cyclopean images. (a) compares of how predictions based on “single position” and “offset position” stimuli explain the measured fMRI responses in V1, V2, and V3. In V1 and V2, it can be reliably distinguished between responses elicited by “single position” and “offset position” stimuli. In V3, the response prediction is not sufficient to distinguish between the two stimulus representations; (b) illustrate the transformation from a representation of two retinal image in V1 to a cyclopean image in V2 onward. Left panel shows the representation of “the position in depth” stimulus in V1 is best explained by the retinal images of the stimulus, while the representation in V2 is best explained by a cyclopean image. The right panel examines the voxels in areas V1 through LO2 that can accurately differentiate between “single position” and “offset position” stimuli.

### 1.3.2 Methods of measuring the location of the cyclopean eye

There is ongoing debate around the exact location of the cyclopean eye. The precise position of the cyclopean eye, or egocentre, can be measured behaviourally in the laboratory using psychophysical techniques (Barbeito & Ono, 1979). Rather than assuming a fixed location, some investigators have developed different methods to estimate the location of the cyclopean eye. Four of these methods will be described briefly: two of them (Funaishi, 1926; Howard & Templeton, 1966) attempt to estimate the egocentre location independently of the law of visual direction, whereas the other two (Fry, 1950; Roelofs, 1959) rely on the law of visual direction and estimate the location based on an observer's response (Ono, 1991- see Figure 1.14).

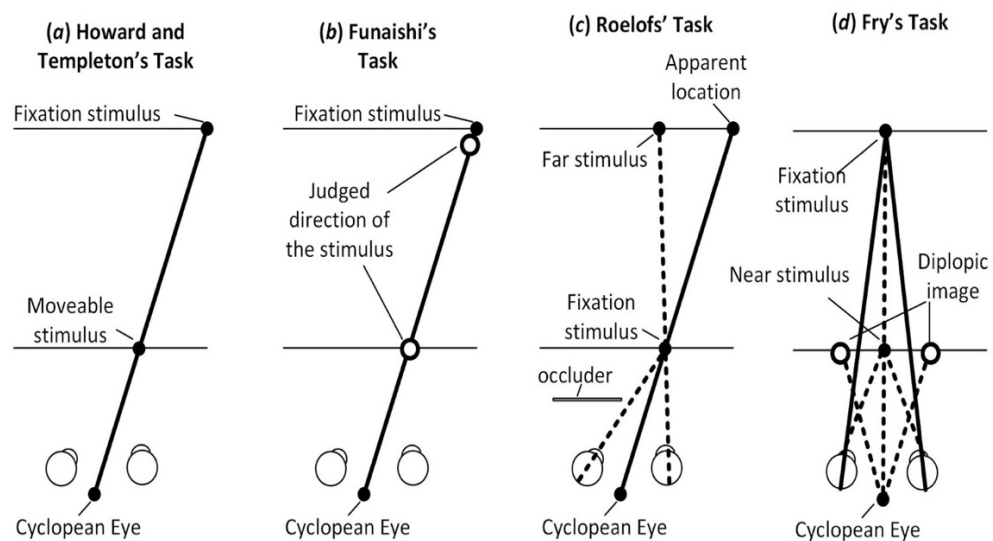


Figure 1.14: Schematic of four methods of locating the cyclopean eye. (a). Howard and templeton's method involve the subject aligning two stimuli, one near and one far, the intersection point of the projected axes from these alignments is the cyclopean eye; (b). For Funaishi's method, the subject fixates on a point and judges the direction of the non-fixated one by pointing to their apparent direction; (c). Roelofs's method, the subject fixates on the front of the tube monocularly with the other eye occluded and indicates a point on the illusory line perceived; (d) Fry's methods instructs the subject to fixate on one of two stimuli and indicate the apparent location of diplopic images produced by the non-fixated stimulus. Figure adapted on the basis of Mitson, Ono, & Barbeito (1976).

In Howard and Templeton's (1966) method, an observer was asked to align two stimuli (near and far) until the imaginary axis joining them was judged to point directly at themselves. The intersection point of the projected axes is taken as the cyclopean eye (see Figure 1.14(a)). Funaishi's (1926) task required an observer to fixate a point and then judge the direction of a non-fixated point placed to the left or right of the fixation point in the same frontal parallel plane. The apparent direction of the targets and lines are projected back through the response locations to estimate the cyclopean eye (see Figure 1.14 (b)). Roelofs's (1959) method required the observer to fixate on the front of a tube with one eye, while the other eye is occluded, and indicate a point on the illusory line that is perceived between them. In accordance with Hering's (1879/1942) principles of visual direction, the tube will appear to be pointing forward along a radial line joining the subject's cyclopean eye and the tube's front, rather than corresponding to its objective direction. As defined above, the apparent direction of the tube is regarded as the projection from its front to a point on the observer's face at which the tube is pointing, such that the projection is considered to pass through the cyclopean eye (see Figure 1.14(c)). For Fry's (1950) measurement, an observer was required to binocularly fixate on one of two stimuli (the farther target in Figure 1(d)) and indicate the apparent location of each diplopic image produced by the non-fixated stimulus (the closer one). The observer used a pointing device to mark these locations, ensuring that the hand used for pointing was not visible to maintain the accuracy of the perceived direction. Lines, projected from the indicated location of the diplopic images back towards the observer, are assumed to pass through the cyclopean eye (see Figure 1.14(d)).

After comparing the predictive validity (the ability to predict responses on other visual direction tasks) and reliability (rest-retest stability) of these four methods, Barbrito and Ono (1979) concluded that the approach proposed by Howard and Templeton (1966) provided the best estimate of the location of the egocentre - the reference point used to perform this task could be located with much greater precision. Howard and

Templeton's method required direct visual judgments, while the other three methods introduced potential sources of error (asking subjects to point to a location in space using their hands) to the visual judgment. Based on the predictive validity of Howard and Templeton's method, the locations determined by it were most effective in predicting individual differences across three different visual direction tasks. As a result, the method's high precision is attributed to the lack of manual pointing responses as a source of variability (Barbrito & Ono, 1979). In addition, individual differences in constant errors associated with pointing to a location in space manually may obscure true variation in egocentre location and inflate estimate reliability, reflecting variations in constant error rather than the true egocentric localization (Barbrito & Ono, 1979; Mitson et al., 1976; Ono et al., 1972). Furthermore, manual pointing errors in different methods could lead to different egocentre locations, which may explain offsets in egocentre location – it's more rightward in the Roelofs's (1959) methods compared with Furnishi's (1926) method.

## 1.4 Individual differences

Ono and Mapp (1995) supported Wells–Hering's laws and emphasized the role of the cyclopean eye in predicting the visual direction of objects. This model outlines key elements of egocentric direction, including the retinal location being stimulated (local sign) and the positions of both eyes (Ono, 1981). However, the cyclopean eye location is a complex and individualized perceptual construct influenced by various factors, including age (e.g., Bian & Andersen, 2013; Norman et al., 2004;), eye position information (Barbeito & Simpson, 1991; Erkelens, 2000; Ono & Weber, 1981; Park & Shebilske, 1991; Simpson 1992; Sridhar & Bedell, 2011), eye dominance (Mapp, Ono & Barbeito, 2003). It has been demonstrated previously that individual differences in measured visual egocentre location can be used to predict individual differences in perceptions of directions (e.g. Ono et al., 1972; Barbeito & Ono, 1979).

An extensive body of research has found that age-related reductions in the ability to process sensory information, including visual acuity (Corso, 1981; Owsley & Sloane, 1990), contrast sensitivity at higher spatial frequencies (Owsley, Sekuler & Siemsen, 1983), and the useful field of view (Sekuler & Ball, 1986). These age-related changes in vision have an effect on spatial abilities (Gazova *et al.*, 2013, Roggiero *et al.*, 2016, Techentin *et al.*, 2014) and visual perception (Bian & Anderson, 2013; Norman *et al.*, 2004), suggesting variability on the ability to process depth perception.

The perceived egocentric visual direction is derived from a combination of eye position information (Bridgeman & Stark, 1991; Bock & Kommerell, 1986) and retinal information (Howard, 1982). Barbeito and Simpson (1991) used an experimental setup where subjects pointed to the apparent direction of a target while one eye's position was varied. The results confirmed the linear relationship between eye position and egocentric visual direction and revealed individual differences in how each eye's position affects egocentric direction. For example, differences in how effectively they integrate retinal information with eye position or how well they combine joint binocular signals and eye position information leads to variations in the cyclopean eye position. In addition, changes in oculomotor control affects the way how retinal information and eye position signals are combined. Moreover, abnormal conditions like strabismus (misalignment of the eyes) affect how visual information is integrated, leading to shifts in the cyclopean eye position (Mollon *et al.*, 2017). Different levels of eye coordination may cause variations in the egocentre location (Cui, *et al.*, 2010), a person with strabismus (misaligned eyes) may have a different egocentric perception compared to a person with normal eye alignment.

Given the high sensitivity to relative direction, the visual system can provide precise information about the object's position relative to its reference frame (Ono, Mapp & Howard, 2002). The differences in visual system sensitivity among individuals may give rise to variation on the

cyclopean eye locations. Individuals often have one dominant eye that exerts more influence in binocular vision, resulting in asymmetries in visual sensitivity when integrating information from both eyes (Ooi & He, 2020) (eye dominance will be further discussed in the next section). For example, someone with a dominant right eye may have the cyclopean point closer to the right visual axis, affecting their sensitivity to certain spatial locations. It has also been found that greater amplitudes and faster peak velocities in dominant eye than non-dominant eye when conducting a sighting task (Oishi et al., 2005), in which different degree of eye dominance can also be considered as a factor leading to variations in the cyclopean eye positions. Moreover, observers' knowledge on "point the rod to themselves" during binocular sighting task are different, which may lead to varied reference frames (e.g., bridge of nose, one eye, or anywhere on the face). The subjective impression based on individual knowledge plays an important role in determining the cyclopean eye location and explaining its variations (Erkelens, 2000; Erkelens et al., 1996; Erkelens & van Ee, 2002; Ono, Mapp, & Howard, 2002) Long-term exposure to specific visual environments or tasks can lead to adaptations in the visual system. For instance, pilots and athletes who rely heavily on precise visual information may experience shifts in their cyclopean eye location due to specialized visual demands (Howard & Templeton, 1966).

The observed variation in individual egocentric localizations highlights the importance of studying individual differences in visual perception, which reflects the inherent diversity of individual's perceptual processing and anatomy. Recognizing and studying these differences can enhance our understanding of how spatial perception is adapted to individual needs and may have practical applications in areas such as virtual reality, and clinical assessment of spatial impairment. Taking into account individual differences in egocentric localization allows developers to tailor visual content to users' natural spatial orientation, enhancing realism and reducing discomfort used in Virtual Reality (VR) and Augmented Reality (AR) systems. For patients with spatial perception disorders, VR and AR



environments can be used to create controlled visual scenarios to gradually correct their spatial misjudgements and improve their functional ability.

## 1.5 Eye dominance

Research moved from developing the specific dominance tests to connecting eye dominance to other visual phenomena in the middle of the 20<sup>th</sup> century. Chamwood (1949) and Francis & Harwood (1952) found evidence of dominance changing when measured with a neural density filter, suggesting that eye dominance could shift to favour the eye with a brighter image. Among these studies, eye dominance was measured with different tasks, such as reaction time (Minucci & Connor, 1964), size distortion (Coren & Porac, 1976), accuracy of bisecting lines (Mefferd & Wieland, 1969), and even marksmanship (Crider, 1943). Interestingly, these early studies noted that eye dominance is not a single, unified phenomenon, suggesting that it may depend on the task itself (Woodhouse, 2009).

### 1.5.1 Different forms of eye dominance

Although the human body is symmetrical, one side may function more efficiently than the other. This difference in efficiency can result in a preference for using the more efficient one, known as the limb dominance, with handedness playing a crucial role in daily activities (Woodhouse, 2009). Similarly, people tend to favour the visual input from one eye than the other when both eyes are open, the preferred eye is known as the dominant eye. The concept of eye dominance was first mentioned by Porta in 1593 (Porac & Coren, 1976), in which an individual aligns a pencil (or a similar object) with a mark on the wall, known as the Rosenbach test (Miles, 1929) or Porta- Rosenbach test (Miles, 1930). When performing this task, the eye used for alignment is the dominant eye. Eye dominance remained largely unexplored until the 20<sup>th</sup> century, when further tests of eye dominance were developed. Mile's (1929) test,

as one the most famous tests, where an individual aligns a target through a small opening in a truncated cardboard cone that is held up to the face. The eye used for alignment refers the dominant eye, though observer is unaware he is sighting with only one eye. Crider (1944) expanded upon this by developing a set of seven sighting tests, including observers look through a ring, or look through a hole in a card, in which remain in use today (Ehrenstein, Arnold-Schulz-Gahmen & Jaschinski, 2005; Handa *et al.*, 2004). Banister (1935) examined the role of eye dominance in daily activities by investigating the impact of dominant eye on marksmanship, showing that right eye dominant individuals behave more accurate when shooting them from the right shoulder.

Since eye dominance is defined based on such a wide range of criteria, its definition is complex and influenced by a variety of theoretical orientations (Porac & Coren, 1976). As a result of this complexity, different measurements of eye dominance show low intercorrelations (Coren & Kaplan, 1973; Crider, 1944; Gronwall & Sampson, 1971; Jasper & Raney, 1937; Washburn *et al.*, 1934). It was initially thought that eye dominance was a single mechanism (Parson, 1924; Porta, 1593), but many scholars have suggested that eye dominance encompasses several, potentially independent factors, resulting in the development of different typologies (Berner & Berner, 1953; Cohen, 1952; Coren & Kaplan, 1973). There is still disagreement regarding the types of dominance and the number of mechanisms involved, with some suggesting as few as two (Berner & Berner, 1953; Cohen, 1952; Walls, 1951) and others suggesting as many as five (Lederer, 1961). Coren and Kaplan (1973) contributed to this debate via an empirical experiment involving a battery of 13 common eye dominance tests, in which they used a non-dichotomous scoring system to assess both the strength and direction of eye dominance. Three different forms of ocular dominance were identified by their factor analysis: sighting, sensory, and acuity dominance. The findings suggested that different tasks or sensory demands can alter the dominance between the eyes, demonstrating eye dominance is not a unitary concept but rather varies depending on the

types of dominance being assessed. Thus, eye dominance is multifaceted, with sighting, sensory, and acuity dominance potentially producing different results.

Despite the recognition of various forms of eye dominance, motor dominance (Walls, 1951), now referred to as the sighting dominance, remains the focus. As is the most commonly measured form of eye dominance, sighting dominance reflects a behavioural selection or preference for one eye's input in situations where both eyes cannot be used simultaneously, or their views are discrepant and cannot be fused (Porac & Coren, 1975). Due to its frequent occurrence and familiarity, sighting dominance is regarded as the "definitive" type of eye dominance (Mapp et al., 2003; Porac & Coren, 1976), and is the most easily measurable simply by having them look through a pinhole (Crider, 1944). Large sample sizes have been used in numerous studies to investigate sighting dominance, revealing reasonable consistency between population norms (Porac & Coren, 1976). Studies have shown that approximately 65% of healthy populations prefer viewing with the right eye, 32% with the left eye, and 3% show no consistent preference (Li et al., 2010; Yang et al., 2010; Zhang et al., 2011). This finding indicates approximately 97% of people use the same eye consistently across a variety of sighting tasks, underscoring the reliability of sighting dominance as a phenomenon. In fact, it has been observed that certain animal species, especially primates, exhibit behaviours associated with sighting dominance, suggesting that primates may have particularly significance in terms of sighting dominance (Porac & Coren, 1976). For example, monkeys exhibit a dominant eye when engaging a sighting task (Cole, 1957; Hall & Mayer, 1966; Kounin, 1938; Kruper et al., 1967; Kruper et al., 1971; Smith, 1970), however, other animal species, like cats, exhibit paw preference but no eye preference (Crinella et al., 1972).

Sensory dominance is more commonly seen in scenarios involving binocular rivalry (Coren & Kaplan, 1973). These scenarios lead to non-fusible images and alternating conscious perceptions where one eye's

view predominates for longer periods as two monocular images are highly discrepant. Thus, sensory dominance can be determined by comparing the duration of each monocular vision in the binocular perception (Cohen, 1952; Coren & Kaplan, 1973). Sensory dominance does not occur in daily situations but arises under specific conditions, such as reduced luminance in one eye or when objects are closer to the face than the near point of convergence, indicating sensory dominance is a distinct phenomenon from sighting dominance. Data from studies by Cohen (1952), Coren and Kaplan (1973), Porc (1974), and Washburn et al. (1934) suggested that 48% of individuals showing a preference for the right eye, 32% for the left eye, and 19% being no dominance. Although sensory dominance tends to favour the right eye, its strength is weaker than sighting dominance, such as that reported by Humphiss (1969), suggests a development increase in the strength of sensory dominance, which is not observed in sighting dominance studies.

Acuity dominance, appears to be markedly different from the previous two forms of eye dominance, refers to the dominance of the eye with higher visual acuity. This form of dominance is evident in situations where the visual acuity of one eye is noticeably reduced than the other, such as amblyopia (Porac & Coren, 1975), or when one is more long-sighted (hyperopic) or short-sighted (myopic) than the other (Woodhouse, 2009). Unlike sighting and sensory dominance, which can shift between the eyes based on external factors like gaze direction or image manipulations (Khan & Crawford, 2001; Meegan et al., 2001), the concept of acuity dominance is based on the physiological of the eyes, with acuity being influence by the efficiency of relationship exists between the brain and the eye (Bruce et al., 1996) and hyperopic and myopic being defined by physical dimensions of the eyeball (Blake & Sekuler, 2006). It is logical to assume that acuity dominance remains stable and unaffected by external manipulations.

However, the boundaries between three types of dominance are not as clear as they might initially seem. For instance, both forms involve

situations where two monocular images differ, either due to the difference in visual acuity (acuity dominance) or due to they are noticeably different from one other (sensory dominance). This suggests a potential relationship between acuity dominance and sensory dominance. If the acuity in one eye is reduced, which will trigger a form of dominance that affects the perceptual system. Small acuity disparities would identify the eye with better acuity as dominant. On the other hand, when there is a noticeable acuity differences, sensory dominance may take over, the eye with a prolonged percept refers as the dominant eye. As a result, acuity and sensory dominance may exist on a spectrum, with acuity dominance representing inherent physiological differences and sensory dominance taking over when those differences are aggravated by external circumstances. Some researchers attempted to connect acuity dominance to sighting dominance (e.g., Porac & Coren, 1975b; Woo & Pearson, 1927), stating that the eye with better visual acuity tends to be the eye chosen for sighting. The only measures of acuity dominance involve situations where dichoptic or non-dichoptic information is tachistoscopically presented (Coren & Kaplan, 1973; Hayashi & Bryden, 1967; Kephart & Revesman, 1953; Perry & Childers, 1972). In these cases, the eye whose input is most frequently reported is the one with better acuity. However, even this relationship does not hold when exposure time is extended to approximately 250 milliseconds (Porac, 1974). Therefore, a normal observer without significant acuity imbalances between the eyes is not particularly dependent on an acuity-dominant eye. This factor may play a role in cases where there is a noticeable difference in acuity between the eyes, as can happen when cataracts or other ocular diseases like macular degeneration emerge.

### 1.5.2 Eye dominance and generalized laterality

The generalized laterality concept suggests that most individuals show consistent lateral preferences across various functions, such as handedness, footedness, and eyedness. Typically, a right-handed

person is also expected to be right-eyed. However, neurological evidence does not support a straightforward correlation between eye dominance and cerebral dominance. The complexity of the visual system, with its bilateral processing of visual input, means that eye dominance does not directly indicate which cerebral hemisphere is dominant. The relationship between eye dominance, handedness, and cerebral dominance is multifaceted and requires a nuanced understanding beyond simple lateral preferences (Porac & Coren, 1976). Several researchers have explored the connection between eye dominance and cerebral dominance by studying the projection of each hemi-retina to its respective cerebral lobe. These investigations have generally focused on whether dominance in the hemi-retina or visual field aligns with the overall eye dominance commonly measured. Some researchers (Jasper & Raney, 1937; Spreen, Miller, & Benton, 1966) employed an ambiguous apparent movement task to determine whether observers resolved the movement in favour of the dominant visual field (i.e., cerebral hemisphere) or the dominant eye. Jasper and Raney observed both behaviours occurred, while Spreen, Miller, & Benton (1966) didn't find any relationship between visual field dominance and eye dominance.

Although there is little physiological relationship between cerebral and ocular lateralization, one could speculate on linking sensorimotor coordination with eye dominance. In tasks requiring continuous visual monitoring and control, such as mirror tracing, the use of the dominant eye does not appear to confer any advantage (e.g., Ong & Rodman, 1972; Schrader, 1971). However, in tasks involving ballistic movements or aiming, such as throwing a basketball or hitting a baseball with a bat, there is some evidence of an eye-hand effect. More accurate performance is often associated with having a dominant eye and dominant hand that are ipsilateral to each other (Adams, 1965; Shick, 1971). This ipsilateral hand-eye dominance has also been shown to benefit sports performance in children (Lavery, 1944) and driving ability in adults (Quinan, 1931).

### 1.5.3 The relationship between the visual egocentre and the dominant eye

Charnwood (1949) and Francis & Harwood (1952) were among the earliest researchers to examine if the evidence of an apparently moving dominant eye could indicate a shifting centre of visual direction. This concept sparked further investigation into the visual egocentre location, where visual information is combined to create a cohesive sense of direction. Important studies by Mitson, Ono, & Barbeito (1976) and Barbeito & Ono (1979) provided a better understanding of locating the visual egocentre, it will be discussed in more in detail in Chapter 4.

The concept of the visual egocentre and the dominant eye are crucial to understanding human visual perception, particularly in determining the origin of visual direction. As mentioned in 1.3.1, the visual egocentre hypothesis proposes that the centre of visual direction is located exactly midway between the two eyes, integrating inputs from the two eyes to form a single visual percept (Hering, 1879/1942; Le Conte, 1881). The dominant eye hypothesis suggests that visual direction originates from one eye, typically the eye preferred during sighting tasks (Parson, 1924; Porac & Coren, 1981; Walls, 1951). Barbeito (1981) investigated both the location of the visual egocentre and the sighting dominant eye, and found that sighting judgments were made from a point between the eyes (the visual egocentre) rather than from the dominant eye, and the preferred eye in sighting tests aligns with the side of the midline where the visual egocentre is located. Ono and Barbeito (1982) evaluated two competing hypotheses regarding the centre of visual direction using a modified hole-in-card test, they found that when observers viewed a distant object through the hole with the sighting dominant eye, the object appeared to be located on a visual axis that is collinear with an egocentre positioned directly between the eyes. In addition, the findings revealed that sighting dominance could vary based on how the task was performed: when observers raised up the card from the left, they tended to use the left eye, when raised up the card from the right, they tended to sight through the

right eye. Barbeito (1981) conducted three experiments to examine the reference point used in sighting tests and the location of the visual egocentre in relation to sighting dominance. Barbeito's research provides compelling evidence that the visual egocentre, rather than the dominant eye, is the primary reference point for judging the visual direction. This has significant implications for understanding visual perception and the mechanisms underlying sighting dominance. However, Barbeito's study focused on a sighting task; whether the dominance of visual egocentre is consistent across different visual contexts, such as depth perception, motion detection, or complex spatial navigation, remains unexplored. In addition, the neurological basis of cyclopean vision and its development over time were not addressed. Porac & Coren (1986) instructed observers to move a point of light until they perceived it as being located straight ahead. They found that those who sighted with the right eye tended to have a rightward bias, while those who sighted with the left eye tended to have a leftward bias, suggesting that the point of reference for judgment is displaced towards the sighting eye.

Elbaum, Wagner, and Botzer (2017) conducted two experiments to compare the tracking accuracy between the visual egocentre, the dominant eye and the non-dominant eye in gaze-interface tracking. The study concluded that the visual egocentre provides more accurate tracking than either the dominant or non-dominant eye, particularly in initial or untrained conditions. This supports the theory of egocentric direction and the results have implications for the design and optimization of human-computer interaction systems. However, although the study acknowledges the concept of eye dominance, it does not delve deeply into the variability of dominance across different tasks and conditions. It is still unknown how eye dominance interacts with other factors, such as task difficulty and individual variations in visual processing.



## 1.6 Short-term monocular deprivation on sensory eye dominance

Brain plasticity refers to the ability of central nervous system (CNS) neurons to rearrange in response to environment inputs, which allows us to learn new knowledge and skills, adapt to environmental changes, and recover from injuries (Bliss & Lomo, 1973; Kandel et al., 2014; Levy & Steward, 1983; Magee & Gruenberge, 2020; Malenka & Bear, 2004; Strettoi, 2022). Visual experience plays a crucial role in shaping neural connections, but its effects are most pronounced during a specific time window, termed the critical period of visual development. Monocular visual deprivation during the critical period results in shrinkage of ocular dominance columns associated with the deprived eye (Adams, Sincich, & Horton, 2007; Baker, Grigg, & von Noorden, 1974; Blakemore, Garey, & Vital-Durand, 1978; Crawford, Blake, Cool, & von Noorden, 1975; Frenkel & Bear, 2004; Wiesel & Hubel, 1963; Hubel & Wiesel, 1969).

The first systematic investigation on critical period was conducted in the visual cortex of cats, Wiesel and Hubel (1963) used extracellular recordings to study the cortical responses in kittens deprived of vision in one eye for a few weeks after birth and found a shift in ocular dominance induced by monocular deprivation. This effect was the most pronounced between 4 and 8 weeks after birth and decrease gradually until 3 months. After the critical period closed, monocular deprivation had little impact on ocular dominance column distribution. Wiesel and Hubel's (1963) research demonstrated the importance of critical period plasticity and suggested monocular deprivation had little impact on ocular dominance column distribution after critical period. Similar findings have been reported in the human visual cortex (Braddick & Atkinson 2011), where the visual cortex undergoes a similar reorganization when the visual experience is poor early in life due to ocular problems such as astigmatism, amblyopia, and congenital cataracts. For example, amblyopia is caused by abnormal visual input from one eye and can lead

to imbalance in the dominant eye and poor visual acuity (Hensch & Quinlan 2018). Amblyopia can be treated by covering the preferred eye with an eye patch and forcing the brain to use signals from the amblyopic eye (Webber & Wood 2005). Since the benefits of this treatment fade with age and are most effective in the early stages of life, it appears that the degree of plasticity peaks early in life and subsequently decreases (Fronius *et al.*, 2014).

However, in the recent decades, there factors have been identified as crucial for regulating developmental plasticity, namely, myelin maturation (McGee *et al.*, 2005), the formation of perineuronal nets from extracellular matrix maturation (Hock *et al.*, 1990; Pizzorusso *et al.*, 2002), and the development of intracortical inhibition (Hensch *et al.*, 1998; Huang *et al.*, 1999; Hensch, 2005). Notably, the last factor (intracortical inhibition) has been highlighted as a key element not only for the regulation of critical periods but also for the recovery of the plasticity in the adult visual system, suggesting that the visual system retains a considerable degree of plasticity even in adulthood (Castaldi *et al.*, 2020; Sagi, 2011; Spolidoro, 2009; Watanabe & Sasaki 2015).

Various mechanisms have been proposed to account for the ongoing plasticity of the adult visual system, with Hebbian and homeostatic plasticity being two of the most influential. Hebbian plasticity involves synaptic alterations triggered by the relationship between pre- and postsynaptic activity, with synaptic strength rising when the presynaptic cell fires just prior to the postsynaptic cell (Hebb *et al.*, 2004). For example, long-term depression (LTD) happens when the postsynaptic neuron fires before the presynaptic neuron, whereas long-term potentiation (LTP) happens when the presynaptic neuron fires first. In contrast, homeostatic plasticity helps the neuronal system return to baseline state after a disturbance by preventing hyperactivity or hypoactivity and regulating general neuronal functions (Turrigiano 1999; Turrigiano 2011; Turrigiano & Nelson, 2000). Studies have found that neuronal replay, a phenomenon where neuronal activity patterns from

experiences are re-expressed during rest or sleep, has been associated with Hebbian plasticity (O'Neill et al., 2010).

The first observation of neuronal replay comes from hippocampal place in rodents (Wilson & McNaughton, 1994), a stronger neural connection formed with neighbouring place cells that corresponds to the animal's next destination (Pfeiffer, 2020). These connections formed during navigation create positive feedback within the system and encourage spontaneous replay (Chenkov et al., 2017; Jackson et al., 2006), which strengthens these connections through repeated co-occurrence of neurons, thus reinforcing synaptic connections according to the Hebbian learning principles (Sadowski et al., 2016). Homeostatic plasticity refers to the global adjustment of synapses to maintain an overall balance of excitatory and inhibitory inputs for optimal neuronal performance, where potentiated synapses undergo downscaling and weakened synapses experience upscaling (Turrigiano, 1999, 2011). Despite their opposite direction, Hebbian and homeostatic plasticity act in concert maintain the equilibrium of neural network activity and promoting optimal functioning of the visual system (Fox & Stryker, 2017; Keck et al., 2017). For example, Hebbian and homeostatic plasticity work together in the consolidation process that occurs in the brain circuits involved in perceptual learning during wakefulness and sleep following training (Bang et al., 2018; Shibata et al., 2017). The consolidation of visual perceptual learning is closely linked to the balance between excitatory and inhibitory (E/I) neurochemical activity in early visual cortex (especially V1, V2 and V3). Specifically, Increased E/I ratios and reaction during weakness favours Hebbian plasticity, while enhanced spindle activity during Non-Rapid Eye Movement Sleep (NREM) is consistent with this mechanism as well (Bang et al., 2014; Tamaki & Sasaki, 2020; Tamaki et al., 2020). In contrast, decreased E/I ratios and increased theta activity during Rapid Eye Movement (REM) favours homeostatic plasticity. This implies that Hebbian plasticity predominates during waking and NREM, while homeostatic plasticity predominates during REM. Though the exact nature of these processes remains unknown the findings support the

involvement of both Hebbian and homeostatic plasticity in determining the plasticity of the visual system during learning and its subsequent stabilization.

Additionally, Hebbian and homeostatic plasticity work together on regulating visual deprivation during adulthood (Keck et al., 2017; Lunghi, Burr, & Morrone, 2011, 2013). Monocular visual deprivation takes the form of altering the input of one eye for a period of years (long-term deprivation) down to hours (short-term deprivation), resulting in shifting eye dominance towards deprived eye (Bang, Hamilton-Fletcher, & Chan, 2023; Lunghi, Burr, & Morrone, 2011, 2013; Wang, McGraw, & Ledgeway, 2021; Zhou, Clavagnier, & Hess, 2013). The change of eye dominance is driven by alternated brain activities in visual cortex, in which the C1 component of visual evoked potentials, alpha band peak, and the amplitude of V1 BOLD activity increase in the deprived eye but decrease in the non-deprived eye (Bang, Hamilton-Fletcher, & Chan, 2023; Binda et al., 2018; Lunghi et al., 2015a). Specifically, the effect of deprivation on BOLD responses in V1 is associated with eye dominance shifts, where V1 voxels that initially favoured the non-deprived eye shift towards the deprived eye. This supports the concept of homeostatic plasticity, where the brain enhances signals from deprived eyes to maintain network balance. An alternative interpretation is that increased signals from the deprived eye are due to a release from adaptation (inhibition) (Binda et al., 2018; Zhang et al., 2009). It remains unclear whether monocular deprivation effects are due to homeostatic plasticity or adaptation release, but both mechanisms appear to result in the same output, that is maintaining overall brain activity (Bang, Hamilton-Fletcher, & Chan, 2023; Binda et al., 2018).

### 1.6.1 Short-term plasticity

Short-term plasticity, as an important determinant of the information processing and response properties of neural circuits, refers to the dynamic changes in synaptic transmission including synaptic facilitation,

enhancement, enlargement and inhibition (Zucker, 1989). Research using ultra high field functional magnetic resonance imaging (fMRI) has found short-term plasticity effects in the adult's primary visual cortex (V1) compatible with changes in ocular dominance (Binda et al., 2018). The classic paradigm of monocular deprivation is a powerful method used to investigate short-term plasticity, in which one eye is patched for a few days during development weakens the cortical representation of the deprived eye, resulting in a stable shift of ocular dominance columns in V1 ((Hensch & Quinlan, 2018; Wiesel & Hubel, 1963, 1965). The initial demonstration of short-term plasticity on healthy adults was conducted by Lunghi, Burr, and Morrone (2011), who observed a paradoxical enhancement of the deprived eye signal after patching with a translucent occluder for 150 minutes. This post-patching effect has been observed across psychophysical (Lunghi et al., 2011, 2013; Zhou, Clavagnier, & Hess, 2013; Zhou, Reynaud, & Hess, 2014; Zhou et al., 2017), electrophysiological (Lunghi & Sale, 2015; Zhou et al., 2015), and brain imaging studies (Binda et al., 2018; Chadnova et al., 2017; Lunghi et al., 2015) in humans. During this period, the contrast gain of the deprived eye increases while that of the non-deprived eye decreases, suggesting a form of homeostatic plasticity in visual processing (Min, Baldwin, & Hess, 2019).

SED was subsequently measured after removing the patch with a binocular rivalry (BR) task by viewing a dichoptic display with horizontal grating patches presented to one eye and vertical grating patches to the other eye. Findings revealed that the previously patched eye dominated perception for up to 90 minutes (Figure 1.15). Bai et al. (2017) demonstrated that short-term monocular deprivation leads to distinct effects in binocular rivalry measured by presenting incompatible stimuli to each eye. As inputs from both eyes tend to compete rather than fuse, relative durations of monocular perception were used to estimate ocular dominance plasticity during binocular rivalry tasks. Wang, McGraw, and Ledgeway (2020, 2021) demonstrated that eliminating visual input to one eye with an opaque patch could effectively enhance the subsequent

relative dominance of the previously patched eye in a BR task. Notably, an opaque eye patch that eliminates all visual input can also shift subsequent binocular balance towards the patched eye (Chadnova et al., 2017b; Zhou et al., 2013), suggesting a possible role for retinal adaptation to light. However, Wang, McGraw, and Ledgeway (2021) compared three types of monocular treatments (an opaque, a diffusing lens, and an inverting prism) and found that all three manipulations altered dominance duration and predominance during the BR task in favour of the treated eye. Such similar effects help rule out possibility of retinal adaption. A binocular combination task involves presenting fusible stimuli to each eye, in which perception is based on the level of contribution of each eye to binocular vision. Changes in ocular dominance resulting from short-term patching are indexed using various combination tasks, such as phase combination, motion combination, and contrast combination (Zhou et al., 2013; Min, Balwin & Hess, 2019). Additionally, Kim, Kim, and Blake (2017) used eye patching and continuous flash suppression (CFS), two distinct deprivation regimes that lasted for 15 minutes each. While both methods increased the dominance of the deprived eye during the BR task, but CFS had a stronger effect. When a higher contrast pattern was utilized in the CFS regime, dominance effects were weaker and dissipated faster, indicating that complete suppression during CFS is a more efficient way to alternate ocular dominance.

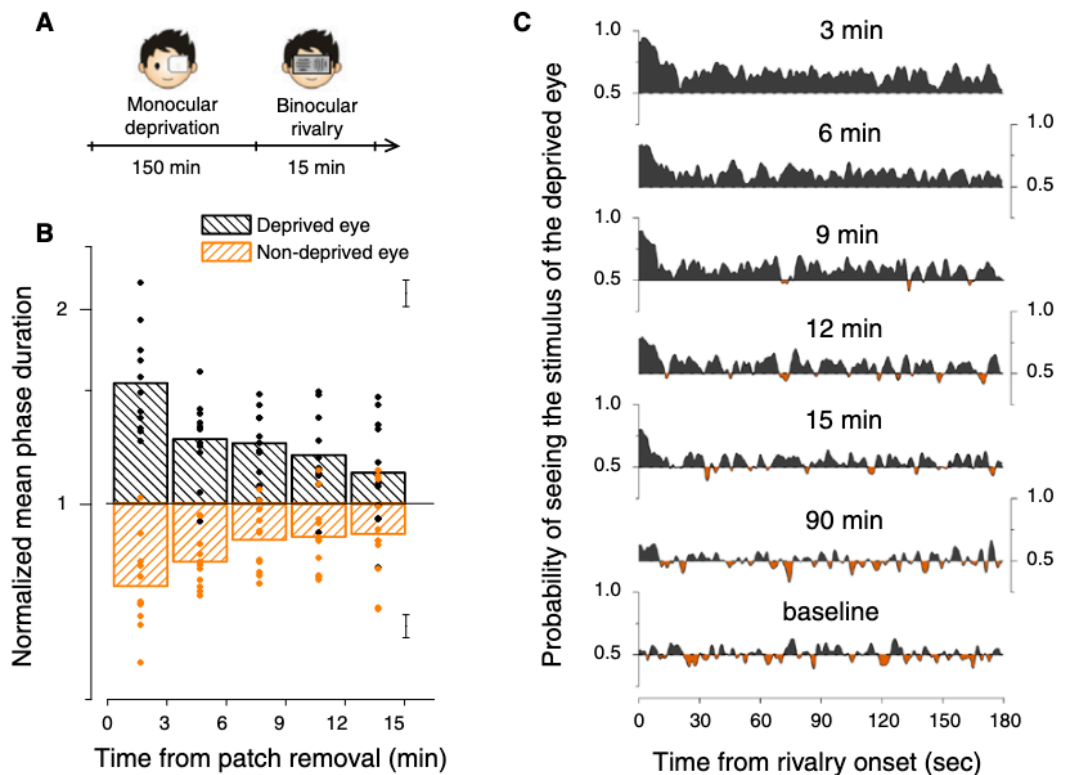


Figure 1.15: The effect of 90-minute monocular deprivation on mean phase durations. (a) Following 150 minutes of monocular patching, observers participated in five consecutive sessions of binocular rivalry, viewing Gabor patches oriented vertically for one eye and horizontally for the other. (b) The relative phase durations of the two stimuli, expressed as a fraction of each observer's mean baseline phase duration, were recorded over time after the patch removal. Data points represent individual measurements, and bars represent group averages with standard error of the mean (s.e.m.) indicated by the bar symbols on the right. (c) The average proportion of time observers reported seeing the stimulus presented to the deprived eye was calculated as a function of time from the start of each session and smoothed with a Gaussian window of one-second time constant. For at least six minutes post-deprivation, this probability remained above chance, indicating a consistent predominance of the stimulus seen by the deprived eye. Image from Lunghi et al. (2011).

## 1.6.2 Timescale

As one of the key parameters that make ocular dominance plasticity fundamentally different from conventional monocular deprivation, the deprivation duration is an important parameter of sensory eye dominance plasticity following short-term monocular deprivation (Iny et al., 2006; Pham et al., 2004; Prusky, Alam, & Douglas, 2006; Sato & Stryker, 2008; Tagawa, Kanold, Majdan, & Shatz, 2005). In a series of studies, Lunghi

et al. (2013) used a translucent lens patching 150 minutes, which deprived the eye of spatial information while maintaining average luminance at a comparable level to the other eye. This post patching effect lasts for 30 - 90 minutes and decayed over time. Lunghi et al. (2013) also observed that temporary dynamics of rivalry returned to pre-deprivation levels within 15 - 30 minutes after the end of the deprivation for luminance stimuli, whereas the effect of monocular deprivation could last up to 3 hours for chromatic stimuli. This finding suggests that the adult visual cortex maintains a high degree of plasticity even after the critical period, and adult visual cortex is more sensitive to colour pathway (parvo pathway) (see Figure 1.16). The relative dominance of the deprived eye changes depending on the deprivation durations, ranging from several minutes to hours. For example, the deprivation effect lasted only about 3 minutes after 30 minutes of patching (Lunghi et al., 2013) (Figure 1.17). It has been found that the enhancement of the patching effect by extending the deprivation period is modest when considering both the magnitude and the duration of the effect (Min et al., 2018). The transience of this effect implies a lack of structural changes by modulating the contrast gain mechanism to enhance the response to weak stimuli, which sharply contrasts with the long-term impacts of extensive monocular deprivation during the critical period of early life. Such impacts can be permanent or semi-permanent (Blakemore, Garey, & Vital-Durand, 1978; Dews and Wiesel, 1970; Olson and Freeman, 1980; Swindale, Vital-Durand, & Blakemore, 1981).



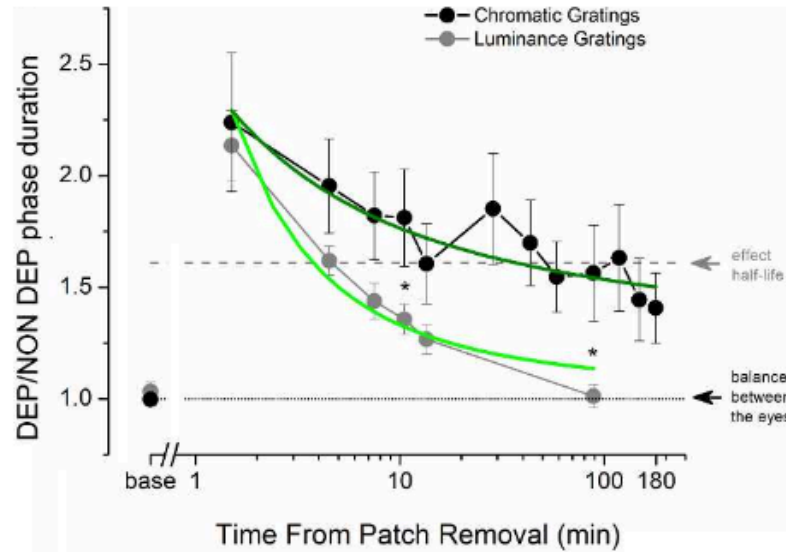


Figure 1.16: The timecourse of the patching effect of 150-minute monocular deprivation. The ratio of deprived to non-deprived eye phase duration as a function of the time since patch removal measured with chromatic or achromatic stimuli. Image from Lunghi et al. (2013).

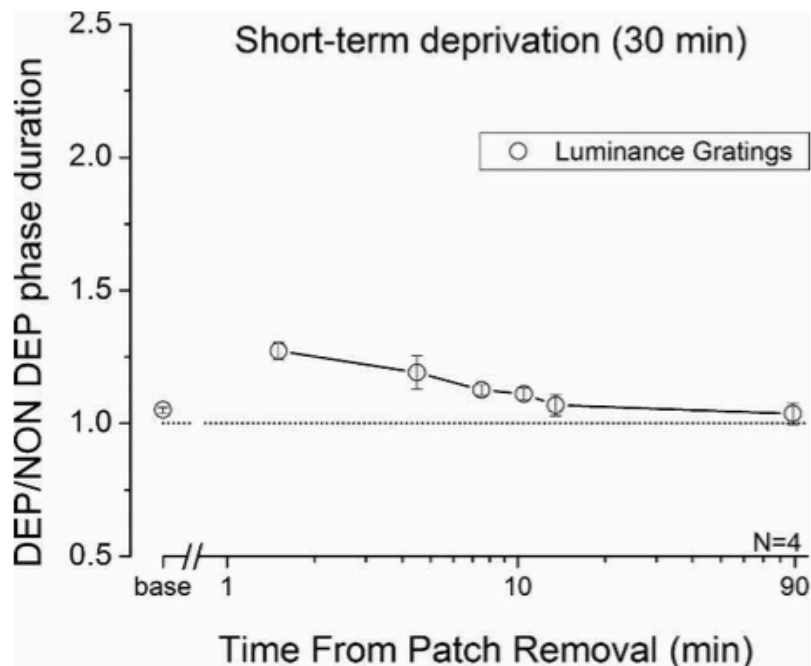


Figure 1.17: The timecourse of the patching effect of 30-minute monocular deprivation. It only included achromatic stimuli. Image adapted from Lunghi et al. (2013).

### 1.6.3 The mechanisms underpinning shifts in eye dominance

Following monocular patching, the relative perceptual contribution of each eye to binocular tasks will vary based on whether the previously deprived eye becomes more sensitive or the other eye becomes less sensitive. However, there is conflicting evidence to support this proposal. Lunghi et al.'s (2011) original study found no change in each eye's contrast distribution threshold following monocular deprivation. Baldwin and Hess (2018) conducted a dichoptic masking task to measure the effect of patching by evaluating contrast thresholds for detecting a stimulus presented to one eye while a mask was shown to the other. Two types of masks were compared: a parallel mask measured with the same spatial properties in both eyes, and a cross-oriented mask where the mask was orthogonal to the target. In addition to the direction observation indicating that monocular sensitivity remains unchanged following monocular deprivation. However, the indirect evidence can be inferred from Baldwin and Hess's results showing that the magnitude of the deprivation effect revealed by different binocular tasks was not correlated across subjects (see Figure 1.18). Therefore, a correlation would be expected if the changes in binocular balance are driven by a single effect, such as altered monocular sensitivity following monocular deprivation.

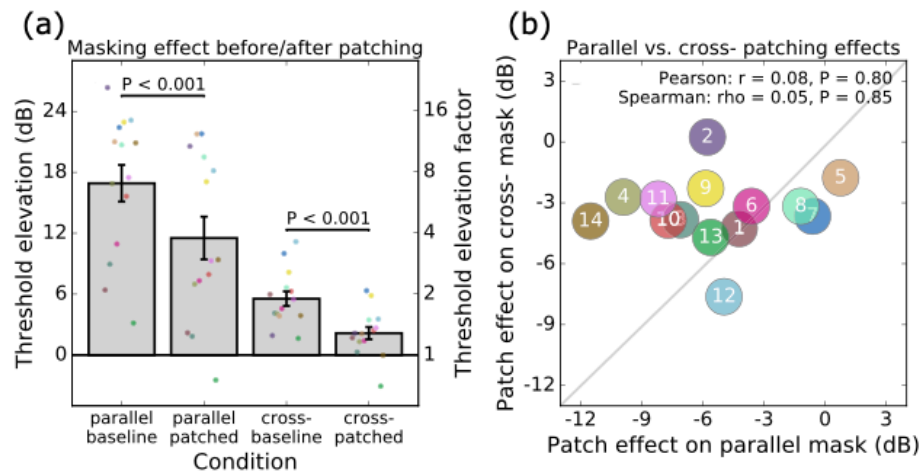


Figure 1.18: The effect of patching on dichoptic masking strength is depicted in two panels. (a) For both parallel and cross-oriented dichoptic masks, 150-minute-deprivation significantly reduced subsequent masking effect (as indicated by threshold elevation) of the previously deprived eye. (b) patching effect, indicating no significant correlation between the parallel and cross-oriented masking effects. Image adapted from Baldwin and Hess (2018).

The findings of Baldwin and Hess (2018) have demonstrated reduced monocular detection thresholds in the deprived eye and increased thresholds in the non-deprived eye. The reciprocal nature of these monocular contrast threshold effects suggests that the strengthening of the deprived eye and the weakening of the non-deprived eye result from a binocular-based interaction rather than a monocular effect of the deprived eye (Arditi, Anderson, & Movshon, 1981; Ding, Klein, & Levi, 2013; Legge, 1984a; Zhou et al., 2013; Zhou, et al., 2017). Binocular combination has been investigated through various tasks, including contrast detection (e.g., Anderson, & Movshon, 1989; Legge, 1984a), contrast discrimination (e.g., Baker, Meese, & Georgeson, 2007; Meese, Georgeson, & Baker, 2006), contrast matching (e.g., Baker, Meese, & Georgeson, 2007; Legge & Robin, 1981), visual direction (Mansfield & Legge, 1996) orientation discrimination (Bears & Freeman, 1994) and phase perception (e.g., Ding & Sperling, 2006, 2007; Huang *et al.*, 2009). For example, Legge (1984) proposed a quadratic summation model to explain how the visual system combines contrast information from both eyes.

$$C = \sqrt{C_L^2 + C_R^2} \quad (1.1)$$

However, Legge's (1994b) model was unable to explain changes in the shape of binocular contrast contours when additional factors like added noise or contrast adaption were introduced. Anderson and Movshon (1989) proposed a multiple-channel model, suggesting that the visual system processes different aspects of contrast information from each eye through separate processing channels. This model, contrasts with single-channel model that assume all visual information is processed through a single mechanism, allows the visual system to process complex visual information more flexible by dividing tasks into specialized pathways.

Cohn and Lasley (1976) proposed evidence that single channel model was insufficient to predict luminance detection when both eyes received different visual signals. They proposed a two-channel model to account for binocular combination when each eye perceives changes with the same or opposite interocular polarity. According to this two-channel model, one channel for combining two eyes' inputs and the other for calculating the difference between the inputs of two eyes. The following models for binocular combination collectively emphasizes the role of interocular inhibition and gain control in accounting for how the visual system integrates information from both eyes. For instance, Cogan (1987) incorporated interocular divisive inhibition into the summation channel of a two-channel model to detect changes in luminance.

Using fMRI evidence, Moradi and Heeger (2009) proposed an interocular contrast normalization model to emphasise the importance of inhibitory interactions between the eyes in shaping visual perception. To address the limitation in previous models included nonlinear operators that tends to distort phase information when applied to predict the perceived combined binocular visual phase. Ding and Sperling (2006) proposed the gain-control model involving two paths for each eye: single path using linear operations selectively for orientation and spatial frequency and

gain-control path measuring the total contrast energy across all orientations and spatial frequencies for each eye and exerts gain control on the other eye (see Figure 1.19). Models like the interocular contrast normalization (Moradi & Heeger, 2009) and contrast-gain model (Ding & Sperling, 2006) suggest that the brain's mechanism for summing and inhibiting each eye's input are adjusted to maintain optimal visual processing during deprivation, highlighting the role of interocular interactions and neural plasticity in maintaining effective visual perception.

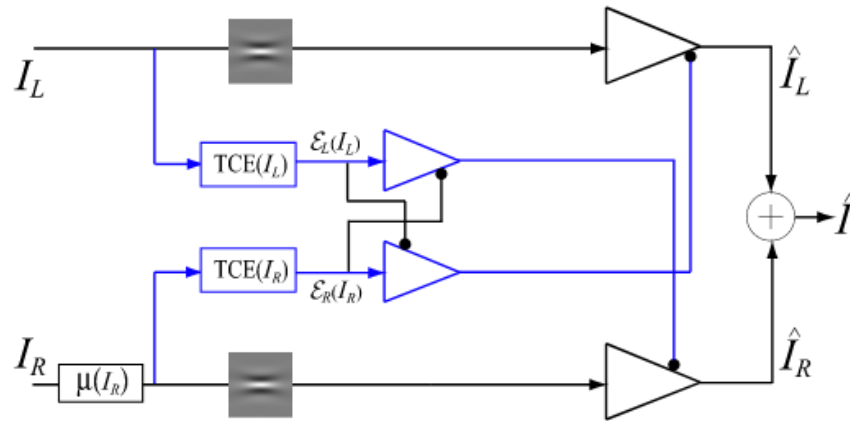


Figure 1.19: Ding-Sperling's (2006) gain control model. This model consists of left and right channel, each containing two mechanisms: single path and gain control path. The single path (black lines) is selective for orientation and spatial frequency, while the gain control path (blue lines) is based on total contrast energy (TCE) and nonselective for orientation and spatial frequency. These two TCE components are proportionally inhibited from each other in the gain control path with their respective TCE outputs, these outputs then exert gain control over the selective gain control of the other eye in single path.  $I_L$  and  $I_R$  represent the input of the left- and right-eye.  $\epsilon_L$  and  $\epsilon_R$  are the total weighted contrast energy to each eye across all orientations and spatial frequencies channels. The outputs  $\hat{I}_L$  and  $\hat{I}_R$  are linearly summed to determine the binocular signal. Image from Ding, Klein, & Levi (2013).

Wang, McGraw, and Ledgeway (2024) examined whether bottom-up (monocular deprivation) and top-down (selective attention) mechanisms of binocular visual plasticity can be independently combined. The results showed that changes induced by one (e.g. short-term monocular deprivation) can be completely counteracted by another (e.g. directing attention to the non-deprived eye). This highlights the independent roles

of sensory deprivation and attentional modulation and underscored the complexity of ocular dominance plasticity (Figure 1.20). On the other hand, other studies have found a reciprocal change in contrast thresholds, with the patched eye showing decreased thresholds and the unpatched eye showing increased thresholds after deprivation. These findings suggested that shifts in eye dominance result from changes in the monocular contrast gain of each eye (Zhou, Clavagnier, & Hess, 2013; Zhou et al., 2017; Zhou, Thompson, & Hess, 2013). Such inconsistency of results might be related to a smaller sample size (only 5 in Zhou, Clavagnier, & Hess's (2013) study), and the findings may not be generalizable to a larger population.

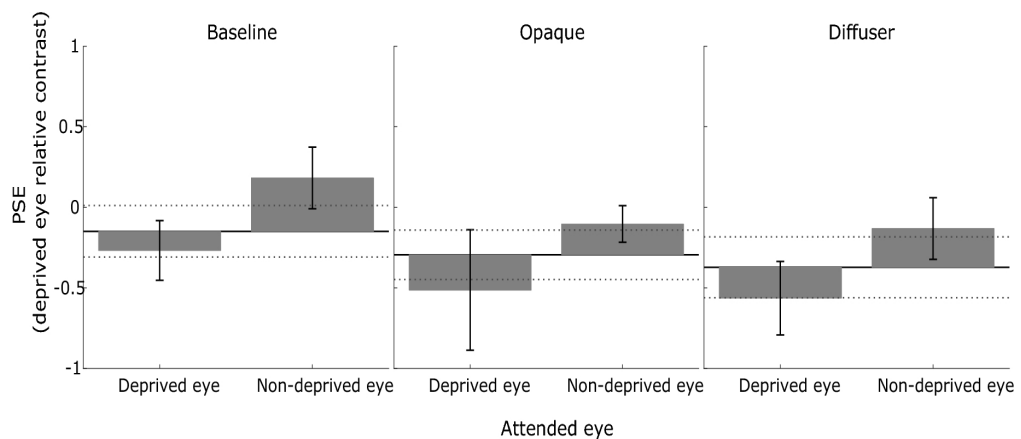


Figure 1.20: The mean point of subjective equality (PSE) regarding the relative contrast of the deprived eye's stimuli is presented for 7 observers under baseline, opaque patching, and diffuser conditions.

The horizontal solid line represents the PSE in neutral condition, while dotted lines indicate the  $\pm 1$  SEM across the group. The bars represent the PSE for attending to the deprived eye and non-deprived eye conditions, relative to the neural condition. Error bars represent  $\pm 1$  SEM across the group. It is evident that although deprivation shifts the dominance toward the deprived eye, this deprivation effect can be completely counteracted by selectively attending to the non-deprived eye's grating. Image from Wang, McGraw, & Ledgeway (2024).

#### 1.6.4 Plasticity in Ocular Dominance: Implications for Amblyopia

Ocular dominance plasticity influences the development and treatment of amblyopia, commonly known as "lazy eye," a developmental disorder characterized by impaired vision in one eye due to abnormal visual

experiences during early childhood (Barrett *et al.*, 2004; Crawford & Harwerth, 2004). Amblyopia is the leading cause of monocular vision loss in children and adults (Birch, 2013), with reduced visual acuity and contrast sensitivity in the amblyopic eye, along with disrupted cortical binocular connections leading to deficits in depth perception (Birch, 2013; Daw, 1998; Mitchell & MacKinnon, 2002; Simons, 2005). Monocular deprivation has been widely used to induce amblyopia in young animals, as this condition often results from disrupted interocular correlation (Harrad, Sengpiel, & Blakemore, 1996).

Hubel and Wiesel investigated the effects of monocular deprivation (Wiesel & Hubel, 1963; Hubel, Wiesel, & LeVay, 1977; LeVay, Wiesel, & Hubel, 1980) on the visual system's structure and function, establishing several key principles. First, they identified the primary visual cortex (striate cortex, V1, Brodmann's area 17) as the main site of abnormality caused by deprivation. Second, they highlighted the importance of the age at which deprivation occurred and its duration, introducing the concept of a critical period for visual development. Finally, they proposed a model explaining cortical changes due to abnormal early visual experiences, emphasizing a competitive interaction between the cortical inputs from both eyes. However, early studies were primarily conducted on animals, raising questions about the relevance of monocular deprivation-induced amblyopia to common human forms of the condition. Although monocular deprivation has often been used as a method to induce amblyopia in young animals (e.g., von Noorden, 1973; von Noorden *et al.*, 1970), a tailored experimental protocol is essential for developing more effective treatments for human amblyopia.

Short-term monocular deprivation, in the form of part-time occlusion of the unaffected eye, is a key treatment for childhood amblyopia (Campos, 1995; Webber, 2007; Webber & Wood, 2005). This approach is similar to the recovery of visual acuity loss seen with reversal deprivation (Blakemore, Garey, & Vital-Durand, 1978; Swindale, Vital-Durand, & Blakemore, 1981), although such plastic changes are effective only

before the closure of the critical period of visual development (Blakemore, Garey, & Vital-Durand, 1978; Blakemore & van Sluyters, 1974; Dews & Wiesel, 1970; Epelbaum et al., 1993). The degree of interocular inhibition in amblyopia patients is closely related to the severity of perceptual impairment and the differences in interocular vision (Holopigian *et al.*, 1988; Li *et al.*, 2011; Sireteanu & Fronius, 1981). This association highlights the complex interplay between neural and sensory mechanisms that contribute to amblyopia (Cakir et al., 2024; Li et al., 2011; Maehara et al., 2011; Meire & Giaschi, 2017).

Strong evidence suggests that brief monocular deprivation alters sensory eye dominance (SED), which may be key to understanding amblyopia patch therapy (Lunghi et al., 2016; Lunghi et al., 2019; Wang, McGraw & Ledgeway, 2021, 2024; Zhou, Thompson, & Hess, 2013). It is generally thought that the effects of short-term monocular deprivation are temporary, but they can reveal important aspects of visual plasticity. Therefore, there is a crucial need to quantify sensory eye dominance induced by short-term monocular deprivation to develop more targeted and effective amblyopia treatment plans that leverage the brain's plasticity.

### 1.6.5 Quantifying neural plastic changes on sensory eye dominance

To create a coherent cyclopean perception, observers rely more on one eye than the other, such eye dominance is crucial in a variety of clinical settings (Bossi, et al., 2018). Therefore, assessing eye dominance provides valuable insights for clinical applications: such as the treatment of amblyopia (e.g., Birch, 2013; Bossi et al., 2017; Kehrein, Kohnen, & Fronios, 2016), diagnosis of age-related macular degeneration (Wiecek et al., 2015), and monovision correction or presbyopia (Rodriguez-Lopez et al., 2023).



Sensory eye dominance (SED) refers to the relative contribution of each eye to the unified, cyclopean visual perception under conditions where different images are presented to each eye (Ooi & He, 2001). When both eyes contribute equally, observers experience an enhanced contrast sensitivity with both eyes (e.g., Baker et al., 2007; Baker, Meese, & Summers, 2007) and stereopsis (e.g., Cumming & DeAngelis, 2001; O'Connor et al., 2010). Though there is no standard clinically test for binocular summation, stereoacuity forms the basis of clinical binocular assessment where visual researchers use innovative psychophysical methods to measure SED (Li et al., 2010). Standard tests of eye dominance involve the hole-in-card test (Gould, 1910), the point-a finger test (Roth, Lora, & Heilman, 2002; Khan & Crawford, 2001), the near-point convergence test (Cheng et al., 2004; Seijas et al., 2007), the Worth's 4-dots test (Seijas et al., 2007), the distance fixation disparity test (Seijas et al., 2007), and the modified Baglioni striated lens test (Bruce, 2001). Standard tests of eye dominance offer a range of methods for assessing eye dominance, providing valuable insights for clinical applications.

SED measurements are categorized based on whether they create a coherent cyclopean perception or induce binocular rivalry. The first type involves presenting observers two dichoptic sine-wave gratings that differ in phase and contrast. Observers are instructed to identify the position of the middle dark stripe in a phase-shifted grating that results from binocular summation (Ding & Sperling, 2006; Huang et al., 2009; Huang et al., 2010; Kwon et al., 2014; Zhou, Huang, & Hess, 2013), which allows for quantifying "balance point" based on the interocular contrast difference that produces equal contributions from each eye (see Figure 1.21 (a)). Another measurement incorporates contrast manipulation into a global task, like motion coherence paradigms (e.g., Black et al., 2011; Hamm et al., 2017; Li et al., 2010), where observers discriminate the direction of the moving dots involving both signal dots and noise dots (see Figure 1.21 (b)). This measurement requires determining the contrast of the signal dots in dichoptic settings and the percentage of

moving dots required for reliable direction discrimination. Observers perceive a coherent cyclopean percept in both measurements, and the relative contrast of the optimal performance is termed as “balance point”, which quantifies SED.

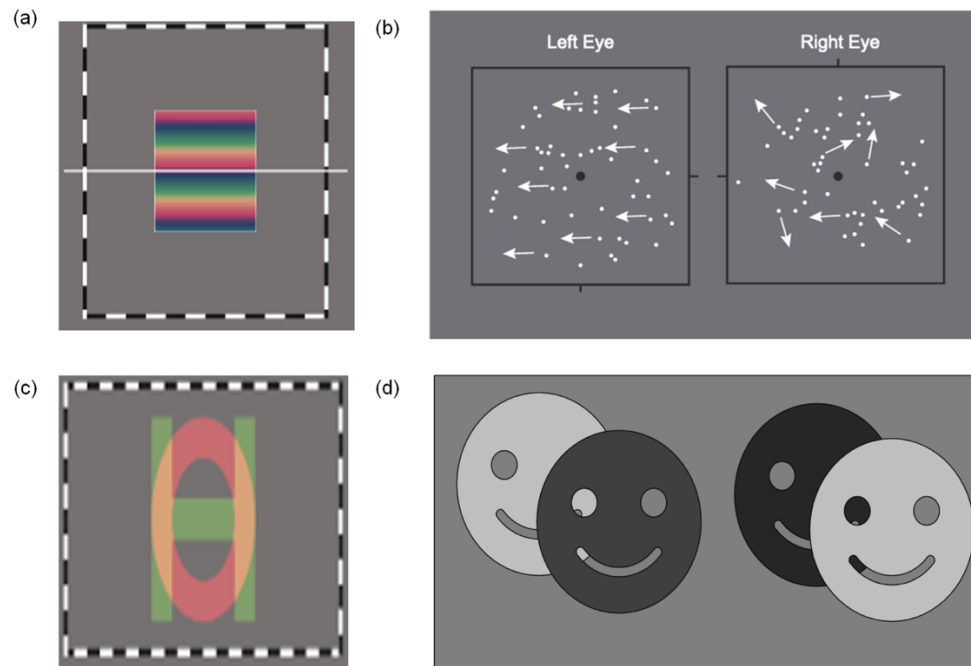


Figure 1.21: Schematic representation in the contrast-balance-point tasks for demonstration. (a). Phase combination test ( $90^\circ$ ), observers aim to demonstrate the position of the middle dark stripe of the grating resulting from binocular summation; (b). Dichoptic motion coherence threshold measurement, the dots presented to the left eye move to the left direction and form the signal dot population, while dots viewed by the right eye move in random directions and represent the noise population; (c). Letter-strength (overlapping) measurement: the rivalrous letters of differing contrast presented to each eye to determine the interocular balance point; (d). Dichoptic opposite contrast-polarity of the same symbol: each symbol consists of one dark and one light component, observers quantified SED by determining the lightest one. Image adapted from Bossi et al. (2018).

The second category involves rivalrous stimuli, where different images fall on corresponding retinal location of both eyes may lead to either binocular rivalry or diplopia. The extend of conflict between the two eyes' images indicates the degree of SED. Kwon et al. (2015) quantified this by using spatially overlapping rivalrous letter pairs of differing contrast (See Figure 1.21(c)), whereas Bossi et al. (2017) used dichoptic stimuli with opposite contrast polarity versions of the same symbols (See Figure

1.21(d)). The objective of both cases is to measure the “contrast balance point”, which indicates the contrast mixture required for equal perceptual influence from each eye, which quantifies SED.

Together, these methods provide a comprehensive way to evaluate both the integration and conflict of visual information from both eyes and enhance our understanding of binocular vision and its anomalies. Based on the research presented here, it seems crucial to account for the magnitude of the neural plastic changes in SED due to different viewing conditions when assessing the effects of ocular dominance. Though various paradigms have been developed aimed at promoting ocular rebalancing, there has been a notable lack of investigation into the neural mechanisms underlying SED and its plasticity. Research on how to quantify the plasticity in eye dominance measured with alignment tasks has been even more limited in recent years. Purver and White (1994) investigated how individuals coped with monocular preference in a binocular alignment task through a partially occluded fenestrated screen positioned 2 meters from the eyes of the viewer. Among the 97 subjects, most alternated between the eyes to varying extents, with only four subjects exclusively using one eye. About half of the subjects were categorized as moderately dominant, depending on the frequency with which they used either eye for fixation. These findings suggest a discrepancy in behaviour compared to the hole-in-the-card test (e.g., Ehrenstein, Arnold-Schulz-Gahmen, & Jaschinski, 2005; Zeri et al., 2011), where subjects often show consistent preference for one eye. Quantifying eye dominance through psychophysical and neurophysiological methods provides valuable insights into the mechanisms underlying visual processing and plasticity. From a clinical perspective, measures that provide a quantitative assessment of SED strength have potential applications in various contexts, including the selection of appropriate low vision aids and the treatment of amblyopia. In these cases, it is crucial to determine not only which eye is dominant but also the strength of this dominance. The technique described herein provides valuable information about the magnitudes of plastic changes,

making it particularly useful for clinical applications and optimizing therapeutic strategies.

## 1.7 Overview

The visual brain is responsible for determining the visual direction of objects in space relative to the viewer. It has been suggested that directional judgments are made relative to a single point, termed the visual egocentre, typically assumed to lie midway between the two eyes (e.g., Herings, 1868/1977; Howard, 1982; Julesz, 1971). Competing theories have proposed that either the egocentre location shifts towards the eye receiving the more visible image (Mansfield & Legge, 1996) or the binocular visual direction is determined from a weighted average of the oculocentric directions (Banks et al., 1997). This thesis aims to focus on the precise computational principles governing the egocentre position and the plasticity of cyclopean perception in ten psychophysical experiments.

The starting point of the thesis in Chapter 3 attempts to discriminate between competing models of perceived visual direction using new stimuli (1 dimensional noise patterns) and additional control experiments. In Chapter 4, the visual egocentre location is measured physically by using a monocular and binocular sighting task. Chapter 5 examines whether short-term monocular deprivation also has consequences on judging the visual direction of objects in space, relative to the viewer (the visual egocentre), and compares the effect of patching dominant eye and non-dominant eye on the visual egocentric localization. Chapter 6 investigates on quantifying the magnitude of neural plastic changes in SED induced by short-term monocular deprivation.

## Chapter 2. General methods

Fechner (1860) introduced a method known as psychophysics, which examines the relationship between psychological sensations and the physical stimuli that give rise to them. The experiments presented in this thesis employed psychophysical techniques to investigate perceived visual direction and sensory eye dominance. In the computer-based experiments (Experiments 1-4), a binocular alignment task was used to compare two existing competing models regarding binocular visual direction. A custom-built sighting apparatus was used for the rest of experiments (Experiments 5-10) to measure the visual egocentre location of each participant using a binocular sighting task. This method has the advantage of providing a physical estimate of visual egocentre position based on subjective responses, albeit with some individual differences. This chapter describes methodological approaches used in the present work. For more specific details in each experiment, please refer to methods section in the relevant experimental chapters.

### 2.1 Observers

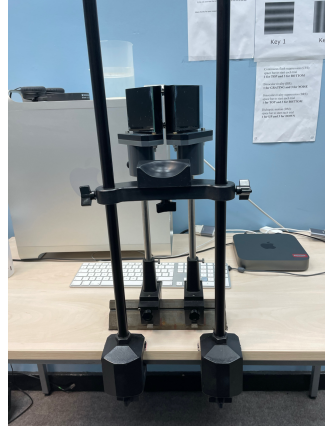
This work investigated human binocular vision in the general population (including the author S1), who had normal or corrected-to-normal vision and no history of ocular disease. All the experiments reported were conducted with the approval of University of Nottingham, School of Psychology Ethics Committee and all participants gave informed consent. All experiments adhered to the general principles of the Declaration of Helsinki.

All participants had their stereovision assessed using the TNO test (Lam´eris Ootech, Nieuwegein, The Netherlands). The participant utilized red-green anaglyph spectacles to discern the orientation of a cyclopean object depicted within random-dot stereograms. The smallest disparity at which accurate identification could be reliably achieved was recorded as

a measure of stereoacuity. The results demonstrated that stereoacuity was within the normal range for all individuals assessed (Baskaran et al., 2023). In line with typical psychophysical research, each study involved a small participant group but with many repeated trials, with the exception that a relatively larger sample size was employed in Experiments 6 (Chapter 4). The primary aim of this experiment was to evaluate the magnitude of individual variations in the egocentre location.

## 2.2 Apparatus & stimuli

Stereoscopic stimuli were grey-scale images generated using an Apple Macintosh computer running custom software written in PsychoPy and presented on two identical LCD monitors (22-inch Samsung Sync-Master 2233RZ; 1024 × 768pixel resolution; 60 Hz refresh rate; 318cd/m<sup>2</sup> maximum luminance). The effectiveness of employing these displays in vision experiments, considering their spatial, timing, and luminance attributes, has been previously confirmed (Wang & Nikolic, 2011). The two monitors were temporally synchronised by driving with the dual outputs from the same video card. They were carefully calibrated using a Minolta Luminance Meter LS-110, such that their luminance output was a linear function of the digital representation of the image. The noisy-bit method was applied to each colour channel separately and was used to increase the number of effective intensity levels available on each display (Allard & Faubert, 2008). Our setup measured disparities down to 2.8arcmin, with effective bit-depth sufficient for luminance but ultimately constrained by pixel granularity.



(a)



(b)

Figure 2.1: Wheatstone mirror stereoscope.

(a) The Wheatstone stereoscope used in this experiment to achieve dichoptic presentation of two images.

(b) An observer can see the left display through the left mirror and the right display through right mirror independently.

A Wheatstone mirror stereoscope (Figure 2.1) was employed to enable the dichoptic presentation of the stimuli, which produced an optical viewing distance of 231.5cm. The pair of full-silvered mirrors in the stereoscope were set at an angle of approximately  $\pm 45^\circ$  with respect to the median plane of the head, but participants could adjust the angle manually (if necessary) using a sprung screw, to align the monocular images and ensure stable fusion of the two images. We checked that only one image could be seen by a single eye once the stereoscope was aligned. The stimuli were presented on a uniform grey background ( $159 \text{ cd/m}^2$ ), which was surrounded by a high contrast black and white peripheral fusion frame, along with a pair of vertically and horizontally oriented nonius lines, to facilitate stable binocular fusion and provide an alignment check during runs. A chin rest was employed to stabilise participant's head and minimise movement during the experiment. The stimuli used in Experiment 1 (see section 3.2.1) were two vertically-separated Gabor patches with a luminance profile of the general form:

$$L(x, y) = \exp\left[-\frac{x^2 + y^2}{2s^2}\right] \cos(2\pi f x) \quad (2.1)$$

Where  $x$  and  $y$  represent the horizontal and vertical dimensions of the screen,  $s$  is the Gaussian envelope space constant, and  $f$  is the carrier spatial frequency. The sinusoidal waveform was always presented in cosine phase, with respect to the centre of the Gaussian envelope. The lower Gabor patch consisted of equal contrast stimuli in each eye, while the upper Gabor contained a contrast difference between the eyes that could be manipulated (see Figure 2.2). One eye's stimulus was presented at a fixed Michelson contrast of 25%, while the other eye's image was set to a lower contrast to achieve the required interocular contrast ratios (including 1:1, 1:4 and 4:1 between two stimuli). In the second condition, a Michelson contrast of 50% was assigned to one image, while the same contrast ratios were tested.

We measured the horizontal location at which the target with equal contrast in each eye appeared vertically aligned with the other target, which was presented at different relative visual depths (and had different contrasts in each eye). The vertical centre-to-centre distance between the upper and lower Gabor patches was 126arcmin. There was a small black fixation square (3.41 x 3.41 arcmin) presented in the centre of each display between the upper and lower Gabor stimuli.

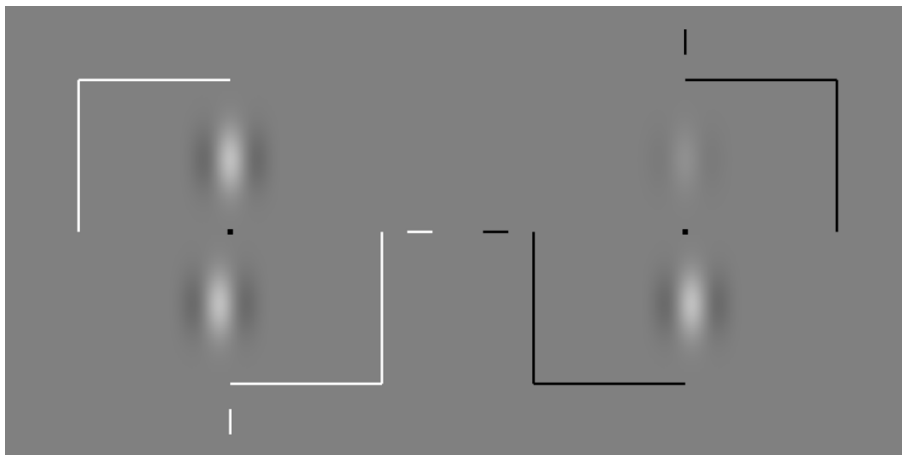


Figure 2.2: A pair of vertically-separated Gabor patches used in Experiment 1. The stereo percept in crossed fusion is two Gabor targets vertically above each other. The upper targets have different contrast between the left and right eyes, while the lower ones have equal contrast in the two eyes.



In Experiments 2-4, the stimuli were changed to Gaussian-windowed, one-dimensional noise patches (Gaussian SD  $0.35^\circ$ ; bar width  $0.06^\circ$ ) generated using custom software written in the C++ programming language. The difference between Experiment 2 and 3 was whether the stimuli were correlated or uncorrelated noise patterns for the upper and lower targets (Figure 2.3). The size of fixation marker was changed to a larger square ( $7.80 \times 7.80$  arcmin) to make it more prominent, which helped participants maintain fixation and reduced unwanted eye movements. The horizontal location of the lower patch was adjusted until it appeared align with the upper patch.

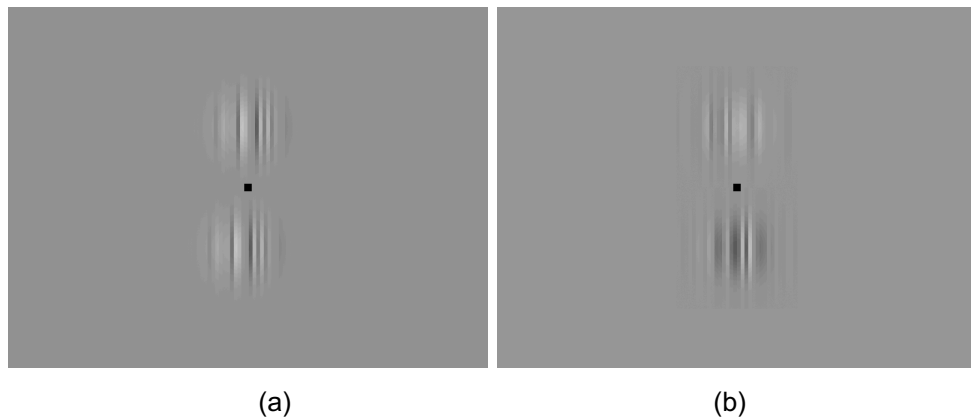


Figure 2.3: An example of noise patterns.

- (a) Two vertically-separated, Gaussian-windowed, 1-dimensional correlated noise patches used in Experiment 2;
- (b) Uncorrelated noise patches used in Experiment 3 and 4.

In experiments 5-8, a custom-built sighting apparatus was used that consisted of a stainless-steel rod (19cm length, 0.25cm diameter located approximately 34cm from bridge of nose) mounted on a Thorlabs' PR01/M Metric Precision Rotation platform. The rod could be smoothly and continuously rotated by hand through a full  $360^\circ$ , measured by the  $1^\circ$  graduation marks on the side of the stage when the steel locking thumbscrew was unlocked (Figure 2.4). The micrometre could provide  $\pm 5^\circ$  of fine adjustment measured with 5 arcmin resolution by the vernier scale when locked the thumbscrew. As shown in Figure 2.4 (b), the PR01A/M Adapter Plate was attached to the top of the PR01/M Rotation Stage, in which a PM5(/M) stainless steel clamping arm was mounted in the centre

of the adapter plate and the distance from the adapter plate centre to the contact point that holds the rod is 2.286cm.

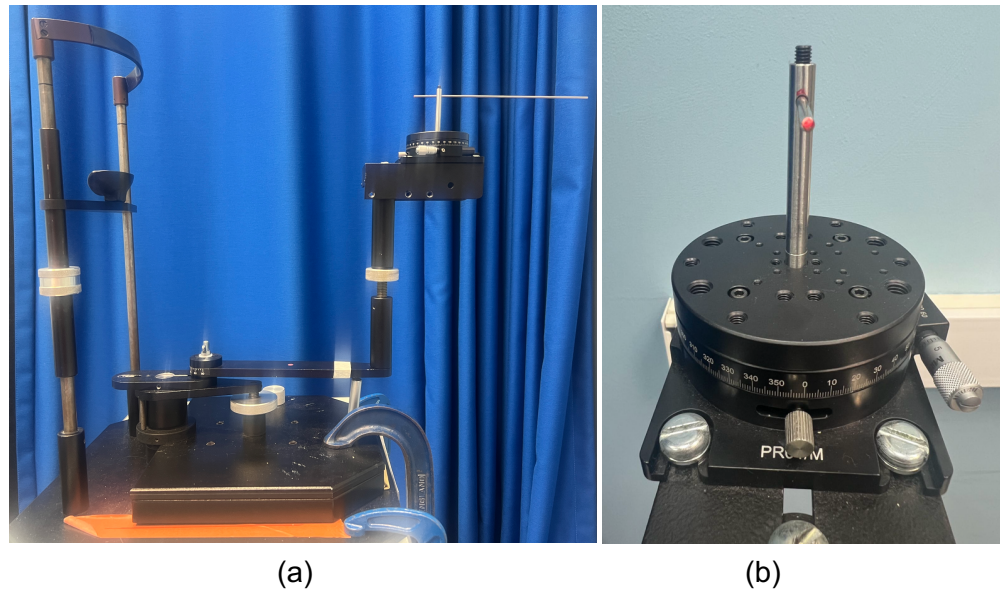


Figure 2.4: The custom-built apparatus used in the experiment. (a) The custom-built apparatus used in the experiment placed on the specially constructed table; (b) The participant was instructed to rotate the high-precision stage to make the rod move in the horizontal plane during the monocular and binocular sighting task.

In Experiments 9 and 10, the apparatus was modified by replacing the horizontal rod with a vertically oriented wooden toothpick (5cm height) - mounted on the steel clamping arm (Figure 2.5(b)). A 360-degree scale was added under the arm of the apparatus so that the rotation angle of the arm could be read precisely. The stimuli consisted of a fixed set of 19 vertical lines, each 5cm in height, arranged in a horizontal row on a white wall with corresponding numbers displayed below them. These lines were spaced 10cm apart, positioned 119cm above the floor, and located 100cm from the pointer of the apparatus (see Figure 2.5 (a)). These stimuli were designed for observers with an inter-pupil distance (IPD) of approximately 6 cm, with one of them being in front of the bridge of the nose (number 0), nine of them being to the left of the bridge of the nose (numbers -1 to -9), and nine were to the right of the bridge of the nose (numbers 1 to 9).

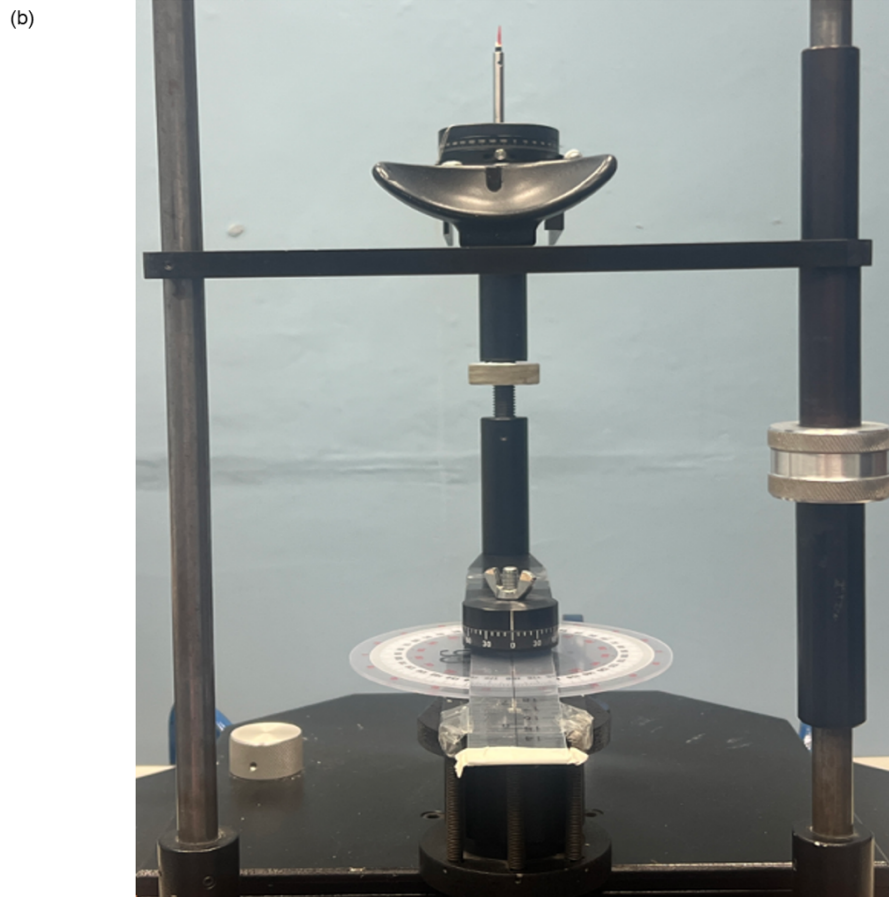
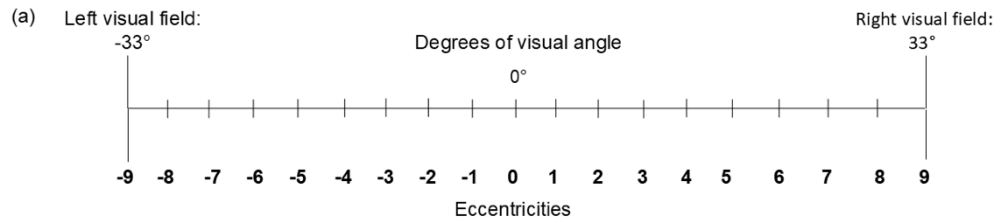


Figure 2.5: Apparatus used in Experiment 9-10.(a) Pre-set 19 horizontal scale markers used to establish the alignment task in different eccentricities; (b) The apparatus used in Exp. 9-10, it was changed on the basis of that used in Exp.5-8.

A pair of two 35mm diameter unmounted linear glass polarizing filters were inserted into one side of an optical trial lens frame. Polarizers can be utilized in pairs to control light attenuation. When the transmission axes of the polarizers are parallel maximum light transmission occurs. Conversely, if they are placed perpendicular, known as "crossed," transmission is minimized as all possible polarization states are effectively filtered out. As shown in Figure 2.6 (a), filter A will polarize the light in a certain transmission axis, all the polarized light passes through

the filter B (in the same direction with filter A) will not be affected. In this manner. The maximum intensity of light is transmitted. Adjusting the angle between the transmission axes allows for varying levels of attenuation. The angular difference between the polarization axes of the filters directly affects the extent of light attenuation. As shown in Figure 2.6 (b), when filter A and B have the transmission axes perpendicular to each other, the intensity of the transmitted light drops to zero.

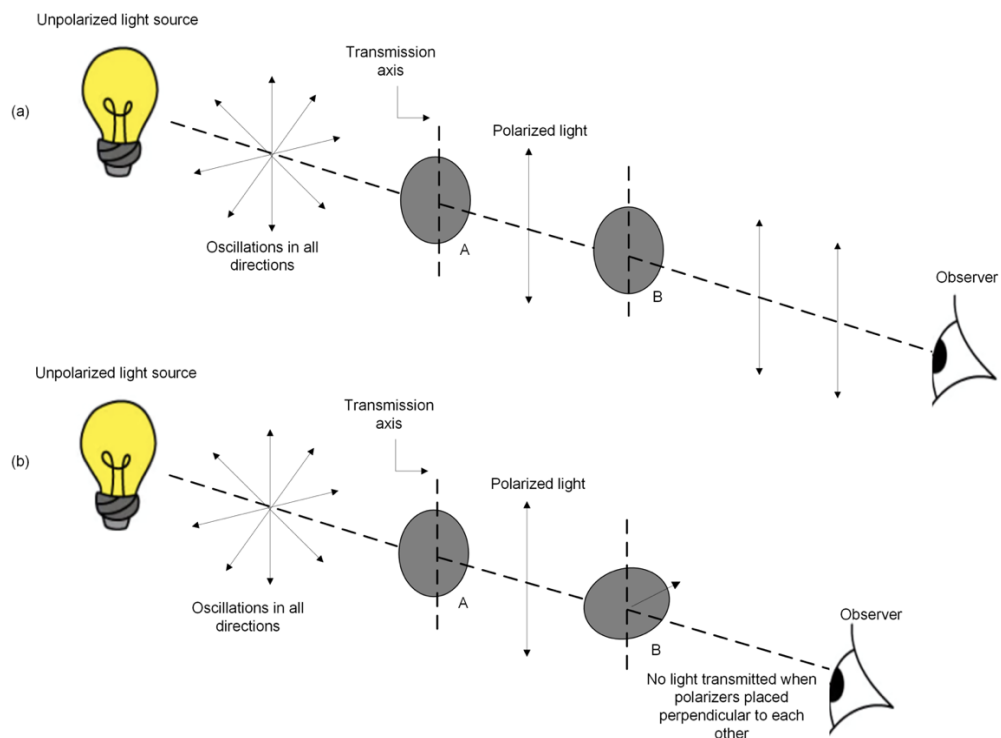


Figure 2.6: How two polarizer filters work together to attenuate the light intensity.

(a) When two polarizers were placed in the same direction, in which the maximum intensity of the light is transmitted; (b) When the second filter was rotated through  $90^\circ$ , the intensity of transmitted light is zero.

## 2.3 Luminance calibration

The single-lens-reflex (SLR) luminance meter LS-110 enables precise aiming and ensures the viewfinder shows the exact area to be measured. This optical system is also flareless, which eliminates the effects of light from the outside of the measurement area. In order to conduct

Experiments 9–10, an SLR luminance meter was set up on a tripod 60cm from the table. The distance between the luminance meters and the linear polarizers was 100cm, and the light source was positioned 20cm behind linear polarizers. The vertical height of the light source, linear polarizers, and SLR luminance meters from the table was the same. (see Figure 2.7 (a)). A square of black card, with a central, circular aperture (1cm diameter) was positioned such that light passed through the centre of each filter (see figure 2.7 (b)).

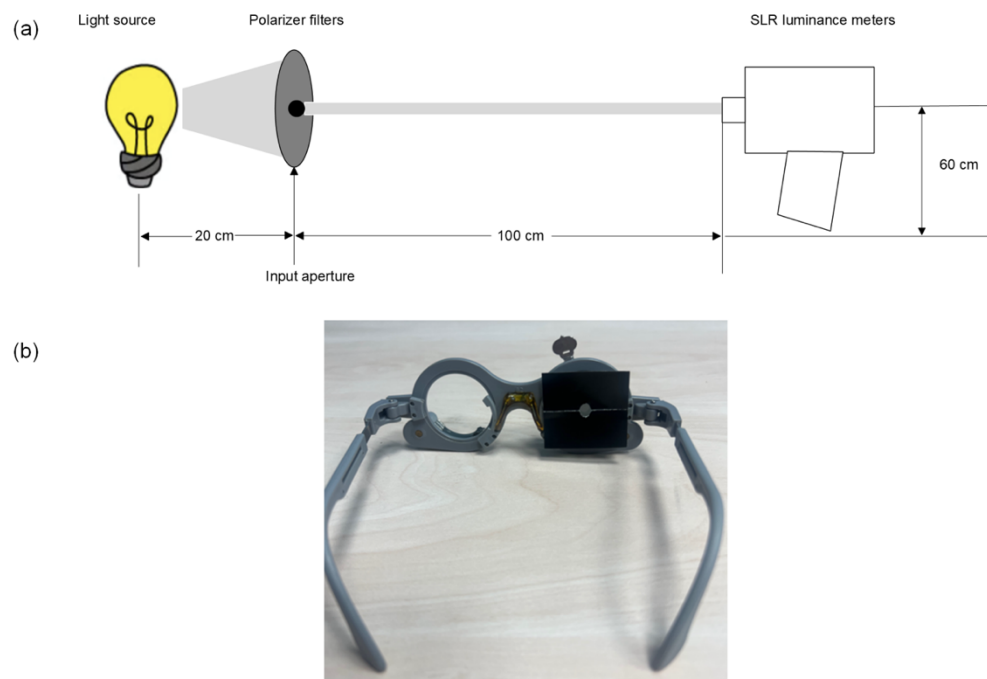


Figure 2.7: Luminance calibration in Experiment 9-10.

(a) The apparatus setting for luminance calibration, the distance between the luminance metre to polarizers, as well as the polarizers to the light source are marked in the figure; (b) Two polarizers are inserted on the lens frame, there is a black card with an aperture in the centre to make sure the light goes through the centre of each polarizer.

A Minolta luminance meter (LS-110) was used to measure the luminance at the surface of the polarising filters. First, luminance readings were taken without any filters to establish the baseline luminance level. Then one polarizer was added to the frame and another series of readings of luminance were made under the same lighting conditions. Finally, a second polarizer was placed in front of the first polarizer. Thereafter, a series of readings were taken as the orientation of the second polarizer

was systematically incremented from parallel ( $0^\circ$ ) until it was perpendicular ( $90^\circ$ ) relative to the first polarizer. We then continued to rotate the second polarizer until it reached  $180^\circ$ , bringing it back to a parallel orientation with the first polarizer. The intensity of plane-polarized light changes as a function of the angle between two linear polarizers. According to Malus's Law (Morus, 2005), the intensity of transmitted light  $I(\theta)$  through two linear polarizers is proportional to the square of the cosine of the angle  $\theta$  between light's initial polarization direction and the axis of the second polarizer. This relationship can be expressed mathematically as:

$$I(\theta) = I_0 \cos^2(\theta) \quad (2.2)$$

where  $I_0$  represents the initial intensity of the light after passing through the first polarizer. The transmitted intensity gradually decreases as the angle  $\theta$  increases from  $0^\circ$  to  $90^\circ$ , it reaches zero when the polarizers are perpendicular (i.e., at  $\theta=90^\circ$ ). This explains how the relative orientation of the polarizing filters modulates the intensity of the plane-polarized light. The luminance of each measurement is plotted in Figure 2.8.

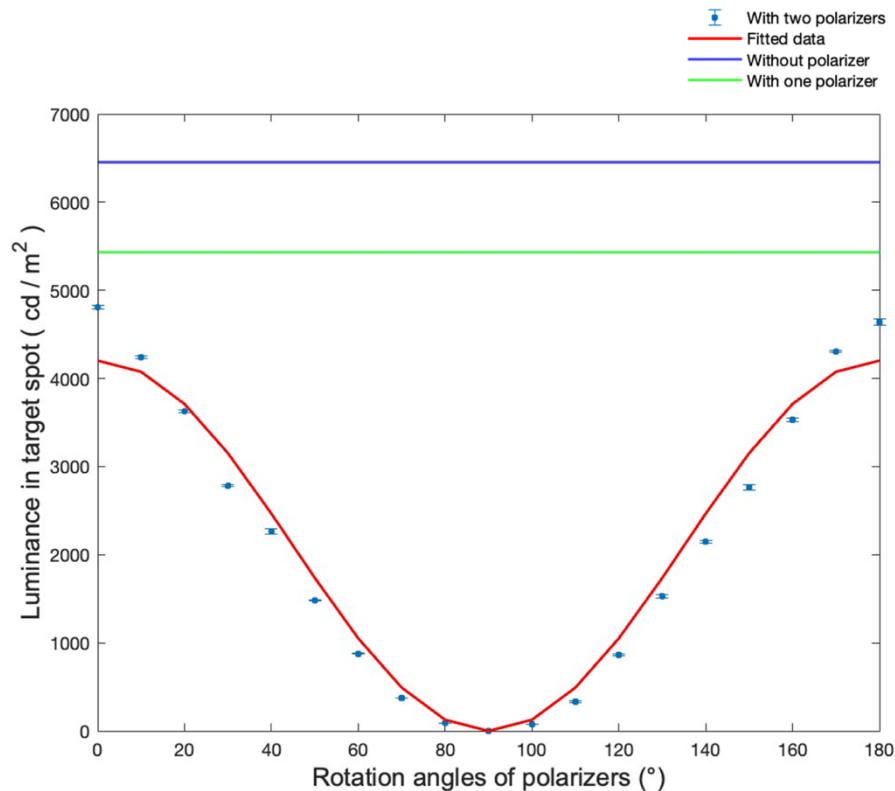


Figure 2.8: The luminance measured without polarizer (blue line), only one polarizer (green line) and two polarizers (light blue dots) rotated from parallel to perpendicular direction and then parallel again. Red curve line indicates how well Malus's Law fits the data with polarizers. The data points are shown with error bars indicate standard deviation.

## 2.4 Procedure

The psychophysical tasks used are explained in detail below. Participants were provided with short periods of practice before any formal data collection began.

### 2.4.1 Measuring binocular visual direction (Experiments 1-4)

A binocular horizontal alignment task was conducted to investigate which visual features were used to make a directional judgment. These experiments used the method of adjustment and completed in a dimly lit room. The method of adjustment is a psychophysical technique where

participants directly manipulate the stimuli until it perceptually matches a reference (Fechner, 1860/1966). This method is a simpler and quicker tool compared with other methods, and participants have an active role to adjust the stimuli. However, it depends more on participants' subjective judgments, which may lead to bias and individual variations. A typical trial sequence is illustrated in Figure 2.9. At the beginning of each trial the participant was required to view the binocular fixation marker and maintain stable binocular fusion. The presentation of stimuli was initiated by a key press. In the experiment, the upper target with different interocular contrast ratios between two eyes' stimuli was located on the vertical midline at the same plane with the fixation marker, while the lower target with equal contrast presented at different relative depths with the upper targets. The stereo targets were displayed for 1 second, following which the observer was required to adjust the location of lower target until the upper and lower stimuli were perceived to be vertically aligned. Then the current location of lower Gabor was recorded as the point of perceived alignment (PPA). The adjustment approach is a potent tool in this experiment that enables accurate and personalized identification of the perceived alignment point at which participants can adjust the alignment to meet their subjective perception properly.



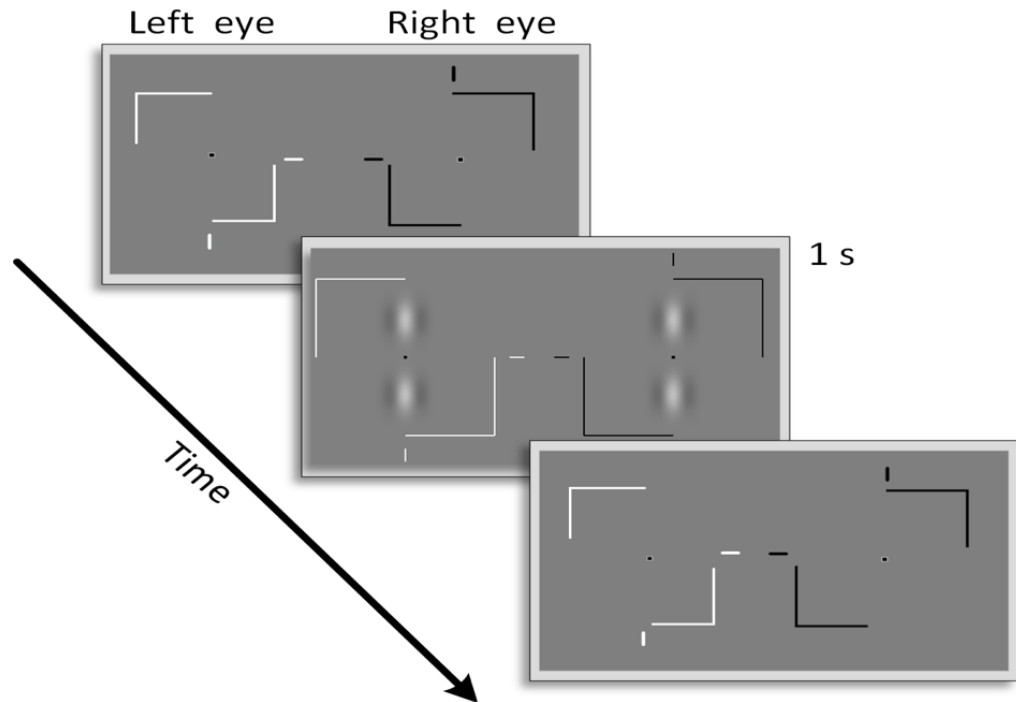


Figure 2.9: Schematic representation of one trial. After fixation point, stereo Gabor patches were separately presented to two eyes for 1 sec (mixed-contrast target was presented at the top half of the screen, while the equal-contrast target was presented at the bottom half of the screen). Then a blank field with fixation point would replace the stimuli, where participant had to press one of four keys (coarse or fine adjustment) to reduce the misalignment of the stereo Gabor patches. When the mixed-contrast target and the equal-contrast target appeared to be vertically aligned, pressed 'space' key. 10 alignments estimates were collected for each combination of contrast ratio and equal contrast Gabor disparity.

## 2.4.2 Measuring the visual egocentre location (Experiments 5-8)

As the results would be compared with physical interpupillary distance and locate the exact position of the visual egocentre relative to the head, head circumference and interpupillary distance were measured before starting the visual direction task. In experiment 5-6, both monocular and binocular sighting tasks were measured to demonstrate the visual egocentre location. Participants were instructed to rotate the orientation of a rod in the horizontal plane until it pointed directly to the right eye, left eye or directly towards himself/herself during binocular viewing. Measurements were made along the horizontal azimuth for each of a

range of eccentricities spanning  $\pm 52.5^\circ$ . relative to the centre of the head. The mean point of intersection of the extensions of the rod's axis at each eccentricity, were used to derive estimates of the monocular visual directions and location of the binocular egocentre. Monocular measures give an estimate of the locations of the two eyes in the head which can be compared to the physical inter-pupil distance (IPD). In experiments 7-8, a binocular sighting task measured along the horizontal azimuth for each of a range of eccentricities spanning  $\pm 30^\circ$ . relative to the centre of the head, referred as the baseline visual egocentre location.

### 2.4.3 Quantifying sensory eye dominance (Experiments 9-10)

The stimuli consisted of 19 vertical lines, each 5cm in height, arranged in a horizontal row on a white wall, with numbers displayed below each line. These lines were spaced 10cm apart, positioned 119cm above the floor, and located 100cm from the pointer of the apparatus. The visual field extends to  $35.64^\circ$  in both the left and right visual fields relative to the fixation point at  $0^\circ$ , as shown in Figure 2.5. Participants were asked to rotate the orientation of the arm and align the pointer to the predetermined markers both monocularly and binocularly: the rotation angle of the protractor scale was used to determine the egocentric angle. Following alignment between the pointer and the scale marker under binocular viewing, we then reduced the luminance to the dominant eye until perception switched to the fellow eye by rotating the angle of external polarizer from  $0^\circ$  to  $90^\circ$ . The angle of the polarizer at this transition was taken to indicate a balance point for a shift in eye dominance. The switch to a monocular image result from the suppression of the reduced-luminance image in the dominant eye. In fact, the procedure we use here is similar to that used to test the depth of suppression in individuals with amblyopia - where a S-bias is used to reduce the luminance of a target presented to the dominant eye until perception switches to the amblyopic eye (Crawford & Griffiths, 2015). In

the following process, the external polarizer was rotated from 90° to 180°, progressively increasing contrast to the dominant eye until physiological diplopia reappeared, and this rotation angle was recorded as well. The same procedure was repeated for the other two eccentricities (0° and 12°), and each measurement was repeated three times in this predetermined order. This setting aims to explore if subtle, rapid adjustments can be observed using alignment tasks with help of linear polarizers.

## 2.5 Curve fitting

The data reported in some of the experiments were fitted with curves, the fitting procedures are detailed as follows.

In Experiment 5-6, the visual egocentre was taken to be a least-squared approximation to the location of the 'true' single intersection, which had the shortest perpendicular offsets to each of the nine lines (see Figure 2.10) (Mitson, Ono, & Barbeito, 1976). The objective is to estimate the convergence point  $(x, y)$  of nine lines by minimising the sum of squared perpendicular distances from  $(x, y)$  to each line. The lines are defined by their coefficients  $(A_i, B_i \text{ and } C_i)$  using the nonlinear least squares fitting method in MATLAB:

$$F(x, y) = \sum_{i=1}^9 \left( \frac{A_i x + B_i y + C_i}{\sqrt{A_i^2 + B_i^2}} \right)^2 \quad (2.3)$$

Where A and B affect the slope of and the orientation of each line, C determines the line's position relative to its origin. The point  $(x, y)$ , in Euclidean coordinates, has the shortest perpendicular distance to each of the 9 lines. This method ensures that the selected point is optimally located relative to all lines, balancing distances and finding a point that minimises overall variation.

In Experiment 8, the magnitude of deprivation effect as a function of timecourse for each eye with respect to the median plane, and the corneal plane, respectively, was fitted with a power function with three parameters (a, b and c) (Lunghi *et al.*, 2013):

$$y = ax^b + c \quad (2.4)$$

Where y is the magnitude of the deprivation effect, x is the time elapsed in minutes expressed in log, a is the amplitude and b defines the decay rate, while c is the lowest deprivation effect.

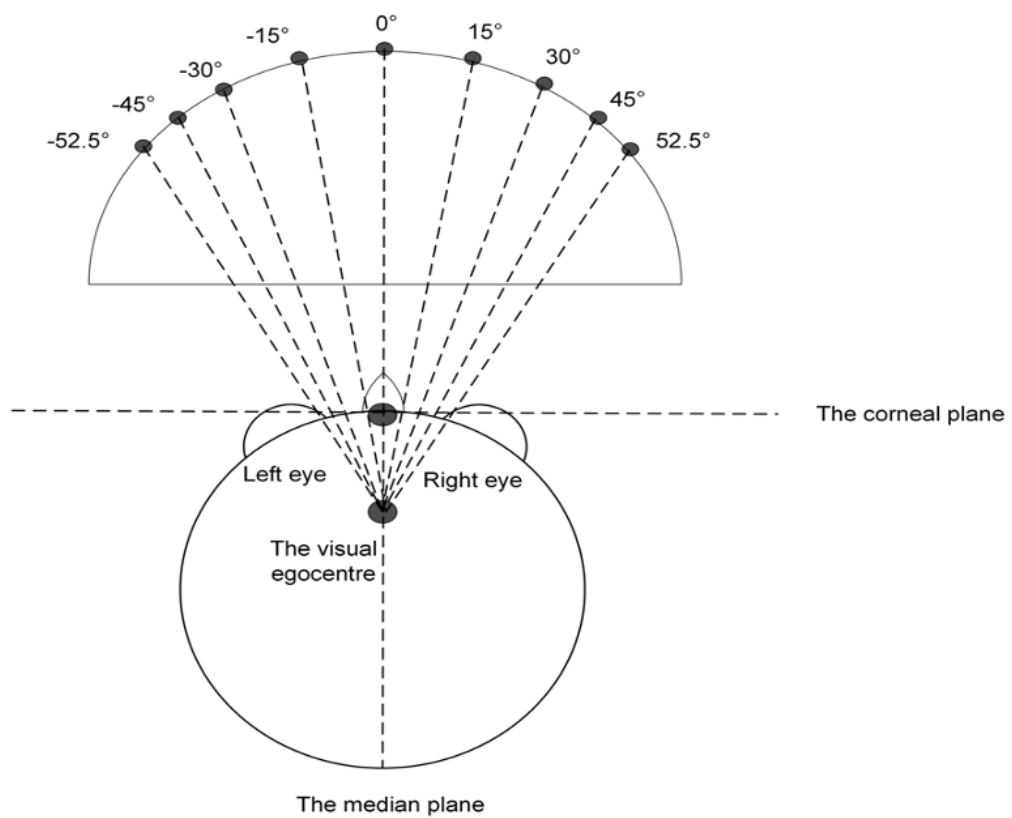


Figure 2.10: Measurements were made along the horizontal azimuth for each of a range of eccentricities spanning  $\pm 52.5^\circ$  relative to the median plane of the head.

## Chapter 3. Establish the best fitted model for binocular visual direction

### 3.1 Introduction

Understanding the fundamentals of visual perception is a central goal of neuroscience and an essential part of understanding the sensory systems in living organisms. To perceive the three-dimensional layout of a scene, both the depths and visual directions of the objects within it need to be determined when perceiving the three-dimensional layout of an object. Strictly speaking, all animals with forward-facing eyes have binocular vision (Howard & Rogers, 1995), which is a large region of binocular overlap for animals to code visual depth. Organisms with binocular vision are able to exploit the slight differences between the images received by the two eyes, a phenomenon called binocular disparity. The ability to utilize these retinal disparities to make extremely fine relative-depth judgments is a process termed stereopsis. Binocular stereopsis creates the impression of depth from binocular cues, which underlies our ability to discriminate between differences in depth. A key step in this process, and a computational challenge faced by the brain, is how to combine the information from the two eyes to achieve a single, unified representation of the world and determine the visual direction of objects in space relative to the viewer.

When determining the direction of a visual object with respect to the viewer's head, it is necessary to take into account both the positions of the images in the eyes (the oculocentric component) and the angle of the eyes with respect to the head (the eye-position component) (Howard & Rogers, 1995). A robust framework for studying headcentric, egocentric visual direction is provided by a model commonly attributed to Hering, with origins traceable to Wells a century earlier (Ono, 1981). This model encompasses the essential components of egocentric direction, namely

the retinal location stimulated (local sign information) and the positions of both eyes (eye information), in accordance with two subsystems proposed by Gregory (1958, 1966): the retinal-image system and the eye-head system work together to combine the local sign signal and eye position signal to determine the visual direction.

To fully capture the phenomenology of egocentric direction, an origin of perceived direction, referred to as the cyclopean eye (or the visual egocentre), serves as a reference point. Collectively, these three elements—retinal location, eye positions, and the cyclopean eye—offer a comprehensive depiction of headcentric, egocentric visual direction and form the foundation for a model of egocentric localization (Barbeito & Simpson, 1991). The cyclopean eye refers to the location from which judgments of relative direction are made. Our everyday visual experience tells us that this is accomplished effortlessly, but nonetheless, the underlying mechanisms are still poorly understood.

The conventional model, initially formulated by Wells (1792) and Hering (1879) and subsequently expanded upon by Ono (1981) and other researchers, proposes that binocular visual direction is determined by averaging the information from monocular images. Furthermore, this model asserts that the resultant visual perception gives the impression that the participant is viewing the target from a single position located in the midway between the two eyes, referred as the visual egocentre (or the cyclopean eye). Figure 3.1 shows an illustration of the conventional model. The participant is fixating on a point along the median plane of the head, so both eyes are in primary gaze. The two thick lines represent the visual axes. Additionally, there is a binocular target present accompanied by its corresponding visual lines. The angles  $\alpha_L$  and  $\alpha_R$  between the visual axes and lines correspond to the oculocentric direction of the target for the left and right eye, respectively. The binocular visual direction is determined by the angle between the median plane and a line originating from the midpoint of the interocular axis and extending to the target. This angle  $\alpha_B$  can be approximated using the subsequent equation:

$$\alpha_B = (\alpha_L + \alpha_R)/2 \quad (3.1)$$

Despite the traditional geometrical model's intuitive appeal, evidence suggests that the position of the visual egocentre is not stable and that the calculation of binocular visual direction may be more complex than previously assumed (Mitson, Ono, & Barbeito, 1976). Indeed, it has been demonstrated that behavioural estimates of visual direction can be reliably altered by changing the input (e.g., luminance contrast) to one eye leaving other aspects of features, including stereoscopic depth, relatively unchanged. Verhoeff (1933) presented different luminance intensities stereograms to the two eyes and found that the relative direction of the features in the stereogram is systematically biased towards the perspective of the eye perceiving the image with greater luminance intensity. This effect is also observed in the binocular observation of real three-dimensional scenes. These findings challenge the traditional geometrical principles, suggesting that binocular visual direction is the average of the directions measured from both eyes. Instead, the left and right direction signals are weighted by factors such as luminance, image resolution, and ocular dominance, either at or prior to the stage of binocular combination.

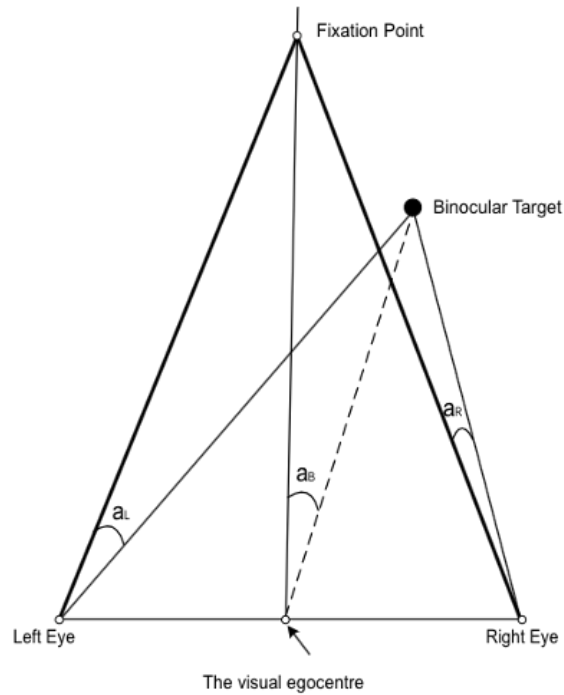


Figure 3.1: The geometry of the conventional model. The participant is fixating directly on a point situated within the median plane of the head so that the eyes are in primary gaze position. The visual axes are indicated using two thick lines. A target is presented, accompanied by its corresponding visual lines depicted as thin lines. The angles  $\alpha_L$  and  $\alpha_R$  are the angles between the visual axes and the lines of the left and right eye, respectively. The angle  $\alpha_B$  corresponds to the binocular visual direction of the target, as estimated based on the conventional theory. This angle is equivalent to the angle formed between the head's median plane and a line extending from the midpoint of the interocular axis to the target. The dashed line extending from the visual egocentre through the apparent location of the target signifies the binocular direction line. Illustration adapted from Banks et al., (1997).

On the basis of previous studies, Mansfield and Legge (1996) assessed the influence of interocular contrast differences on the perceived visual direction of binocularly vertically-aligned Gabor targets, in which the top Gabor patch was positioned with a disparity and varying monocular contrasts to create different interocular contrast ratios while bottom Gabor patch always had equal contrast in both eyes. Participants were instructed to adjust the horizontal position of the bottom Gabor patch to align it vertically with the top Gabor patch, different contrast ratios were tested by varying the contrast in one eye while keeping the other eye's contrast constant in this experiment.



Supported by data showing that the visual direction of binocularly viewed features is biased towards the eye with the higher contrast image, Mansfield and Legge (1996) proposed a new model where the relative alignment of depth features is determined by a maximum-likelihood combination of the direction signals from both eyes. This model explains the change in visual direction caused by interocular contrast differences in terms of choosing the most likely direction based on the noisy estimates from the left and right eyes. Unlike other models, this model accounts for visual direction in either monocular or binocular viewing conditions. There are two critical parameters in the model:  $k$  represents the exponent describing the relationship between image contrast and direction uncertainty, and  $W$  ( $W_L/W_R$ ) refers to the ocular dominance between the two eyes.  $W > 1$  indicates a stronger weighting of the left eye's input, and  $W < 1$  means a weaker weighting of the left eye's input. The following equation (2) describes the relationship between binocular visual direction, ocular dominance and the contrast ratio ( $Q$ ) of the stimuli presented to the two eyes  $C_L/C_R$  (Mansfield & Legge, 1996).

$$\hat{B} = \frac{WQ^{2k}\hat{L} + \hat{R}}{WQ^{2k} + 1} \quad (3.2)$$

The data that changes in the binocular visual direction of the mixed-contrast target can be accurately predicted based on the monocular vernier acuities reinforced the finding that visual direction is determined by a weighted combination of signals from both eyes and influenced by contrast. This was achieved by measuring monocular vernier acuity as a function of the lower Gabor and assessing the binocular visual direction of a mixed-contrast Gabor. This maximum-likelihood model essentially states that the egocentre location moves toward the eye receives more visible image when the visual input to one eye is compromised.

However, Banks and colleagues (1997) criticized that Mansfield and Legge's (1996) interpretation on cyclopean eye position was inappropriate. They argued Mansfield and Legge's task was an alignment

task, in which the perceived changes in alignment could be explained without assuming shifts in the visual egocentre position. Banks *et al.* (1997) suggested an egocentre task would be required where participants indicate the body part with which targets appear to be aligned and thus provide information relevant to the position of the visual egocentre. Banks *et al.* (1997) further demonstrated that changes in vergence (the angle between the eyes when focusing on a point) influenced perceived direction, though they did not empirically test these assumptions. This was contrary to Mansfield and Legge's (1995, 1996) assertion that perceived direction was independent of eye position. Therefore, Banks *et al.* (1997) argued that the observed effects could be fully explained by the conventional theory of binocular visual direction with a simple modification for differential weighting of eye signals based on contrast, in which a weighted average of oculocentric direction is assumed to determine the binocular direction of a target, specifically,

$$\alpha_B = W\alpha_R + (1 - W)\alpha_L \quad (3.3)$$

Where  $\alpha_B$ ,  $\alpha_L$  and  $\alpha_R$  represent binocular direction, left visual direction and right visual direction, respectively.  $W$  is defined as the weight given to the oculocentric direction of the target in the right eye, ranging from 0 to 1.  $W > 0.5$  represents a greater contrast in the right eye, while  $W < 0.5$  represents a greater contrast in the left eye. According to this modified conventional model, the perceived shift of the binocular direction of an object when the visual input to one eye is degraded is characterized by a rotation of the binocular direction line about a fixed cyclopean eye, while the position of the cyclopean eye itself does not change. These observations, when weighted by the monocular visual direction, are consistent with the conventional geometry model. They asserted that the perceived relative binocular direction was affected by the eye position although interestingly they did not formally collect any empirical data to test these assertions. Although Banks *et al.* (1997) presented some informal demonstrations in their paper, based on the ability to free fuse pairs of stereoscopic images, to support their model, they did not test the

predictions of their model in a systematic manner in the laboratory and thus crucially its validity remains untested. Figure 3.2 describes the difference of these two models, in which the upper patch was located on the vertical midline ( $X = 0$  arcmin) with a disparity ( $Z$ ) of 0 arcmin. The solid lines show the model of Mansfield and Legge (1996), while the dashed lines correspond to the model of Banks *et al.* (1997). Different contrast ratios between the two eyes are depicted by different colours and symbols.

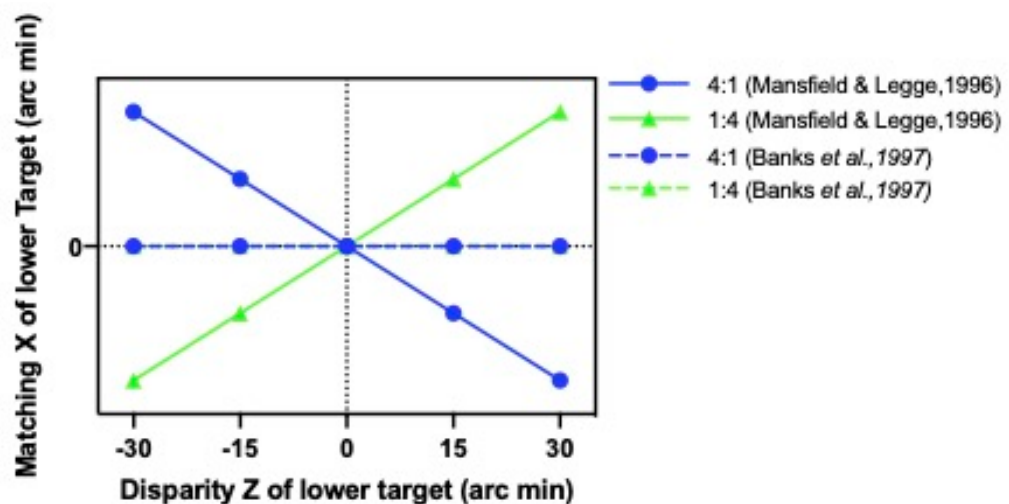


Figure 3.2: The difference of two models.

The solid lines represent the model predictions of Mansfield and Legge (1996) and the dashed lines represent those of Banks *et al.* (1997). Different colours and symbols depict different contrast ratios between the left and right eyes. The solid lines show that the location of egocentre shifts towards the eye receiving a more visible image, whereas the dashed lines describe that the location of egocentre is fixed, but the vergence of egocentre changes when one eye receives a higher contrast image.

Despite the fact that all of these explanations provide qualitative accounts of binocular visual direction, none has been widely accepted. Consequently, considerable uncertainty persists about the precise computational principles governing egocentricity and plasticity in cyclopean perception. To identify which model best predicts psychophysical performance across diverse viewing conditions, this study evaluates competing models of binocular visual direction. Moreover, it aims to uncover the mechanism by which a binocular feature is assigned a single visual direction, where the left and right eyes indicate different directional information.

Even though each of these explanations can qualitatively explain the binocular visual direction, none has been widely accepted, and the geometrical averaging rule remains the predominant explanation for binocular visual direction. Consequently, much uncertainty remains concerning the precise computational principles governing the egocentre position and the plasticity of cyclopean perception in general. Therefore, current study aims to test competing models of binocular visual direction and establish which model best accounts for psychophysical performance under a broad range of viewing conditions, then determine the mechanisms of how a single visual direction is assigned to a binocular feature for which the left and right eyes are signalling different directions.

## 3.2 Experiment 1: The effects of contrast on binocular visual direction - a replication of Mansfield and Legge's (1996) study

### 3.2.1 Methods

#### 3.2.1.1 Observers

Three participants (the authors) with normal or corrected-to-normal vision and no history of ocular disease participated in this experiment (age range: 30-51years, mean age:  $44 \pm 9.90$ years). Before formal data collection began, the TNO stereo test (Laméris Ootech, Nieuwegien, The Netherlands) was administered to ensure each of the participants had normal stereo vision and thus were able to perceive the depth and 3-dimension structure of visual information (range from 60 to 120arcsec). The experiment was approved by School of Psychology Ethics Committee at University of Nottingham and participant gave informed consent before the experiment. Participants gave informed consent before the experiment and all experimental procedure conformed to the guidelines laid out in the Declaration of Helsinki.

### 3.2.1.2 Apparatus and stimuli

The experimental task was conducted in a dimly lit room. Stereoscopic stimuli were grey-scale images generated using an Apple Macintosh computer running custom software written in the C programming language and presented on two identical LCD monitors (22-inch Samsung Sync-Master 2233RZ; 1024 × 768-pixel resolution; 60Hz refresh rate; 318cd/m<sup>2</sup> maximum luminance). The suitability of employing these displays in vision experiments, considering their spatial, timing, and luminance attributes, has been thoroughly documented elsewhere (Wang & Nikolic, 2011). The two monitors were temporally synchronised by driving them using the dual outputs of the same video card. They were carefully calibrated, and gamma-correction was checked using SLR luminance meter LS-110 to ensure that their luminance was a linear function of the digital representation of the image. For precise control of luminance contrast the number of intensity levels available on each display was increased using the noisy-bit method (Allard & Faubert, 2008).

The observer was instructed to view the stimuli dichoptically using a Wheatstone mirror stereoscope (Figure 3.3), producing an effective viewing distance of 231.5cm from mirror to each display. The pair of full-silvered mirrors in the stereoscope were nominally set at an angle of  $\pm 45^\circ$  with respect to the median plane of the head, but observer could adjust the angle manually (if necessary) to maintain stable fusion of the two images. A chin rest was employed to stabilise the participant's head and minimise movement during the experiment.



(a)

(b)

Figure 3.3: The apparatus used in the experiment.

(a) The Wheatstone stereoscope used in this experiment to achieve dichoptic presentation of two images; (b) The participant can see the left display through the left mirror and the right display through right mirror independently.

The stimuli displayed on each monitor were identical to those used by Mansfield and Legge (1996) and were comprised of two vertically-separated Gabor patches with a luminance profile of the general form:

$$L(x, y) = \exp [-(x^2 + y^2)/(2s^2)] \cos(2\pi fx) \quad (3.4)$$

Where  $x$  and  $y$  represent the horizontal and vertical dimensions of the screen,  $s$  is the Gaussian envelope space constant set at  $0.35^\circ$ , and  $f$  is the carrier spatial frequency set at  $1.0\text{c/deg}$ . The sinusoidal waveform was always presented in cosine phase, with respect to the centre of the Gaussian envelope. The lower Gabor patch consisted of equal contrast stimuli in each eye, while the upper Gabor contained different contrasts between the eyes that could be manipulated. The stimuli were presented on a uniform grey background ( $159\text{cd/m}^2$ ), which was surrounded by a high contrast black or white fusion frame, along with a pair of vertical and horizontal nonius lines to facilitate stable binocular fusion. The vertical centre-to-centre distance between the upper and lower Gabor patches

was 2.1deg. There was a small black fixation square presented in the centre of each display between the upper and lower Gabor patches (Figure 3.4). The participants were instructed to maintain fixation on this binocular mark, although vergence position could not be confirmed objectively.

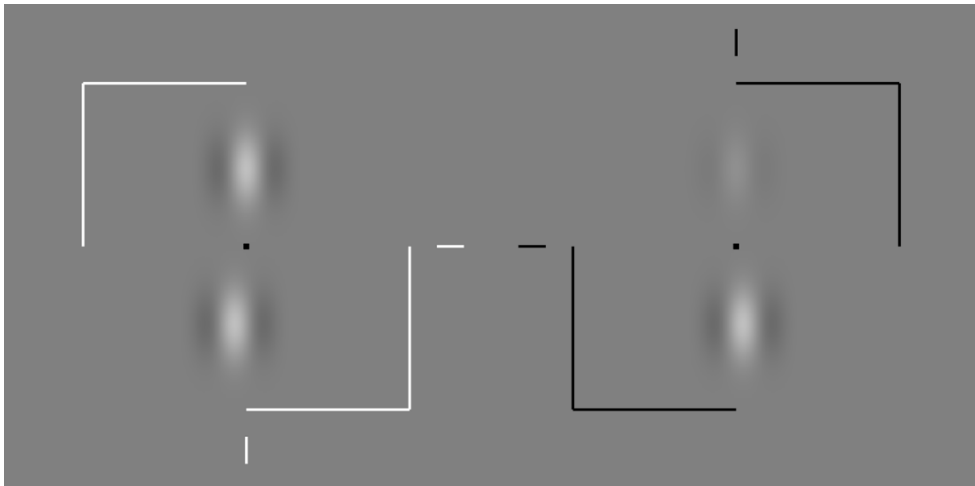


Figure 3.4: Example stereo-Gabor patches used in the experiment. The stereo percept in crossed fusion is two Gabor targets vertically above each other. The upper targets have different contrast between the left and right eyes, while the lower ones have equal contrast in the two eyes.

We measured the horizontal location at which the target, presented with equal contrast in each eye and at varying relative depths, appeared vertically aligned with the upper target, which had different contrasts in each eye. The position of each stereo-Gabor was based on the following parameters (Mansfield & Legge, 1996):

$X$  refers to the horizontal location of the Gabor stimuli as perceived by both eyes, defined as  $(Lx + Rx) / 2$ , where  $Lx$  and  $Rx$  are the horizontal coordinates corresponding to the centre of the left and right stimuli, respectively. It indicates where the stimulus appears to lie along the horizontal plane when the views from both eyes are combined.  $Z$  represents the binocular disparity, defined as difference in the horizontal position of the stimulus as seen by the left and right eye, expressed by  $(Lx - Rx)$ .

### 3.2.1.3 Procedure

The upper Gabor was located on the vertical midline ( $X = 0$  arcmin) with a disparity ( $Z$ ) of 0 arcmin. The stereo-Gabor in the bottom half of the screen had equal contrast between the two eyes' images, while different interocular contrast ratios were obtained for the top images between the two eyes. An alignment task was used to measure the horizontal location ( $X$ ) at which the lower target appeared vertically aligned with the upper target. The disparity ( $Z$ ) of the equal-contrast Gabor was set to either -30, -15, 0, 15, or 30 arcmin correspond to the upper Gabor for alignment estimation. Figure 3.5 is a top-down view of this task to help understand disparity pedestals. Based on these data, we can estimate the visual direction of the mixed-contrast target.

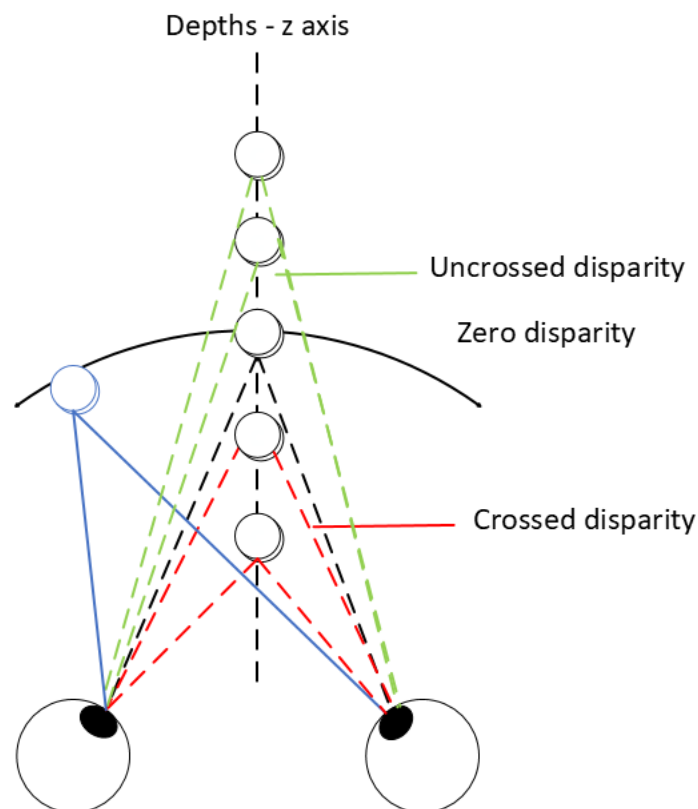


Figure 3.5: A top-down view of this task. The blue-outlined circle represents the upper target (0 arcmin). The black-outlined circle denotes the lower target, positioned at depths ranging from -30 to +30 arcmin. Targets in front of the upper target (crossed disparity) are connected with red dashed lines, while targets behind it (uncrossed disparity) are linked with green dashed lines.



The observer initiated each trial by pressing the “enter” key on a standard computer keyboard. At the beginning of each trial, the initial horizontal location of the lower Gabor was set randomly. The stereo Gabor targets were then displayed for 1s, following which the participant was required to indicate (by pressing one of four keys) whether the lower Gabor appeared to be vertically-misaligned to the left or right of the upper target. These four keys represent either a coarse or fine adjustment in either direction. In the subsequent trial, the X-location of the lower Gabor was adjusted in the correct direction (by either 1.5arcmin or 15arcmin based on the key response) to minimize the misalignment (Figure 3.6). This adjustment was achieved by adding equal increments to both  $Lx$  and  $Rx$  while keeping the disparity of the equal-contrast Gabor constant. Once the participant was confident that the upper and lower stimuli were perceived to be vertically aligned, the current location of lower Gabor was recorded as the point of perceived alignment (PPA).

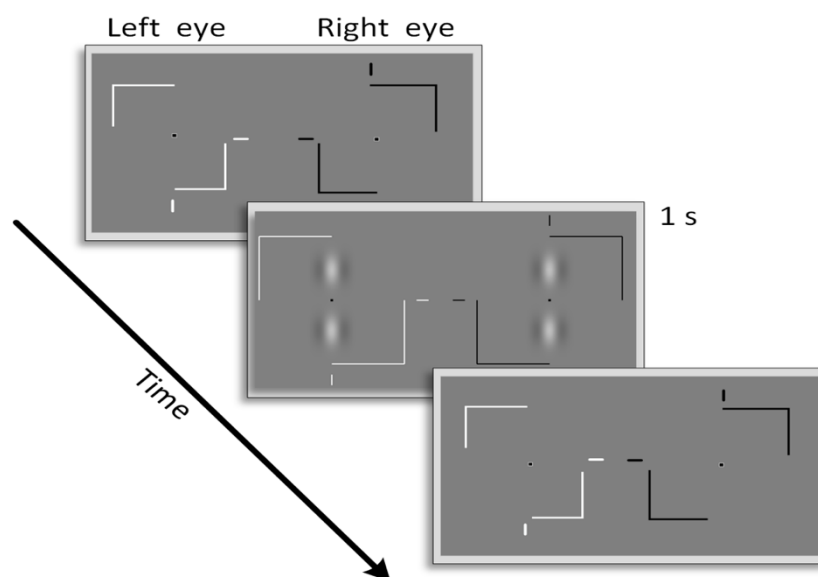


Figure 3.6: Schematic representation of one trial. After achieving stable fixation, a pair of stereo Gabor patches were presented to two eyes for 1 s (mixed-contrast target was presented at the top half of the screen, while the equal-contrast target was presented at the bottom half of the screen). The Gabor stimuli were then removed (only the fixation stimuli remained on screen), and the participant had to press one of four keys to reduce the perceived misalignment of the stereo Gabor patches. When the mixed-contrast target and the equal-contrast target appeared to be vertically aligned, the participant pressed the ‘space’ bar. 10 alignments estimates were collected for each combination of contrast ratio and equal contrast Gabor disparity. There were 15 trials in each session.

For the upper Gabor, one eye's image was presented at the fixed contrast (C), while the other eye's image was set to a lower contrast to achieve the required interocular contrast ratio. For the first condition, C was set to 25% (Michelson contrast) and the contrast ratios were 1:1, 1:4 and 4:1. In the second condition, C was set to 50% and the contrast ratios were also 1:1, 1:4 and 4:1. For each contrast ratio, the task was completed with the left eye exhibiting a higher contrast than the right eye and then the converse configuration. Trials from two independent alignment tasks were randomly interleaved so that it was impossible for the participant to predict which eye would receive the higher contrast image. 10 alignment estimates were collected for each combination of contrast ratio and equal contrast Gabor disparity. There were 15 trials in each contrast condition.

### 3.2.2 Results

The data from three participants measured with a fixed contrast C of 25% and 50% are shown in Figure 3.7 and are plotted in the same manner as Mansfield and Legge (1996). In each graph the location (X) where the lower Gabor appeared to be vertically aligned with the upper Gabor (the PPA) is plotted as a function of the lower Gabor's disparity (Z). Each point is the mean of ten alignment estimates and the error bars above and below each data point represent the standard error of the mean (SEM).

If Mansfield and Legge's (1996) model was used to establish the binocular visual direction, then the PPA depends on both the lower Gabor's disparity and the upper Gabor's contrast ratios, that is the PPA may shift closer to the left eye when the left eye is presented with a higher contrast image and the opposite is true when the right eye is presented with a higher contrast image. On the other hand, all of the PPAs would be expected to be along the  $X = 0$  horizontal line if the data were consistent with the modified conventional model. The difference between them is whether the PPA has large bias towards the more visible image.

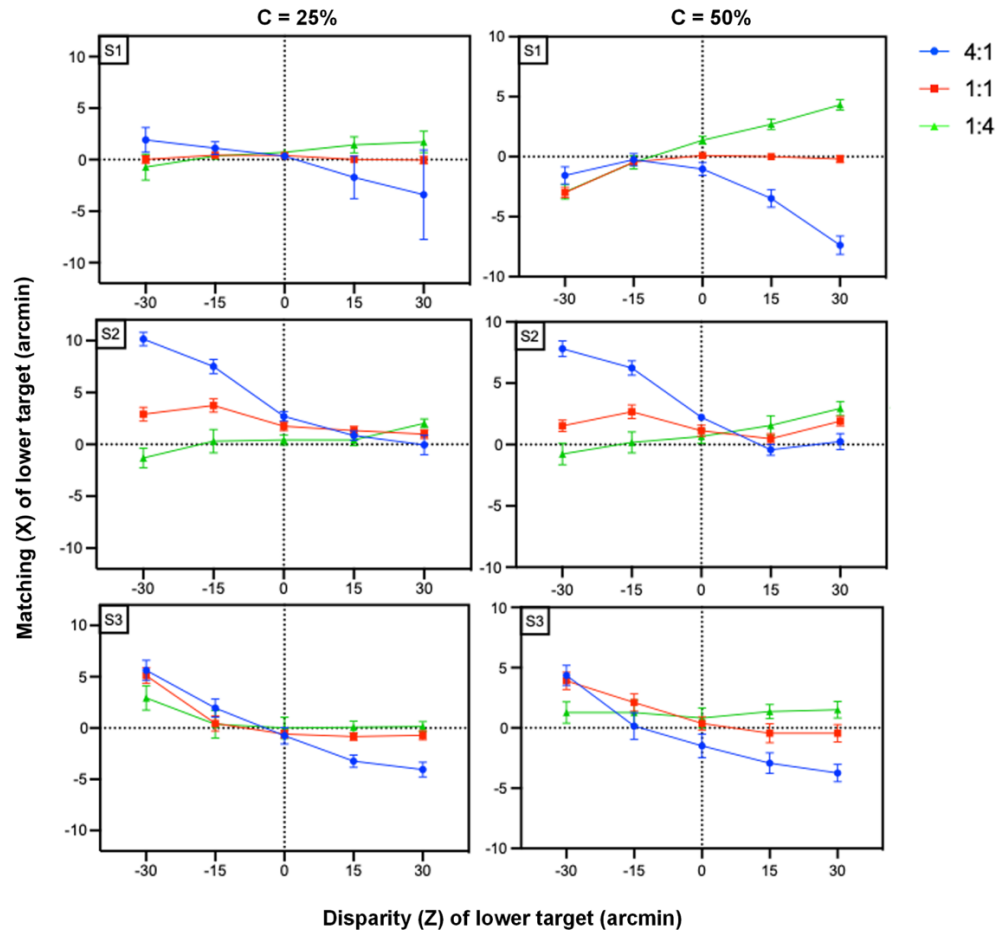


Figure 3.7: Data from three participants with a fixed contrast  $C$  of 25% and 50%. The disparity of the upper Gabor was always 0 arcmin. Each data point represents the  $X$  location of lower Gabor that appears vertically aligned with the upper Gabor. The contrast ratios between the left and right eye are depicted by the different coloured symbols and lines as indicated in the legend at the right of each plot. Error bars represent the SEM calculated across repetitions of the task for each observer.

According to Figure 3.7, for disparities greater than 0 arcmin, such that the lower Gabor appears in front of the upper Gabor, the PPAs lie to the below of the true (physical) alignment when the left eye views a higher contrast image than the right eye. While for disparities less than 0 arcmin (lower Gabor is behind the upper Gabor), the PPAs lie to the above of the true alignment when the left eye has a higher contrast. When the right eye has greater contrast, the opposite is true. This suggests a weighting of visual inputs that is related to the contrast difference between the eyes. However, a point to note is that these data, like those of Mansfield and Legge (1996), show considerable individual differences. Even though data are collected in the same contrast conditions (i.e.,  $C = 25\%$ ), the

discrepancy in the PPAs for all three subjects are quite different. The data from S1 and S3 exhibit a similar trend, but the data from S2 is somewhat different. For disparity is less than 0 arcmin, the PPAs for S2 is more than 10arcmin removed from the point of geometrical alignment when the left eye receives a more visible image. In addition, data of the same participant measured with different contrast conditions also exhibited different behaviours. For example, the PPAs for S1 measured in  $C = 25\%$  contrast condition lie along the  $X = 0$  horizontal line, but the discrepancy observed in the  $C = 50\%$  contrast condition shows more than 5arcmin removed from the horizontal line when disparity is greater than 0arcmin.

Linear regression analyses were conducted to quantify the relationship between contrast ratios (4:1, 1:1, and 1:4) measured in two contrast conditions (25% and 50%) for each participant. While inter-participant variability is evident, a consistent directional pattern emerges across conditions. In terms of 25% contrast condition, participants elicited uniformly strong negative relations for 4:1 contrast ratio (*all  $\beta \approx -0.97$ ,  $p < .01$* ), while the 1:4 contrast ratio showed positive effects for two participants (S1 and S2:  $\beta \approx 0.90$ ,  $p < .05$ ). The 50% contrast condition produced participant-specific effects for 4:1 contrast ratio with only S2 showed significant positive relationship ( $\beta \approx 1$ ,  $p < .01$ ), while the 1:4 contrast ratio showed positive effects for all participants ( $\beta \approx 0.96$ ,  $p < .05$ ). 1:1 contrast ratio shows weak and non-significant effects (*all  $p > .05$* ).

In summary, the results from Experiment 1 indicate that binocular visual direction is biased towards the visual line from the eye that receives higher contrast image, but an alignment task, rather than egocentre task, could not directly explain whether the cyclopean eye position. Instead, modified conventional model can explain these changes of perceived visual direction without assuming a wandering cyclopean eye. There are a number of unresolved methodological issues with Mansfield and Legge's (1996) original study that have yet to be adequately resolved. For example, they only showed a subset of the results obtained for their first experiment (measuring the PPAs as function of lower Gabor disparity)

and these exhibited marked individual differences between the three participants tested but these were not adequately addressed. Furthermore, they also did not present the PPA settings made by these same participants in subsequent experiments, designed to test their model, in which several methodological details were changed, thus the generality of the findings is uncertain. These important issues will be explored further in the next experiment.

### 3.3 Experiment 2: Egocentric visual direction using one-dimensional correlated noise stimuli

The results of Experiment 1 show some qualitative differences with respect to the published data from Mansfield & Legge (1996), despite the fact that we employed an identical procedure, and these may have arisen due to the following issues. First, like Mansfield and Legge (1996), we did not measure eye movements and although our participants were well practiced on psychophysical tasks, they may have made eye movements (i.e., had unstable vergence) rather than maintaining fixation on the central square. According to Hering's (1879/1942) laws, visual directions do depend on eye movements under specific viewing conditions (Erkelens, 2000). This criticism was levelled by Banks *et al.* (1997) and could contribute to some of the inconsistencies reported. Second, the Gabor stimuli used in Experiment 1 were constructed such that the sinusoidal waveform was always in cosine phase with respect to the centre of the Gaussian envelope, so they were unbalanced and had an overall luminance offset with respect to the uniform background. The magnitude of this luminance offset is directly proportional to the contrast of the Gabor presented to each eye. Mansfield and Legge (1996) acknowledged this luminance artefact in their original study but played down its importance even though previous research has shown that interocular luminance differences can produce changes in visual

direction (e.g., Francis & Harwood, 1951). Furthermore, the Gabor stimuli used in this, and previous research, may not be optimal stereoscopic stimuli for studying the mechanisms of visual direction because they have an inherent ambiguity due to their periodic structure. That is, they can give rise to disparity mismatches (“false correspondence”) that can lead to misperceptions of depth (Prince & Eagle, 2000) in stereoscopic displays. In Experiment 2, we sought to exercise greater experimental control over the stimuli by using windowed visual noise patterns in the same vertical alignment task. This modification is particularly effective to reduce such inherent ambiguity present in periodic stimuli. Unlike structured or repetitive patterns, visual noise lacks a periodic organization, minimizing the risk of spurious matches in stereopsis. By using windowed noise, we ensure that local disparity cues are unambiguous, thereby improving the reliability of depth perception judgments. This approach allows us to isolate the mechanisms of visual direction more precisely, as the stochastic nature of noise eliminates the confounding effects of regularity in the stimulus.

### 3.3.1 Methods

#### 3.3.1.1 Observers

Six observers participated in this experiment (S1, S2 and S3 participated in Experiment 1 also participated in Experiment 2; age range: 30-51years, mean age:  $35.83 \pm 10.82$ years). The observers all had normal or corrected-to-normal vision and no history of ocular disease. Before formal data collection began, the TNO stereo test was administered to ensure each of the observers had normal stereo vision and thus were able to perceive the depth and 3-dimension structure of visual information (range from 60 to 120arcsec).

### 3.3.1.2 Apparatus and stimuli

The apparatus was identical to that used in Experiment 1, but stereoscopic stimuli were changed to vertically-separated, Gaussian-windowed, one-dimensional, aperiodic noise patches (Gaussian SD:  $0.35^\circ$ ; bar width:  $0.06^\circ$ ). The stimuli used were correlated noise samples for the upper and lower targets, in which the upper and lower noise pairs had the same texture on any one trial (see Figure 3.8).

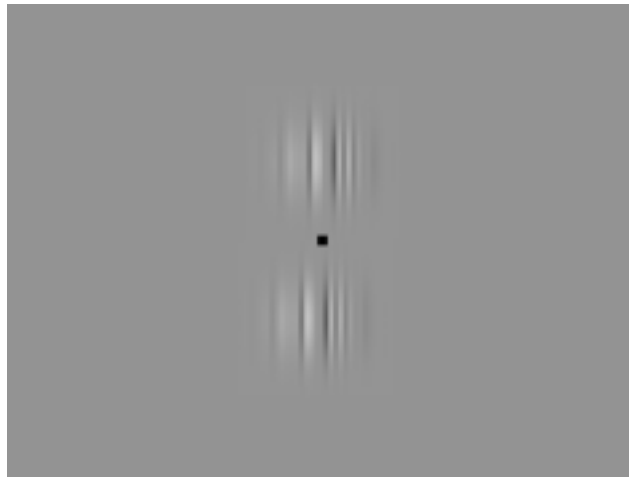


Figure 3.8: Two vertically-separated, Gaussian-windowed, 1-d correlated noise patches used in Experiment 2, in which the upper and lower patches were in the same patterns.

To investigate performance under a wide range of viewing conditions three stereoscopic depths were used for the upper noise target, either 0, +30 or -30 arcmin relative to the fixation marker, in separate runs of trials. The contrast ratio between the left and right images for the upper noise patch was varied, in an identical manner to that used in the first experiment, to provide ratios of 4:1, 1:1 and 1:4. The lower noise target always had equal contrast in each eye, which was presented at five different stereoscopic depths (range  $\pm 60$  arcmin) relative to upper target. The size of fixation marker was increased to make it more prominent from 3.41 arcmin to 7.80 arcmin, to help participants maintain stable fixation and reduce eye movements. The horizontal location of the lower patch was adjusted until it appeared aligned with the upper patch.

### 3.3.1.3 Procedure

The procedure was identical to that used in Experiment 1 with the exception that another two disparity conditions were measured for the upper patch, in which the upper patch was located on the vertical midline ( $X = 0$ ) with a disparity ( $Z$ ) of 0, +30 and -30arcmin. The lower patch was located at five different stereoscopic depths, which were -30, -15, 0, +15, or +30arcmin when the upper patch disparity was 0 arcmin disparity condition; and 0, +15, +30, +45, or +60arcmin when the upper patch disparity was +30 arcmin; and -60, -45, -30, -15, or 0arcmin when the upper patch disparity was -30 arcmin.

In each adjustment procedure, the initial horizontal location of the lower patch was set randomly. In order to help minimise potential eye movements, the presentation of the stereo patches was reduced from 1 s to 150ms. As Experiment 1 showed that the absolute stimulus contrast ( $C$ ) used had little to no effect on performance, in Experiment 2, a 50% Michelson contrast level was used for the upper patch for one eye, and the other eye's image was set to a lower contrast to achieve the required interocular contrast ratio.

### 3.3.2 Results

The data for one representative participant (S3) measured with correlated noise patches is depicted in Figure 3.9. and shows the  $X$  locations at which the lower target appeared to be vertically aligned with the upper target (the PPAs). It is evident that the PPAs are dependent on the contrast ratios of the upper targets and disparity depths of the lower targets. The perceived binocular direction of the upper target appears to be biased towards the eye with the more visible image. This is consistent with the results of Experiment 1. However, different from the view of Mansfield and Legge (1996), the result suggests the direction perceived with both eyes is not straightforwardly determined by one eye but rather computed. As shown in Figure 3.9(b) measured in the same disparity



condition with Experiment 1, the PPAs do not show apparent displacement with the  $X = 0$  horizontal line. When fixating on an object, the vergence angle, formed by simultaneously moving two eyes in opposite directions to maintain single vision, provides a powerful depth cue. A larger vergence angle (eyes turning inward) indicates the object is closer, while smaller vergence angle (eyes turning outward) indicates a farther object. It highlights the importance of ocular vergence in perceiving the visual direction, but the effect of ocular vergence on visual direction changes depending on different viewing conditions, indicating that the environment and context in which we view objects can alter how vergence affects our perception. These observations are thought to be consistent with the modified conventional model proposed by Banks *et al.* (1997), indicating that our brain computes the binocular visual direction by averaging the directions seen by each eye separately. Such averaging is weighted, implying some visual inputs may be given more importance than others in the computation process.

According to Figure 3.9(a), the upper target has a crossed disparity of +30arcmin relative to the fixation marker, while the lower target has disparities ranging from 0 to +60arcmin. The observer fixates behind the target, resulting in  $\alpha_L$  and  $\alpha_R$  with equal magnitudes but opposite in sign ( $\alpha_L$  is clockwise or negative). When the weight  $W$  in Equation (3) is 0.5, indicating equal contrast between the two eyes (as shown by the red lines in Figure 3.9). So  $\alpha_B$  is the average of  $\alpha_L$  and  $\alpha_R$ ,  $\tan \alpha_B$  therefore equals to 0 calculated from the average of  $\tan \alpha_L$  and  $\tan \alpha_R$ . The target is perceived as being in the middle between the two eyes. If the weight  $W$  in Equation (3) is greater than 0.5, the right eye receives a higher contrast image (the green lines in Figure 3.9), causing  $\alpha_B$  to be biased towards the value of  $\alpha_R$  and the PPA appears to the left of the true alignment. Conversely, if  $W$  is less than 0.5, the left eye receives a higher contrast image (the blue lines in Figure 3.9). Therefore,  $\alpha_B$  is biased towards the value of  $\alpha_L$ , suggesting PPA is farther to the right of the true alignment. In Figure 3.9(b), the upper patch is at the same disparity as the fixation marker, while the lower patch has disparities from -30 to +30arcmin. All

three lines lie along the  $X = 0$  horizontal line, indicating that the target is perceived in the head's median plane. Figure 3.9(c) describes the upper target with an uncrossed disparity of -30arcmin relative to the fixation marker, while the lower target with disparities ranging from -60 to 0arcmin. In this condition, the participant fixates in front of the target, making  $\alpha_L$  and  $\alpha_R$  equal in magnitude but their reversed signs compared to Figure 3.9(a). When both eyes receive images with equal contrast, the target is perceived in the head's median plane. In instances where the right eye receives a higher contrast image (indicated by the green lines in Figure 3.9), the perceived point of alignment (PPA) is displaced to the right of the true alignment. Conversely, when the left eye receives a higher contrast image (represented by the blue lines in Figure 3.9), the PPA moves to the left. These findings are consistent with the modified conventional model, which posits that the shift in perceived visual direction is attributable to the rotation of ocular vergence rather than an alteration in the cyclopean eye.

Figure 3.10 is a replot of the data for the same subject from Figure 3.9 to give a clearer picture of the data. Disparity ( $Z$ ) has been converted to the physical distance in centimetres from the participant. Similarly,  $X$  has been converted into centimetres displaced from the midline. The left and right visual lines passing through the mixed-contrast target are also plotted. The PPAs map out the line of depths which appeared aligned with the mixed-contrast targets for each contrast ratio. A linear least squares method was used to find the best fitting straight line through these points for each contrast ratio (different colours represent different contrast ratios).

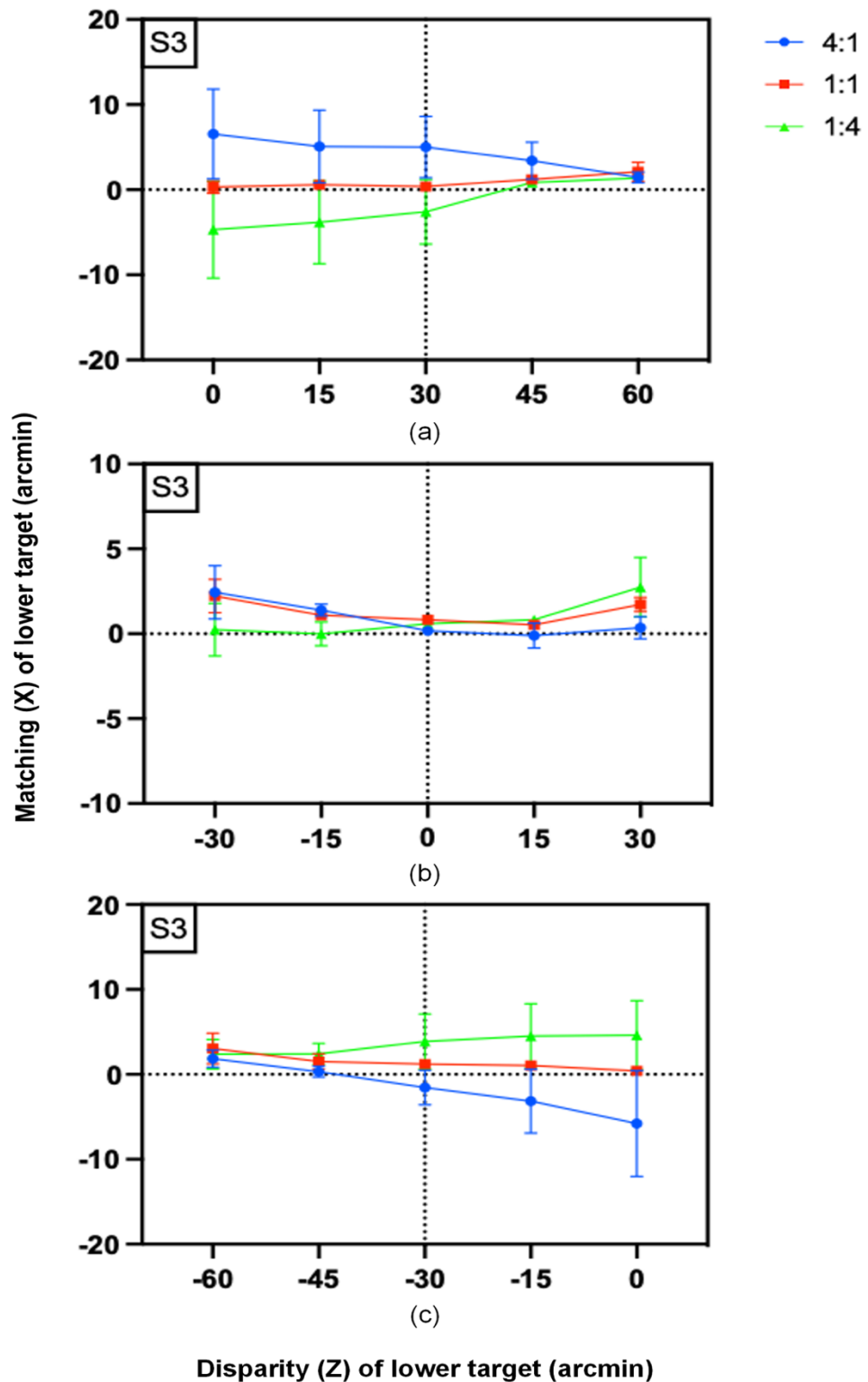


Figure 3.9: The example data of an observer measured in correlate patterns. The disparity of upper Gabor was set at +30, 0 and -30 arcmin. Each data point represents the X location of lower noise patch that appears vertically aligned with the upper patch (the PPA). The contrast ratios between the left and right eye are described in different colour of lines as indicated at the right of each diagram. Error bars represent the SEM calculated across repetition of the task.

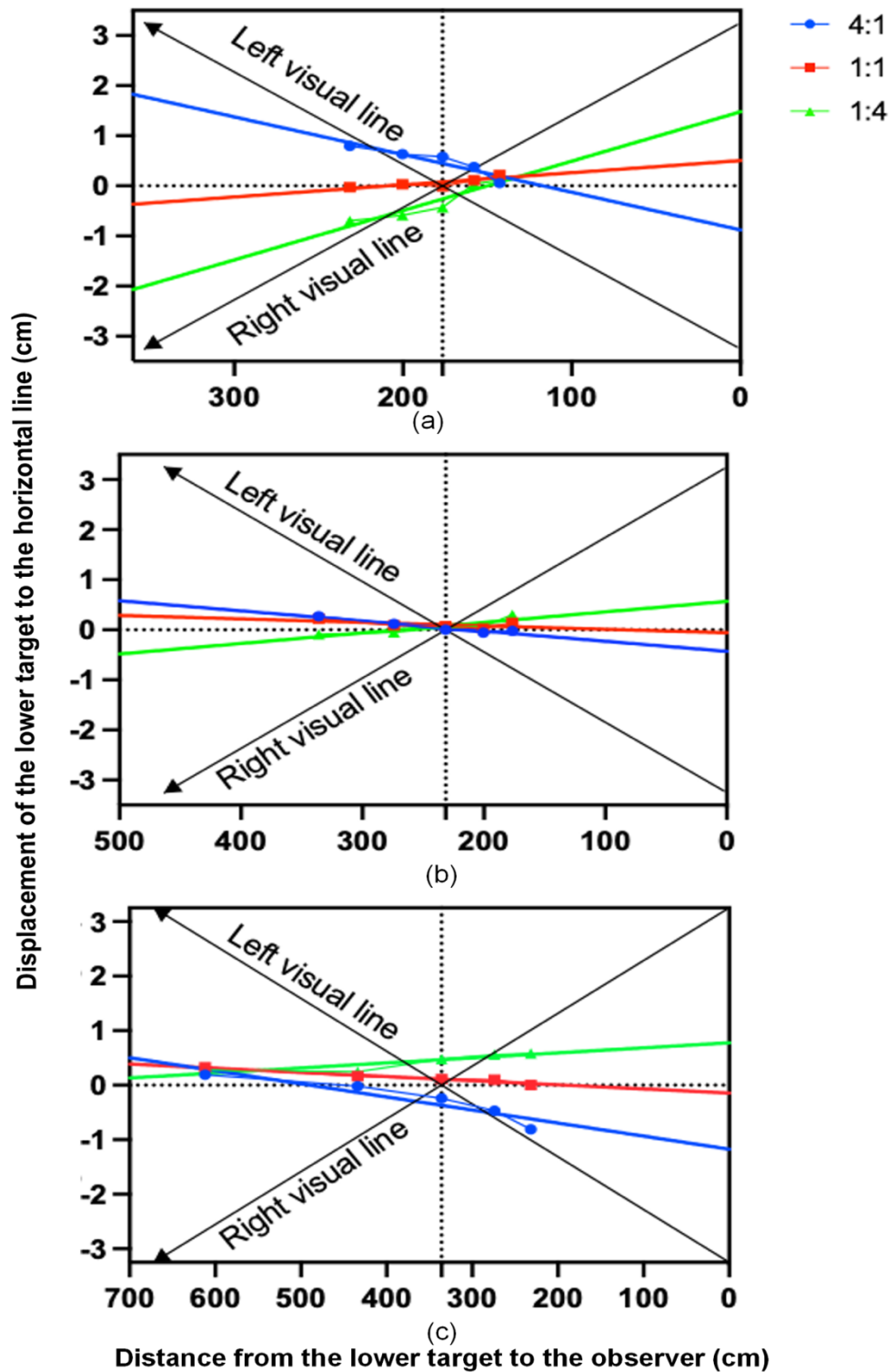


Figure 3.10: Data with correlated patterns from one participant is replotted with X and Z converted into physical distances (cm). The black lines represent the visual lines from the left and right eyes passing through the upper target. The contrast ratios between the left and right eye are described in different colour of lines as indicated at the right of each diagram. Situation a, b and c represent the upper target was located at +30, 0 and -30arcmin, which has been converted to the physical distance in centimetres. Unequal contrast in the left and right eye bias PPAs to the visual line with higher contrast image.

Accordingly, Figure 3.11 maps out the binocular visual line fitter with the PPAs that lower and upper targets appear to be vertically aligned. These points must have the same visual direction since they are perceptually aligned. The straight line, viewed as the binocular visual line, is fitted to the PPAs between the mixed- and equal-contrast targets. The orientation of this line with respect to the veridical direction (straight ahead) indicates the change in visual direction of the mixed-contrast target caused by the interocular contrast difference, with the formula:

For the purposes of describing the data, the angle  $B$  is taken as a measure of the binocular visual direction of the mixed contrast target. Based on Figure 3.11, it is evident that the shift in perceived visual direction can be readily explained by a rotation of the binocular direction line about a fixed cyclopean eye, rather than a change in the location of the cyclopean eye. With the incorporation of varying weights assigned to the monocular measurements of direction, in this manner, the binoculus rotates to the eye receiving the higher contrast image. Therefore, these observations are entirely congruent with the modified conventional theory of binocular visual direction.

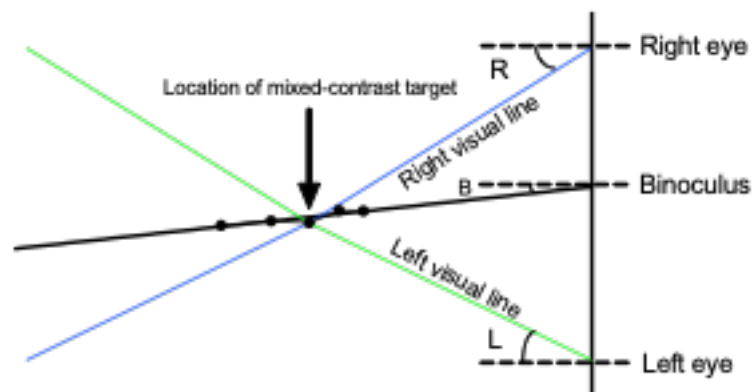


Figure 3.11: A straight line, viewed as the binocular visual line, is fitted to the PPAs between the mixed and equal contrast target. Compared to straight ahead, the angular ( $B$ ) indicates a change in visual direction due to the unequal monocular contrasts.  $L$  and  $R$  represent the orientation (with respect to the straight ahead) of the left and right visual lines passing through the location of mixed-contrast target.

The relationship between interocular contrast ratio and perceived visual direction was modelled using a linear fit:

$$Y = BX + D \quad (3.5)$$

Where  $B$  represents the slope, quantifying sensitivity to contrast imbalance,  $D$  is intercept representing baseline bias.

Table 3.1, 3.2, and 3.3 show the best fitting parameters for six participants measured with correlated patterns. The disparity of the equal-contrast (lower) targets was positioned at either +30, 0 or -30arcmin, respectively.  $B$  indicates the binoculus angle ( $^{\circ}$ ),  $D$  is the distance (cm) away from the midline and the goodness of fit indicated by  $R^2$ . For six participants, the value of  $D$  is below 0.3 cm, suggesting that the shift of the perceived visual direction is due to the rotation of ocular vergence instead of changing the visual egocentre location. The  $R^2$  values show a strong fit across most conditions, particularly for S1, S2, and S3 ( $R^2 > 0.9$  in several cases), confirming that robustness of the model.

Table 3.1: Fit results (Eq. 3.5) of the binocular visual direction from 6 observers when the upper target disparity was fixed at +30arcmin measured with correlated noise patches. The estimates of the three parameters  $B$  ( $^{\circ}$ ),  $D$  (cm) and the goodness of fit described by  $R^2$  are shown.

L:R	Correlated patches								
	4:1			1:1			1:4		
	$B$ ( $^{\circ}$ )	$D$ (cm)	$R^2$	$B$ ( $^{\circ}$ )	$D$ (cm)	$R^2$	$B$ ( $^{\circ}$ )	$D$ (cm)	$R^2$
S1	-0.22**	0.19	0.99	0.07**	-0.05	1.00	0.20**	-0.20	0.93
S2	-0.11*	0.16	0.82	0.11	-0.01	0.71	0.31**	-0.18	1.00
S3	-0.17**	0.20	0.91	0.06*	-0.01	0.77	0.22**	-0.18	0.92
S4	-0.11*	0.24	0.76	0.08	-0.03	0.75	0.12	-0.21	0.39
S5	-0.02	0.14	0.49	0.03	-0.01	0.29	0.11**	-0.11	0.99
S6	0.04	0.14	0.60	0.09**	-0.01	0.92	0.17**	-0.16	0.98

Note: \*  $p < 0.05$ , \*\*  $p < 0.001$

Table 3.2: Fit results (Eq. 3.5) of the binocular visual direction from 6 observers when the upper target disparity was fixed at 0arcmin measured with correlated noise patches. The estimates of the three parameters  $B$  ( $^{\circ}$ ),  $D$  (cm) and the goodness of fit described by  $R^2$  are shown.

L:R	Correlated patches								
	4:1			1:1			1:4		
	$B$ ( $^{\circ}$ )	$D$ (cm)	$R^2$	$B$ ( $^{\circ}$ )	$D$ (cm)	$R^2$	$B$ ( $^{\circ}$ )	$D$ (cm)	$R^2$
S1	-0.15*	0.04	0.92	-0.05	-0.01	0.58	0.06	-0.04	0.57
S2	-0.06*	-0.03	0.84	0.14*	-0.01	0.85	0.25*	0.02	0.93
S3	-0.08*	0.01	0.77	-0.02	0.03	0.48	0.09*	0.01	0.85
S4	0.01	0.03	0.51	0.02	0.02	0.24	0.04	0.02	0.52
S5	-0.05	0.03	0.69	-0.07	0.01	0.67	0.01	0.06	0.52
S6	-0.06	0.03	0.37	0.00	0.04	0.50	0.03	0.04	0.54

Note: \*  $p < 0.05$

Table 3.3: Fit results (Eq. 3.5) of the binocular visual direction from 6 observers when the upper target disparity was fixed at -30arcmin measured with correlated noise patches. The estimates of the three parameters  $B$  ( $^{\circ}$ ),  $D$  (cm) and the goodness of fit described by  $R^2$  are shown.

L:R	Correlated patches								
	4:1			1:1			1:4		
	$B$ ( $^{\circ}$ )	$D$ (cm)	$R^2$	$B$ ( $^{\circ}$ )	$D$ (cm)	$R^2$	$B$ ( $^{\circ}$ )	$D$ (cm)	$R^2$
S1	-0.18**	-0.12	0.97	-0.24**	-0.11	0.98	0.06*	-0.03	0.77
S2	-0.18*	-0.23	0.94	-0.07	-0.07	0.38	0.28**	0.22	0.97
S3	-0.24**	-0.18	0.99	-0.07*	0.00	0.87	0.09**	0.15	0.81
S4	-0.12	-0.17	0.39	0.01	0.01	0.45	0.13*	0.24	0.83
S5	-0.09*	-0.13	0.84	-0.08*	-0.02	0.94	-0.02	0.14	0.55
S6	-0.17**	-0.15	0.96	-0.06	0.00	0.71	-0.17**	-0.15	0.96

Note: \*  $p < 0.05$

Figure 3.12 illustrates the effects of different contrast ratios between the left and the right eye measured with correlated patterns at three depth (-30arcmin, 0arcmin, and 30arcmin) on two fitting parameters:  $B$  ( $^{\circ}$ ) and  $D$ (cm). The y-axis in the left panel represents the binocular angle and in the right panel represents the distance (cm) away from the midline, while x-axis in both panels indicates the contrast ratio between the left and the right eye (4:1, 1:1, 1:4). Bars with different colours correspond to -30 disparity (blue), 0 disparity (green), and -30 disparity (brown). Error bars indicate standard error of mean (SEM). Individual data points are overlaid to show variability across participants. As shown in the Figure 3.12, the

greater disparities result in greater deviations in binocular alignment, but both the changes in binocular angle and displacement remain within  $\pm 0.3$ .

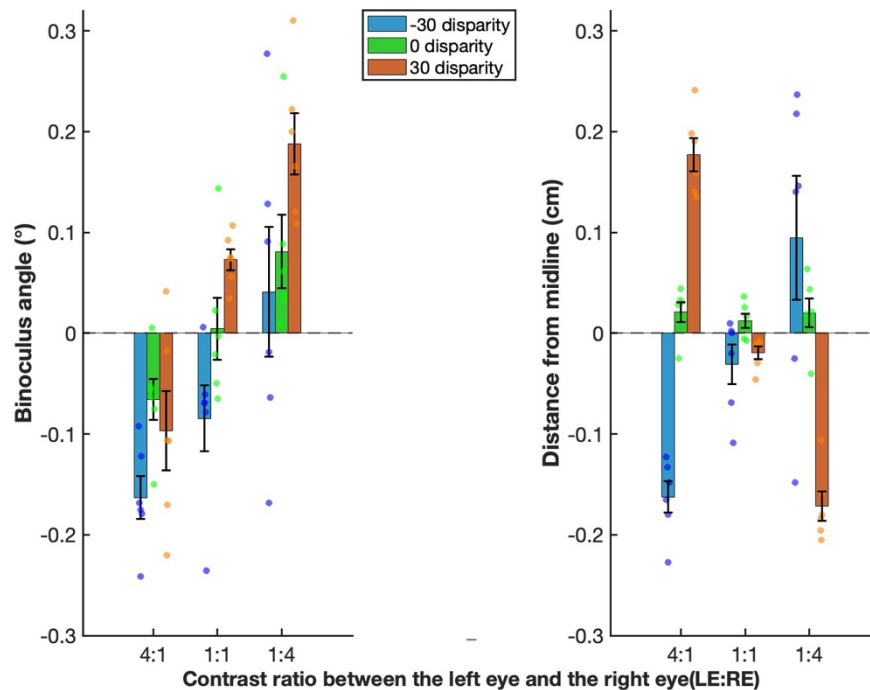


Figure 3.12: The effect of contrast ratio between the left and right eye (LE:RE) measured with correlated patterns across three disparity conditions: -30arcmin (blue), 0arcmin (green), and 30arcmin (brown) on two fitting parameters: B (°) (left ) and D(cm) (right). Error bars indicate standard error of mean (SEM), individual data points are overlaid to illustrate variability across participants.

## 3.4 Experiment 3: Egocentric visual direction

using one-dimensional uncorrelated noise

stimuli

### 3.4.1 Methods

#### 3.4.1.1 Observers

Six observers that participated in Experiment 2, also participated in Experiment 3.



### 3.4.1.2 Apparatus and stimuli

Experiment 3 aimed to investigate the nature of the visual features used by participants to make judgments. That is whether observers used the fine scale spatial detail (e.g. individual noise bars or clusters of bars) or the coarse scale global envelope of the stimuli to support alignment judgements. The stimuli in Experiment 3 were similar to those used in Experiment 2, but crucially the noise samples used for the upper and lower noise pairs were uncorrelated on each trial, rendering only the coarse scale spatial information available to perform the task (see Figure 3.13).



Figure 3.13: Two vertically-separated, Gaussian-windowed, 1-d uncorrelated noise patches used in Experiment 3. The upper and lower targets were quite different.

### 3.4.1.3 Procedure

The procedure was identical to that used in Experiment 2.

## 3.4.2 Results

The data were averaged across the group of 6 participants to demonstrate the overall group result (see Figure 3.14). The data of correlated and uncorrelated noise patches will be different if alignment judgments are based on the finer scale internal structure rather than the coarse scale features. However, the similarity in alignment estimates between correlated and uncorrelated noise patches indicates that these finer details did not impact the observers' judgments. When participants viewed the noise patches, they relied more on the overall shape and

boundaries defined by the Gaussian window, which is a larger, smoother feature. This is likely because coarse scale features are easier to detect. The brain tends to prioritize these features in complex visual environments because they provide essential information about the general structure and layout of objects. This reinforces the idea the brain naturally organizes visual information into whole structures rather than focusing on individual elements. This principle supports the reliance on overall shapes and boundaries, as these provide essential information about the general structure of objects in the visual field (Wagemans et al., 2012).

Table 3.4, 3.5, and 3.6 show the best fitting parameters for six participants measured with uncorrelated patterns. The disparity of the equal-contrast (lower) targets was positioned at either +30, 0 or -30arcmin, respectively.  $B$  indicates the binoculus angle ( $^{\circ}$ ),  $D$  is the distance (cm) away from the midline and the goodness of fit indicated by  $R^2$ . For six participants, the value of  $D$  is below 0.3 cm, suggesting that the shift of the perceived visual direction is due to the rotation of ocular vergence instead of changing the visual egocentre location. The  $R^2$  values show a strong fit across most conditions, confirming that robustness of the model.

Figure 3.15 illustrates the effects of different contrast ratios between the left and the right eye measured with uncorrelated patterns at three depth (-30arcmin, 0arcmin, and 30arcmin) on two fitting parameters:  $B$  ( $^{\circ}$ ) and  $D$ (cm). The y-axis in the left panel represents the binocular angle and in the right panel represents the distance (cm) away from the midline, while x-axis in both panels indicates the contrast ratio between the left and the right eye (4:1, 1:1, 1:4). Bars with different colours correspond to -30 disparity (blue), 0 disparity (green), and -30 disparity (brown). Error bars indicate standard error of mean (SEM). Individual data points are overlaid to show variability across participants. As shown in the Figure 3.15, the greater disparities result in greater deviations in binocular alignment, but both the changes in binocular angle and displacement remain within  $\pm 0.3$ .

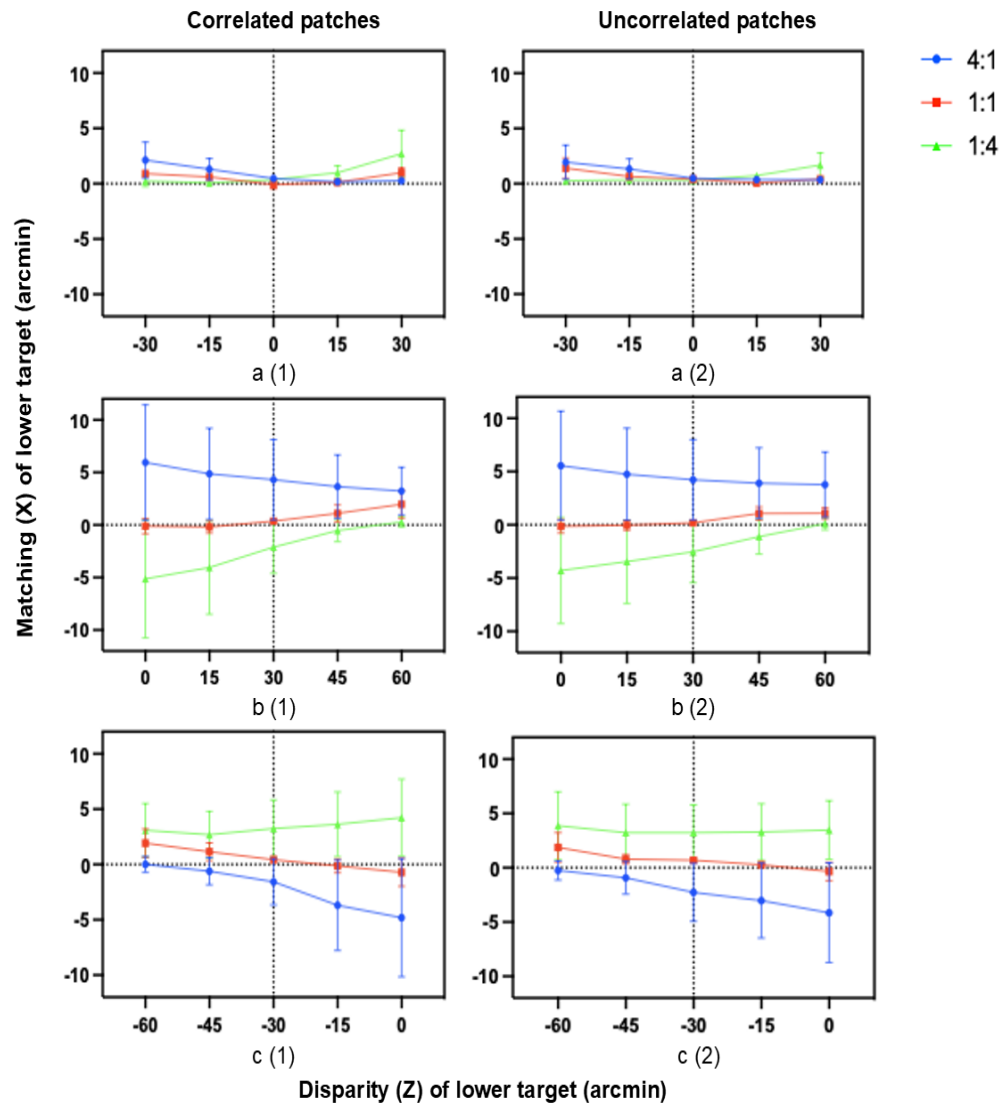


Figure 3.14: Group data of six participants in correlated and uncorrelated patterns. The disparity of upper Gabor was set at 0, +30 and -30arcmin. Each data point represents the X location of lower noise patch that appears vertically aligned with the upper patch. The contrast ratios between the left and right eye are described in different colour of lines as indicated at the right of each diagram. Error bars represent the SEM calculated across repetition of the task.

Table 3.4: Fit results (Eq. 3.5) of the binocular visual direction from 6 observers when the upper target disparity was fixed at +30arcmin measured with uncorrelated targets. The estimates of the three parameters  $B$  ( $^{\circ}$ ),  $D$  (cm) and the goodness of fit described by  $R^2$  are shown.

L:R	Uncorrelated patches								
	4:1			1:1			1:4		
	$B$ ( $^{\circ}$ )	$D$ (cm)	$R^2$	$B$ ( $^{\circ}$ )	$D$ (cm)	$R^2$	$B$ ( $^{\circ}$ )	$D$ (cm)	$R^2$
S1	-0.18*	0.20	0.89	0.04	-0.05	0.74	0.17**	-0.17	0.91
S2	-0.10*	0.13	0.88	0.09**	-0.04	0.91	0.21**	-0.16	0.94
S3	-0.10*	0.19	0.76	0.00	0.02	0.01	0.21**	-0.16	0.99
S4	-0.01	0.18	0.06	0.03	0.00	0.50	0.07	-0.17	0.45
S5	-0.02	0.13	0.55	0.04	0.00	0.44	0.08	-0.11	0.76
S6	0.02*	0.16	0.81	0.07*	0.00	0.82	0.15**	-0.15	0.95

Note: \*  $p < 0.05$ , \*\*  $p < 0.01$

Table 3.5: Fit results (Eq. 3.5) of the binocular visual direction from 6 observers when the upper target disparity was fixed at 0arcmin measured with uncorrelated targets. The estimates of the three parameters  $B$  ( $^{\circ}$ ),  $D$  (cm) and the goodness of fit described by  $R^2$  are shown.

L:R	Uncorrelated patches								
	4:4			1:1			1:4		
	$B$ ( $^{\circ}$ )	$D$ (cm)	$R^2$	$B$ ( $^{\circ}$ )	$D$ (cm)	$R^2$	$B$ ( $^{\circ}$ )	$D$ (cm)	$R^2$
S1	-0.13*	0.05	0.87	-0.04	0.00	0.41	-0.01	-0.05	0.53
S2	-0.07	-0.01	0.69	0.03	0.00	0.45	0.13*	0.02	0.84
S3	-0.07*	0.02	0.77	-0.02	0.00	0.65	0.06*	0.01	0.85
S4	0.01	0.02	0.58	0.03	0.01	0.74	0.05*	0.00	0.77
S5	0.04**	0.02	0.92	-0.02	0.01	0.22	-0.01	0.05	0.45
S6	-0.03	0.03	0.32	-0.05	0.04	0.73	0.03	0.05	0.33

Note: \*  $p < 0.05$ , \*\*  $p < 0.01$

Table 3.6: Fit results (Eq. 3.5) of the binocular visual direction from 6 observers when the upper target disparity was fixed at -30arcmin measured with uncorrelated targets. The estimates of the three parameters  $B$  ( $^{\circ}$ ),  $D$  (cm) and the goodness of fit described by  $R^2$  are shown.

L:R	Uncorrelated patches								
	4:1			1:1			1:4		
	$B$ ( $^{\circ}$ )	$D$ (cm)	$R^2$	$B$ ( $^{\circ}$ )	$D$ (cm)	$R^2$	$B$ ( $^{\circ}$ )	$D$ (cm)	$R^2$
S1	-0.17**	-0.12	0.99	-0.18*	-0.08	0.88	-0.08**	-0.03	0.92
S2	-0.10**	-0.17	0.97	-0.05**	-0.04	0.91	0.09*	0.11	0.87
S3	-0.14**	-0.14	0.99	-0.04	0.02	0.61	0.04	0.14	0.53
S4	0.01	-0.11	0.54	0.02	0.03	0.32	0.02	0.15	0.48
S5	-0.15	-0.17	0.75	-0.04	-0.01	0.64	-0.01	0.17	0.03
S6	-0.16**	-0.14	0.99	-0.09**	-0.01	0.94	-0.05	0.15	0.56

Note: \*  $p < 0.05$ , \*\*  $p < 0.01$

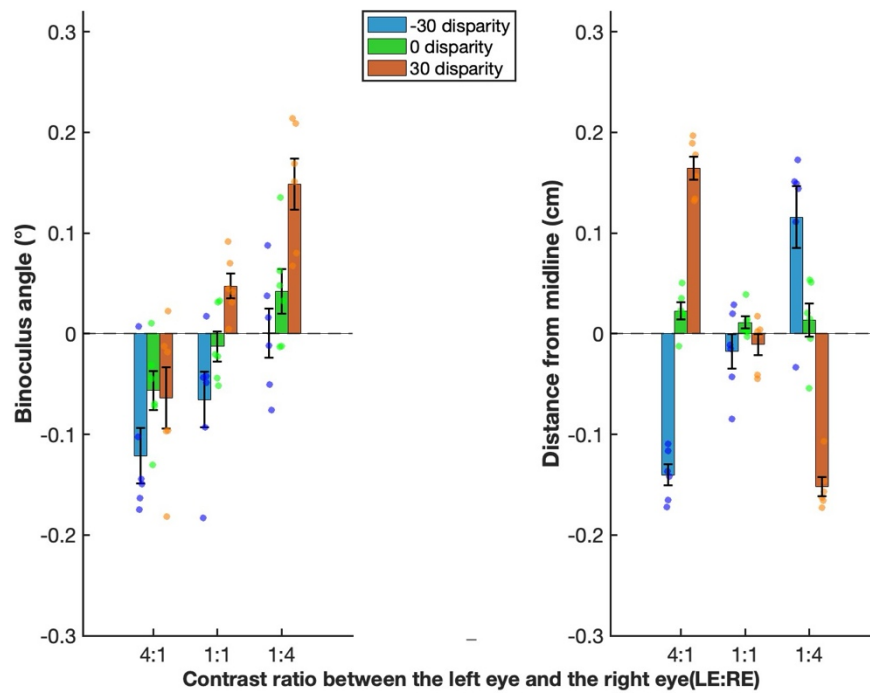


Figure 3.15: The effect of contrast ratio between the left and right eye (LE:RE) measured with uncorrelated patterns across three disparity conditions: -30arcmin (blue), 0arcmin (green), and 30arcmin (brown) on two fitting parameters:  $B$  ( $^{\circ}$ ) (left) and  $D$ (cm) (right). Error bars indicate standard error of mean (SEM), individual data points are overlaid to illustrate variability across participants.

## 3.5 Experiment 4: Comparison with longer presentation.

Experiment 3 showed that there was no difference between the patterns of results found using correlated and uncorrelated one-dimensional noise patterns. However, it is unknown if this consistency was a consequence of the very brief duration (150ms) of the stimuli, as participants may not have sufficient time to process and compare the fine internal spatial details of the two vertically-separated stereo patches containing the same noise sample in Experiment 2. Indeed, there is much evidence that stereoscopic-depth perception may be mediated by two distinct systems (transient versus sustained stereopsis), operating over different timescales and with different properties (e.g. Schor, Edwards, & Pope, 1998). If this was the case, participants are able to utilise fine spatial scale information when it is available for a sustained period of time, one might expect a different result using correlated versus uncorrelated patterns when the stimuli are presented for a longer duration.

### 3.5.1 Methods

#### 3.5.1.1 Participants

Six participants participated in Experiment 3, also participated in Experiment 4.

#### 3.5.1.2 Apparatus and stimuli

This experiment used both the correlated and uncorrelated noise patterns as stimuli.

#### 3.5.1.3 Procedure

The procedure was identical to that used in Experiment 3 with the exception that the presentation of stereo patches lasted 1s, which was

consistent with Experiment 1. Only one disparity condition was measured in this experiment, in which the upper patch was located at fixation (0arcmin). The disparity of the lower patch ranged from -30 to +30arcmin. The same contrast parameters were measured to that used in Experiment 3.

### 3.5.2 Results

Our findings with brief presentation (150ms) stimuli were robust and not dependent on the operation of a transient stereo vision mechanism as we obtained similar results even with a much longer presentation which should favour a sustained stereo mechanism (see Figure 3.16). Since there is no difference between the results using correlated and uncorrelated targets, this suggests that alignment judgements were made using the overall coarse spatial scale of the Gaussian envelope (window) rather than the finer scale internal structure. Figure 3.16 depicts the data of all six participants when disparity of the upper noise patch was located at 0 arcmin and measured with both correlated and uncorrelated patterns. Consistent with Figure 3.14b, the perceived visual direction remains along the  $X = 0$  horizontal line, regardless of different interocular contrast differences. This indicates that the visual direction does not shift towards the eye with the more visible image.

Figure 3.17 depicts the best fitting straight lines to the alignment data, which is a replot of the data for the six subjects from Figure 3.16. Similarly, Z and X have been transformed into physical distance (cm). The left and right visual lines passing through the mixed-contrast target are also plotted. In Figure 3.17, the best fitting straight line through these points for each contrast ratio (different colours represent different contrast ratios) are considered to represent the binocular visual line. According to Figure 3.17, the displacements from the  $X = 0$  horizontal line for participants were generally minimal, not exceeding 1cm. However, participants S1 and S2 showed slightly larger displacements, which were still less than 1 cm, especially when their right eye received a higher contrast image. This

may be due to their right eye dominance influencing their judgments. No significant differences were observed between correlated and uncorrelated patterns, indicating that alignment judgments were based on the overall coarse structure. Therefore, the results were consistent with the modified conventional model (Banks *et al.*, 1997), which posited that the cyclopean eye is fixed and does not shift towards the eye with a higher contrast image. The fitted parameters (Eq.3.3) for binocular visual direction under three contrast ratios with correlated patterns are presented in Table 3.7 and visualized in Figure 3.18. The uncorrelated patterns are presented in Table 3.8 and visualized in Figure 3.19.

The distance (D value) was consistent small (with  $D < 0.06$ ) across all conditions and participants, indicating no systematic deviation from the midline. Figure 3.18 and Figure 3.19 demonstrates the effects of interocular contrast difference on binocular visual direction judgments for correlated targets and uncorrelated targets, respectively. The y-axis in the left panel represents the binocular angle and in the right panel represents the distance (cm) away from the midline, while x-axis in both panels indicates the contrast ratio between the left and the right eye (4:1, 1:1, 1:4). Error bars indicate standard error of mean (SEM). Individual data points are overlaid to show variability across participants. The stable displacement confirms that the cyclopean eye is fixed rather than shifting to the eye receiving a more visible image.



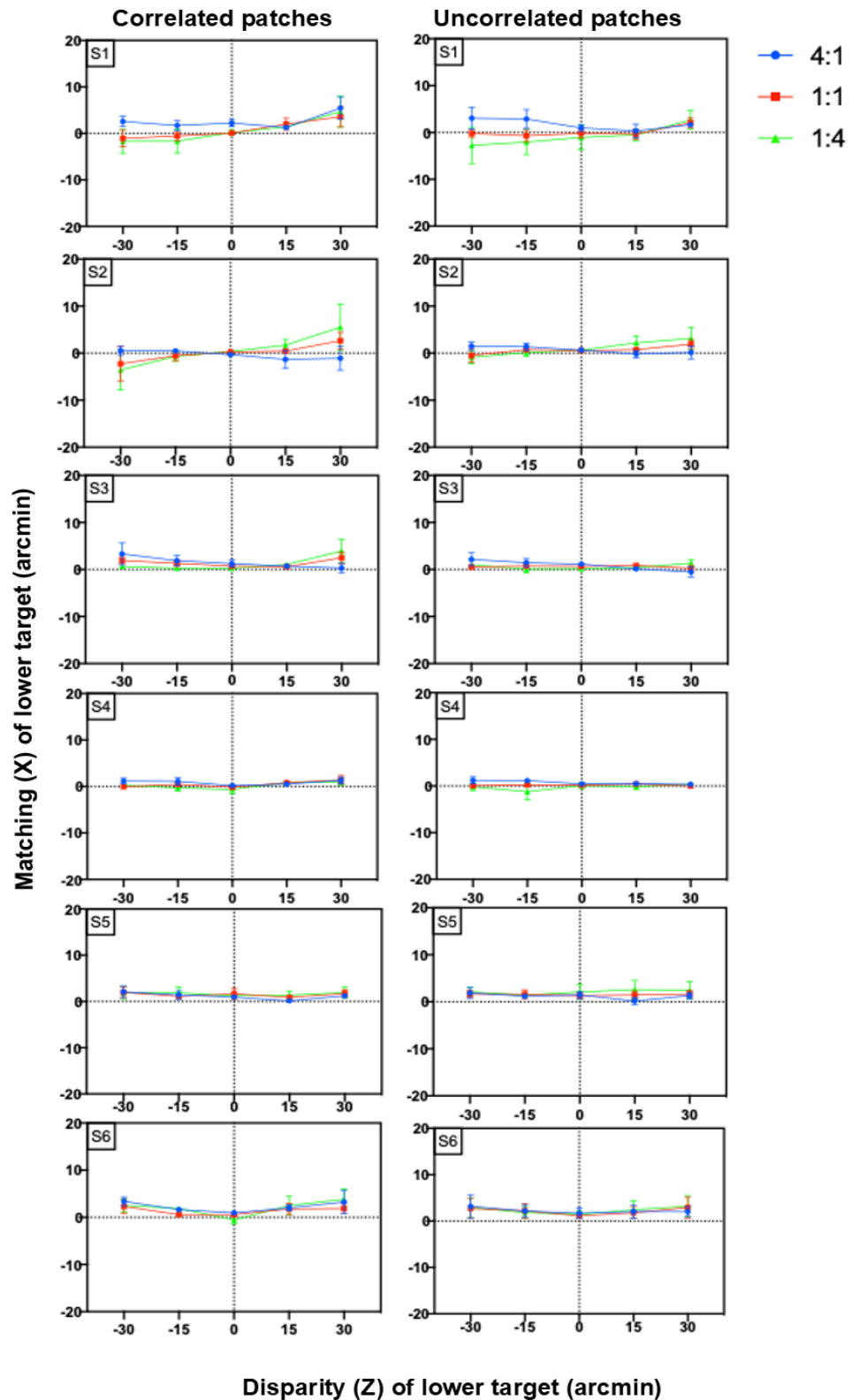


Figure 3.16: Individual data of six observers viewing with correlated and uncorrelated patterns. The upper Gabor was located at 0arcmin. Each data point represents the X location of lower noise patch that appears vertically aligned with the upper patch. The contrast ratios between the left and right eye are described in different colour of lines as indicated at the right of each diagram. Error bars represent the SEM calculated across repetition of the task.

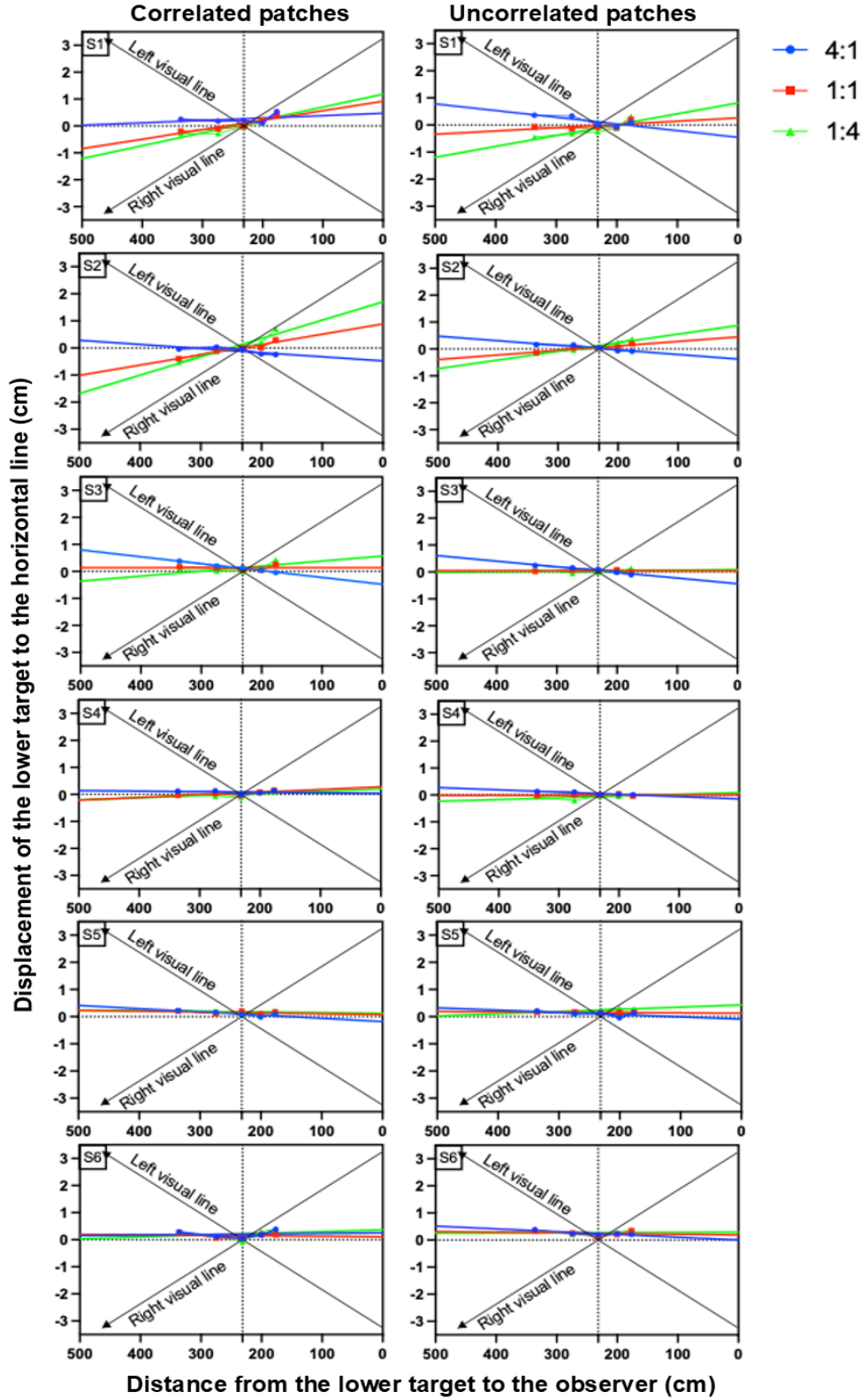


Figure 3.17: Data from 6 observers with 1s presentation is replotted with X and Z converted into physical distances when viewing with both correlated and uncorrelated patterns. Each data point represents the X location of lower noise patch that appears vertically aligned with the upper patch. The contrast ratios between the left and right eye are described in different colour of lines as indicated at the right of each diagram. Error bars represent the SEM calculated.

Table 3.7: Fit data (Eq. 3.5) of the binocular visual direction from 6 observers when the upper target disparity was fixed at 0 arcmin measured with correlated targets and longer presentation. The estimates of the three parameters  $B$  ( $^{\circ}$ ),  $D$  (cm) and the goodness of fit described by  $R^2$  are shown.

	Correlated patches								
	4:1			1:1			1:4		
	$B$ ( $^{\circ}$ )	$D$ (cm)	$R^2$	$B$ ( $^{\circ}$ )	$D$ (cm)	$R^2$	$B$ ( $^{\circ}$ )	$D$ (cm)	$R^2$
S1	0.05	0.06	0.18	0.15**	0.01	0.95	0.20*	0.00	0.89
S2	-0.07	-0.02	0.73	0.15*	-0.01	0.90	0.27*	0.01	0.94
S3	-0.10**	0.03	0.96	0.01	0.03	0.61	0.08	0.03	0.51
S4	-0.03*	0.01	0.82	0.00	0.00	0.50	0.03	-0.02	0.32
S5	-0.04	0.03	0.55	-0.01	0.04	0.47	-0.01	0.04	0.44
S6	0.02	0.05	0.47	0.00	0.04	0.40	0.04	0.05	0.42

Note: \*  $p < 0.05$ , \*\*  $p < 0.01$

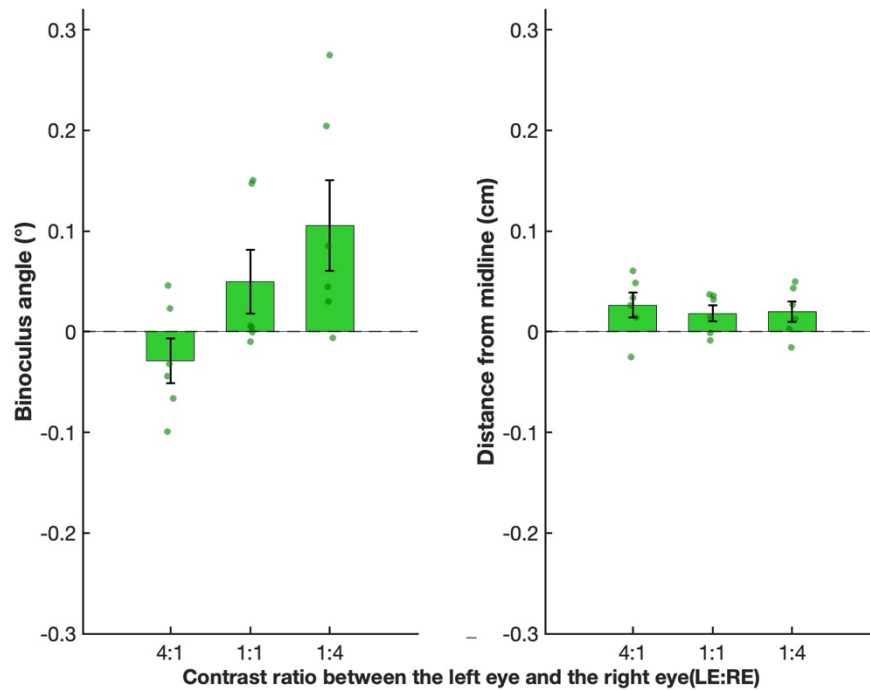


Figure 3.18: The effect of contrast ratio between the left and right eye (LE:RE) measured with correlated patterns at 0 arcmin on two fitting parameters:  $B$  ( $^{\circ}$ ) (left) and  $D$  (cm) (right). Error bars indicate standard error of mean (SEM), individual data points are overlaid to illustrate variability across participants.

Table 3.8: Fit results (Eq. 3.5) of the binocular visual direction from 6 observers when the upper target disparity was fixed at 0 arcmin measured with uncorrelated targets and longer presentation. The estimates of the three parameters  $B$  ( $^{\circ}$ ),  $D$  (cm) and the goodness of fit described by  $R^2$  are shown.

	Uncorrelated patches								
	1:4			1:1			4:1		
	$B$ ( $^{\circ}$ )	$D$ (cm)	$R^2$	$B$ ( $^{\circ}$ )	$D$ (cm)	$R^2$	$B$ ( $^{\circ}$ )	$D$ (cm)	$R^2$
S1	-0.09	0.03	0.53	0.06	-0.01	0.41	0.17*	-0.04	0.83
S2	-0.07**	0.01	0.92	0.07*	0.01	0.82	0.13**	0.02	0.97
S3	-0.09**	0.02	1.00	0.00	0.01	0.42	0.02	0.01	0.41
S4	-0.03*	0.01	0.82	0.00	0.00	0.40	0.03	-0.02	0.32
S5	-0.03	0.03	0.22	0.00	0.04	0.44	0.03	0.06	0.51
S6	-0.03	0.06	0.46	0.00	0.06	0.50	0.01	0.06	0.45

Note: \*  $p < 0.05$ , \*\*  $p < 0.01$

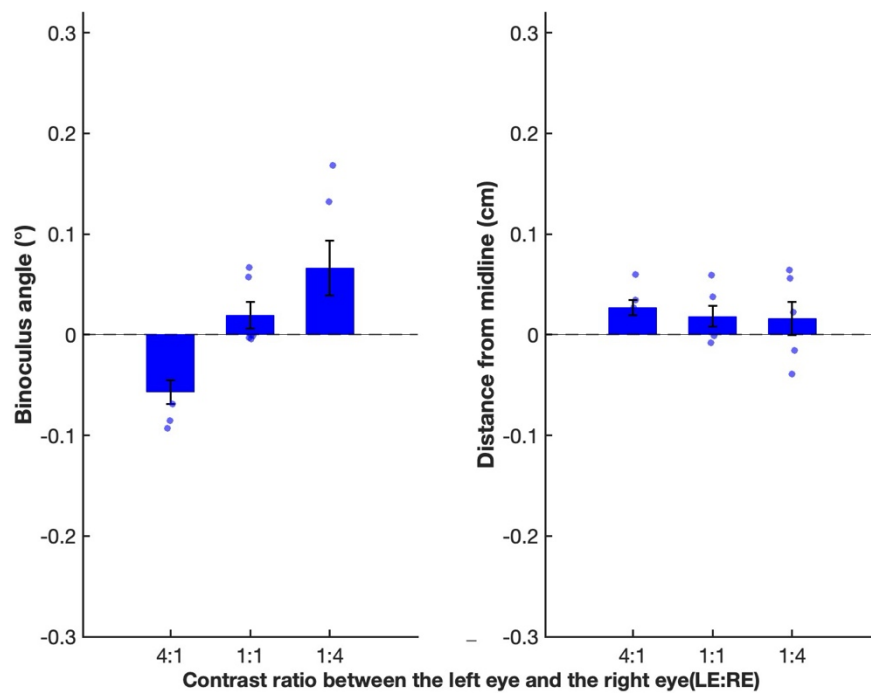


Figure 3.19: The effect of contrast ratio between the left and right eye (LE:RE) measured with uncorrelated patterns at 0 arcmin (on two fitting parameters:  $B$  ( $^{\circ}$ ) (left) and  $D$  (cm) (right). Error bars indicate standard error of mean (SEM), individual data points are overlaid to illustrate variability across participants.

### 3.6 Discussion

When the target image appears at different locations in the two eyes, estimates of binocular visual direction become ambiguous. This ambiguity arises because identical retinal disparities can result from different real-world configurations. To resolve this conflict, the brain must rely on additional cues—such as occlusion, perspective, or prior knowledge—to disambiguate the perceived direction. The perceived visual direction of the fused image is from the left and right eye (e.g., Walls, 1951), it is perceived as if viewing from one imagery eye, the cyclopean eye (or the visual egocentre) which is believed as the average of the monocular images (e.g., Hering, 1879; Ono, 1981; Wells, 1792). It has long been established that differences in target luminance between the eyes affect perceived visual direction (Charnwood, 1949; Francis & Harwood, 1951; Verhoeff, 1933, 1935). This finding led Mansfield and Legge (1996) to propose a novel model based on which the most likely direction given the noisy direction estimations communicated by the left and right eyes is selected. This model takes into consideration variations in visual direction affected by interocular contrast differences. According to the theory of Mansfield and Legge (1996), the cyclopean eye was not fixed, but rather was able to shift along the interocular axis in response to the relative contrast ratios presented to each eye. Nevertheless, Banks et al. (1997) argued that their findings cannot be explained by a wandering cyclopean eye, as the alignment task is unable to pinpoint the location of the cyclopean eye without assuming a wandering cyclopean eye, Banks et al. (1997) modified the conventional model by adding varying weights allocated to the monocular direction measurements.

Figure 3.20 describes the predictions of these two models measured at three different stereoscopic depths, in which the upper patch was located on the vertical midline ( $X = 0$  arcmin) with a disparity ( $Z$ ) of 0, +30, and -30 arcmin. The solid lines show the model of Mansfield and Legge (1996), while the dashed lines correspond to the model of Banks et al. (1997). Different contrast ratios between the two eyes are depicted by different

colours and symbols. The tendency of the solid lines is constant throughout stereoscopic depth settings, suggesting that the perceived visual direction is biased to the eye receives a higher contrast image. The dashed lines behave very differently in three stereoscopic depth conditions, suggesting that the cyclopean eye is fixed in the middle between the two eyes, but the binocular direction line can rotate relative to this cyclopean eye to change perceived visual direction if the two eyes' inputs are unbalanced.

The results of this study suggest that both depths and interocular contrast differences have an effect on perceiving the binocular visual direction. In line with earlier research showing that interocular brightness differences (e.g., Charnwood, 1949) impact visual direction, interocular contrast imbalance also somewhat influences how one perceives visual direction. As there was no difference between the results using correlated and uncorrelated luminance-balanced, aperiodic, one-dimensional noise stimuli with either relatively brief or longer presentation durations, suggesting that alignment judgments were made based on using the overall coarse spatial scale of the Gaussian envelope rather than the finer scale internal structure. For visual decision-making, this phenomenon indicates that the brain prioritizes broader and more prominent features, indicating the brain arranges visual information into whole structures instead of concentrating on individual components (Wagemans et al., 2012).

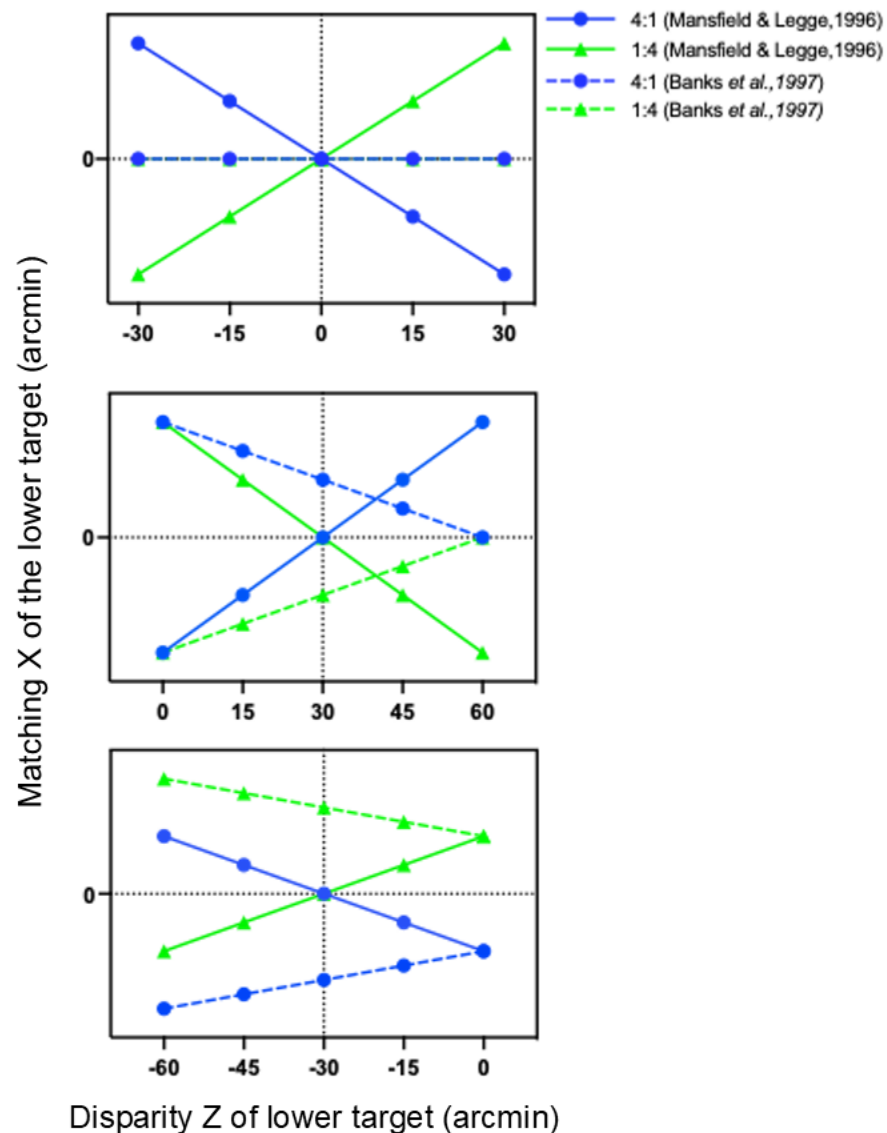


Figure 3.20: The prediction of two models. The solid lines represent the model predictions of Mansfield and Legge (1996) and the dashed lines represent those of Banks *et al.* (1997). Three depths conditions were compared: 0 arcmin (top), 30 arcmin (middle) and -30 arcmin (bottom). Different colours and symbols depict different contrast ratios between the left and right eyes. The solid lines show that the location of egocentre shifts towards the eye receiving a more visible image, whereas the dashed lines describe that the location of egocentre is fixed, but the vergence of egocentre changes when one eye receives a higher contrast image.

The results are more biased toward the modified conventional model (Bank *et al.*, 1997) based on the best fitting parameters of binocular angle and displacement from the midline. Therefore, binocular visual line changes are caused by ocular vergence rather than the location of the cyclopean eye when contrast imbalances occur between the two eyes.

The influence of contrast sensitivity varies depending on the area of the visual field when discussing contrast imbalances between the two eyes. Due to the high density of cone photoreceptors in the fovea, the central region of the visual field is the most contrast sensitive. As contrast sensitivity declines from the fovea to the peripheral retina, the peripheral retina is more sensitive to low light levels (Wright & Johnston, 1983). Which portion of the retina is exposed to the stimuli depends on the eye position, and this has a distinct effect on contrast sensitivity. Consequently, when contrast imbalance occurs between the two eyes, changes in perceived visual direction may be attributed to changes in eye position or vergence. Mansfield and Legge (1996), on the other hand, did not record eye movement because they believed that eye position would not influence directional judgments. Consequently, they were unable to take into account the variation in vergence in all experimental situations.

Furthermore, Mansfield and Legge (1996) highlighted the distinction between detecting stereo depth and visual direction, suggesting that the geometrical model is not straightforward if the images from the left and right eye are not stereoscopically integrated. Stereo depth perception necessitates that the stimulus be detected in both eyes (Hawken, Parker, & Simmons, 1987; Simmons, 1992; Simmons & Kingdom, 1994), whereas visual direction can be determined as long as the stimulus is detectable in either one or both eyes. Consequently, the accuracy of stereo depth judgments is constrained by the noise in the least sensitive monocular channel (Legge & Gu, 1989), while binocular visual direction judgment is constrained by the noise in the most sensitive monocular channel. There is a critical interocular contrast ratio, beyond which achieving stereo fusion becomes impossible (Smallman & McKee, 1995). This can potentially explain the diplopia that was reported by our participants in some cases when viewing the correlated one-dimensional noise conditions, especially when the upper patch was presented with a disparity of -30arcmin.



As predicted by the fusion theory, dichoptic stimuli with a small disparity were perceived as single. When the upper target was located at a depth of -30arcmin (an uncrossed disparity), the target moved back to the fixation point, and the subject perceived a sense of plasticity in the depth difference between the fixation marker and target. In terms of Panum's fusional area, this disparity corresponds to the outer border of binocular single vision (Ogle, 1952). Therefore, there is a reported difficulty in fusing the stimuli, and thus diplopia is perceived. As fusion may not always be achieved in all cases, the relative direction between the two targets is determined by the eye that can see both targets if the contrast in one eye is below the detection threshold. However, an absolute direction alignment task should be employed if they want to conclude there is a wandering cyclopean eye shifting along the interocular axis. In terms of a fixed cyclopean eye, whether it is located centrally or non-centrally, the origin of all visual directions remains consistent. However, the origin of a wandering cyclopean eye changes depending on the stimulus setting; the direction of objects relative to the participant must be continually recalibrated (Mapp & Ono, 1999).

The binocular visual line, an imaginary line that depicts the combined direction of gaze from both eyes, rotates markedly when two eyes receive unequal contrast images, according to Banks *et al.*'s (1997) theory. As a result, the brain gives more weight to the eye presented with a higher-contrast image. As compared with the minor shifts in cyclopean eyes, this rotation is more substantial. In many studies, the terms effective viewpoint and cyclopean eye have been blurred (e.g., Charnwood, 1949; Francis & Harwood, 1951; Erkelens & van de Grind, 1994). The effective viewpoint refers to the actual position where objects are observed. Erkelens and colleagues (1996) characterized it as a local centre of direction that could be situated at the left eye, the right eye, or midway between the eyes. The position of this local centre of direction varies depending on whether the alignment targets are situated near a region that was monocularly occluded. The cyclopean eye represents the perceived point from which egocentric direction judgments are formed,

essentially signifying the perceived “self” location. Accordingly, their claim that the effective viewpoint moves to the eye receiving higher contrast does not differ much from their initial argument that the cyclopean eye moves, and, as such, it is subject to all the same criticisms discussed by Banks et al. (1997).

In summary, the results of the current study are consistent with models in which binocular visual direction is computed by a weighted average of the monocular directions and favour coarse-scale information. Nonetheless, future work should aim to develop tasks that can measure the location of the cyclopean eye directly, as the current experiments cannot decisively establish its precise location within an individual. Understanding how human binocular vision determines the directions of objects in space relative to the viewer has important implications not only for basic science but for many ocular diseases where input to one eye is modified, such as cataracts and amblyopia.

# Chapter 4. Measurement of the visual egocentre location

## 4.1 Introduction

When determining the direction of a visual object relative to the head, it is necessary to take into account the positions of the images in the eyes (the oculocentric component) and the angle of the eyes with respect to the head (the eye-position component) (Howard & Rogers, 1995). A visual object fixated by the two eyes has a different (monocular) direction in each eye, yet it's judged to have a single direction in space. Though our two eyes receive distinct images, the visual system combines them into a single unified representation of world, termed the cyclopean view. This concept was first proposed by Alhazen in the eleventh century - he used the term "centre" rather than "cyclopean eye". Later, Hering (1868/1977), during a discussion on binocular visual direction, introduced the concept of a hypothetical body anchor point to serve as a reference for judging the direction of objects relative to the viewer. The point, situated midway between the two eyes, has been given various names, such as the "cyclopean eye", "projection centre", "binoculus" and the "visual egocentre" (Howard, 1982). The idea of a cyclopean eye acting as a reference for visual direction persisted without substantial challenge for almost a century (see Fry, 1950) until Walls (1951) introduced a new theory of egocentric localization. According to Walls, visual direction is referenced against the dominant eye's visual line (or sighting dominance) rather than against a hypothetical interocular projection centre. Julesz (1971) extended Hering's ideas and proposed that the processing of cyclopean perception resides at a central location in the human brain. The first opportunity for the visual system to combine outputs from each eye into a single unified representation is the primary visual cortex (area V1 in primates). Hubel and Wiesel (1962, 1968) found that a majority of the cortical cells in area 17 of the cat and area 18 of the monkey could

be driven binocularly. More recent evidence from neuroimaging in humans suggests that V1 provides a representation of the stimulus position in each eye, while responses in V2 and other extrastriate cortical regions are better predictors of the location of cyclopean images (Barendregt et al., 2015).

Wells's (1792) three propositions together illustrate how visual direction is affected by the alignment of objects with various visual axes and visual lines. According to Proposition I, even when an item is directly aligned with the optic axis, it appears to be viewed in the common axis, indicating that visual perception changes from the optic axis to the common axis. A shift in perception from the common axis to the individual axis of the eye is indicated by Proposition II, which demonstrates that an object aligned with the common axis does not appear to be on it, but rather on the axis of the eye that is unable to see them. The first two propositions, as special cases of Proposition III, can therefore be deduced from it. Proposition III, as the core proposition of Wells's theory, describes a more complex and comprehensive phenomenon of visual direction perception, covers the perceptual shift in different situations, and reveals the influence of binocular disparity on stereopsis. Wells's theory not only explains why the objects' position we see may not correspond to their actual positions, but also demonstrates an early attempt to codify the relationship between the physical and perceived locations of objects in the visual field.

Wells (1792) focused on the descriptive observation of how objects are perceived in different visual axes instead of relying on constructs, but his research was not widely understood or recognized until Hering (1879/1942) developed a comprehensive explanation of visual direction. Hering (1879/1942) posited that the direction of an object is determined by projecting the retinal image to a hypothetical "cyclopean eye", based on retinal points in both eyes corresponding to the visual direction. Hering's law incorporated hypothetical constructs such as the cyclopean eye, corresponding points, and identical visual direction, focusing on how the brain combines images from two eyes to create a unified visual

direction. Accordingly, researchers have devoted a great deal of effort to understanding how people determine the location of the cyclopean eye (or the visual egocentre) and to formalizing the various principles of visual direction (González, Steinbach, & Ono, 1999). There is ongoing debate on the exact location of the cyclopean eye. One of the hypotheses, had been remained unchallenged for nearly a century, suggested that the cyclopean eye is located at the midway between the two eyes (Fry, 1950; Hering, 1868/1977, 1879/1942; Le Conte, 1881). Walls (1951) proposed that the egocentric visual direction is determined by the sighting dominant eye, or the dominant eye (Parson, 1924; Porac & Coren, 1981; Rubin & Walls, 1969; Sheard, 1926). This phenomenon of the non-sighting eye being temporarily suppressed during the visual alignment task led to this hypothesis. These two hypotheses led to one question - where is the exact position of the visual egocentre (or the cyclopean eye)? The precise position of the visual egocentre can be measured behaviourally in the laboratory using psychophysical techniques, and a number of different methods have been developed for this purpose (Barbeito & Ono, 1979).

Four of these methods will be described briefly: two of them (Funaishi, 1926; Howard & Templeton, 1966) attempt to estimate the egocentre location independently of the law of visual direction, whereas the other two (Fry, 1950; Roelofs, 1959) rely on the law of visual direction and estimate the location based on an observer's response (Ono, 1991 - see Figure 1.14 in Chapter1). In Howard and Templeton's (1966) method, an observer was asked to align two stimuli (near and far) until the imaginary axis joining them was judged to point directly at themselves. The intersection point of the projected axes is taken as the egocentre (see Figure 1.14 (a)). Funaishi's (1926) task required an observer to fixate a point and then judge the direction of a non-fixated point placed to the left or right of the fixation point in the same frontal parallel plane. The apparent direction of the targets and lines are projected back through the response locations to estimate the egocentre (see Figure 1.14 (b)). Roelofs's (1959) method required the observer to fixate on the front of a

tube with one eye, while the other eye is occluded, and indicate a point on the illusory line that is perceived between them. In accordance with Hering's (1879/1942) principles of visual direction, the tube will appear to be pointing forward along a radial line joining the subject's egocentre and the tube's front, rather than corresponding to its objective direction. As defined above, the apparent direction of the tube is regarded as the projection from its front to a point on the observer's face at which the tube is pointing, such that the projection is considered to pass through the egocentre (see Figure 1.14 (c)). For Fry's (1950) measurement, an observer was required to binocularly fixate on one of two stimuli (the farther target in Figure 1(d)) and indicate the apparent location of each diplopic image produced by the non-fixated stimulus (the closer one). The observer used a pointing device to mark these locations, ensuring that the hand used for pointing was not visible to maintain the accuracy of the perceived direction. Lines, projected from the indicated location of the diplopic images back towards the observer, are assumed to pass through the egocentre (see Figure 1.14 (d)).

After comparing the predictive validity (the ability to predict responses on other visual direction tasks) and reliability (rest-retest stability) of these four methods, Barbrito and Ono (1979) concluded that the approach proposed by Howard and Templeton (1966) provided the best estimate of the location of the egocentre - the reference point used to perform this task could be located with much greater precision. Howard and Templeton's method required direct visual judgments, while the other three methods introduced potential sources of error (asking subjects to point to a location in space using their hands) to the visual judgment. Based on the predictive validity of Howard and Templeton's method, the locations determined by it were most effective in predicting individual differences across three different visual direction tasks. As a result, the method's high precision is attributed to the lack of manual pointing responses as a source of variability (Barbrito & Ono, 1979). In addition, individual differences in constant errors associated with pointing to a location in space manually may obscure true variation in egocentre

location and inflate estimate reliability, reflecting variations in constant error rather than the true egocentric localization (Barbrito & Ono, 1979; Mitson et al., 1976; Ono et al., 1972). Furthermore, manual pointing errors in different methods could lead to different egocentre locations, which may explain offsets in egocentre location – it's more rightward in the Roelofs's (1959) methods compared with Furnishi's (1926) method. We choose to employ a similar paradigm based on the approach used by Howard and Templeton (1966), but in order to reduce errors in the alignment between the two stimuli, we used a rod instead. The rod is free to rotate until its near front side (the one closer to the observer) directly toward the observer. In order to explore the true individual variations in the egocentre location that eliminates the effects of measurement error or systematic biases, both binocular and monocular sighting tasks are conducted based on this paradigm to investigate the egocentre locations and correlate the horizontal separations with the physical Inter-Pupil distance (IPD) among individuals. Individual difference studies can be used to compare visual characteristics between different populations, such as gender differences, age differences, and differences between patients with certain diseases and normal people (Mollon et al., 2017). These variations can give us deeper understanding of the workings of the visual system and are crucial in the clinical domains, such as investigating the biological causes of illnesses and linking specific visual characteristics to specific clinical symptoms.

## 4.2 Experiment 5: Variation in the location of the visual egocentre measured using a monocular and binocular sighting task

### 4.2.1 Methods

#### 4.2.1.1 Observers

Twenty-six participants ( $N = 26$ , age range: 23-53years, mean age:  $30.76 \pm 7.76$ years) took part in this experiment. The participants all had normal or corrected-to-normal vision and no history of ocular disease. Before formal data collection began, the TNO stereo test (Lam´eris Ootech, Nieuwegein, The Netherlands) was presented orthogonally at a distance of approximately 40cm. The observer utilized red-green anaglyph spectacles to discern the orientation of a cyclopean object depicted within random-dot stereograms. The smallest disparity at which accurate identification could be reliably achieved was recorded as a measure of stereoacuity. We first presented Plate III to ensure each of the participants had normal stereo vision and thus was able to perceive the depth and 3-dimension structure of visual information (range from 60 to 120 arcsec). The observer then was presented with Plate V-VII, in which six pairs of figures are characterized by retinal disparities of 480, 240, 120, 60, 30 and 15arcsec, respectively. It would be used for exact determination of stereoscopic sensitivity. The experiment was approved by the School of Psychology Ethics Committee at the University of Nottingham. Participants gave informed consent before the experiment and all experimental procedure conformed to the guidelines laid out in the Declaration of Helsinki.

#### 4.2.1.2 Apparatus and Stimuli

We used a custom-built sighting apparatus consisted of a stainless-steel rod (19cm length, 0.25cm diameter located approximately 34cm from



bridge of nose) mounted on a Thorlabs' PR01/M Metric Precision Rotation platform, which could be smoothly and continuously rotated by hand through a full 360°, measured by the 1° graduation marks on the side of the stage when the steel locking thumbscrew was unlocked (Figure 4.1). The micrometre could provide  $\pm 5^\circ$  of fine adjustment, measured with 5 arcmin resolution, by means of a Vernier scale. As shown in Figure 4.1, the PR01A/M Adapter Plate was attached to the top of the PR01/M Rotation Stage, in which a PM5(/M) stainless-steel clamping arm was mounted in the centre of the adapter plate and the distance from the adapter plate centre to the contact point that holds the rod was 2.286cm. Using this apparatus, the visual egocentre was measured using both a monocular and a binocular sighting task. During the task, the participant sat at a specially constructed table with their head supported by a chin rest. They fixated on the front end the rod (coloured red) and rotated the orientation of the rod in the horizontal plane until it pointed to either their right eye, left eye or directly towards them during binocular viewing. Fine adjustments could be made using a screw mechanism on the edge of the stage. The entire stage could be rotated in an arc around the participant's head to vary the viewing angle.

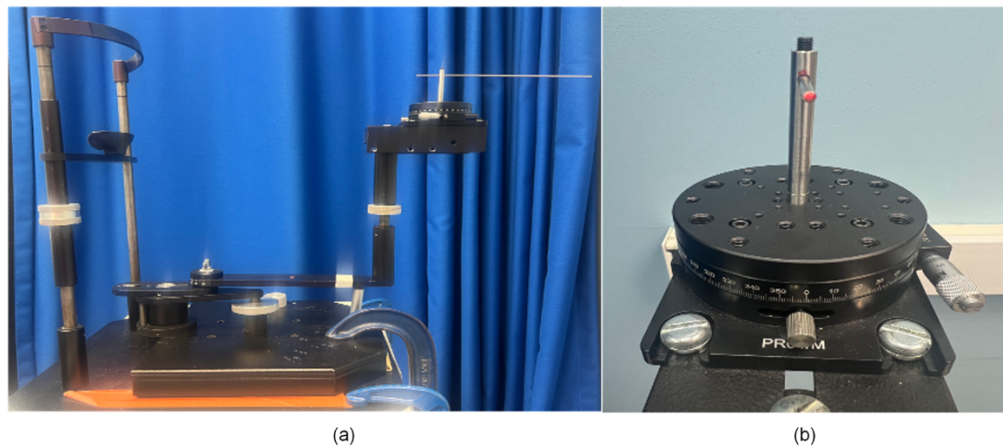


Figure 4.1: The apparatus used in the experiment.  
 (a). The custom-built apparatus used in the experiment placed on the specially constructed table; (b) The high-precision stage used to move the rod in the horizontal plane during the monocular and binocular sighting task.

#### 4.2.1.3 Procedure

At the beginning of the experiment the individual's head circumference was measured using a flexible tape measure. The participant was then instructed to place their head in the sighting apparatus using the head restraint and chin rest, and the distance from the front end of the rod to the bridge of the nose as well as from the centre of rotation to the bridge of the nose were measured. Then the participant was instructed to fixate on the red-coloured front end of the rod, during which the inter-pupillary distance (IPD) was measured with a ruler. After these measurements were complete, the participant was asked to adjust the orientation of the rod in the horizontal plane until its front end was pointing directly towards their right or left eye (monocular conditions), or directly towards them during binocular viewing. Measurements were made along the horizontal azimuth for each of a range of eccentricities spanning  $\pm 52.5^\circ$ , relative to the centre of the head (9 eccentricities:  $0^\circ$ ,  $15^\circ$ ,  $30^\circ$ ,  $45^\circ$ ,  $52.5^\circ$ ,  $-15^\circ$ ,  $-30^\circ$ ,  $-45^\circ$ ,  $-52.5^\circ$ ), as shown in Figure 4.2. Within each experimental session, each task was measured five times, each time constituted a single trial that consisted of a set of nine single eccentricities made in a manner appropriate to the task in question. The order of these judgments within a trial was randomly assigned. Trial judgments were made with both left eye, right eye, and binocularly. Within each trial, the starting position was randomized. Subjects were given one practice trial before the start of each task. The mean intersection of the extensions of the rod's axis at each eccentricity gave a direct measure of visual direction (termed measured egocentre). The point was taken to be a least-squared approximation to the location of the 'true' single intersection, which had the shortest perpendicular offsets to each of the nine lines (Mitson, Ono, & Barbeito, 1976). The perpendicular distance from a point (x, y) to each of the nine lines was determined using the nonlinear least squares method in MATLAB with three fitted parameters (A, B and C):

$$F(x, y) = \sum_{i=1}^9 \left( \frac{A_i x + B_i y + C_i}{\sqrt{A_i^2 + B_i^2}} \right)^2 \quad (4.1)$$

Where A and B affect the slope of and the orientation of each line, C determines the line's position relative to its origin. The point (x, y), in Euclidean coordinates, has the shortest perpendicular distance to each of the 9 lines. This method ensures that the selected point is optimally located relative to all lines, balancing distances and finding a point that minimises overall variation. This estimate was compared to the averaged egocentre, established by viewing the same rod monocularly and finding the midpoint of the left and right eyes' sighting measurements.

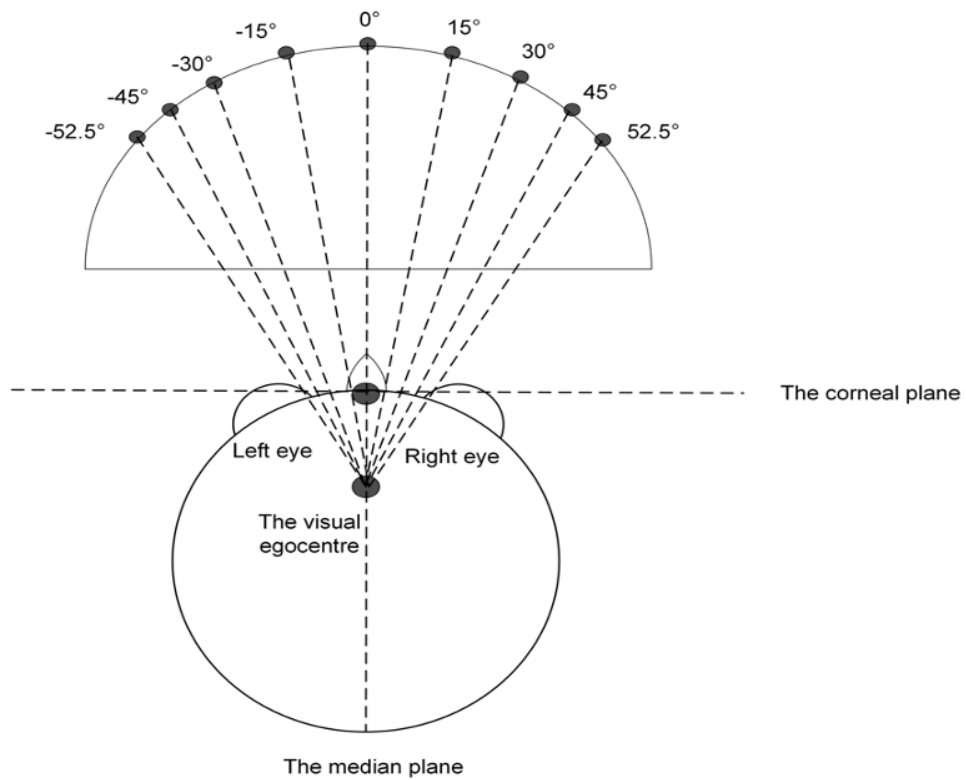


Figure 4.2: Schematic representation of the experiment. Measurements were made along the horizontal azimuth for each of a range of eccentricities spanning  $\pm 52.5^\circ$  relative to the median plane of the head.

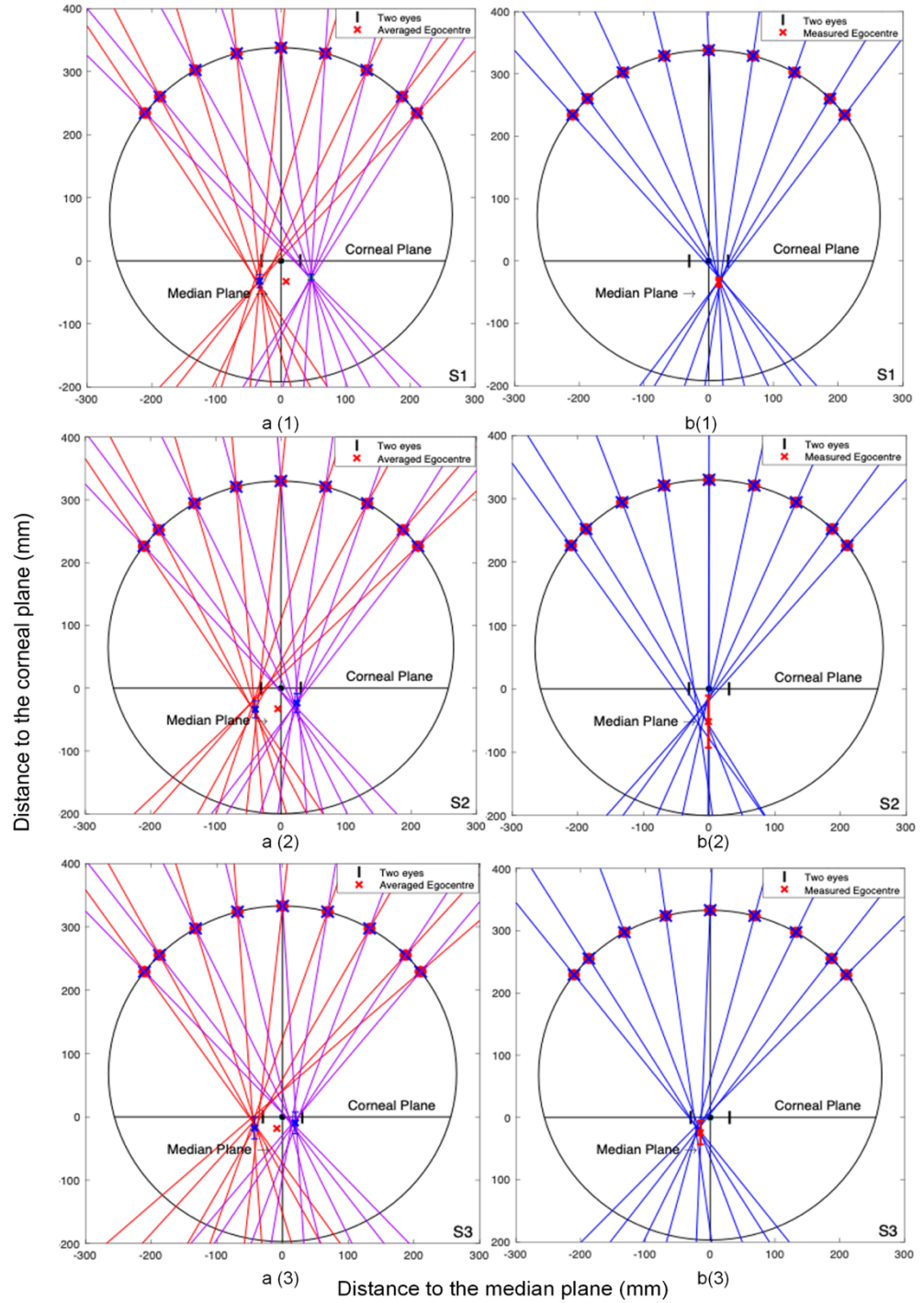


Figure 4.3: Three representative sets of data for both monocular and binocular measures. Left column a(1), a(2), and a(3) show monocular measurements where red lines represent the left eye sighting direction, and purple lines represent the right eye sighting direction. The blue crosses represent the intersections of these lines separately for the left and right eyes and the red cross represents the average of these two locations. Right column, b(1), b(2), and b(3) provide a direct estimate of the binocular visual egocentre location for each participant, indicated by the red cross. Error bars represent  $\pm 1$  standard deviation, calculated across five repetitions of the task.

## 4.2.2 Results

The visual egocentre location was established using a least squares method and represents the mean point of intersection of the extensions of the rod's axis in its various azimuthal locations. Three representative participants' data (S1, S2 and S3), measured with monocular and binocular viewing, are shown in Figure 4.3. In Figure 4.3a, monocular measures give an estimate of the locations of the two eyes in the head, derived from the sighting task, which can be compared to the physical IPD measured at the start of the experiment. The red lines indicate the left eye sighting direction while the purple lines indicate the right eye sighting direction. The blue crosses represent the intersections of these lines separately for the left and right eyes. The blue crosses for the left eye of S1, S2, and S3, are located 33.00 (SD = 1.93), 39.25 (SD = 2.40), and 42.74 (SD = 2.93) mm to the left of the median plane of the head, respectively. The blue crosses for the right eye of these same participants are positioned 46.69 (SD = 0.72), 24.55 (SD = 2.78) and 19.41 (SD = 2.76) mm right of the median plane, respectively. The "averaged egocentre" (i.e. half the distance between the monocular sighting estimates indicated by red cross on each plot in Figure 4.3a) is located 7.88 (SD = 0.6) mm to the right of the median plane and 32.76 (SD = 9.46) mm behind the corneal plane for S1, 4.60 (SD = 0.65) mm left of the median plane and 32.78 (SD = 17.35) mm behind the corneal plane for S2, and 8.67 (SD = 1.41) mm left of the median plane and 18.28 (SD = 20.13) mm behind the corneal plane. The horizontal separation between the locations of the two eyes in the head, derived from the monocular sighting task, for the same three representative participants are 79.69, 63.80, and 62.15mm, respectively.

Figure 4.3b shows the results of the binocular sighting task which provide a direct estimate of the binocular visual egocentre location (hereafter termed "measured egocentre") for each participant, indicated by the red cross in each plot. The measured egocentre of S1 is located 15.59 (SD = 0.86) mm to the right of the median plane, and 33.94 (SD = 7.44) mm

behind the corneal plane, indicating a marked bias towards the right eye's location. The measured egocentre of S2 is situated 0.06 (SD = 0.01) mm to the right of the median plane, and 30.89 (SD = 26.64) mm behind the corneal plane. The measured egocentre location of S3 is located 15.15 (SD = 2.12) mm left of the median plane, and 24.56 (SD = 18.80) mm behind the corneal plane, indicating a bias towards their left eye.

Figure 4.4(a) compares the frequency of objective IPD (red bars) with the eye separation estimated from the monocular sighting task (blue bars) for the entire group of 26 participants. To assess the degree of association between the IPD and monocular measures, the Pearson correlation coefficient was calculated for the entire sample as shown in scatterplot in Figure 4.4(b). Although there is considerable variation in the estimates based on the monocular sighting measures (mean  $74.22 \pm 9.59$ mm), which are generally higher than their equivalent IPD (mean  $62.04 \pm 2.76$ mm), the two were nonetheless significantly correlated ( $r_{(24)} = 0.416$ ,  $p < 0.05$ ). Monocular sighting estimates reflect the perceptual location of the fovea whilst viewing the end of the rod, whereas the IPD is the distance measured between the centres of pupils. Under normal distance viewing conditions there is an angular offset of about 5 degrees between the optical and the visual axes (termed kappa), with the fovea in each eye displaced horizontally in the temporal plane relative to the intersection point of the optical axis and the posterior pole (Artal, 2014). Moreover, when fixating on a relatively near object, the eyes will converge, so the distance between the pupil centres (the near IPD) will be smaller than when looking farther away. This inward eye rotation will also displace the fovea outwards, so the distance between them (derived from the monocular sighting data) will increase compared to more distant viewing. Consequently, one might reasonably expect the inter-fovea distance to be greater than the IPD.

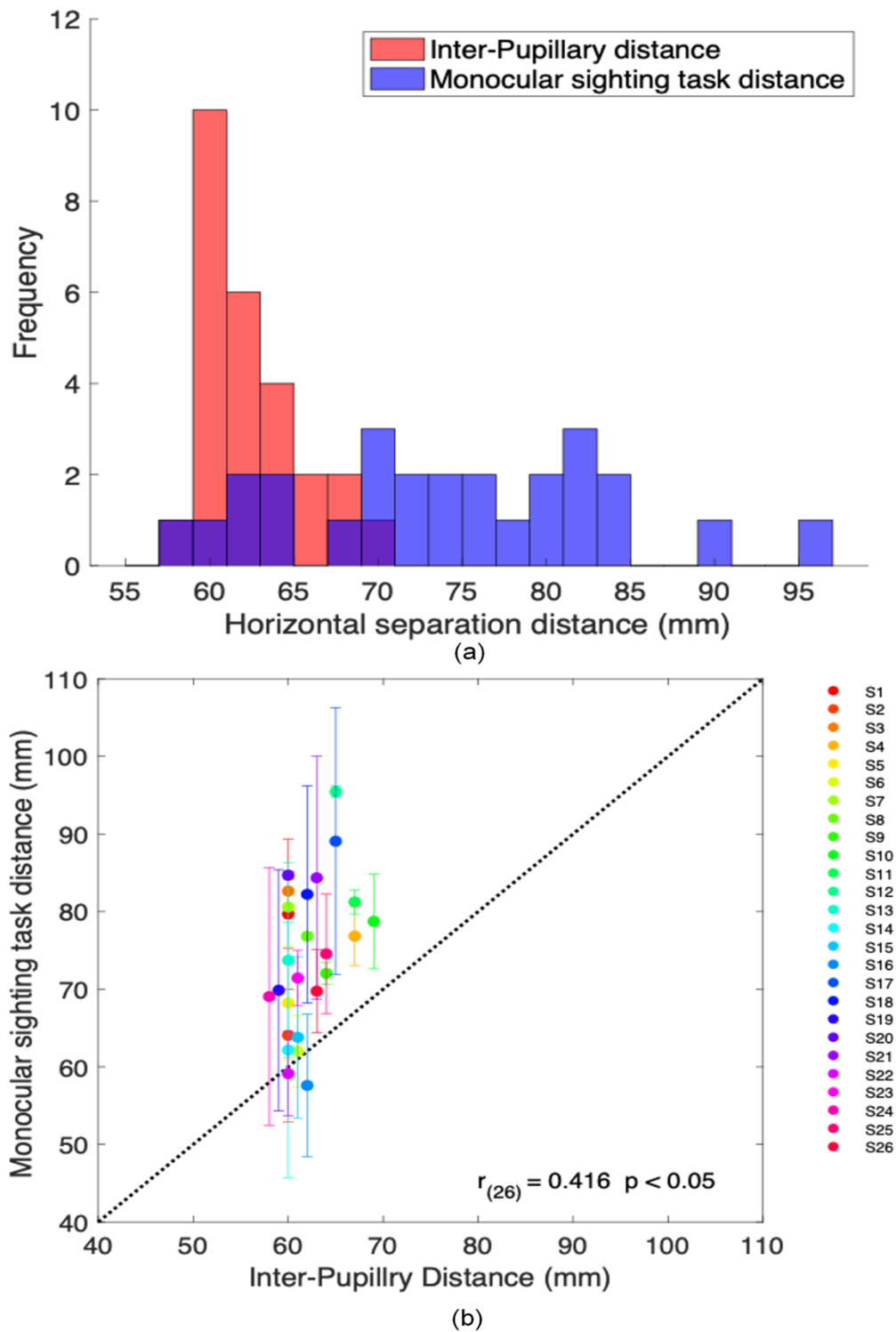


Figure 4.4: The comparison between IPD and monocular sighting task distance across 26 participants. (a). The frequency of IPD (red bars) and monocular sighting distance estimates (blue bars) in the sample; (b). Scatterplot showing the degree of association between these two horizontal distances, with error bars indicating the standard deviations of monocular sighting measures for each participant.

The measured egocentre locations are plotted against the averaged egocentre locations separately for each participant in Figure 4.5 to reveal the individual variation within our sample of participants, representing asymmetries between half distance between monocular sighting estimates and the binocular sighting egocentre locations with respect to the median and the corneal plane of the head. In Figure 4.5(a), the green area represents the visual egocentre situated to the right of the median plane of the head, while the blue area indicates the visual egocentre is situated to the left of the median plane. It is possible to identify the sighting dominant eye for each individual by using the information of measured egocentre location in this figure. In Figure 4.5(b), the yellow area shows the egocentre is located in front of the corneal plane and the purple area indicates the egocentre is behind the corneal plane. The group measured egocentre is located on average 0.41 (SD = 11.13) mm to the right of the median plane of the head and 24.63 (SD = 13.85) mm behind the corneal plane, but considerable individual differences in its location are evident in both conditions. Similar to the binocular estimates, all the monocular estimates are positioned behind the corneal plane. However, in relation to the median plane, binocular estimates can be situated to either the left or the right.

It is clear from Figure 4.5 that the measured egocentre and the averaged egocentre estimates fall close to a diagonal line with unity slope. The Pearson correlation coefficient was calculated to quantify the potential relationship between these two locations with respect to the median plane and the corneal plane. Performance on these two tasks is significantly and positively correlated, although estimates based on the median plane show a weaker correlation than those based on the corneal plane ( $r_{(24)}$  of 0.537 vs. 0.682, respectively).



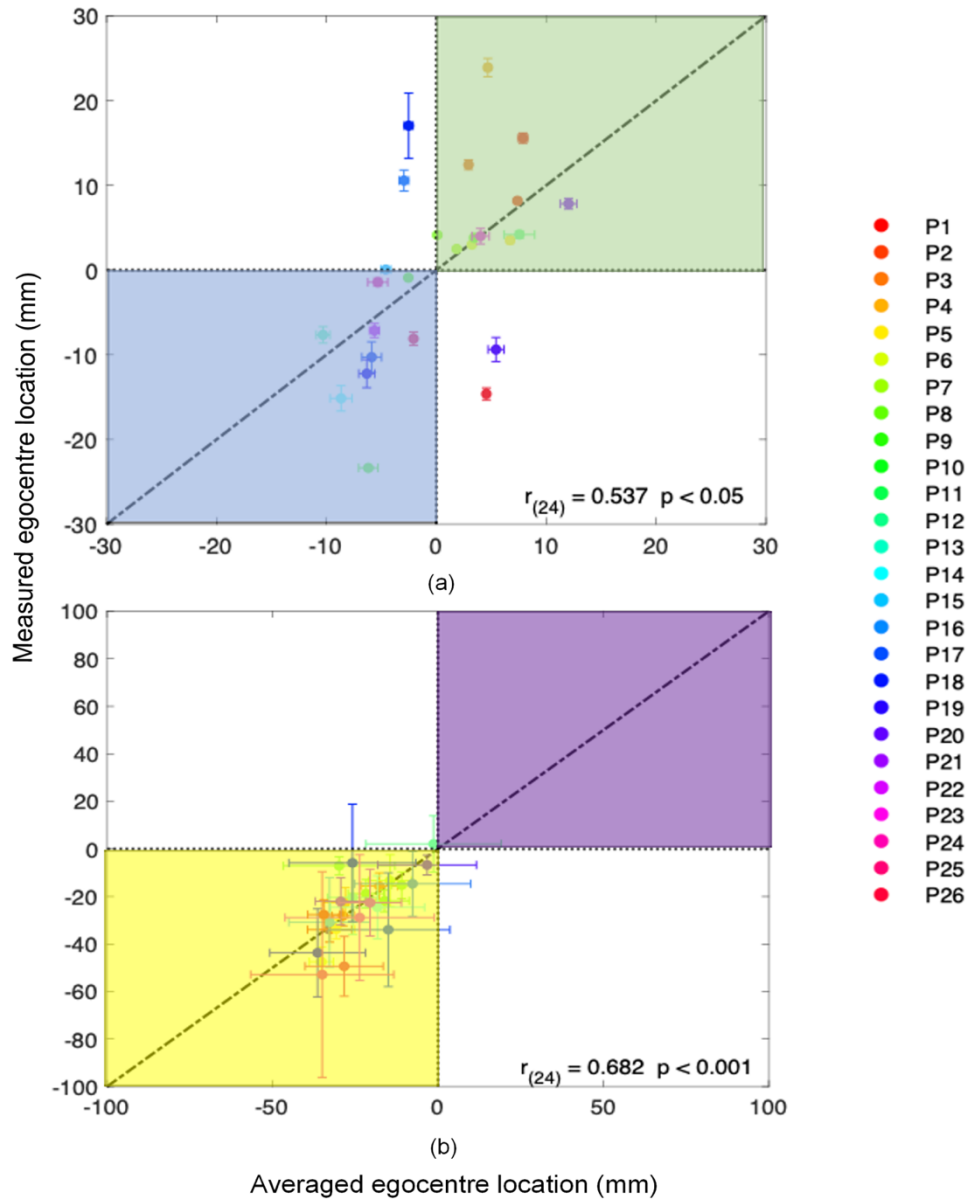


Figure 4.5: Measured egocentre location plotted against averaged egocentre location for all 26 participants, estimates measured (a) with respect to the median plane, (b) with respect to the corneal plane. Vertical and horizontal error bars represent the SEM calculated across repetitions of the measurement for each participant. The Pearson correlation coefficient between these two sets of measurements is also shown on each plot.

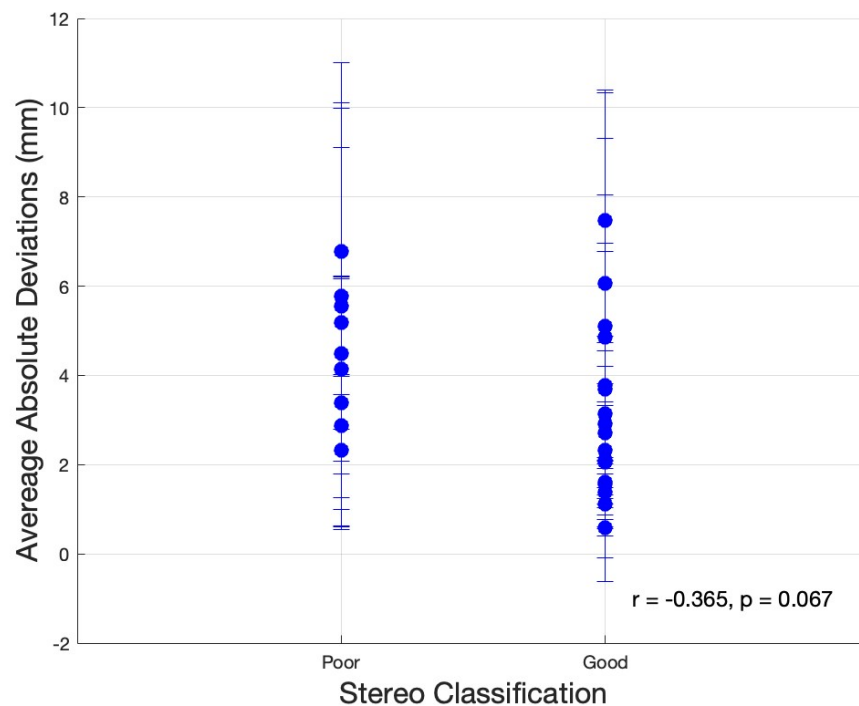


Figure 4.6: The relationship between average absolute deviations from the median plane and stereo classification. Stereoacuity measures were classified into relative good (stereoacuity  $\leq 60$ arcsec) and relative poor (stereoacuity  $> 60$  arcsec). Each blue point represents an individual participant, with error bars indicating variability in the measurements of average absolute deviations.

A repeated measures ANOVA was conducted to compare the variances in performance within subjects across five measurements to the variation between subjects. The analysis revealed a between-subjects variance of 50.43 and a within-subject variance of 27.24, suggesting a significant difference between these two variances,  $F_{(25,100)} = 1.85$ ,  $p < .05$ . The data demonstrates that there is greater variability between subjects compared to the consistency of responses within the same individual. As demonstrated by the findings supporting the Howard and Templeton technique in the Barbeito and Ono (1979) study, the minimisation of the noise measurement is crucial for building confidence in our results. In this manner, it convinces that the variations observed are more likely due to true individual variation, such as differences in egocentric position, rather than noise associated with each measurement process. In terms of investigating the relationship between egocentric localization and corresponding processing mechanism. observers were classified into two

groups based on their TNO stereoacuity scores: Good ( $\text{TNO} \leq 60\text{arcsec}$ ) and Poor ( $\text{TNO} > 60\text{arcsec}$ ). A Point Biserial Correlation was conducted to examine the relationship between stereo classification and egocentre deviations. The results revealed a negative correlation ( $r = -0.365$ ), suggesting observers with relatively good stereopsis tended to exhibit less egocentre deviations compared to those with relatively poor stereopsis. However, the correlation was not statistically significant ( $p = .067$ ). Figure 4.6 illustrates the relationship between egocentre deviations (y-axis) and stereo classification (x-axis).

### 4.3 Discussion

Since Hering (1879/1942) devised his principles of visual direction, the visual egocentre has often been assumed to lie at the midpoint of the interocular axis. The actual location of the visual egocentre, however, may deviate somewhat from this midpoint because different measurements have been found to yield varied results (Milson, Ono, & Barbeito, 1976). Thus, much uncertainty exists concerning the location of the egocentre, and its variation with the normal adult population, despite its fundamental importance to our understanding of binocular vision.

This study performed a monocular and binocular sighting task to explore the variability of visual egocentre location across a relatively large sample of individuals. The binocular sighting measure allowed a direct estimation of the location of the visual egocentre, which is typically behind the corneal plane of the head and close to the median plane, but there were marked individual variations in its position.

The sighting task procedure under monocular viewing required the participant to close one eye, a manipulation that is known to lead to apparent egocentric direction shifts with each alternation of monocular vision. This illusory displacement is termed the monocular egocentric

direction (MED) illusion (Park & Shebilske, 1991). Ono and Gonda (1978) explored the relationship between apparent movement, eye movements, and phoria (latent eye misalignment) when subjects alternate monocular viewing between their left and right eyes, showing that lateral heterophoria significantly affects monocular perception of direction and apparent movement. The MED illusion is a result of the interaction between retinal images and eye movements, influenced by lateral heterophoria. As the procedure of monocular sighting measurements were conducted in 9 different eccentricities across the horizontal plane, assuming all information from retinal displacements had been eliminated when transitions were made between blocks, there still existed individual differences in perceiving visual direction due to lateral heterophoria even though the participant was instructed to rotate the rod to point at the opened eye (Park & Shebilske, 1991). Therefore, another possible explanation of the variations of the horizontal distance estimates under monocular viewing is a shift in eye position caused by lateral heterophoria which may place the critical stimulus on a visual line different from the visual axes under binocular fusion, leading to an apparent displacement.

Binocular sighting is believed to provide a direct estimate of the visual egocentre (Mitson, Ono, & Barbeito, 1976; Ono, Angus, & Gregor, 1977; Porac & Coren, 1981, 1986). The mean location of the visual egocentre across individuals lies close to the median plane and behind the corneal plane of the head, which is consistent with the results of Howard and Templeton (1966), suggesting that the visual information from both eyes is combined to create a single perceptual egocentre located midway between the two eyes and behind the corneal plane, i.e., midway between the interocular axis and interaural axis. Their work provides a detailed analysis of the mechanisms underlying spatial orientation and perception. Anecdotal studies suggest that when young children are asked to look through a tube, they do so by placing the tube between the two eyes instead of in front of one eye, known as the cyclops effect (Church, 1966, 1970). This behaviour was observed in 2-year-olds and some 3-year-olds but decreased with age (Barbeito, 1981, 1983). It had

also been reported that the cyclops effect occurs in young strabismic children and in children under 4 years of age who have one eye enucleated two years earlier (Dengis et al., 1993). The cyclops effect was found in visual tasks such as aligning a line or a moving stimulus with a head landmark (the bridge of the nose or edge of the pinna) among older observers (5.8 to 22.8 years), but less so in binocular observers matched by age (González, Steinbach, Gallie, & Ono, 1999). However, Dengis (1998) tested participants with normal vision, concomitant strabismus, or one eye enucleated, of varying ages. The results found that individuals with normal binocular vision or common strabismus aligned the stimuli with the midline of the head, whereas monocular removers aligned with the centre located 75% of the way to the other eye. This finding suggests that cyclops effect is independent of age, instead, it is related with egocentre location, which serves to reconcile the impressions derived from the two vantage points (Howard, 1982).

The fovea is a small central area of the retina with the highest visual acuity due to its densely packed exclusively with cone photoreceptors, which are highly responsible for specialised for spatial vision. The fovea provides a stable frame of reference allowing accurate and stable spatial judgments and navigation. and the brain must prioritize the integration of information from this region to form a clear and detailed visual perception (Howard & Rogers, 2012). The visual egocentre serves as a reference point from which the information of directions and distances is perceived. When the human eye gazes at an object, it automatically rotates to ensure that the target image falls on the fovea. In this manner, this location can balance the convergence angle and parallax information of the visual axes of both eyes, thus optimizing the integration of visual information and ensuring the accuracy and stability of spatial perception. If the visual egocentre is located before the corneal plane, it may lead to an imbalance in binocular input, which in turn affects the accuracy of depth perception and spatial localization (Howard & Templeton, 1966; Purves, et al., 2001; Roger & Graham, 1979). It will be difficult for the visual egocentre to align with the optical axes if it is located in front of the

corneal plane. As a result of this misalignment, the brain may combine visual inputs from both eyes differently. The disparity between images from each eye, for instance, might result in distortions in perception of depth and spatial awareness (Kandel *et al.*, 2014). Our findings support the notion that the visual egocentre is located behind the corneal plane, where enables the brain to effectively merge the slightly different views from each eye, thus maintaining a coherent and stable perception of space.

Current study demonstrates convincingly that there is considerable individual variation in the location of the visual egocentre. It has been demonstrated previously that individual differences in measured visual egocentre location can be used to predict individual differences in perceptions of directions (e.g. Ono *et al.*, 1972; Barbeito & Ono, 1979). From the view of oculomotor coordination, visual direction can be conceptualized based on the signals from two subsystems proposed by Gregory (1958, 1966): the retinal-image system and the eye-head system, which provides crucial framework how visual direction is established. The retinal-image system integrates retinal and eye position signals independently before combining information into the cyclopean eye. Simultaneously, the eye-head system uses joint binocular local signals and joint eye position signals to determine visual direction directly. Variations in how these subsystems combine and process visual information can affect the location of the visual egocentre. For example, differences in how effectively they integrate retinal information with eye position or how well they combine joint binocular signals and eye position information leads to variations in the visual egocentre location.

In addition, changes in oculomotor control affects the way how retinal information and eye position signals are combined. Different levels of eye coordination may cause variations in the egocentre location (Cui *et al.*, 2010), a person with strabismus (misaligned eyes) may have a different egocentric perception compared to a person with normal eye alignment. Swanson, Wade, and Ono (1990) expanded on previous work by

proposing that retinocentric and eye movement signals are weighted and combined for each eye to create an egocentric representation. They demonstrated that left and right retinocentric signals merge to form a binocular retinocentric representation, while left and right eye position signals combine to produce a binocular eye movement signal. Both retinocentric and eye movement signals are weighted and combined for each eye to form a unified egocentric representation. In this manner, individuals weigh retinocentric and eye movement signals in different ways depending on the characteristics of their visual system or a particular visual task may lead to variations on the egocentric localization. For example, some people may focus more on retinal information when determining spatial location, whereas others may prioritize eye movement signals. This difference in weighting can affect the perceived location of the visual egocentre. Individual differences on the egocentre location can be attributed to different integration on the retinal-image and eye-head system, as well as different weights on retinocentric and eye movement signals. Recognizing these variations emphasizes the significance of both retinal and eye signals in identifying visual egocentre location and helps to explain why people may perceive their visual direction differently.

Mitson, Ono, and Barbeito (1976) investigated three different methods (Funaishi, 1926; Howard & Templeton, 1966; Roelofs, 1959) for measuring the location of the visual egocentre and found the mean egocentre location was near the median plane, but estimates ranged within around 10 mm on either side of the median plane. In the present experiment, the visual egocentre locations of ten participants (38%) showed a deviation toward the side of the sighting dominant eye. This result inevitably raises the question, where is the point of origin of visual direction, the cyclopean eye or the sighting eye? Barbeito (1981) investigated the relationship between sighting dominance and the processing of visual direction and demonstrated that the reference point for sighting is the visual egocentre instead of a true preference for one eye. Barbeito (1981) further explained that the apparent preference for

one eye in sighting task stems from the requirement for monocular viewing, which aligns with the eye closest to the egocentre rather than indicating a dominant eye for processing visual directions. Therefore, sighting dominance can be explained as resulting from the egocentre being off-centred, combined with the design of the sighting tests that require monocular viewing. As a result, the eye selected for monocular viewing is simply the one closest to the visual egocentre.

We found a moderate correlation between egocentric location for the median plane with stereo threshold, which supports the notion that variations in stereo acuity are associated with changes in the egocentric localization. Individuals whose egocentre location deviate more from the median plane tend to show poorer stereoscopic acuity, indicating that stereoscopic visual acuity provides a unique sensation of depth perception. One possible explanation is that stereo acuity refers to the ability to distinguish slight disparities received by the two eyes and utilize differences to perceive depth, poorer stereo acuity leads to less precise binocular integration. In the case of poor stereoacuity, the highly adaptive visual system may compensate for these differences through adaptive adjustment adapt by changing the perceived egocentre location (greater deviation from the median plane) to optimize spatial coherence (Webster, 2015). These compensatory adjustments come in a variety of forms, for example, to keep visual and proprioceptive signals coordinated and to adapt to physiological changes like fatigue or injury, sensory-motor control must be continually recalibrated (Shadmehr et al., 2010, Wolpert et al., 2011). Similarly, stereopsis is modified to account for changes in spatial sensitivity (Webster et al., 2002). This suggests many aspects of adaptation remain stable throughout the life cycle, and it is critical for stabilizing visual perception of the many optical and neural changes that do occur.

Porac and Coren (1986) suggested that biases in egocentric localization stem from the habitual suppression of input from the non-sighting eye in various stimulus situations, leading to a reliance on the monocular



information from the sighting eye for directional judgments. If this bias results from the frequent use of the sighting eye for determining visual direction, it can be predicted that directional judgments will be more reliable when using the sighting eye compared to the non-sighting eye. However, Porac and Coren (1986) did not concur that sighting dominance determines the perceived direction of a target, as the magnitude of the deviations were insubstantial. Instead, they asserted that sighting dominance undoubtedly plays a crucial role in sensorimotor coordination and effective interaction with visual targets.

In summary, the observed variation in individual egocentric localizations highlights the importance of studying individual differences in visual perception, which reflects the inherent diversity of individual's perceptual processing and anatomy. Recognizing and studying these differences can enhance our understanding of how spatial perception is adapted to individual needs and may have practical applications in areas such as virtual reality, and clinical assessment of spatial impairment. Considering individual differences in egocentric localization allows developers to tailor visual content to users' natural spatial orientation, enhancing realism and reducing discomfort used in Virtual Reality (VR) and Augmented Reality (AR) systems. For patients with spatial perception disorders, VR and AR environments can be used to create controlled visual scenarios to gradually correct their spatial misjudgements and improve their functional ability.

# Chapter 5. Short-term monocular deprivation biases the location of the visual egocentre

## 5.1 Introduction

Neural brain plasticity refers to the ability of central nervous system (CNS) neurons to reorganise in response to learning, environmental changes, or injuries. CNS activity can be modulated in various ways due to environmental inputs (Bliss & Lomo, 1973; Kandel et al., 2014; Levy & Steward, 1983; Magee & Grienberge, 2020; Malenka & Bear, 2004; Strettoi et al., 2022). occurs in two forms with opposite effects: Hebbian and homeostatic. Hebbian plasticity is a correlation-based mechanism that progressively modifies network properties, while homeostatic plasticity promotes network stability (Turrigiano & Nelson, 2000). The interaction between these forms of plasticity has been most clearly illustrated by studies of abnormal visual input, such as monocular deprivation, during development. This interaction leads to structural and functional changes in the visual cortex, where Hebbian processes, such as long-term depression (LTD), are followed by increases in synapse strength (Keck et al., 2007). Disruptions to visual input, particularly during a critical developmental window of heightened plasticity known as critical period, can lead to long-term remodelling of neural architecture (Hensch, 2004, 2005; Shonkoff & Phillips, 2000). However, the extent to which this plasticity persists in the adult brain remains unclear.

Early studies on monocular visual deprivation date back to the mid-20th century. Wiesel and Hubel (1963a) used extracellular recordings to study cortical responses in kittens deprived of vision in one eye, finding a shift in ocular dominance due to monocular deprivation. Similar findings were later observed in mice and other young animals, where monocular

deprivation caused a shift in ocular dominance of cortical neurons, along with reduced visual acuity in the deprived eye (e.g., Allard et al., 1991; Douglas, Alam, & Prusky, 2004; Fischer et al., 2007; Gordon & Stryker, 1996; Tagawa et al., 2005). Over the past fifty years, studies have shown that ocular dominance shifts induced by monocular deprivation during critical periods reflect structural changes in the brain (Wiesel, 1982). In ocular dominance plasticity, if one eye receives less input during early development, its neural connections weaken, while those of the non-deprived eye expand, becoming functionally and anatomically dominant. This imbalance leads to the expansion of ocular dominance columns in the non-deprived eye and a corresponding shrinkage in the deprived eye (Crair et al., 1997). Sensitivity to deprivation is highest during the critical period but declines with age. In adult mice, as long as seven days of monocular deprivation is required to alter ocular dominance (Karmarkar & Dan, 2006; Ranson et al., 2012; Sato & Stryker, 2008).

It has been observed that the visual cortex does not lose its capacity for plasticity at the end of the critical period; instead, the nature of this plasticity evolves as the brain matures (Sato & Stryker, 2008). This post-patching effect has since been consistently observed across psychophysical (Lunghi et al., 2011, 2013; Zhou et al., 2013; Zhou et al., 2014; Zhou et al., 2017), electrophysiological (Lunghi & Sale, 2015; Zhou et al., 2015), and brain imaging studies (Binda et al., 2018; Chadnova et al., 2017; Lunghi et al., 2015) in humans. The first demonstration of short-term plasticity in healthy adults was conducted by Lunghi, Burr, and Morrone (2011), who found a paradoxical enhancement of the deprived eye's signal after patching with a translucent occluder for 150 minutes. Wang et al. (2020, 2021) demonstrated that eliminating visual input to one eye with an opaque patch, while effective in generating changes in rivalry dynamics in favour of the patched eye, was not a requirement. They compared three types of monocular treatment (an opaque patch, a diffusing lens and an inverting prism) and found that all three manipulations altered dominance duration and predominance during binocular rivalry task in favour of the treated eye. Bai et al. (2017)

measured eye dominance before and after removing the phase regularity of an image while maintaining its amplitude spectra and found a shift in eye dominance towards the eye with the impoverished input. This shift was present when measured with a binocular rivalry task, but not with a binocular phase combination task, suggesting that eye dominance plasticity may occur at different stages of visual processing. Binocular combination tasks involve presenting fusible stimuli to each eye, where the combined perception is based on the level of each eye's contribution to binocular vision. Changes in eye dominance resulting from short-term patching have been measured using various combination tasks, such as phase combination, motion combination, and contrast combination (Zhou, Clavagnier & Hess, 2013; Min, Balwin & Hess, 2019). Additionally, Kim et al. (2017) demonstrated that the patching effect can be induced by suppressing one eye without physically depriving it of visual input, using continuous flash suppression.

Previous studies have suggested that changes in monocular input may alter binocular balance through selective attention mechanisms (Wang *et al.*, 2021; Dieter, Melnick, & Tadin, 2016). During short-term deprivation, the contrast gain of the deprived eye increases, while the non-deprived eye's gain decreases. This process suggests a form of functional eye dominance plasticity in which the visual system adjusts to maintain balance between the eyes (Min *et al.*, 2019). This functional dominance change is temporary in nature, the recovery of post-deprivation effect occurs over a period of 30 – 90 minutes in adults (Lunghi et al., 2011; Zhou et al., 2013), suggesting that patching one eye can only temporarily introduce an imbalance before the original balance is restored. Consequently, the mechanisms underpinning shifts in eye dominance remain unresolved, but may involve unbalanced inter-ocular suppression, attentional shifts in eye selection or both.

Virtually all of the tasks up to this point have looked at how sensory representation is altered when input to one is changed in some way. However, sensory signals need to be transformed so that motor

behaviour can be applied. For example, an object may first be detected (sensory component) and then its location determined relative to the body or head (transformed) of an observer and then finally acted upon by pointing at it (motor component). In fact, it was originally thought that the neural pathways subserving visual perception and visual control of motor actions were completely independent (Goodale & Milner, 1992). Therefore, to understand this behaviour, it is necessary to know not just how binocular sensory judgements are influenced by altered visual input, but in what way the resulting motor output is affected. To address this, the current study aimed to explore whether short-term monocular deprivation also has consequences on judging the visual direction of objects in space, relative to the viewer. We sought to compare the effect of patching dominant and non-dominant eyes on visual egocentric localization judgements. This study will help us determine whether the same residual plasticity is also observed for estimates of visual direction that might act to compensate for situations where input to one eye is compromised, either through developmental anomalies or ocular disease.

## 5.2 Experiment 6: What is the optimum period of monocular visual deprivation?

### 5.2.1 Methods

#### 5.2.1.1 Observers

One participant (the author, female) had normal or corrected-to-normal vision and no history of ocular disease participated in this experiment. Before formal data collection, the TNO stereo test (Laméris Ootech, Nieuwegien, The Netherlands) was administered to ensure the participant had normal stereo vision and thus was able to perceive the depth and 3-dimension structure of visual information (range: 60-120 arcsec). The experiment was approved by the School of Psychology

Ethics Committee at the University of Nottingham. Participants gave informed consent before the experiment and all experimental procedure conformed to the guidelines laid out in the Declaration of Helsinki.

#### 5.2.1.2 Apparatus and stimuli

Using the apparatus same with Chapter 4, the visual egocentre was measured using both a monocular and a binocular sighting task. During the task, the participant sat at a specially constructed table with their head supported by a chin rest. They fixated on the front end the rod (coloured red) and rotated the orientation of the rod in the horizontal plane until it pointed to their right eye, left eye or directly towards them during binocular viewing. Fine adjustments could be made using a screw mechanism on the edge of the stage. The entire stage could be rotated in an arc around the participant's head to vary the viewing angle (see Figure 5.1).

#### 5.2.1.3 Procedure

The distance from the front of the rod to the bridge of the nose and from the rotation point of the apparatus to the bridge of the nose were measured. Measurements were made along the horizontal azimuth for three eccentricities relative to the centre of the head ( $0^\circ$ ,  $30^\circ$ ,  $-30^\circ$ ), as shown in Figure 5.1.

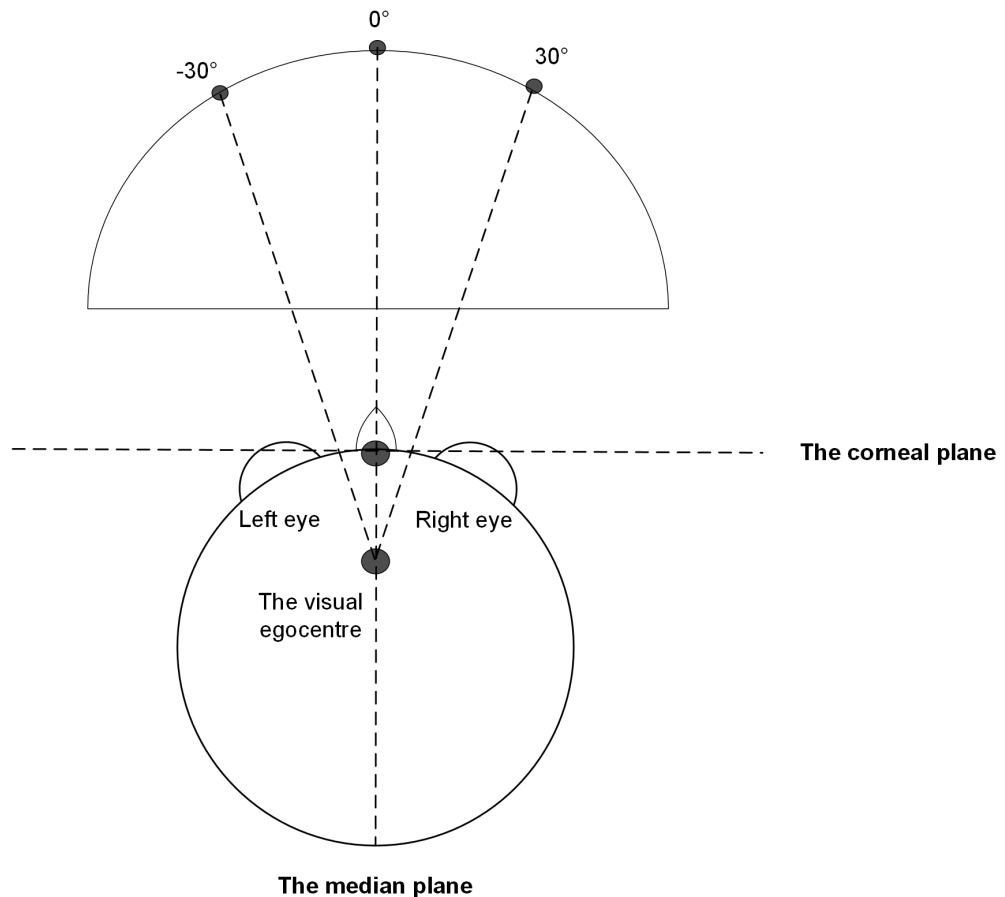


Figure 5.1: Schematic representation of the experiment. Measurements were made along the horizontal azimuth for each of three eccentricities spanning  $\pm 30^\circ$  relative to the median plane of the head.

Within an experimental session, each eccentricity was measured five times. The order of these judgments within a session was randomly assigned. For each trial, the starting position of the rod was randomized. The mean intersection of the extensions of the rod's axis at each eccentricity gave a direct measure of visual direction, referred as the baseline egocentre position (See Figure 5.2). This point was taken to be a least-squared approximation to the location of the 'true' single intersection, which had the shortest perpendicular offsets to each of the three lines (Mitson, Ono, & Barbeito, 1976). Monocular measures (not shown on the figure) were used as control data to confirm that any observed shifts were attributed to changes in binocular visual direction rather than monocular shifts.

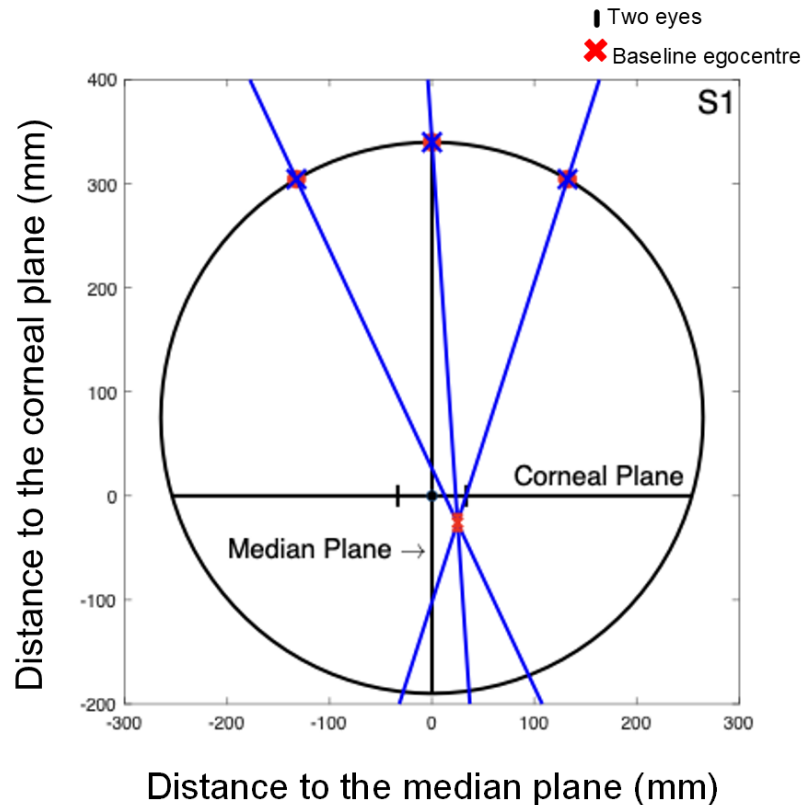


Figure 5.2: The baseline visual egocentre location of the observer. Two short lines represent the monocular estimates for each eye, and red cross represents the baseline egocentre location under binocular viewing conditions. Three blue lines represent measurements from three eccentricities. Vertical and horizontal error bars represent the standard deviation calculated across five repetitions of the task.

We first determined sighting eye dominance by identifying which eye the baseline egocentre location favoured. The non-dominant eye was positioned farther from the visual egocentre. Then non-dominant eye (in this case, the left eye) was covered with an opaque patch for 30, 60 and 90 minutes in separate testing sessions conducted on different days. During the patching period, the non-dominant eye received no visual input, while the observer was free to continue their routine activities. We measured the effects of monocular treatment to determine whether each treatment condition altered eye balance compared to baseline measures. After patch removal for each session, the visual egocentre location was remeasured three times at an interval of 0, 3, 6, 9, 12, 15, 30, 45, 60, 90, 120 minutes (see Figure 5.3).



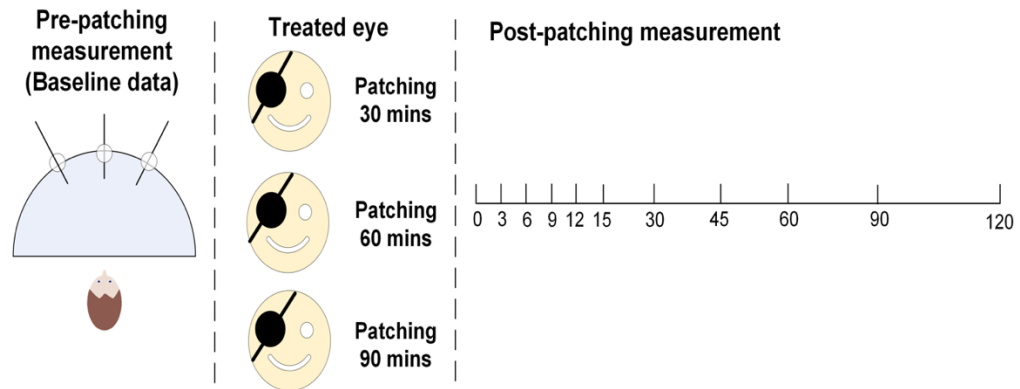


Figure 5.3: Schematic illustration of the experimental procedure. The baseline egocentre location was measured before applying an opaque patch to the non-dominant eye for 30, 60, and 90 minutes in separate sessions. After patching, the visual egocentre location was remeasured every 3 minutes during the first 15 minutes, every 15 minutes for the next 45 minutes, and finally, every 30 minutes during the remaining 60 minutes.

## 5.2.2 Results

The least squared method was used to calculate the visual egocentre location, which represents the mean point of intersection of the extensions of the rod's axis in various positions. Figure 5.4 shows the changes in the visual egocentre location relative to the median plane for this observer. In the figure, the red dashed line indicates the baseline visual egocentre location, while the green line illustrates how monocular treatment impacts sensory dominance balance across the three treatment conditions (wearing an opaque patch for 30, 60, and 90 minutes, respectively). Positive y-values indicate the egocentre is positioned to the right of the median plane, while negative y-values indicate it is positioned to the left.

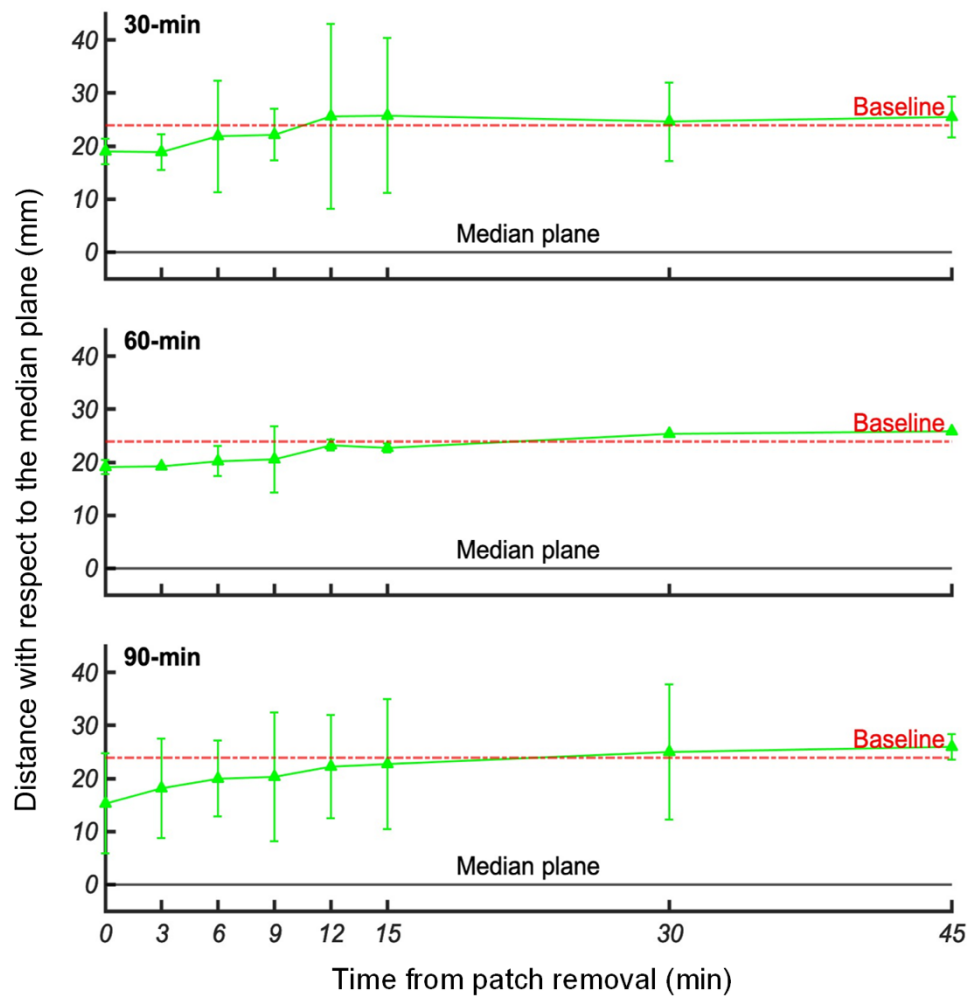


Figure 5.4: The visual egocentre for the median plane in Experiment 6. This observer's data represent the mean distance from the median plane, measured continuously for 45 minutes after 30-minute (top), 60-minute (middle), and 90-minute (bottom) monocular treatments with an opaque patch. Vertical and horizontal error bars indicate the standard deviation (SD) across five repetitions of the task. The black lines represent the median plane, while the red lines indicate the baseline egocentre location for the median plane. The green lines show how the egocentre location changes after patch removal. Positive y-values indicate the egocentre is positioned to the right of the median plane, while negative y-values indicate it is positioned to the left.

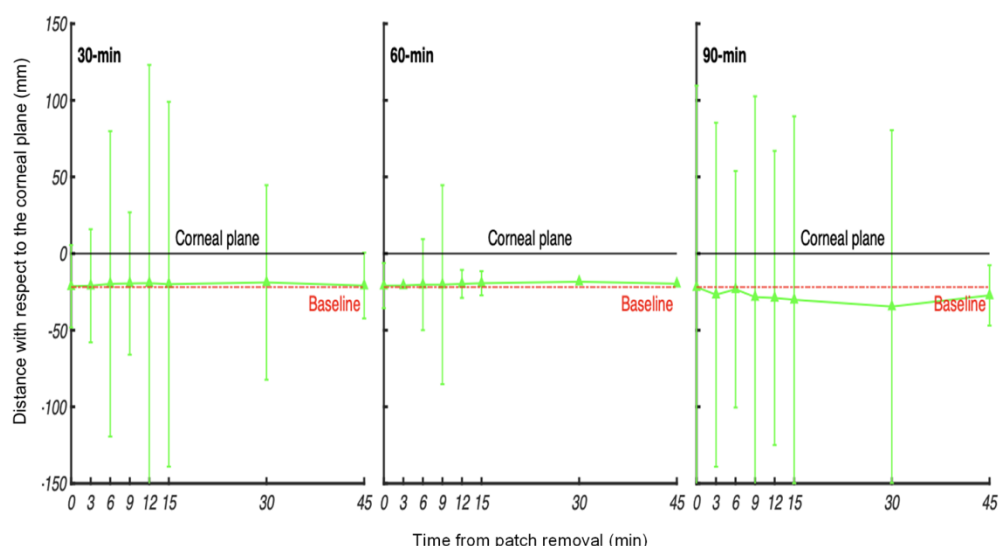


Figure 5.5: The results for the corneal in Experiment 6.

This observer's data represent the mean distance from the corneal plane, measured continuously for 45 minutes after 30-minute (left), 60-minute (middle), and 90-minute (right) monocular treatments with an opaque patch. Vertical and horizontal error bars indicate the standard deviation (SD) across five repetitions of the task. The black lines represent the corneal plane, while the red lines indicate the baseline egocentre location for the corneal plane. The green lines show how the egocentre location changes after patch removal. Positive y-values indicate the egocentre is positioned in front of the corneal plane, while negative y-values indicate it is positioned behind the corneal plane.

The baseline measure of the binocular egocentre was located 23.91 (SD = 1.53) mm right of the median plane and 22.61 (SD = 8.62) mm behind the corneal plane, suggesting this observer has strong right eye dominance (see Figure 5.2). To quantify changes in egocentre location after monocular deprivation, the displacements relative to the median plane are depicted in Figure 5.4 for all monocular treatment conditions. As shown in Figure 5.4, the immediate displacements of each monocular treatment condition at the time of patch removal (at 0-min) were  $d_{30\text{mins}} = 4.92\text{mm}$ ,  $d_{60\text{mins}} = 4.61\text{mm}$  and  $d_{90\text{mins}} = 8.65\text{mm}$  in the median plane. Figure 5.5 shows the displacements relative to corneal plane for all monocular treatments. The black lines represent the corneal plane, while the red lines indicate the baseline egocentre location for the corneal plane. The green lines show how the egocentre location changes after patch removal. Positive y-values indicate the egocentre is positioned in

front of the corneal plane, while negative y-values indicate it is positioned behind the corneal plane. The immediate displacements of each monocular treatment condition at the time of patch removal (at 0-min) were  $d_{30\text{mins}} = 0.58\text{mm}$ ,  $d_{60\text{mins}} = 0.97\text{mm}$  and  $d_{90\text{mins}} = 0.01\text{mm}$  in the corneal plane. A repeated measures ANOVA was conducted to compare the effects of 30-min, 60-min, and 90-min on the visual egocentre location. There was a significant effect of duration on the median plane ( $F_{(2, 28)} = 5.035$ ,  $p < .05$ ), indicating that the duration of monocular deprivation significantly influenced egocentre location. However, there was no significant effect for data relative to the corneal plane ( $F_{(2, 28)} = 34.60$ ,  $p = .053$ ). The post-deprivation effect rapidly declined within the first 6-15 mins for three patching conditions before gradually reaching a plateau back at baseline. Among these three treatment conditions, post-hoc pairwise comparisons revealed no statistically significant differences between monocular treatment conditions for the data relative to the median plane ( $p = .051$ ). Although the size of the induced shift following patch removal is similar between 30- and 60-min occlusion, the effect dissipates more quickly with the shorter deprivation period. Therefore, the patching duration was slightly extended to account for potential long-lasting effects in some of the observers. A 60-min treatment period was used in the following experiment, providing more flexibility in post-treatment measurements while avoiding excessively long patching durations.

## 5.3 Experiment 7: Can egocentre location be modified by short-term monocular deprivation on the non-dominant eye?

### 5.3.1 Methods

#### 5.3.1.1 Observers

Ten observers took part in this experiment (age range: 25-53years, mean age:  $35.20 \pm 10.00$ years), all had normal or corrected-to-normal vision and no history of ocular disease. Before formal data collection began, the TNO stereo test was administered to ensure each of them have normal stereo vision and thus was able to perceive the depth and 3-dimension structure of visual information (range from 60 to 120arcsec).

#### 5.3.1.2 Apparatus and stimuli

The apparatus was identical to that used in the Experiment 6.

#### 5.3.1.3 Procedure

The procedure was identical to that used in the Experiment 6. The visual egocentre was measured for each observer to obtain a baseline visual egocentre location, from which we could determine the non-dominant eye (the eye that was located farther from the visual egocentre) for each observer. The non-dominant eye was selected for firstly patching because patching the dominant eye would leave little room for detecting any significant shift in the egocentre. Since the egocentre is already close to the limit set by monocular estimates (as shown in Figure 5.2) and the dominant eye already has a strong influence on visual direction, patching the dominant eye would likely result in minimal displacement. In contrast, patching the non-dominant eye provides a better opportunity for rebalancing sensory input, making it more effective in detecting shifts in

the egocentre. Three representative observers' baseline data are shown in Figure 5.6. Then they were asked to wear an opaque patch on non-dominant eye for 60 mins, during which observers were free to engage in routine activities. Upon patch removal, the visual egocentre location was remeasured three times at 0, 3, 6, 9, 12, 15, 30, 45mins. (see Figure 5.7).

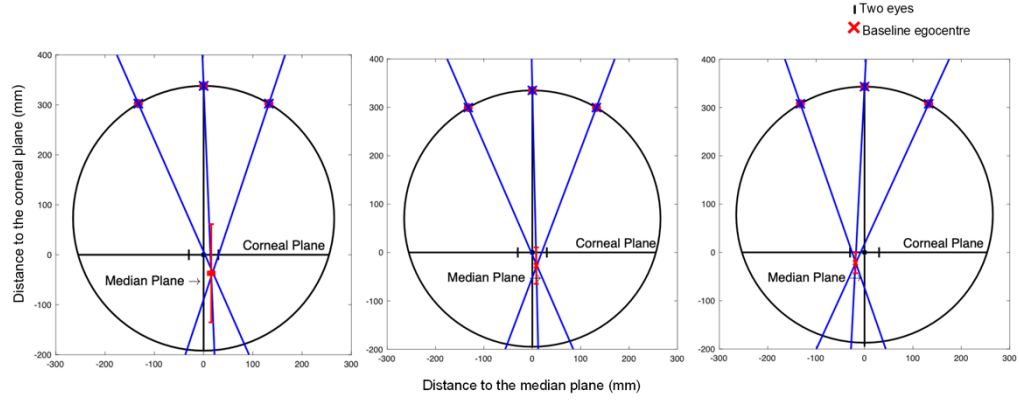


Figure 5.6: The baseline visual egocentre location of the three representative observers. Two short lines represent the monocular estimates for each eye, and red cross represents the baseline egocentre location under binocular viewing conditions. Three blue lines represent measurements from three eccentricities. Vertical and horizontal error bars represent the SD calculated across X repetitions of the measurement for each observer.

#### 5.3.1.4 Mixed-effects model analysis

The analysis of covariance (ANCOVA) was used to investigate the effect of time on post-deprivation egocentre positions while controlling individual differences in baseline egocentre position, using the *fitlme* function in MATLAB (MathWorks, version R2022a). ANCOVA allows us to isolate time's effect on egocentre recovery while adjusting for baseline location's influence (Vickers & Altman, 2001). A linear regression model was defined as following:

$$\text{Post-deprivation egocentre} = \beta_0 + \beta_1 \cdot \text{Baseline} + \beta_2 \cdot \text{Time} + \epsilon \quad (5.1)$$

Where post-deprivation egocentre is the dependent variable,  $\beta_0$  is the intercept,  $\beta_1$  is the coefficient for baseline egocentre location controlling for individual differences,  $\beta_2$  is the coefficient for time on egocentre

recovery, and  $\epsilon$  is the error term representing the residual variability not explained by this model.

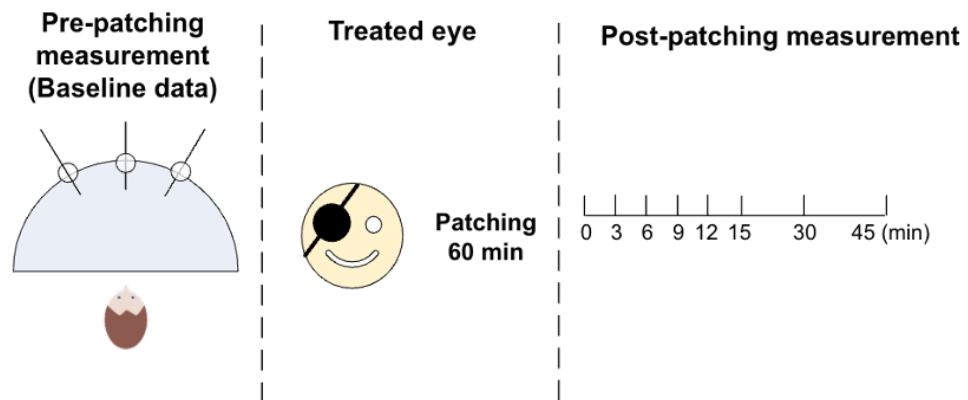


Figure 5.7: The schematic illustration of the procedure of Exp.7. The baseline egocentre location was measured before wearing an opaque patch on non-dominant eye for 60mins. Then the visual egocentre location was remeasured every 3-minute in the first 15mins, then every 15-minute in the following 30mins.

### 5.3.2 Results

The visual egocentre locations of ten observers were remeasured with binocular sighting task for 45 minutes following the removal of the patch. At the moment of patch removal (0-min), the average group egocentre shifted 1.80mm (SD = 8.74) to the left of the median plane and 19.16mm (SD = 16.51) behind the corneal plane. Figures 5.8 and 5.9 illustrate the changes in egocentre location, relative to the median and corneal planes, for each observer after removing the patch from the non-dominant eye. Based on baseline measurements (represented by the red dashed line in each figure), eight participants were right-eye dominant, one was left-eye dominant, and one showed no clear sensory dominance. The green line tracks how egocentre location changed over the 45 minutes following patch removal, positive y-values indicate the egocentre is positioned to the right of the median plane, while negative y-values indicate it is positioned to the left. Figure 5.8 reveals a leftward shift in nine participants, with one participant (S8) showing a rightward shift toward the deprived eye, consistent with previous findings (e.g., Lunghi et al., 2011; Wang et al., 2020). We also examined the variability in monocular

deprivation effects across observers. Notably, at the time of patch removal (0-min), S10 exhibited the largest shift in egocentre location, with a displacement of 13.31mm (SD = 5.36) from baseline. In contrast, S8 showed the smallest effect, with only a 0.58mm (SD = 1.56) displacement from baseline. Additionally, S4 and S5 showed long-lasting effects, with their egocentre not returning to baseline after 45 minutes, while the effects in S8 returned to baseline within 9 minutes.

The data for the median plane in Figure 5.8 suggests that 60-mins of monocular deprivation reliably shifts eye dominance immediately after patch removal, and the effect gradually dissipates to baseline levels around 12-15mins after removing the patch, but some level of individual variation was seen across the 10 participants. The baseline measurement of the egocentre was located on average 5.76 (SD = 8.57) mm right of the median plane of the head. Following 60-minute monocular deprivation, the egocentre was located on average 2.01 (SD = 8.91) mm left of the median plane upon immediate re-exposure to normal binocular vision. A repeated measures ANOVA was conducted to investigate the effect of short-term monocular deprivation on egocentre location,  $F_{(7,56)} = 2.198$ ,  $p = .048$ , suggesting the egocentre location changes significantly over time after monocular deprivation. There was no significant interaction between subjects and post-deprivation time slots,  $F_{(7,56)} = 0.226$ ,  $p = .978$ , indicating that changes in egocentre location were consistent across ten observers. The results of ANCOVA showed that both baseline egocentre location and time play significant role in post-deprivation egocentre location,  $F_{(2,6)} = 19.1$ ,  $p = .005$  and explained 76.1% of variance in the post-deprivation egocentre,  $R^2 = 0.761$ .



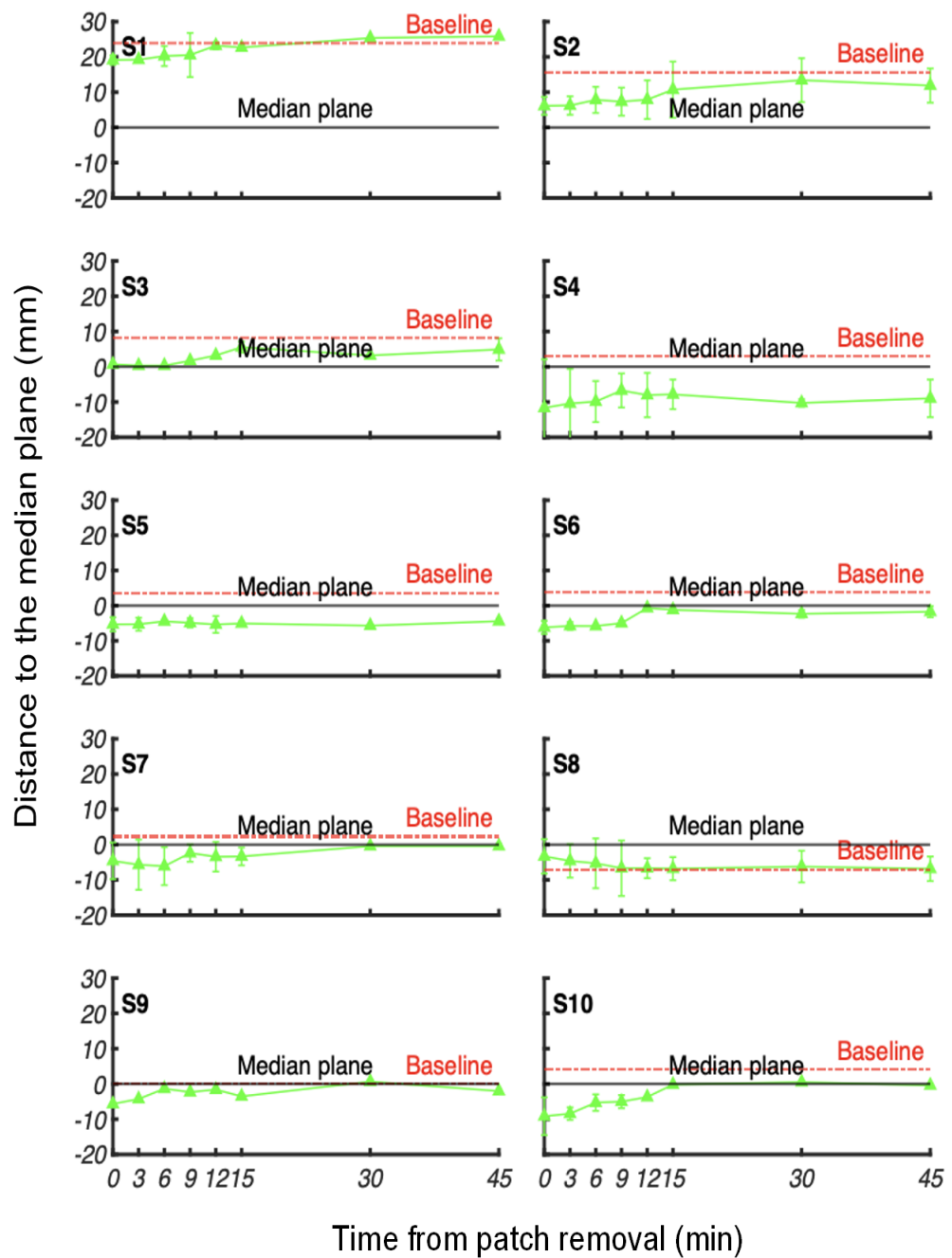


Figure 5.8: The egocentre location (relative to the median plane) of 10 participants was monitored for 45 minutes after removing the eye patch from the non-dominant eye. The black lines indicate the median plane of the head, while the red dashed lines represent each participant's baseline data for the median plane. The green solid lines with triangles illustrate the changes in data over the subsequent post-patch durations. Vertical and horizontal error bars represent the standard deviation calculated across three repetitions of the measurement for each participant. Positive y-values indicate the egocentre is positioned to the right of the median plane, while negative y-values indicate it is positioned to the left.

In terms of egocentre with respect to the corneal plane, the baseline egocentre was located on average 26.62 ( $\pm 10.35$ ) mm behind the corneal plane of the head (shown in Figure 5.9), this measure also exhibited individual differences between participants. Following 60-minute of monocular deprivation, the egocentre was located on average of 19.80 ( $\pm 15.08$ ) mm behind the corneal plane upon re-exposure to binocular vision immediately. A repeated measures ANOVA was conducted to investigate the effect of short-term monocular deprivation on egocentre location,  $F_{(7,56)} = 0.655$ ,  $p = .709$ , suggesting that changes in egocentre location with respect to the corneal plane over time were not statistically significant. There was no significant interaction between subjects and post-deprivation time slots,  $F_{(7,56)} = 0.827$ ,  $p = .569$ , indicating that variation in egocentre location for the corneal plane was consistent across ten observers. The results of ANCOVA showed that the effect of time on post-deprivation egocentre location for the corneal plane was not statistically significant,  $F_{(2,6)} = 0.836$ ,  $p = .396$ , the model explained 12.2% of the variance in egocentre location.

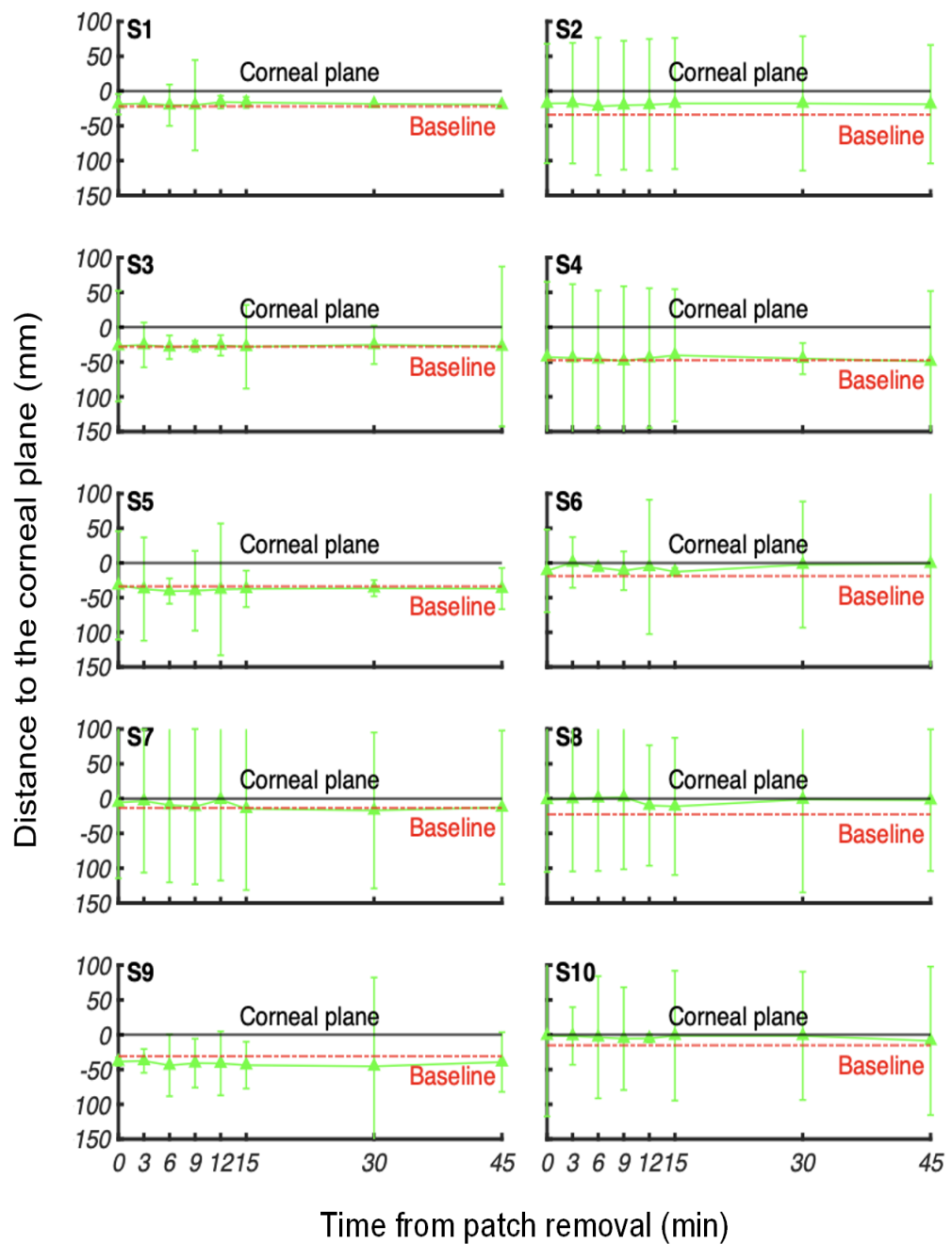


Figure 5.9: The egocentre location (relative to the corneal plane) of 10 participants was monitored for 45 minutes after removing the eye patch from the non-dominant eye. The green solid lines with triangles illustrate the changes in data over the subsequent post-patch durations. Vertical and horizontal error bars represent the standard deviation calculated across three repetitions of the measurement for each participant. The black lines represent the corneal plane, while the red lines indicate the baseline egocentre location for the corneal plane. The green lines show how the egocentre location changes after patch removal. Positive y-values indicate the egocentre is positioned in front of the corneal plane, while negative y-values indicate it is positioned behind the corneal plane.

## 5.4 Experiment 8: Shifts in egocentre location after patching the dominant eye

The previous data on patching from sensory task suggested that previously deprived eye tends to be favoured (e.g., Lunghi et al., 2011; Wang et al., 2020). While our findings in Experiment 7 examined these effects on the non-dominant eye, if this also holds for egocentre location, the opposite direction will be expected based on which eye is patched, providing a new insight into the dynamics of visual dominance and plasticity. Therefore, this experiment mirrors the design of the Experiment 7 on the non-dominant eye, its focus on patching dominant eye allows us to examine whether the same phenomenon occurs for egocentric localization.

### 5.4.1 Methods

#### 5.4.1.1 Observers

Nine participants took part in this experiment (age range: 23-53years, 4 females and 5 males, mean age:  $35.56 \pm 10.54$ years), who had also attended Experiment 7.

#### 5.4.1.2 Apparatus and stimuli

The apparatus was identical to that used in Experiment 7.

#### 5.4.1.3 Procedure

The procedure was identical to that used in Experiment 7, with the exception that an opaque patch was placed on the dominant eye for 60mins for all participants.

#### 5.4.1.4 Data analyse

A mixed-effects model analysis was used to compare different monocular conditions (dominant vs non-dominant patching) and time course, using the *fitlme* function in MATLAB (MathWorks, version R2022a). These models incorporate both fixed effects and subject-specific random effects. It was assumed that all random effects were uncorrelated. A linear regression model was defined as following:

$$\text{Post-deprivation egocentre} = \beta_0 + \beta_1 \cdot \text{Patching Eye} + \beta_2 \cdot \text{Timecourse} + \beta_3 \cdot (\text{PatchingEye} \cdot \text{Timecourse}) + u_i + v_i + \epsilon \quad (5.2)$$

Where post-deprivation egocentre is the dependent variable,  $\beta_0$  is the intercept,  $\beta_1$  is the coefficient representing Patching Eye (non-dominant eye patching vs. dominant eye patching),  $\beta_2$  is the coefficient for time on egocentre recovery,  $u_i$  is the random intercept for participant  $i$  capturing baseline egocentre variability,  $v_i$  is random slope for participant  $i$  representing individual differences in the effect of time on egocentre recovery, and  $\epsilon$  is the error term representing the residual variability not explained by this model.

#### 5.4.2 Results

The changes of visual egocentre location induced by 60-min monocular deprivation of the dominant eye were compared with the data of the non-dominant eye, aiming to determine whether there are any potential direction differences in the egocentric shift. To facilitate comparison between non-dominant and dominant eye patching, the shifts of egocentric localization following 60-min deprivation was normalized for each observer by subtracting individual baseline measurement from the post-deprivation data. This normalized data allows to analyse the relative change in egocentric localization, ensuring that any subsequent shifts in egocentric localization could be attributed specifically to the monocular deprivation effects, rather than individual variations in baseline

measurements. Figure 5.10 and 5.11 represent deviations from the individual's baseline in relative to the median, and corneal plane, respectively, with zero indicating no shift from baseline. The baseline measurement (black line) serves as the reference point for each observer, representing their egocentric localization under normal binocular viewing conditions. Figure 5.10 describes the effect of monocular deprivation on the egocentre position for both the non-dominant and the dominant eye across 9 observers (S1-S9). Positive y-values indicate the egocentre is positioned to the right of the baseline, and negative y-values indicate it is positioned to the left. X-axis represents time (in minutes) from patch removal. Another two lines in each subplot depict the non-dominant eye patching (red), and dominant eye patching (blue). According to Figure 5.10, the red lines, representing the egocentric shifts following non-dominant eye patching, show a range of variability across observers. In observers such as S1, S4, S6 and S9, the non-dominant eye patching led to larger deviations from baseline in the earlier minutes, indicating a markable shift in egocentric localization and then gradually return to around baseline level except S4, S5, and S6. The blue lines, representing egocentric shifts following dominant eye patching, tend to exhibit larger shifts in the earlier minutes before returning to baseline for some of the observers (e.g., S2, S4, S5, S6, and S7), though some observers (e.g., S4, S5, and S7) still need extra time to return to the baseline. Overall, the data in Figure 5.10 suggests that short-term monocular deprivation induced a consistent shift in the egocentre location and gradually returned to a stable level at around 12–15mins after the patch was removed for all nine observers, with the shifts always moving toward the median plane of the head rather than the previously deprived eye.

Figure 5.11 describes the effect of monocular deprivation on the egocentre position relative to the corneal plane for both the non-dominant and the dominant eye across 9 observers (S1-S9). Positive y-values indicate the egocentre is positioned in front of the baseline and negative y-values indicate it is positioned behind. X-axis represents time (in minutes) from patch removal. Two lines in each subplot depict the non-dominant eye patching (red), and dominant eye patching (blue). The red lines in each subplot represent the shifts after non-dominant eye patching, in observers such as S2 and S9, the shifts show a greater deviation within the first few minutes following patch removal. Some observers, such as S4, S5, S7, and S9 show larger initial shifts following dominant eye patching (blue lines in each subplot) compared to those after non-dominant eye patching. According to Figure 5.11, both non-dominant and dominant eye patching tend to shift towards the corneal plane and then return to baseline overtime after 15-45 minutes, however, the varying magnitude and duration of these shifts based on whether the non-dominant or dominant eye is patched further demonstrate that eye dominance plays an important role in post-deprivation.

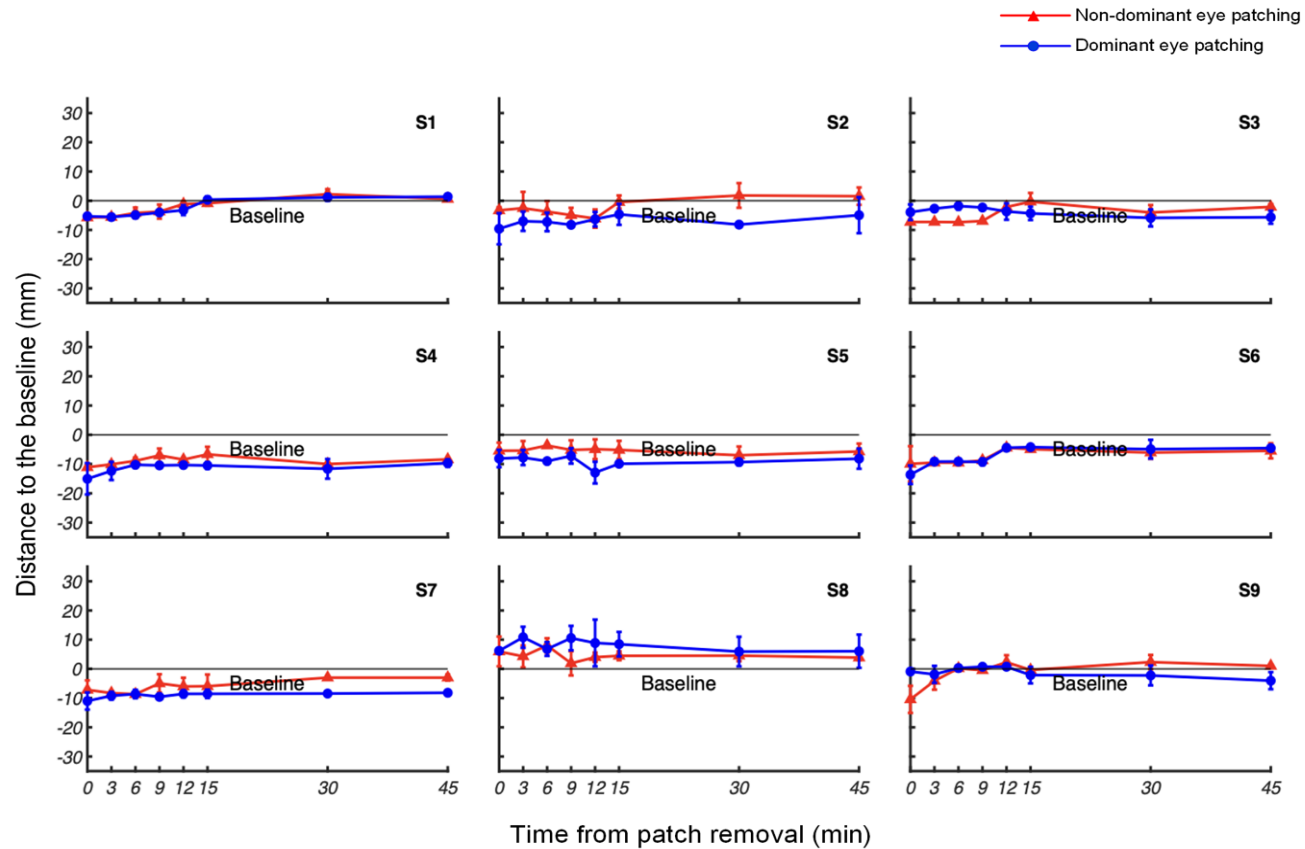


Figure 5.10: Comparison of individual egocentre positions relative to the median plane between patching the non-dominant eye (red lines) and the dominant eye (blue lines). Positive y-value represents the data is at the right of the baseline, while negative y-value represents the data is to the left. The black dashed line represents the baseline for the median plane. Vertical and horizontal error bars represent the SD calculated across repetitions of the measurement for each participant.



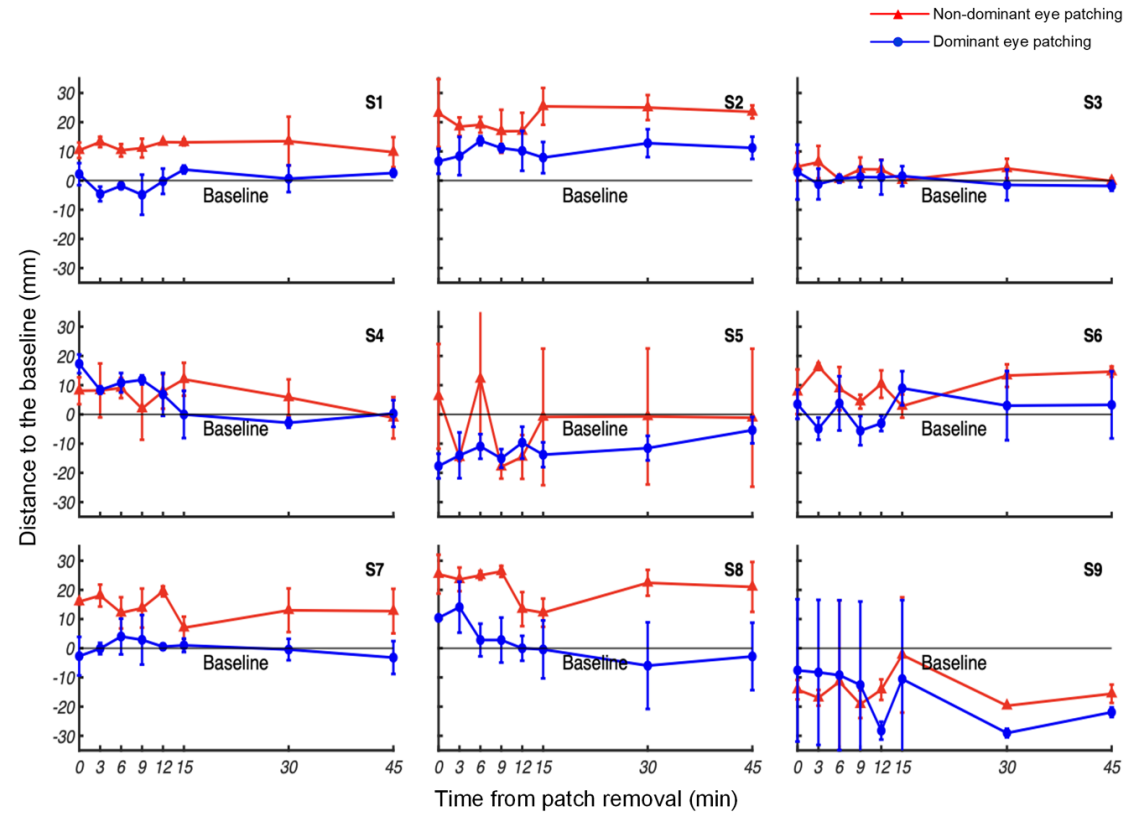


Figure 5.11: Comparison of individual egocentre positions relative to the corneal plane between patching the non-dominant eye (red lines) and the dominant eye (blue lines). Positive y-value represent the data is positioned in front of the baseline, while negative y-value is positioned behind. The black dashed line represents the baseline data for the corneal plane. Vertical and horizontal error bars represent the SD calculated across repetitions of the measurement for each participant.

To compare the differences of patching the non-dominant and dominant eye, the averaged egocentre location in relative to the median and corneal plane was calculated as presented in Figure 5.12(a). The green line describes how the averaged data changes after removing the patch from non-dominant eye over the following 45 mins, while the blue line depicts the data for patching of the dominant eye. The egocentre location was located on average 1.21 (SD = 9.06) mm left of the median plane after removing the patch from the non-dominant eye, compared with the that of 1.12 (SD = 10.18) mm left of the median plane following the dominant eye patching. A one-way analysis of covariance (ANCOVA) was performed to compare the effect of patching conditions (non-dominant or dominant eye patching) on egocentric shift for the median plane, while controlling for baseline measurements. There was no significant effect of patching conditions on egocentric shifts,  $p = .986$ , suggesting that egocentric shifts for the median plane did not differ between non-dominant and dominant eye patching conditions. The covariate baseline shift was found to be a significant predictor of egocentric shifts,  $F_{(1,140)} = 209.79$ ,  $p < .001$ , with a strong positive association ( $\beta = 0.985$ ), indicating a higher baseline data was associated with greater egocentric shifts.

This finding suggests that individual differences in baseline egocentric localization significantly influence the post-patching shifts. Therefore, both non-dominant and dominant eye patching move the egocentre location in exactly the same direction, suggesting that the egocentric shift is not eye-specific and occurs at a higher level where the identity of each input has been lost. As can be seen from Figure 5.12(a), the egocentre location was shifted immediately after patch removal, the shift dissipated within the first 9 mins before gradually reaching an equilibrium. When we compared the egocentre location recorded 45 mins following patch removal from the non-dominant eye and dominant eye, it was located on average 2.02 (SD=10.95) mm right of the median plane (non-dominant eye) and 0.58 (SD =10.95) mm right of the median plane (dominant eye). A repeated measures ANOVA performed with Time (8 levels: 0, 3, 6, 9,

12, 15, 30, 45 minutes) and Conditions (non-dominant and dominant eye patching) as with-in subject factors to investigate changes in the egocentre location with respect to the median plane. The repeated measures ANOVA revealed a significant main effect of time on egocentric shifts for the median plane,  $F_{(15,120)} = 52.27$ ,  $p < .001$ , suggesting that egocentric shifts varied significantly overtime and the shifts occurred regardless of which eye was patched previously.

In terms of egocentre location relative to the corneal plane, the averaged baseline egocentre location was located 27.88 (SD = 10.31) mm behind the corneal plane (Figure 5.12 (b)). The immediate egocentre position was averaged located 21.85 (SD=4.44) mm behind the corneal plane after removing the patch from the non-dominant eye, compared with the location of 27.06 (SD=12.51) mm behind the corneal plane after the patch was removed from the dominant eye. A one-way analysis of covariance (ANCOVA) was performed to compare the effect of patching conditions (non-dominant or dominant eye patching) on egocentric shift for the corneal plane, while controlling for baseline measurements. There was no significant effect of patching conditions on egocentric shifts,  $p = .868$ , suggesting that egocentric shifts for the corneal plane did not differ between non-dominant and dominant eye patching conditions. The covariate baseline shift was found to be a significant predictor of egocentric shifts,  $F_{(1,140)} = 31.77$ ,  $p < .001$ , with a stronger positive association ( $\beta = 0.622$ ), indicating a higher baseline data was associated with larger egocentric shifts. This finding suggests that individual differences in baseline egocentric localization significantly influence the post-patching shifts. Therefore, the egocentric shift for the corneal plane is not eye-specific and occurs at a higher level where the brain is no longer distinguishing between inputs from the non-dominant and dominant eye. A repeated measures ANOVA was conducted to examine the effect of time on the corneal plane shifts following monocular deprivation. The analysis revealed a significant main effect of time on egocentric shifts for the corneal plane,  $F_{(15,120)} = 18.84$ ,  $p < .001$ ,

suggesting that observed shifts in the corneal plane varied significantly overtime.

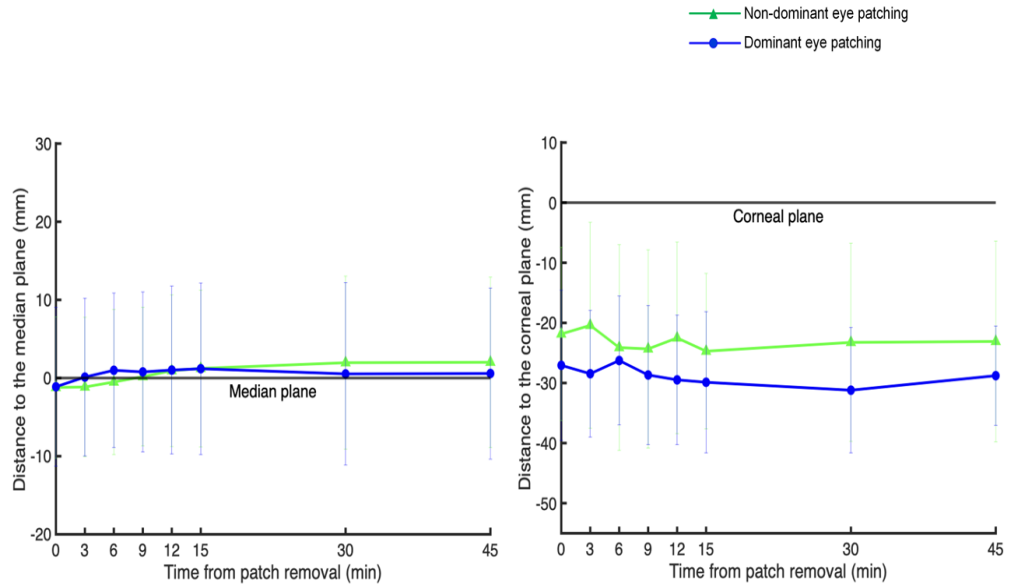


Figure 5.12: The changes of the egocentre location after the end of monocular treatment for the non-dominant eye compared with the dominant eye averaged across all the participants. Vertical and horizontal error bars represent the SD calculated across participants.

A power function was fitted to calculate the egocentric shifts from the median plane and corneal plane at 8 time points following the removal of monocular patch, in the form of the following equation:

$$y(t) = a * t^b + c \quad (5.3)$$

The relationship between  $y(t)$  is the egocentric shifts from the median and corneal plane, and time  $t$  after patch offset was captured. The parameters  $a$ ,  $b$ , and  $c$  were fitted the data to determine the initial magnitude of the egocentric shift immediately after removing the patch, the rate of change overtime, and the asymptote value that the egocentric shift approaches, respectively. The method of nonlinear least-squares was used for fitting, while  $R^2$  represents the goodness of fit for each model.

The power function fit the data is better for the median plane than the corneal plane, particularly in the non-dominant eye patching condition

where 89% of the variance was explained by the model compared with 80% of variance for the dominant eye patching condition. In contrast, the corneal plane in both patching conditions showed weaker fits, particularly in the non-dominant eye patching, where the model only explained 20% of the variance (see Table 5.1 for fitted results).

## 5.5 Discussion

The influence of short-term monocular deprivation on inter-ocular balance in adults has recently been demonstrated by highlighting an increased relative contribution from the deprived eye on a range of binocular tasks (e.g. Lunghi et al., 2011; Zhou et al., 2013; Wang et al., 2021). However, the mechanisms underpinning shifts in sensory eye dominance following deprivation are still unresolved, particularly under binocular viewing conditions. This issue was addressed by judging the visual direction of object in space relative to the viewer (the egocentre location) following short-term monocular deprivation. Here, we found monocular deprivation for 60mins induced a marked shift in the egocentre location. Unlike previously reported studies (e.g. Lunghi et al., 2011, 2013; Zhou et al., 2013; Wang et al., 2020, 2021), we found 60-min monocular deprivation induced a marked shift in the egocentre location, the shift was always towards the direction of the median plane of the head, rather than the eye that had been deprived. This effect was found for occlusion of dominant and non-dominant eyes, where movement in opposite direction would be anticipated, and in most cases returned to baseline levels after ~15mins. However, shifts with respect to the corneal plane did not show a similar pattern. Our findings unequivocally reveal the remarkable plasticity of the adult visual system, consistent with previous assumptions (Gibert & Li, 2012; Lunghi et al., 2013; Wang et al., 2024), highlighting visual cortex has life-long, experience-dependant plasticity.

Table 5.1: Fits results (Eq. 5.3) of the time course of the egocentre location. The estimates of three parameters (a, b and c) (with 95% confidence intervals shown in brackets), and the goodness of fit indicated by  $R^2$  are shown below.

<b>Monocular treatment</b>			<b>a</b>	<b>b</b>	<b>c</b>	<b><math>R^2</math></b>
Non-dominant eye	For the median plane		0.53(-0.44, 1.5)	0.52(0.08, 0.97)	-1.48(-2.81, -0.14)	0.89
	For the corneal plane		-1.06(-10.09, 7.96)	0.21(-1.42, 1.83)	-21.42(-29.25, -13.58)	0.20
Dominant eye	For the median plane		-0.63(-6.28, 5.02)	-0.19(-1.19, 0.82)	1.15(-3.42, 5.72)	0.80
	For the corneal plane		-0.82(-4.82, 3.19)	0.37(-0.77, 1.50)	-26.84(-31.05, -22.62)	0.41

One of the best-known studies of experience-dependent changes in brain function was binocular visual responsiveness of neurons in the V1 can be altered by monocular visual deprivation during a critical period of postnatal development (Daw, 1995; Wiesel, 1982; Wiesel & Hubel, 1963b). It highlights that while cortical circuits are most sensitive to sensory experience during early postnatal development, there is much less plasticity in the mature brain (e.g., Berardi *et al.*, 2000; Hensch, 2004). However, our results demonstrate that the adult human visual system possesses a significant degree of functional plasticity, which is consistent with recent studies that even after the critical periods ends, monocular visual deprivation can still lead to an ocular dominance shift in visual cortical neurons in mice though the characteristics of shift – such as magnitudes, mechanisms, duration and other features - differ from those observed in critical period plasticity (Antonini *et al.*, 1999; Fischer *et al.*, 2007; Hofer *et al.*, 2006; Lehmann & Löwel, 2008; Morishita & Hensch, 2008; Pham *et al.*, 2004; Sato & Stryker, 2008; Sawtell *et al.*, 2003; Tagawa *et al.*, 2005;).

The cerebral cortex primarily consists of two types of neurons: glutamatergic (excitatory) and GABAergic (inhibitory), each contributing differently to visual cortical plasticity, particularly in term of binocular responsiveness and adaptivity to changes like monocular deprivation (Kameyama *et al.*, 2010). While earlier studies using genetically modified mice with different GABA levels found GABAergic plays an important role in regulating critical periods by either enhancing or inhibiting GABAergic function to affect visual cortical plasticity (Hensch, 2005; Hensch *et al.*, 1998), but result in uncertainties about the inherent differences between GABAergic and excitatory neurons regarding their plasticity. Kameyama *et al.* (2010) used transgenic mice with normal GABA expression levels demonstrated that GABAergic neurons are more binocularly in responses than excitatory neurons and exhibit greater plasticity especially after ends of the critical period, indicating that GABAergic neurons play a crucial and sustained role in visual plasticity beyond early development. They revealed that monocular deprivation reduced the

responsiveness of GABAergic neurons to the deprived eye and excitatory neurons increased the responsiveness to the non-deprived eye, which aligns with Hebbian synaptic plasticity, suggesting that neural connections are strengthened or weakened based on activity.

In adults, an enhancement of the deprived eye's signal induced by short term (around 2-hour) monocular visual deprivation has been observed (Bai et al., 2017; Binda & Lunghi, 2017; Castaldi et al., 2020; Chadnova et al., 2017; Lunghi et al., 2011, 2013, 2015; Lunghi & Sale, 2015c; Lunghi et al., 2019; Min et al., 2018; Wang et al., 2020; Zhou et al., 2013, 2014, 2015). Ongoing research has shown that the persistence of plasticity into adulthood allows for continued adaptability in response to new experiences, learning and injury recovery (Gibert & Li, 2012). A key feature of plasticity in the adult primary visual cortex is the connection field, which links contour elements in the visual field through long-range horizontal connections formed by cortical pyramidal cells (Gibert & Wiesel, 1989; Stettler et al., 2002). These connections allow for integrating information across the large areas of the visual field, encoding new information and recovering from the sensory disruptions in adulthood (Gibert & Li, 2012). The impact of shifts in the egocentric location in this chapter highlights the adaptability of the visual system, which is supported by research that short-term monocular visual deprivation leads to perceptual adjustments as a form of homeostatic plasticity (Turrigiano, 2012). Consistent with research on ocular dominance plasticity that short-term monocular deprivation alters the balance of visual inputs from both eyes (Bai et al., 2017; Ramamurthy & Blaser, 2018), suggesting that adult plasticity can recalibrate spatial perception based on altered sensory input. Kurzawski et al. (2022) investigated short-term monocular (2-hour) deprivation in the human visual thalamus, especially the lateral geniculate nucleus (LGN) and occipital lobe, in response to short-term monocular masked stimulation.

Using ultra-high field (7T) functional magnetic resonance imaging (fMRI), they found evidence of short-term plasticity effect in the ventral occipital



lobe (vPulv), where representation of the deprived eye was enhanced compared to the non-deprived eye. This effect is similar to previously observed plasticity in the visual cortex and has been associated with behavioural shifts in ocular dominance. In contrast, no such effects were observed in the dorsal occipital lobe or LGN, suggesting short-term monocular deprivation affects the special subregions of the thalamus differently and highlighting that visual thalamus, specifically the vPulv, has a unique capacity for short-term plasticity in response to altered sensory input. The observed vPulv plasticity aligns with my research on short-term monocular deprivation effect on the egocentre location. This supports the notion that short-term monocular deprivation triggers rapid adaption not only in the visual cortex but in the subcortical structures like the thalamus, which play a crucial role in visual perception. The link between change in thalamus and changes visual perception highlights the interconnected plasticity of both cortical and subcortical regions, suggesting that the shifts of egocentric location may involve contributions from both cortical and subcortical regions (Wilke et al., 2009), and thereby allowing for rapid recalibration of spatial perception and sensory input balance.

Min et al. (2018) investigated the impact of short-term monocular deprivation on ocular dominance with a binocular phase combination task, during which the dominant eye of each participant was patched for 2 hours over 5 consecutive days to examine if repeated short-term monocular deprivation leads to cumulative effects. An enhanced contribution of the deprived eye to binocular vision was found, but this effect did not accumulate over repeated sessions, suggesting that the effect of short-term monocular deprivation is transient and follows an all-or-none pattern, regardless of the duration or repetition of the deprivation. However, this finding contrasts with our observation that egocentric shifts are related to short-term monocular deprivation. Min et al. (2018) argued that ocular dominance changes induced by short-term monocular deprivation are driven by a fast homeostatic plasticity mechanism that quickly restore balance between the eyes after deprivation ends. The

observed all-or-nothing effect is because this mechanism does not gradually build over time or with repeated deprivation. In contrast, the shift in the visual egocentre may involve a more sustained or cumulative change beyond the fast homeostatic adjustments, suggesting that distinct forms of plasticity may characterize different aspects of visual processing.

We achieve a cohesive sense of direction by assessing the direction of objects in visual space relative to the visual egocentre, integrating perspectives from both eyes' distinct vantage points. With symmetrical convergence, objects along corresponding visual lines are regarded as being perceived from a point approximately midway between the two eyes. This reference point is present from childhood, and it has been shown that young children (between 1.8 – 5 years of age) with normal binocular vision, comitant strabismus, or had undergone eye enucleation (Dengis et al., 1993a) instinctively position a tube at the bridge of the nose when instructed to look through it at targets, a phenomenon known as the 'cyclops effect' (Barbeito, 1983; Church, 1966). This effect reduces with age as children start to sight monocularly by the age of around 5 years old. The observation that children default to aligning relative to the middle of their head, regardless of the quality of binocular vision they possess, suggesting that a cyclopean projection centre may be innate, which aligns with Hering's hypothesis that the visual direction of an object is determined with reference to an egocentre located midway between the two eyes (Hering, 1879/1942; Ono, 1979,1991).

This midline egocentre has been consistently demonstrated in individuals with normal binocular vision or strabismus (Ono & Weber, 1981), whether they are viewing binocularly or monocularly. The presence of a median egocentre supports a unified sense of visual direction to integrate inputs from both eyes, in which this integration reconciles local retinal information and eye position information projecting to a single visual egocentre to provide a coherent perception of visual space (Dengis et al.,1998). Dengis et al. (1993b) further examined whether the surgical

correction of strabismus affects the egocentre location in children with strabismus. They used a modified Roelof's (1959) method to measure the egocentric position of three groups of children: children with horizontal strabismus before and after surgery, children with vertical strabismus before and after surgery, and a control group of children with normal binocular vision. The results found no significant differences between the egocentric position of strabismus group and that of the control group, which remained at the midline before and after surgery, despite changes in eye position.

My observations extend the understanding of visual egocentre flexibility by showing that 60-min monocular deprivation caused a marked shift in the egocentre location toward the median plane rather than the previously deprived eye aligns with the findings on egocentre stability in children with strabismus. Similar to how children use the cyclops effect during monocular task, the stability of the egocentre position demonstrates visual system prioritizes a central egocentric alignment for spatial stability even when sensory input is temporarily altered. However, my findings on short-term monocular visual deprivation and shifts in the visual egocentre location demonstrates that the relative visual input, rather than the visual direction of a particular eye is more important on egocentre position.

To conclude, our study has demonstrated functional changes in perceived visual direction for adults with normal vision induced by short-term monocular deprivation. The cyclops effect in adults suggests that visual egocentre starts from a unified spatial reference point that is based on the median plane of the head, implying that the visual system defaults to a centrally aligned egocentre. Barbeito (1981) conducted two experiments using common sighting tasks that requires participants to align an object through monocular viewing to investigate the relationship between sighting dominance and visual direction processing. The findings suggested that monocular sighting dominance is not an innate feature of the visual system, but a visual experience learned from a range of tasks where using a single eye is beneficial (e.g., shooting, using a

telescope or a microscope). Over time, monocular sighting dominance becomes context-specific and influenced by individual experiences and needs, resulting in consistent patterns. However, the shift toward the median plane induced by short periods of visual deprivation may to some extent break this learned monocular preferences and shifts the egocentre back to a more innate state, a median plane alignment. This reset provides an insight on treating certain conditions where one eye becomes dominant (e.g., amblyopia or strabismus). By breaking down the established monocular preference, brief periods of monocular visual deprivation can promote a more balanced inputs from both eyes and foster a better binocular function and coordination.

# Chapter 6. The magnitude of plastic changes in eye dominance measured using an alignment task

## 6.1 Introduction

In humans and higher mammals with forward-facing eyes, a significant portion of the visual field is seen by both eyes (Boff et al., 1986). However, bilateral structures in the body rarely demonstrate complete equality. Typically, one eye is favoured in processing visual information or exhibits physiological superiority, leading to its classification as dominant. For instance, individuals who consistently use their right hand for writing or eating are described as having a dominant right hand, or right-handedness. The most commonly measured form of eye dominance, called sighting dominance, reflects a behavioural preference for input from one eye when both eyes cannot be used simultaneously, or when their views are discordant and cannot be fused (Porac & Coren, 1975). Due to its frequency and ease of measurement—often tested by having individuals look through a pinhole (Crider, 1944)—sighting dominance is considered the “definitive” measure of eye dominance (Mapp et al., 2003; Porac & Coren, 1976).

A common scenario illustrating this phenomenon occurs when someone points at a distant target with a finger. Double vision arises as the target stimulates non-corresponding retinal spots, creating two images of the finger. This visual interference requires the brain to rely on input from one eye to resolve the alignment challenge, suppressing the other eye’s input to eliminate double vision. Thus, one eye typically dominates in completing the task.

A dominant eye is characterized by its superior ability in behavioural coordination, monocular perception (Porac & Coren, 1976). Population studies indicate that approximately 65% of healthy individuals prefer viewing with the right eye, 32% with the left eye, and 3% show no consistent preference (Li et al., 2010; Yang et al., 2010; Zhang et al., 2011). These findings suggest that approximately 97% of individuals consistently favour one eye over the other when performing sighting tasks. Similar patterns have been observed in other species, particularly primates (Cole, 1957; Hall & Mayer, 1966), while some animals, like cats, exhibit paw preference without showing eye preference (Crinella et al., 1972).

While eye dominance exhibits some plasticity in adults, most research has focused on rebalancing eye inputs rather than exploring the underlying neural mechanisms. Messe, Georgeson, and Baker (2006) proposed a two-stage model, suggesting that the visual system modulates each eye's input through contrast gain control and binocular combination. However, this model does not fully account for other aspects of binocular vision, such as depth perception and stereopsis. Recent studies, such as Kam and Chang's (2021) work on dichoptic training tasks, suggest that changes in eye dominance may occur at early stages of the visual processing pathway, like the lateral geniculate nucleus (LGN) or the primary visual cortex (V1). Animal studies have documented interocular inhibitory interactions in the LGN (Guillery & Colonnier, 1970), and diffusion-weighted imaging in humans has shown that optic radiation microstructure can predict eye dominance (Chan & Chang, 2022). These findings suggest that both subcortical and cortical mechanisms contribute to eye dominance.

Based on the research presented here, it is crucial to account for the magnitude of neural plastic changes in eye dominance resulting from different viewing conditions when assessing the effects of eye dominance. While various paradigms have been developed to promote eye rebalancing, there has been a notable lack of investigation into the neural

mechanisms underlying eye dominance and the magnitude of its plasticity. Furthermore, research on quantifying plasticity in eye dominance measured through alignment tasks is limited. Purves and White (1994) investigated how individuals manage monocular preference in a binocular alignment task. They used a partially occluded fenestrated screen positioned 2 meters from the viewer, allowing simultaneous sight of a target with both eyes. In this setup, the line of sight from one eye interacts with the screen, offering insights into how monocular preference influences binocular alignment. Among 97 subjects, about half were categorized as moderately dominant, based on the frequency of eye fixation. These findings reveal a discrepancy compared to the hole-in-the-card test (e.g., Ehrenstein, Arnold-Schulz-Gahmen, & Jaschinski, 2005; Zeri et al., 2011), where subjects often show a consistent preference for one eye. This suggests that when faced with a task requiring a choice between the views of each eye, some individuals prioritize one eye, while a significant portion assigns similar importance to both monocular views. This complexity complicates the decision of which eye to utilize, leading to alternating behaviour. The current study aims to investigate whether the weighting of monocular views can be measured during the depth-based alignment of visual targets across a range of eccentricities. This investigation involves monitoring binocular perception to assess how the brain balances input from each eye and examining the extent of neural adaption induced by short-term monocular deprivation, which seeks to clarify the mechanisms that governs sensory integration in response to monocular input imbalance.

## 6.2 Experiment 9: Measuring visual alignment of targets in depth across a range of horizontal eccentricities

### 6.2.1 Methods

#### 6.2.1.1 Observers

Nine participants (age range: 23-53years, mean age:  $34.33 \pm 11.48$ years) had normal or corrected-to-normal vision and no history of ocular disease participated in this experiment. Before formal data collection, the TNO stereo test (Laméris Ootech, Nieuwegien, The Netherlands) was administered to ensure the participants had normal stereo vision and thus were able to perceive the depth and 3-dimensional structure of visual information (stereo threshold range of 60 to 120arcsec). The experiment was approved by School of Psychology Ethics Committee at University of Nottingham. Participants gave informed consent before the experiment and all experimental procedure conformed to the principles laid out in the Declaration of Helsinki.

#### 6.2.1.2 Apparatus and stimuli

The stimuli consisted of 19 vertical lines, each 5-cm in height, arranged in a horizontal row on a white wall, with numbers displayed below each line. These lines were spaced 10-cm apart, positioned 119 cm above the floor, and located 100cm from the pointer of the apparatus. The visual field extends to  $33^\circ$  in both the left and right visual fields relative to the fixation point at  $0^\circ$ , as shown in Figure 6.1(a).

The adjustable apparatus was custom-built and consisted of a wooden toothpick (5-cm in height) with the tip highlighted in red to serve as a pointer. The pointer was positioned approximately 40cm from the bridge of the nose and mounted on a high-precision rotation stage (see Figure



6.1 (b)). A 360-degree protractor was attached under the arm of the apparatus, allowing the experimenter to read the rotation angle directly. Using this apparatus, visual alignment of targets in depth was measured at various eccentricities during both monocular and binocular alignment tasks.

#### 6.2.1.3 Procedure

The observer viewed the stimuli in a well-lit room, seated at an adjustable table and their head supported by a chin rest. The line of sight was perpendicular to the wall when the observer fixated on number Zero. The observer was instructed to adjust the arm of the apparatus until the pointer appeared aligned with the predetermined marker on the wall, this was repeated both monocularly and binocularly. After each measurement, the experimenter recorded the rotation angle from the protractor. This procedure was used to establish baseline data. Each measurement was repeated three times, across 19 marker locations in a randomized order, totalling 171 trials. First, we measured sighting alignment under monocular and binocular viewing conditions; this provided an estimate of monocular visual direction and perceived egocentric visual direction. Next, the non-dominant eye was covered with an opaque patch for 60 minutes, during which all visual input to that eye was eliminated. The observer was free to engage in routine activities while patched. After the patch was removed, visual alignment was remeasured both monocularly and binocularly. The viewing distance was then adjusted to further investigate changes in relative depth between the two alignment targets. The distances between the pointer and the scale were either 50cm, 100cm, or 200cm.

#### 6.2.1.4 Data analysis

A linear mixed-effects model analysis was conducted to examine the relationship between various eccentricities and the perceived visual direction, using the *fitlme* function in MATLAB (MathWorks, version

R2024a). The model had fixed effects of *Viewing Distance* (50cm, 100cm, and 200cm) and random effects of *Eccentricity* allowing for random intercepts across a range of eccentricities.

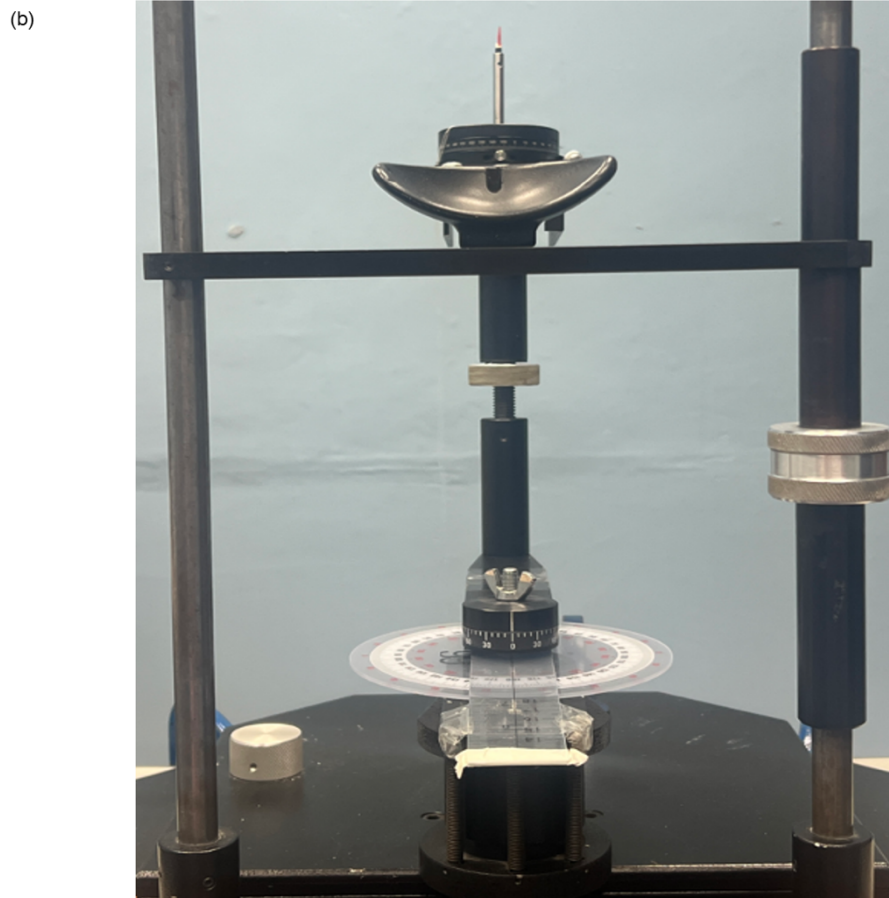
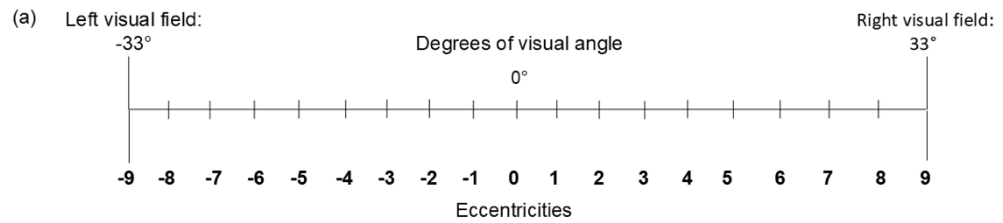


Figure 6.1: Apparatus used in the experiment. (a) 19 pre-set horizontal scale markers were used in the alignment task each at a different eccentricity, with the visual field extends  $33^\circ$  in both the left and right visual field relative to the fixation point at  $0^\circ$ ; (b) The custom-built apparatus used in the experiment placed on the specially constructed table, a  $360^\circ$  scale was added under the arm of the apparatus so that the rotation angle of the arm could be read precisely.

## 6.2.2 Results

The mean settings for monocular and binocular alignment, representing monocular visual direction and egocentric visual direction, are shown as a function of the horizontal scale measured under both viewing conditions for three representative subjects in Figure 6.2. The data were highly consistent, with the error bar (standard error) being smaller than the data symbol. Eye dominance can be determined by identifying which eye the egocentric visual direction is biased towards, based on the three alignment settings. As shown in Figure 6.2, the first observer (a) demonstrates strong right eye dominance, with the egocentric direction (red line) nearly overlapping the direction of the right eye (blue line). In contrast, the third observer (c) shows left eye dominance, where the egocentric direction (red line) almost overlaps the direction of the left eye (green line). The second observer (b) shows no strong eye preference, with the binocular egocentric direction (red line) positioned between the two monocular visual directions.

To explore the generalizability of these findings, different viewing distances were tested with the same three observers, examining variations in the relative depth between the two alignment targets. Figure 6.3 presents data from one representative observer at viewing distances of 50cm (a), 100cm (b), and 200cm (c), measured from the moveable pointer to the fixed markers on the wall. As shown in Figure 6.3, the perceived visual direction changes linearly with the horizontal scaling of the 19 eccentricities across three depth planes. A linear regression was conducted to examine the relationship between different viewing distances and perceived egocentric direction. Table 6.1 provides a summary of the slopes of the linear regressions for binocular alignment at these different depths averaged by 9 subjects. The slopes decreased gradually as viewing distances increase, with slopes of 1.816, 1.279, and 0.790 for 50cm, 100cm, and 200cm, respectively. All p-values were statistically significant ( $p < .001$ ) and  $R^2$  represented a high degree of fit

( $R^2 > 0.994$ ) highlighting a high reliability of the alignment data at varying distances.

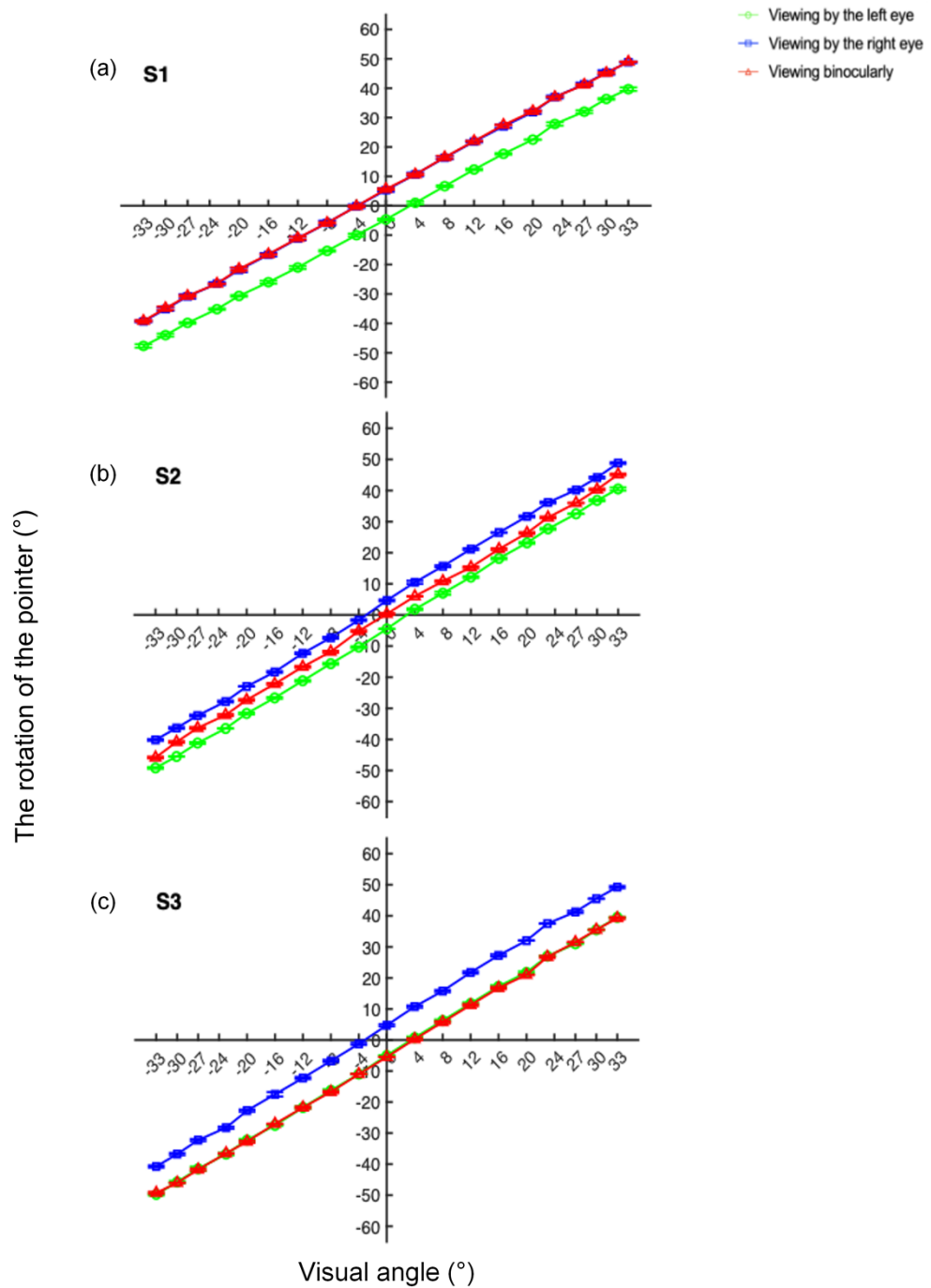


Figure 6.2: The data of three representative observers measured at 100cm from the moveable pointer to the fixed markers on the wall. The rotation of pointer is shown as a function of fixed horizontal scaling location viewed by the left eye (green line with circle), the right eye (blue line with square) and two eyes (red line with triangle).

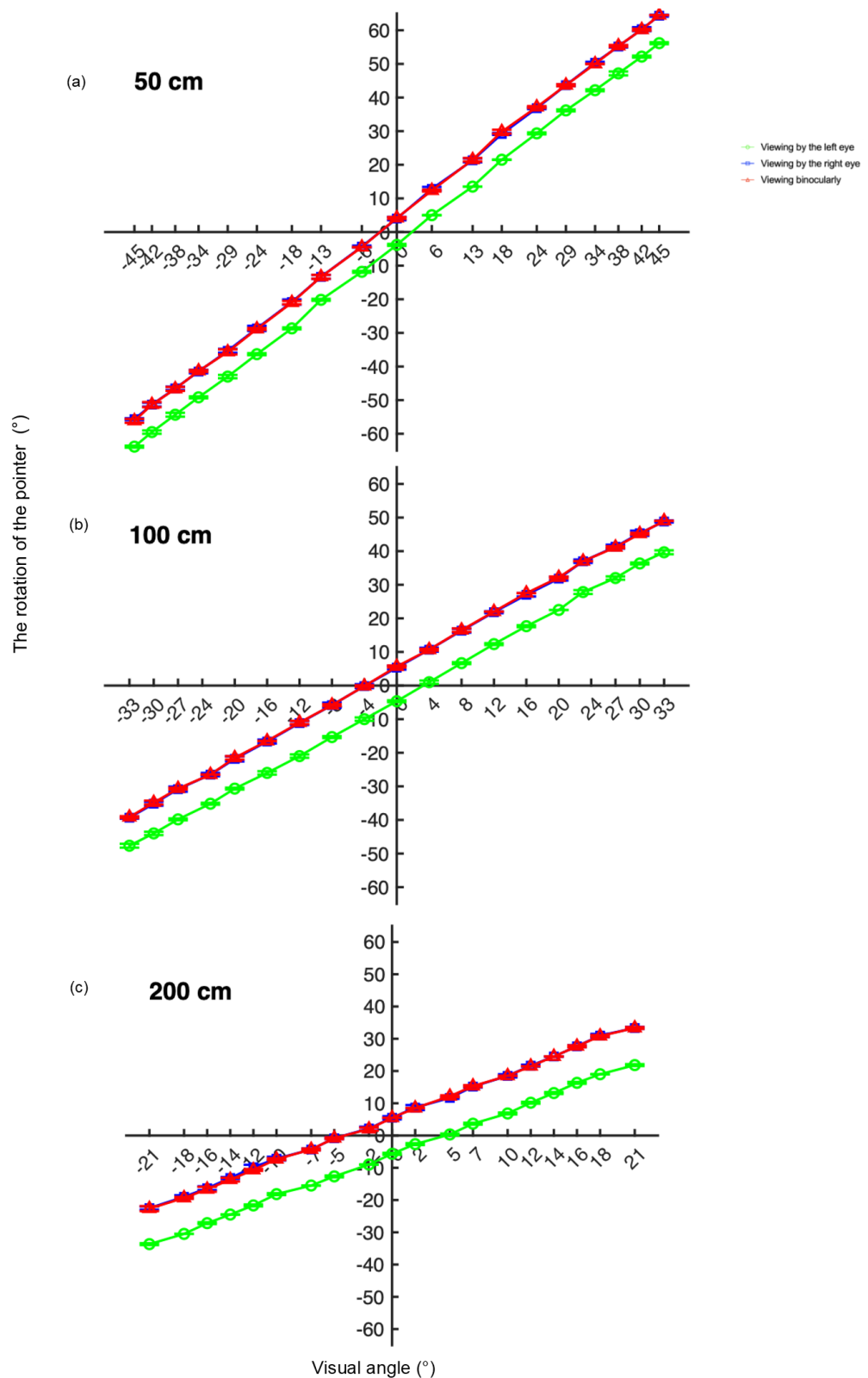


Figure 6.3: The data in different absolute distance of one representative participant measured across three viewing distances: 50cm (a), 100cm (b) and 200cm (c), from the moveable pointer to the fixed markers on the wall. The rotation of pointer is shown as a function of fixed horizontal scaling location viewed by the left eye (green line with circle), the right eye (blue line with square) and two eyes (red line with triangle).

Table 6.1: Slopes calculated from linear regressions to the settings of monocular and binocular alignment at different depths.

Viewing distance (cm)	Viewing	Slope (b)	Std. Error	p-value	R <sup>2</sup>
50	Left eye	1.810	0.032	0.000	0.995
100		1.274	0.013	0.000	0.998
200		0.779	0.003	0.000	1.000
50	Right eye	1.811	0.033	0.000	0.994
100		1.281	0.012	0.000	0.998
200		0.784	0.003	0.000	1.000
50	Binocular	1.816	0.033	0.000	0.994
100		1.279	0.013	0.000	0.998
200		0.790	0.003	0.000	1.000

A mixed-effects analysis was conducted to assess the effect of viewing distance on egocentric direction across different eccentricities. The results revealed that neither viewing distance ( $b = 0.008$ ,  $SE = 0.024$ ,  $t_{(55)} = 0.317$ ,  $p = .752$ ) nor the interaction ( $b = 4.105$ ,  $SE = 7.10$ ,  $t_{(55)} = 0.578$ ,  $p = .565$ ) had statistically significant effects on the perceived visual direction. This indicates that different viewing distance did not lead to significant differences in the egocentric direction.

Three subjects were instructed to wear an opaque patch over their non-dominant eye for 60 minutes, with alignment measurements taken at varying viewing distances. Figure 6.4 displays post-deprivation alignment data for one representative subject at viewing distances of 50cm (a), 100cm (b), and 200cm (c) under both monocular and binocular conditions. A mixed-effects analysis was conducted to assess the effect of conditions (baseline and post-deprivation) and viewing distance on egocentric direction across different eccentricities. The data revealed no significant main effects for conditions ( $b = 0.070$ ,  $SE = 3.996$ ,  $t_{(110)} = 0.018$ ,  $p = .986$ ) or viewing distances ( $b = 0.009$ ,  $SE = 0.021$ ,  $t_{(55)} = 0.415$ ,  $p = .679$ ). The interaction was also non-significant ( $b = -0.001$ ,  $SE = 0.030$ ,  $t_{(55)} = -0.041$ ,  $p = .968$ ), suggesting that 60 minutes deprivation does not alter eye dominance in this setting for the three subjects.

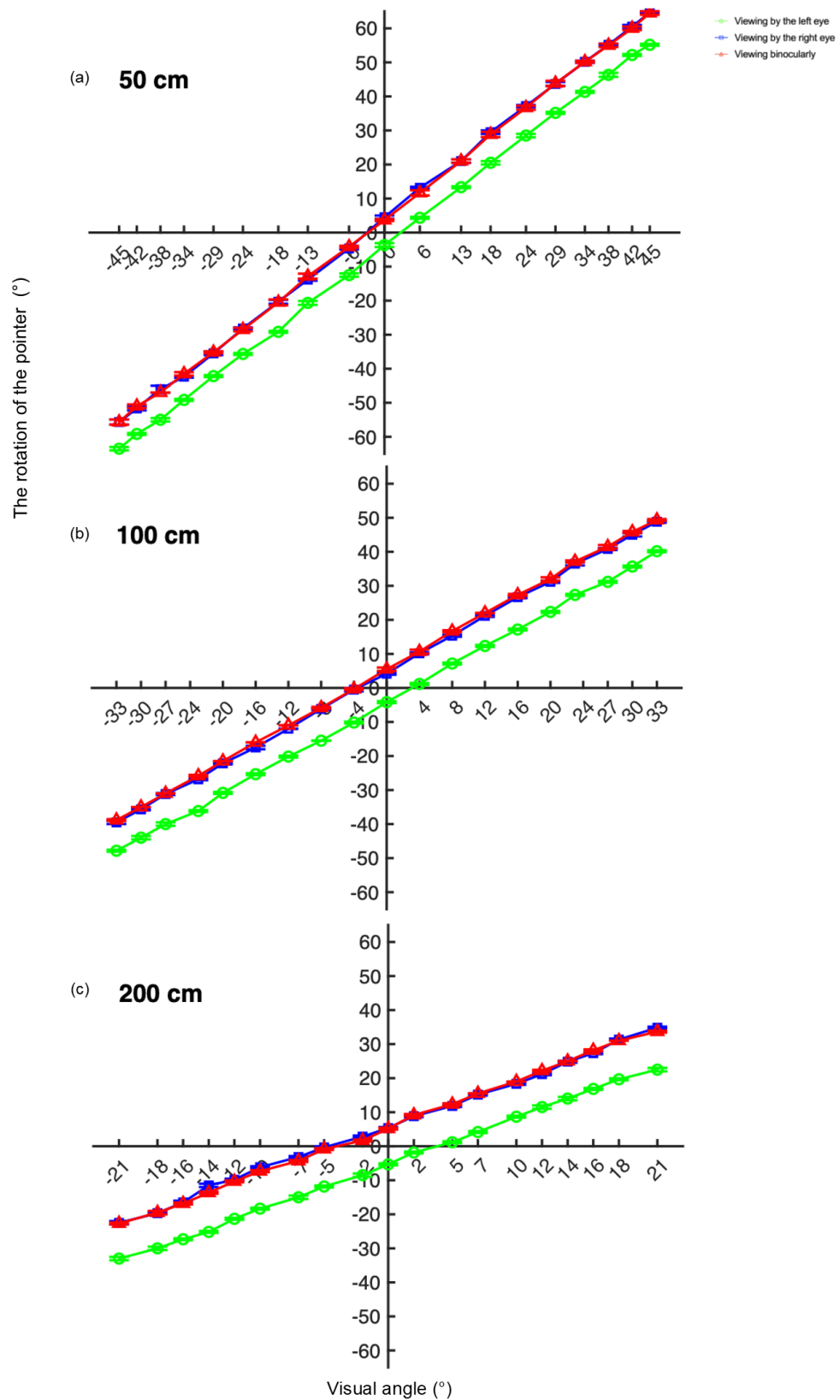


Figure 6.4: The post-deprivation data of one representative participant in different absolute distance measured across three viewing distance: 50cm (a), 100cm (b) and 200cm (c), from the moveable pointer to the fixed markers on the wall. The rotation of pointer is shown as a function of fixed horizontal scaling location viewed by the left eye (green line with circle), the right eye (blue line with square) and two eyes (red line with triangle).

In summary, we examine the effect of short-term monocular deprivation on perceived visual direction across varying viewing conditions (50cm, 100cm, and 200cm). The primary goal was to investigate whether 60-min monocular deprivation could lead to a shift in eye dominance, as measured by visual alignment data under monocular and binocular viewing conditions. As previous studies have demonstrated that monocular deprivation can induce temporary shifts in eye dominance by altering the input balance of two eyes (e.g., Kim et al., 2017; Lunghi et al., 2011, 2013; Zhou et al., 2013). However, the lack of significant changes in eye dominance measured in our experimental setup implies that alignment task may not be sensible enough to detect subtle changes in eye dominance following 60-min monocular deprivation. Therefore, more sensitive perceptual manipulations may be required to investigate the extent of neural plastic changes in eye dominance induced by deprivation, which will be explored in the following sections.

## 6.3 Experiment 10: The effects of short-term monocular deprivation on visual alignment in depth

### 6.3.1 Methods

#### 6.3.1.1 Observers

Ten observers took part in this experiment (4 females, age range: 25-53years, mean age:  $35.50 \pm 10.01$ years), all had normal or corrected-to-normal vision and no history of ocular disease. Stereo was measured using the same approach as Experiment 9. The handedness was confirmed for each of 10 observers before experiment.



### 6.3.1.2 Apparatus and stimuli

In this experiment, the apparatus used was identical to that in Experiment 9. Additionally, two 35mm diameter unmounted linear glass polarizing filters were placed inside the optical cell of a trial frame. The lens can rotate 360° around the optical axis. The first polarizer was placed closer to the eye and was held stationary (rear cell), while the second polarizer, referred to as the "analyser" was positioned in front of the first one (front cell). The analyser was rotated from 0° (parallel to the first polarizer) to 90° (perpendicular to the first polarizer) to achieve the desired polarization effect and control the light level entering the eye, and then to 180° to increase the luminance.

#### 6.3.1.2.1 *Linear polarizing filters*

Light, as an electromagnetic wave, has an electric field that oscillates perpendicular to its direction of propagation. Everyday light sources such as sunlight, LED bulbs, and incandescent lights emit unpolarized light, where the electric field direction fluctuates randomly. A linear polarizer restricts the light to a single plane along its direction of propagation (see Figure 6.5). By using two polarizers in combination, we can control the amount of light transmitted. When the polarizers' transmission axes are parallel, maximum light transmission occurs. Conversely, when the polarizers are perpendicular, or "crossed", light transmission is minimized, as all possible polarization states are filtered out. The angle between the transmission axes can be adjusted to achieve varying levels of light attenuation while maintaining binocular vision.

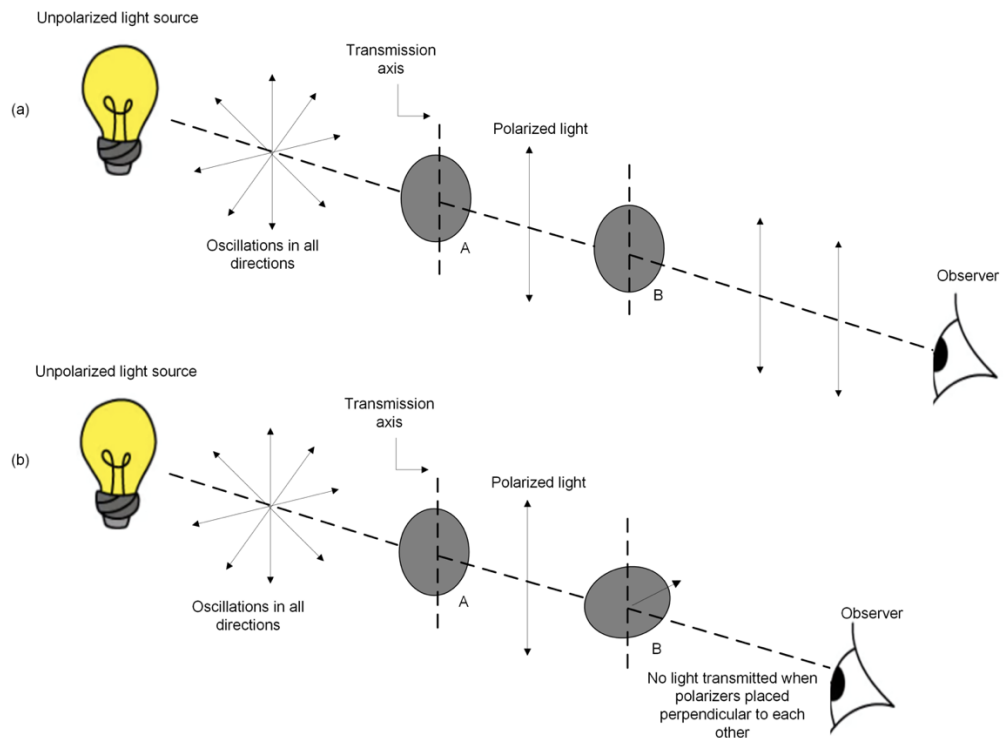


Figure 6.5: How two polarizer filters work together to attenuate the light intensity.

(a) when two polarizers were placed in the same direction, the maximum intensity of the light is transmitted; (b) when the second filter was rotated through  $90^\circ$ , the intensity of transmitted light is zero. By varying the angle between the polarizers, the degree of light entering into the eye can be controlled.

#### 6.3.1.2.2 Luminance calibration

A luminance meter (Konica-Minolta LS-110, Japan) was mounted on a tripod and positioned 100cm away from the linear polarizers and at the same height. The distance between the luminance meter and the linear polarizers was 100cm, with a shielded light source placed 20cm behind the polarizers (see Figure 6.6(a)). The vertical height of the light source, linear polarizers, and luminance meter were the same (60cm above the table). A stop with a central circular aperture ( $1^\circ$  visual angle) was positioned so that light passed through the centre of each filter (see Figure 6.6(b)).

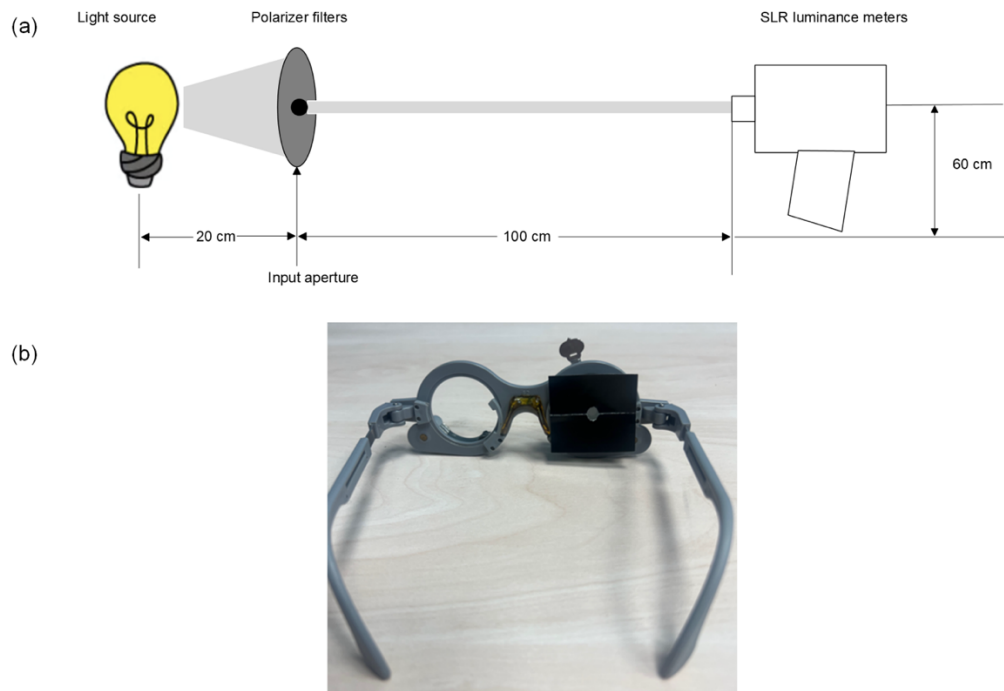


Figure 6.6: Luminance calibration.

(a) The apparatus setting for luminance calibration, the distance between the luminance metre to polarizers, as well as the polarizers to the light source are marked in the figure; (b) Two polarizers are inserted into the cells of one side of a trial frame, there is a black card with an aperture in the centre to make sure the light goes through the centre of each polarizer.

The luminance meter was used to measure the amount of light that passed through the polarizing filters. Firstly, baseline luminance measurements were taken without the filters in place. Then, a single polarizer was added to the setup, and the luminance measurement was repeated under the same lighting conditions. Finally, a second polarizer was placed in front of the first, and a series of luminance readings were recorded as the orientation of the second polarizer was incrementally varied. Starting from a parallel alignment ( $0^\circ$ ) relative to the first polarizer, the second polarizer was rotated until it became perpendicular ( $90^\circ$ ) and then continued rotating until it reached  $180^\circ$ , bringing it back to a parallel orientation with the first polarizer.

According to Malus's Law (Morus, 2005), the intensity of transmitted light  $I(\theta)$ , through two linear polarizers is proportional to the square of the cosine of the angle  $\theta$  between light's initial polarization direction and the

axis of the second polarizer. This relationship can be expressed mathematically as:

$$I(\theta) = I_0 \cos^2(\theta) \quad (6.1)$$

where  $I_0(\theta)$  represents the initial intensity of the light after passing through the first polarizer. The transmitted intensity gradually decreases as the angle  $\theta$  increases from  $0^\circ$  to  $90^\circ$  and reaches zero when the polarizers are perpendicular (i.e., at  $\theta = 90^\circ$ ). The luminance measurement for a range of relative angles between the filters is plotted in Figure 6.7.

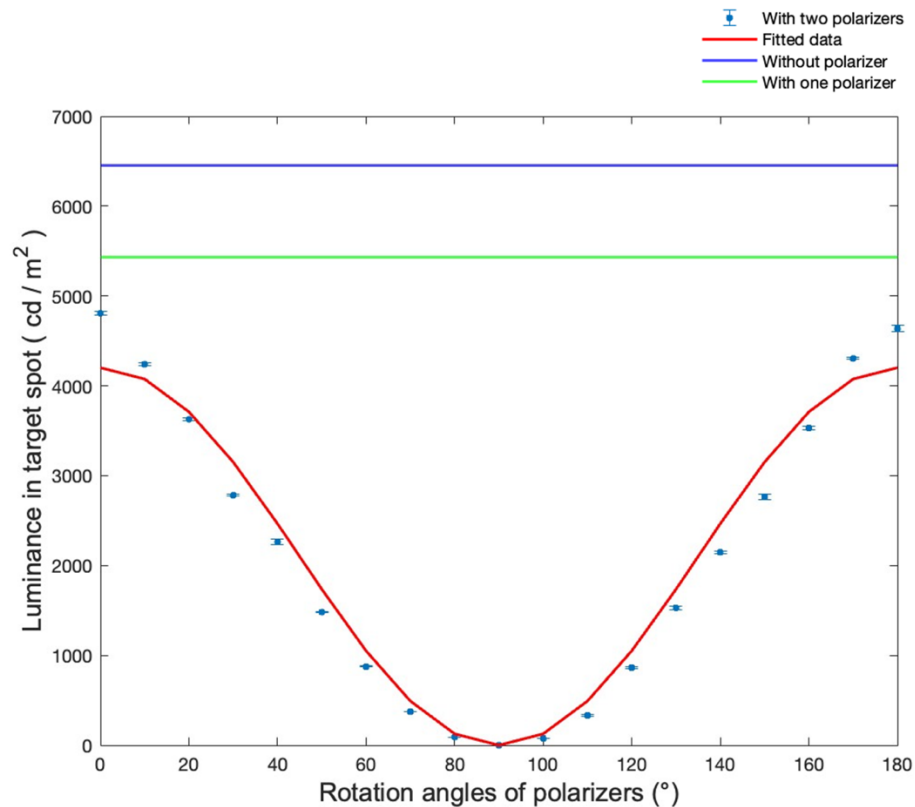


Figure 6.7: The luminance measured without a polarizer (blue line), only one polarizer (green line) and two polarizers (blue dots) rotated from parallel to perpendicular direction and then parallel again. Red curve line indicates how well Malus's Law fits the data with as the relative polarization angle varies. The data points are the mean of X measurements, and the error bars indicate the standard deviation.

### 6.3.1.3 Procedure

Observers were seated at the same table used in Experiment 9, within a well-lit room. They were instructed to adjust the arm of the apparatus until the pointer aligned with a predetermined marker on the wall. In this experiment, only three eccentricities ( $-12^\circ$ ,  $0^\circ$ , and  $12^\circ$ ) were measured monocularly and binocularly to assess each observer's eye dominance. Eye dominance was determined by identifying which eye's monocular alignment corresponds to the alignment observed with both eyes, that eye was considered as the dominant eye. The rotation angles from the binocular measurements were recorded as the baseline data. Each measurement was repeated three times for each eccentricity, randomized in order, resulting in a total of 27 trials. Next, the observer wore a trial frame with polarizers placed over the dominant eye.

The experimenter adjusted the pointer aligned with  $-12^\circ$  eccentricity based on the predetermined baseline egocentric angle. Following alignment between the pointer and the scale marker under binocular viewing, we then reduced the luminance to the dominant eye until perception switched to the fellow eye by rotating the angle of external polarizer from  $0^\circ$  to  $90^\circ$ . The angle of the polarizer at this transition was taken to indicate a balance point for a shift in eye dominance. The switch to a monocular image result from the suppression of the reduced-luminance image in the dominant eye. In fact, the procedure we use here is similar to that used to test the depth of suppression in individuals with amblyopia - where a S-bias is used to reduce the luminance of a target presented to the dominant eye until perception switches to the amblyopic eye (Crawford & Griffiths, 2015). In the following process, the external polarizer was rotated from  $90^\circ$  to  $180^\circ$ , progressively increasing contrast to the dominant eye until physiological diplopia reappeared, and this rotation angle was recorded as well. The same procedure was repeated for the other two eccentricities ( $0^\circ$  and  $12^\circ$ ), and each measurement was repeated three times in this predetermined order.

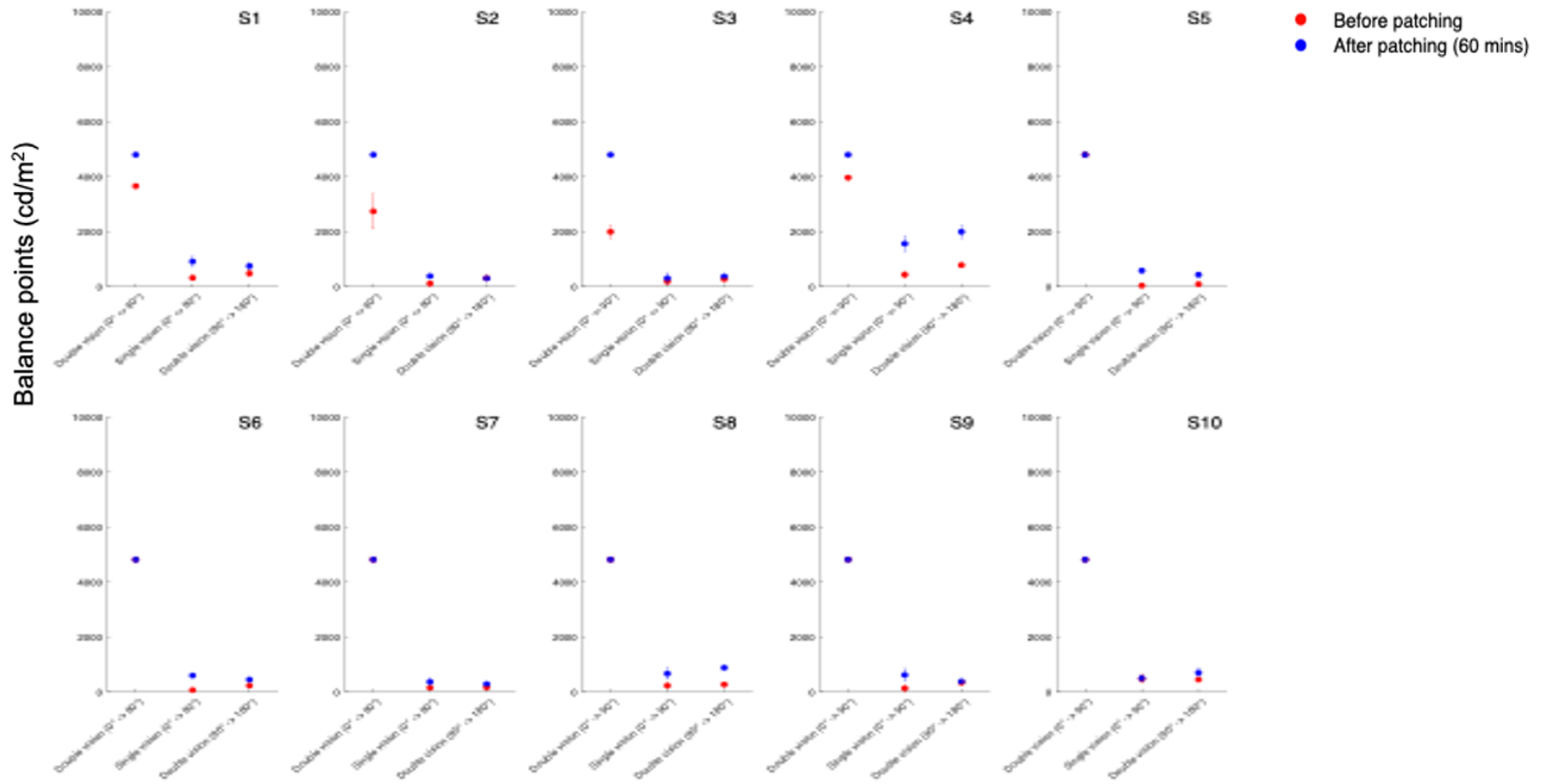
Following these measurements, observers were asked to wear an opaque patch over one eye for 60 minutes, during which they were free to engage in routine activities. After the 60-minute deprivation period, participants underwent repeated measurements in the sequence of  $-12^\circ$ ,  $0^\circ$ , and  $12^\circ$ , with this sequence repeated three times. This allows us to compare the balance points before and after patching and whether this deprivation effect diminish over repeated measurements. This comparison aimed to explore whether short-term deprivation could shift the balance points at which eye dominance changes, providing a more sensitive measure of neural plasticity induced by short-term monocular deprivation. The choice of 60-min deprivation period was guided by the results from Chapter 5 that monocular deprivation for 60 mins induced a marked shift in the egocentre location, though the results in Exp.9 indicated that a 60-min monocular deprivation could not induce significant changes in eye dominance. This experimental setting aims to explore if subtle, rapid adjustments can be observed using alignment tasks with help of linear polarizers.

### 6.3.2 Results

Figures 6.8, 6.9, and 6.10 display these balance points for each of the ten participants measured at three eccentricities ( $-12^\circ$ ,  $0^\circ$ , and  $12^\circ$ ). Based on alignment measurements, four participants (S1 – S4) exhibited strong dominance in one eye (three with right-eye dominance and one with left-eye dominance), while the remaining participants (S5 – S10) showed no strong eye preference. According to baseline data (represented by red dots in the figures), participants with a dominant eye tended to align the target with that eye. As luminance to the dominant eye was reduced, they experienced physiological diplopia. Further reductions in luminance induced suppression of the dominant eye, resulting in perception through the non-dominant eye alone. When luminance to the dominant eye was gradually increased, the suppressed image reappeared, again resulting in physiological diplopia. After the 60-

minute deprivation on the non-dominant eye, participants underwent repeated measurements in the sequence of  $-12^{\circ}$ ,  $0^{\circ}$ , and  $12^{\circ}$ , with this sequence repeated three times to compare balance points before and after patching and examine how the deprivation effect changes across the three repetitions.

For participants no particular eye dominance, polarizers were placed in front of the right eye for all these participants. These individuals initially experienced physiological diplopia. As luminance to the right eye was reduced, diplopia persisted until suppression occurred, allowing perception through the left eye alone. When luminance to the right eye was increased, the suppressed image reappeared, restoring diplopia. After the 60-minute deprivation on the left eye, participants underwent repeated measurements in the sequence of  $-12^{\circ}$ ,  $0^{\circ}$ , and  $12^{\circ}$ , with this sequence repeated three times to compare balance points before and after patching and examine how the deprivation effect changes across the three repetitions.



The images seen during rotation

Figure 6.8: Balance points for ten participants (S1 to S10) measured at  $-12^\circ$  eccentricity. The red dots represent the baseline luminance values, while blue dots represent the post-patching values. The error bars indicate the standard deviation. X-axis denotes the number of image was seen during rotating the external polarizer, and y-axis represents the corresponding balance point values ( $\text{cd/m}^2$ ).



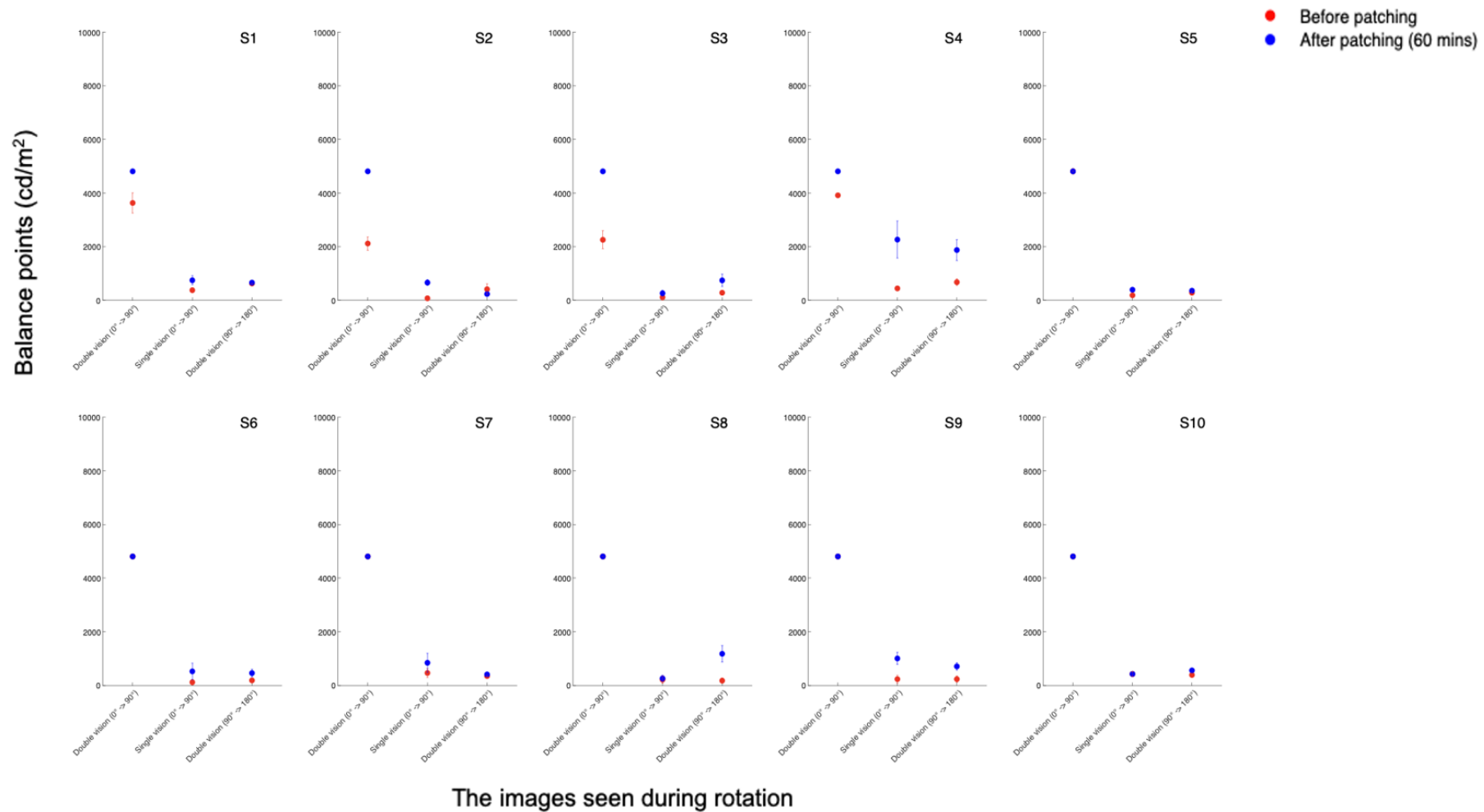


Figure 6.9: Balance points for ten participants (S1 to S10) measured at 0° eccentricity. The red dots represent the baseline luminance values, while blue dots represent the post-patching values. The error bars indicate the standard deviation. X-axis denotes the number of image was seen during rotating the external polarizer, and y-axis represents the corresponding balance point values (cd/m²).

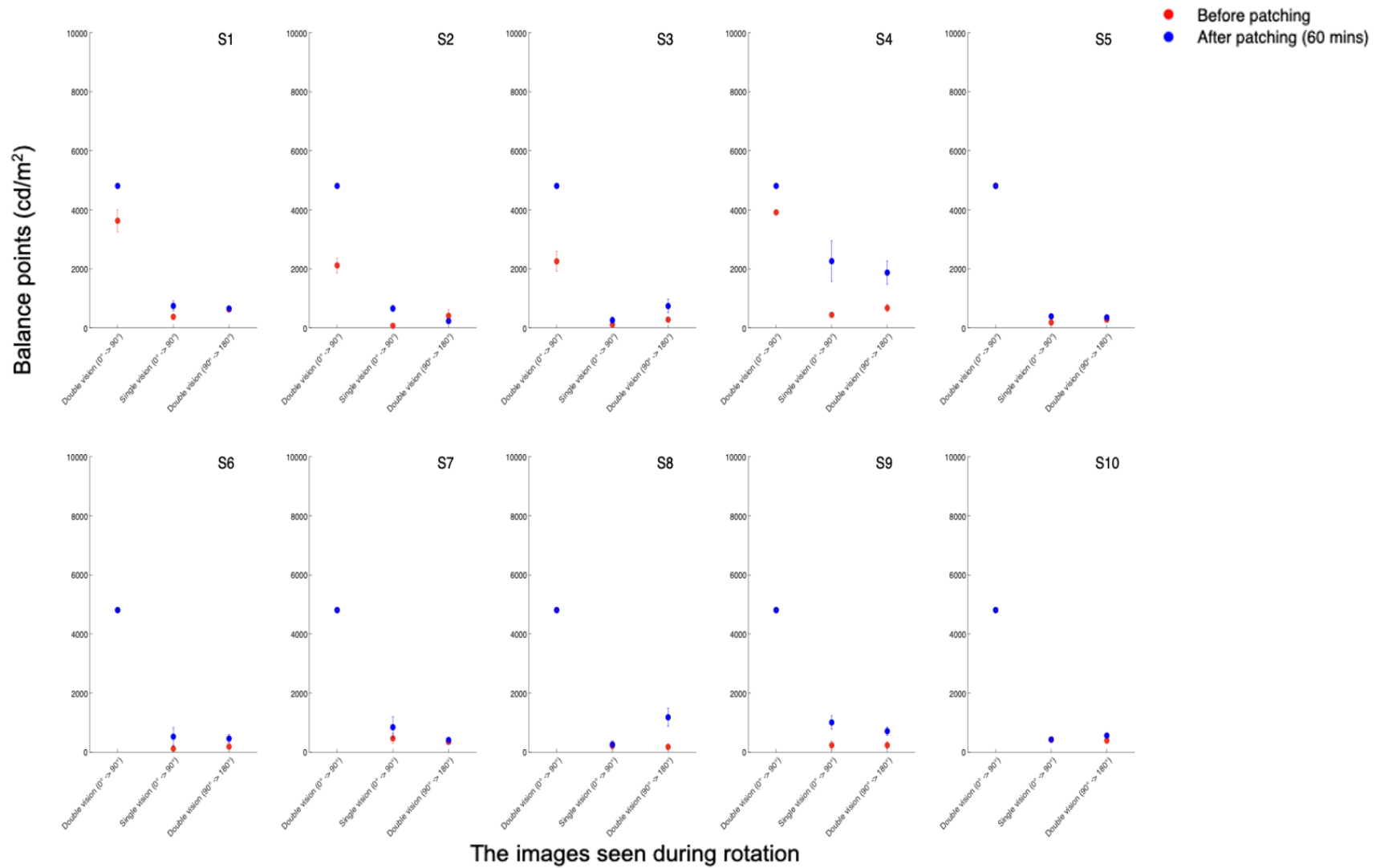


Figure 6.10: Balance points for ten participants (S1 to S10) measured at 12° eccentricity. The red dots represent the baseline luminance values, while blue dots represent the post-patching values. The error bars indicate the standard deviation. X-axis denotes the number of image was seen during rotating the external polarizer, and y-axis represents the corresponding balance point values (cd/m²).

The average luminance values for each vision state (single vision and diplopic vision) across three eccentricities ( $-12^\circ$ ,  $0^\circ$ , and  $12^\circ$ ) are presented in Table 6.2 and displayed in Figure 6.11. For each eccentricity, reductions on one eye results in an initial phase of physiological diplopia, then transitions to single vision perceived through the fellow eye, then suppressed image reappears when increase the luminance to the eye. As for the participants with no strong eye dominance, they perceive the diplopic images as soon as they started the alignment task. Therefore, we just averaged the balance points where perception occurs exclusively through one eye, and then physiological diplopia reappears again. At  $-12^\circ$  eccentricity, a mean luminance value  $215\text{cd/m}^2$  ( $\text{SD} = 149$ ) is needed for perceiving the single image, while a higher luminance of  $331\text{cd/m}^2$  ( $\text{SD} = 200$ ) results in diplopic images. At  $0^\circ$  eccentricity, the mean balance point for single vision is  $264\text{cd/m}^2$  ( $\text{SD} = 149$ ), and for diplopic vision is  $360\text{cd/m}^2$  ( $\text{SD} = 172$ ). At  $12^\circ$  eccentricity, the single vision balance point remains at  $264\text{cd/m}^2$  ( $\text{SD} = 247$ ), with the diplopic balance point at  $349\text{cd/m}^2$  ( $\text{SD} = 119$ ). These measurements provide insight into the balance points of luminance values where dominance shifts, offering a baseline for assessing the effects of monocular.

Table 6.1: Mean balance points ( $\text{cd/m}^2$ ) for perceiving single and diplopic vision measured at three eccentricities across ten observers before deprivation.

Eccentricity ( $^\circ$ )	Vision state	Mean balance point ( $\text{cd/m}^2$ )	SD
-12	Single image	215	149
	Diplopic image	331	200
0	Single image	264	149
	Diplopic image	360	172
12	Single image	264	247
	Diplopic image	349	119

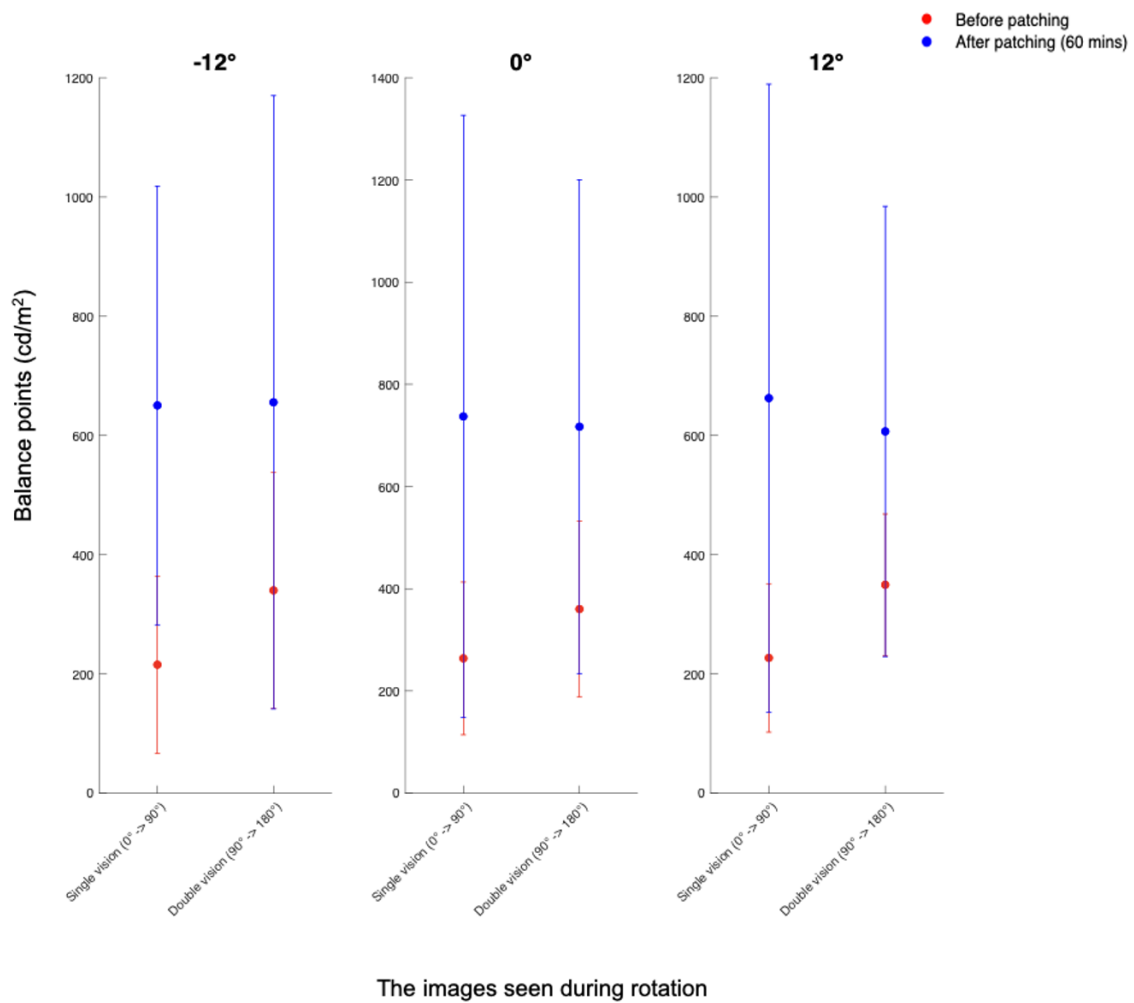


Figure 6.11: Average balance points ( $\text{cd/m}^2$ ) for perceiving single and diplopic vision measured at three eccentricities across ten observers before deprivation. The red dots represent the baseline luminance values, while blue dots represent the post-patching values. The error bars indicate the standard deviation. X-axis denotes the number of image was seen during rotating the external polarizer, and y-axis represents the corresponding balance point values ( $\text{cd/m}^2$ ).

After 60-min monocular deprivation, balance points were remeasured for each participant across three eccentricities. All ten participants perceived the diplopic images as soon as they started the alignment task after removing the patch. Table 6.3 summarizes the average luminance values for each vision state (single vision and diplopic vision) across three eccentricities ( $-12^\circ$ ,  $0^\circ$ , and  $12^\circ$ ) after monocular deprivation across 10 observers.

Table 6.2: Mean balance points ( $\text{cd/m}^2$ ) for perceiving single and diplopic vision measured at three eccentricities after 60-min monocular deprivation across ten observers.

Eccentricity ( $^\circ$ )	Vision state	Mean balance point ( $\text{cd/m}^2$ )	SD
-12	Single image	750	476
	Diplopic image	656	514
0	Single image	804	457
	Diplopic image	717	484
12	Single image	776	677
	Diplopic image	607	378

Inter-ocular differences among 10 participants were calculated by subtracting the balance points when the suppressed image reappeared from the balance points where the suppression occurs, providing a measure of the luminance required to switch perception. The pre-and post-deprivation of inter-ocular luminance difference among 10 participants at three eccentricities is displayed in Table 6.4. A reduction in inter-ocular luminance differences in the post-deprivation data reveals a potential decrease in the deprived eye's luminance contrast threshold, suggesting a reduction in contrast sensitivity for the deprived eye following deprivation. For the participants with strong eye dominance (S1 - S4), positive inter-ocular luminance differences consistently highlighted that the dominant eye is strongly favoured in visual processing, requiring greater luminance to switch perception. Figure 6.12 illustrates the inter-ocular luminance differences before (left panel) and after deprivation (right panel) at three eccentricities for 10 participants, highlighting individual variations in visual processing and adaption among participants. A positive inter-ocular luminance value means the eye with polarizers in front requires a higher luminance to maintain perceptual dominance compared to the fellow eye, whereas a negative value indicates the fellow eye has a higher luminance.

Table 6.3: Pre- and post-deprivation inter-ocular luminance differences at three eccentricities for 10 participants.

	Inter-ocular difference (cd/m <sup>2</sup> )					
	-12 (°)		0 (°)		12 (°)	
	Pre	Post	Pre	Post	Pre	Post
S1	164±77	-164±73	250	-87±150	228±196	-37±257
S2	195±124	-83±25	338±177	-425±104	25 ±115	-458±89
S3	85±57	69±125	170±49	480±172	166±197	321±156
S4	350±150	432±253	233±161	-389±225	152±47	-362±394
S5	55±16	-150±87	95±82	-36±31	85±75	12±98
S6	163±95	-150±87	69±103	-64±163	159±28	309±288
S7	9±87	-81±78	-117±139	-434±307	47±43	-364±241
S8	38±108	216±202	-38±59	917±190	166±119	282±195
S9	210±65	-237±226	0±177	-296±81	94±6	-378±186
S10	-22±181	200±50	-36±126	133±29	93±153	117±126

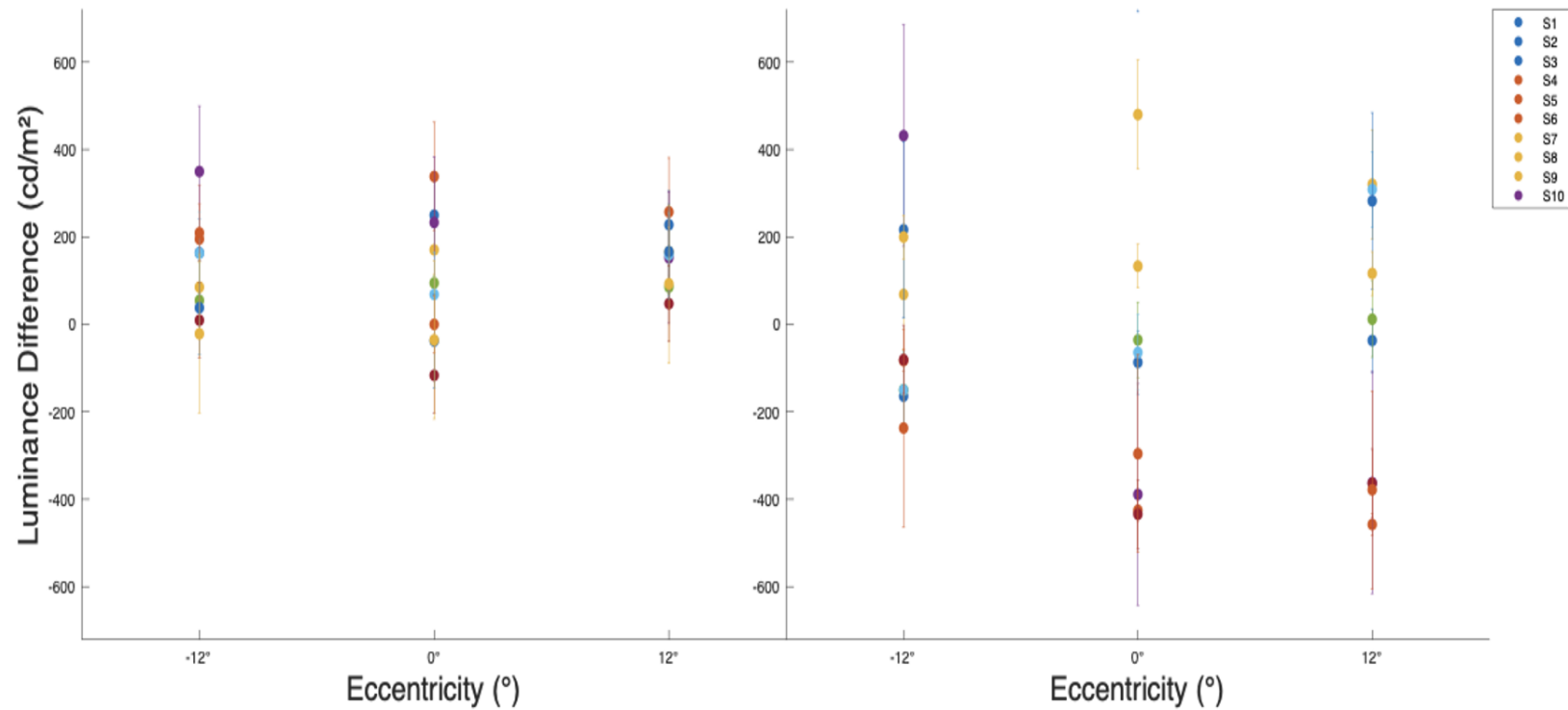


Figure 6.12: Inter-ocular luminance differences across three eccentricities for 10 participants represented dots with different colours. X axis represents three eccentricities, y axis represents inter-ocular luminance differences between the two eyes. Positive y value means the eye with polarizers in front has a higher luminance than the fellow eye, and vice versa for the negative value. The error bars indicate the standard deviation.

Paired t-tests were conducted to compare pre- and post-deprivation balance points for each condition, as displayed in Table 6.5. The results indicated that monocular deprivation induced significant reductions in balance points across all conditions, resulting in measurable changes in eye dominance. A repeated measures ANOVA results indicated that inter-ocular luminance differences did not differ significantly between pre- and post-deprivation ( $F_{(1,57)} = 2.17, p = .146$ ).

Table 6.4: Paired t-test results for changes in balance points induced by monocular deprivation across conditions.

Eccentricity (°)	Vision state	Mean changes (cd/m <sup>2</sup> )	SD	<i>t</i>	<i>p</i>
-12	Single	535	456	-3.71	.0049
	Diplopic	512	354	-2.90	.0176
0	Single	540	607	-2.82	.0202
	Diplopic	357	441	-2.56	.0306
12	Single	663	493	-3.28	.0095
	Diplopic	257	303	-2.68	.0251

To assess the changes in balance points induced by monocular deprivation, the post-deprivation measurements were repeated three times following the sequence: -12°, 0° and 12°. In Figure 6.13, the red, blue, and green dots represent the first, second, and third measurements, respectively, taken after deprivation. Although each measurement was brief, the effects of deprivation gradually diminished with subsequent measurements.



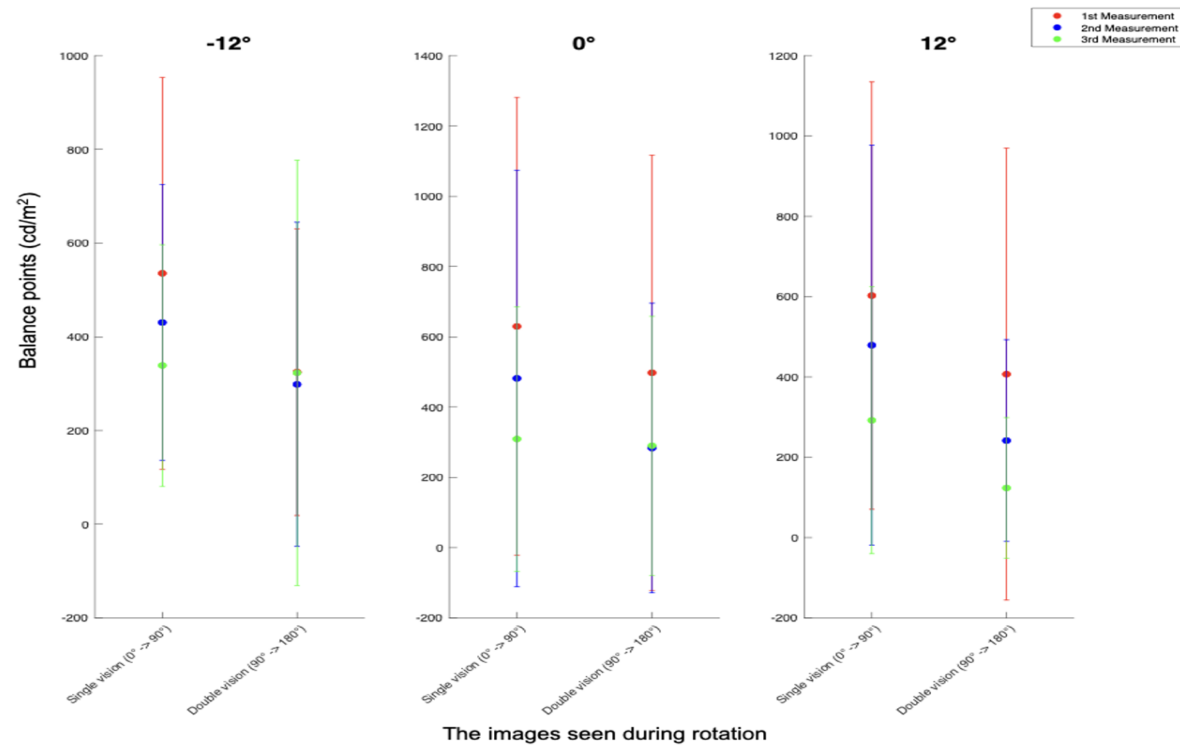


Figure 6.13: Balance points across three eccentricities with sequential measurements after deprivation. The red, blue, and green represent the first, second, and third measurements, respectively. The error bars indicate the standard deviation. X-axis denotes the number of image was seen during rotating the external polarizer, and y-axis represents the corresponding balance point values ( $\text{cd/m}^2$ ). It shows the effects of deprivation gradually diminished with subsequent measurements.

The average changes in balance points, derived from three separate measurements taken following 60 minutes of monocular deprivation are summarized in Table 6.6. A repeated-measures ANOVA was performed on the three post-deprivation measurements. The results revealed a statistically significant main effect among the measurements ( $F_{(2, 18)} = 23.54, p < .001$ ), indicating that balance points were significantly altered after monocular deprivation. However, the absence of a significant interaction suggests that the post-deprivation effects were consistent across different eccentricities, meaning that the deprivation effect was stable regardless of the visual angle tested. This finding further supports the idea that short-term monocular deprivation induces significant changes in eye dominance, with the effect diminishing over time during repeated measures.

Table 6.5: Averaged changes in balance points measured at three eccentricities after 60-min monocular deprivation averaged across ten participants with three separate repetitions.

Eccentricity (°)		-12		0		12	
Vision State		Single	Diplopic	Single	Diplopic	Single	Diplopic
1 <sup>st</sup>	Mean (cd/m <sup>2</sup> )	636	353	730	498	673	407
	SD	546	282	764	619	588	563
2 <sup>nd</sup>	Mean (cd/m <sup>2</sup> )	531	298	582	283	560	242
	SD	422	346	720	412	576	251
3 <sup>rd</sup>	Mean (cd/m <sup>2</sup> )	439	323	309	290	303	124
	SD	431	454	377	368	342	176

## 6.4 Discussion

This study introduces a novel and sensitive method for measuring the extent of eye dominance and quantifying the magnitude of plastic changes induced by short-term monocular deprivation. By employing linear polarizing filters to systematically degrade the visual input to one eye, we were able to precisely determine the balance points at which

perceptual dominance from one eye to the other. This approach offers a quantitative assessment of sensory eye dominance (SED) while providing insights into the dynamic balance of binocular vision.

The key innovation of our methodology is the use of the relative rotation angle of the external polarizers as a quantifiable measure of eye dominance. The size of the rotation angle and its subsequent translation to an inter-ocular luminance difference, indicates the relative influence of the non-dominant eye, effectively capturing the degree to which one eye contributes to the overall visual perception. By averaging these values across multiple eccentricities, we established a reliable measure of each participant's eye dominance before and after deprivation. Our findings revealed that individuals exhibit varying degrees of eye dominance, which could be precisely mapped using this technique. Individuals with stronger eye dominance—where one eye predominantly influences perception—required a larger luminance difference between the eyes to induce a shift in visual perception after monocular deprivation. In contrast, participants with no strong eye dominance exhibited more subtle shifts.

This variability underscores the sensitivity of our method in detecting individual variations in eye dominance, a sensitivity that traditional clinical methods like the hole-in-card test or Worth 4-dots test (Seijas et al., 2007) often lack. After 60 minutes of depriving the non-dominant eye, we observed significant changes in the luminance difference which allowed the non-deprived eye to fully dominate perception. As there is no significant interaction between inter-ocular differences of pre-and post-deprivation data, suggesting that deprivation may have a fixed effect across all participants. The average balance points changed markedly compared to baseline measurements, indicating that short-term deprivation effectively alters the neural weighting of visual input from each eye.

One neural basis of eye dominance is unequal interocular inhibition, this eye dominance can disrupt binocular functions that rely on a balanced

interaction between excitatory and inhibition mechanisms (Sengpiel et al., 1994; Su, He, & Ooi, 2009; Su, He, & Ooi, 2011). The observed shifts suggest that the neural circuits responsible for integrating binocular input remain adaptable, capable of reweighting sensory contributions based on recent visual experiences. This plasticity may involve alterations in inhibitory and excitatory synaptic strengths within visual cortical areas, such as the primary visual cortex (V1), and subcortical structures like the lateral geniculate nucleus (LGN) (Duménieu et al., 2021). Our method provides a practical tool for reducing sensory eye dominance and improving stereopsis for adults. By quantifying the extent of eye dominance and tracking changes of sensory eye dominance over time, researchers can investigate how different factors—such as duration of deprivation, visual tasks, or perceptual suppression of the stronger eye while enhancing excitatory signals in the weaker eye. It provides compelling psychophysical evidence supporting the crucial role of inhibitory activities in driving cortical plasticity, which may broaden therapeutic possibilities for visual dysfunctions linked to sensory imbalance.

One of the key contributions of this study is the confirmation that short-term monocular deprivation induces shifts in eye dominance, a finding that aligns with earlier studies (Lunghi et al., 2011; Zhou et al., 2013). By depriving the non-dominant eye of visual input for 60 minutes, we observed significant changes in the balance points where the previously non-dominant eye became perceptually dominant. This effect, quantified through luminance differences between the two eyes, was especially prominent in individuals with a strong initial eye dominance. This has important implications for both basic visual neuroscience and clinical applications. The shifts in eye dominance observed in this study likely reflect underlying changes in the balance of excitatory and inhibitory signals within the visual cortex. Previous research by Lunghi et al. (2011) proposed that short-term monocular deprivation enhances homeostatic plasticity, wherein the brain compensates for the lack of visual input from one eye by increasing sensitivity to signals from that eye once the

deprivation is lifted. This homeostatic mechanism allows the visual system to adapt dynamically to changes in sensory input, ensuring that visual information is processed efficiently even under altered conditions. Our findings are consistent with this theory. The fact that these changes were most prominent in individuals with high levels of inter-ocular inhibition supports the idea that eye dominance is not a fixed trait but is subject to modulation based on sensory experience.

Furthermore, the temporary nature of these changes raises questions about the long-term potential for altering eye dominance through repeated or prolonged deprivation. While our study focused on short-term effects, it would be valuable to explore whether extended periods of deprivation could result in more permanent shifts in eye dominance. Schwartz & Yatziv (2015) explored how eye dominance can shift following cataract surgery and highlighted that eye dominance is not a static trait but a plastic attribute. They observed 21.2% patients experienced changes of eye dominance following cataract surgery, suggesting that inter-ocular inhibition could adapt to signal quality changes (such as those with visual deterioration associated with development of cataract) and adjust to favour the better eye. Jing et al. (2015) investigated the relationship between sensory eye dominance with interocular refractive difference, known as anisometropia. They found that anisometropic individuals tend to have stronger ocular dominance, with the degree of dominance correlating with the amount of refractive error asymmetry, highlighting the importance of sensory eye dominance on understanding the mechanism of refractive development and providing new ideas for the prevention and treatment of anisometropic.

Yang, Blake and McDonald (2010) used a continuous flash suppression (CFS) paradigm by presenting dynamic noise to one eye and target stimulus to the other eye to examine reaction times for target perception. The dominant eye was expected to quickly break the suppression with a shorted reaction time. In contrast, our approach measured eye

dominance by capturing the inter-ocular luminance threshold to switch perception between the two eyes and providing a sensitive index of eye dominance changes induced by short-term monocular deprivation. This luminance differences-based method allows us to assess not only the strength of each eye's dominance but its adaptability in response with monocular deprivation, providing a valuable insight on treatment of amblyopia or strabismus where long-term adjustments in the balance of visual input between the eyes are desirable. The sensitivity of our measurement technique holds significant potential for clinical applications, particularly in diagnosing and treating binocular vision disorders like amblyopia – an extreme form of eye dominance that is associated with inter-ocular suppression. For example, therapeutic strategies for amblyopia involves patching the dominant eye to stimulate the amblyopic eye, while our approach quantifies how effectively the deprivation intervention alter dominance, offering a method for tracking progress and optimizing treatment efficiency. Clinicians could use this method to monitor patients' responses to treatments like patching, perceptual learning, or dichoptic training, adjusting strategies based on measurable changes in eye dominance.

Ooi et al. (2013) developed a push-pull perceptual learning protocol that simultaneously affects the neural mechanisms of excitatory and inhibitory networks by completely suppressing perception from the strong eye and recalibrating the inter-ocular balance of excitatory and inhibitory interactions. Studies like Wang et al. (2021) have shown that monocular treatments like patching can shift eye dominance, as a measure that can be tracked during therapy or be considered as an outcome measure of any treatment strategy. Furthermore, the method could be adapted for use with different age groups, including children, to assess developmental aspects of eye dominance and neural plasticity. Future research could explore longitudinal studies to determine whether repeated short-term deprivation sessions lead to long-term changes in eye dominance, potentially offering new avenues for early intervention in disorders of binocular vision.

While this study provides valuable insights into the effects of short-term monocular deprivation on eye dominance, there are several limitations that should be addressed in future research. The relatively short duration of the deprivation period. Although we observed significant shifts in eye dominance after 60 minutes of deprivation, it remains unclear whether these changes would persist over longer periods or whether repeated deprivation sessions could lead to more permanent alterations in visual processing.

Future studies should explore the effects of monocular deprivation at different viewing distances and in more naturalistic settings to better understand how these shifts in eye dominance play out in real-world scenarios. Finally, while this study focused on adult participants, it would be valuable to extend the research to younger populations, particularly children with amblyopia or other binocular vision disorders. Children's visual systems are known to be more plastic than those of adults, and the effects of short-term monocular deprivation may be even more pronounced in younger individuals. The study by Knox et al. (2012) demonstrated significant gains in visual acuity and stereo function for amblyopic children who undertook a perceptual learning task that requires participants use both eyes to perform the training. This study highlights binocular treatments, which make use of neural plasticity, can improve the visual function of amblyopic children. Using an iPad binocular treatment for amblyopic children, Li et al. (2014) showed that engaging both eyes during gameplay significantly improved visual acuity, with the gains remaining stable at least three months after treatment. In light of this, it appears that children's visual systems exhibit considerable plasticity, enabling effective adaptation to and improvement even after only a short period of targeted training.

In summary, this study provides a valuable contribution to both vision science and clinical practice by introducing a sensitive and quantitative method for measuring the extent of eye dominance and the magnitude of

neural plastic changes resulting from short-term visual deprivation. The use of linear polarizing filters offers a controlled and precise means to manipulate and assess binocular vision. Our findings highlight the importance of measuring sensory eye dominance. As there is a broad variation in stereo performance among the general population, and it may link to sensory eye dominance. The findings suggest that brief periods of visual deprivation could shift the interocular balance, which may, in turn, enhance depth perception. Although depth perception was not directly measured before and after short-term deprivation in this study, future research could explore this effect further. Additionally, the alignment task used here could serve as a tool to identify individuals with strong eye dominance. For these individuals, short-term monocular deprivation might be a promising method to improve their depth perception, particularly enhancing their experience of three-dimensional world.



## Chapter 7. General discussion

### 7.1 Summary of Findings

This thesis investigates fundamental aspects of human binocular vision through a series of ten psychophysical experiments, specifically examining the neural mechanisms underlying depth computation and the processing of visual direction. The findings provide significant insights into the computational processes governing the visual egocentre—a critical reference point for determining object direction relative to the observer—and neural plasticity associated with our perception of visual direction.

Chapter 3 presents a comparative analysis of two prominent models of binocular visual direction: the maximum-likelihood model (Mansfield & Legge, 1996) and the modified conventional model (Banks et al., 1997). The results demonstrate that both depth perception and interocular contrast differences significantly influence perceived visual direction, corroborating earlier research on the role of luminance differences in binocular perception (Charnwood, 1949; Francis & Harwood, 1951; Verhoeff, 1933, 1935). Contrary to Mansfield and Legge's model—which posits that visual direction results from a maximum-likelihood combination of directional signals from the left and right eyes—our findings suggest that visual direction is computed through the integration of monocular inputs. Using Gaussian-windowed, one-dimensional, aperiodic noise patches in Experiments 3 and 4, we observed that coarse spatial information, rather than fine internal structures, predominantly guides directional judgments. This aligns with established theories emphasizing the significance of shape and boundary cues in object perception (Wagemans et al., 2012), which prioritize holistic properties such as shape over specific internal spatial structures. These shape-based theories focus on emergent and global configurations that define

perceptual organization, while remaining agnostic to internal spatial features.

Chapter 4 examines the visual egocentre location and refines principles of visual direction by exploring variability in egocentric localization within a large population sample. Building on Hering's (1879/1942) foundational principles—which posited that visual direction is governed by a centrally located egocentre along the interocular axis—the study incorporates individual variability in egocentre localization by integrating monocular and binocular cues. The findings indicate that visual direction cannot be universally defined by a static egocentre position but rather involves a dynamic integration of monocular and binocular inputs unique to each individual. This refinement enhances the theoretical framework of binocular vision and supports more personalized approaches in vision science. Compared to alternative methods (Fry, 1950; Funaishi, 1926; Roelofs, 1959), the approach of Howard and Templeton (1966) provides precise egocentre estimates (Mitson, Ono, & Barbeito, 1976). Monocular measures estimate the perceived position of each eye in the head, often exceeding the corresponding interpupillary distance (IPD) due to the misalignment between the visual and pupillary axes by approximately  $5^\circ$  (angle kappa) in the temporal plane (Artal, 2014). Binocular sighting measurements offer direct estimates of the visual egocentre, typically located posterior to the corneal plane and proximal to the median plane, although significant individual variability exists. These results corroborate Howard and Templeton's (1966) earlier research, elucidating individual variations in egocentre localization. Gregory's (1958, 1966) theoretical framework, which posits the existence of two subsystems—the retinal-image system and the eye-head system—further explains how these subsystems integrate signals to establish egocentric visual direction. By combining eye-position and retinal signals, individuals can effectively differentiate between eye movements and object motion. Variations in perceived direction may arise from differences in signal integration, resulting in individual differences in spatial perception. Furthermore, uncertainty in eye-position signals, such as noise or imprecision, can

contribute to variability in aligning retinal input with spatial coordinates. Factors such as sighting dominance and eye dominance further influence egocentric localization. Habitual suppression of the non-sighting eye (Porac & Coren, 1986; Dieter et al., 2017a) may bias directional judgments, favouring input from the dominant eye. Collectively, these factors account for individual differences in perceived visual direction and clarify how eye movements, object motion, and directional judgments contribute to perceptual variability.

Chapter 5 explores eye dominance plasticity in the adult visual system by examining the effects of short-term monocular deprivation on perceived visual direction. The findings highlight the role of interocular imbalance in inducing shifts in the visual egocentre, typically towards the median plane of the head rather than the previously deprived eye. The induced changes suggest that the brain reverts to a location midway between the eyes to localize objects in space relative to the viewer. Consistent with studies by Lunghi et al. (2011) and Zhou et al. (2013), short-term monocular deprivation leads to transient enhancements in visual function in the previously deprived eye. The observed changes in visual direction following occlusion of the non-dominant and dominant eyes were short-lived, returning to baseline levels after 15 minutes. These findings align with the notion that visual deprivation can reinstate higher levels of plasticity in the adult visual cortex (Karmarkar & Dan, 2006; Spolidoro et al., 2009). Such changes may be driven by rapid homeostatic mechanisms that respond to visual disruption.

Chapter 6 introduces a novel and sensitive method for measuring eye dominance and quantifying plastic changes induced by short-term monocular deprivation. By using linear polarizing filters to systematically reduce visual input to one eye, we determined the balance points at which perceptual dominance shifted between the eyes. This method, based on interocular luminance differences, allows precise assessment of the strength and adaptability of eye dominance in response to monocular deprivation. These findings have significant implications for

addressing binocular vision disorders, such as amblyopia, where long-term adjustments in the balance of visual input between the eyes are desirable.

## 7.2 A synthesised framework

The findings presented in this thesis contribute to a comprehensive theoretical framework for understanding binocular interaction and the neural encoding of binocular visual direction. According to Hering's foundational psychophysical laws (1879–1942), visual inputs from both eyes are integrated to form a unified perception, conceptualized as the cyclopean eye. This integration enables the brain to perceive depth and direction in binocular vision. A fundamental computational challenge for the visual system involves the fusion of bilateral ocular information to achieve the cyclopean view and determine the visual direction of objects relative to the observer. Our findings align with the Ding-Sperling-Klein-Levi (DSKL) model, where binocular perception arises from a dynamic interplay between interocular inhibition and gain enhancement (Ding et al., 2013a), involving three distinct layers of processing for each eye. As illustrated in Figure 7.1,  $I_L$  and  $I_R$  represent the signal inputs to narrow-band, orientation-selective spatial frequency channels for the left and right eyes, respectively. The selective signal layer (black lines) processes eye-specific input, receiving both gain control (represented by black filled circles) and gain enhancement (represented by red open circles) from the other eye and outputs to form a combined percept. The non-selective gain-control layer (blue lines) extracts total contrast energy (TCE) across all spatial frequency channels and orientations to apply gain control ( $\varepsilon_L$  and  $\varepsilon_R$  represent contrast energy from each eye) to all three layers separately with varied gain-control efficiency ( $1, \alpha$ , and  $\beta$ ), representing different inhibition strength, to the other eye. The gain-enhancement layer (red lines) extracts image contrast energy (TCE\*) and provides gain enhancement exclusively to the signal layer of the other eye. Gain enhancement complements gain control by amplifying the weaker eye's

input, allowing for a more balanced contribution to the combined binocular percept.

As the two eyes may have different contrast sensitivity, the sensitivity attenuation  $\mu$  was introduced to explain influence from monocular deprivation (Spiegel, Baldwin, & Hess, 2017). The non-selective gain-control layer plays a crucial role in preventing dominance by the deprived eye, functioning as balancing feedback by favouring inputs that stabilize the cyclopean percept along the median plane. The gain-enhancement mechanism, which amplifies the non-deprived eye's input, may inherently maintain binocular balance by promoting symmetry in spatial processing, effectively aligning the combined percept with the median plane rather than favouring the deprived eye. Based on this model, we can explain the reduction of inter-ocular suppression observed in this thesis. As a result of short-term monocular deprivation, the deprived eye's contribution to the selective signal layer is increased, correlated with recalibrated egocentric localization. The sensitivity attenuation  $\mu$  accounts for changes of monocular signal weighting after monocular deprivation would modulate these shifts by exaggerating the deprived eye's gain enhancement. The gain-control efficiencies ( $\alpha$  and  $\beta$ ) regulate the varied strength of inter-ocular inhibition that prevent the deprived eye's overcompensation. The total contrast energy (TCE and TCE\*) further ensures balanced input processing across spatial frequency channels. This mechanism, supported by observed inter-ocular suppression, suggests that binocular vision flexibility adapts to maintain balance, with specific parameters controlling the integration and directionality of visual signals to recalibrate the egocentric localization.

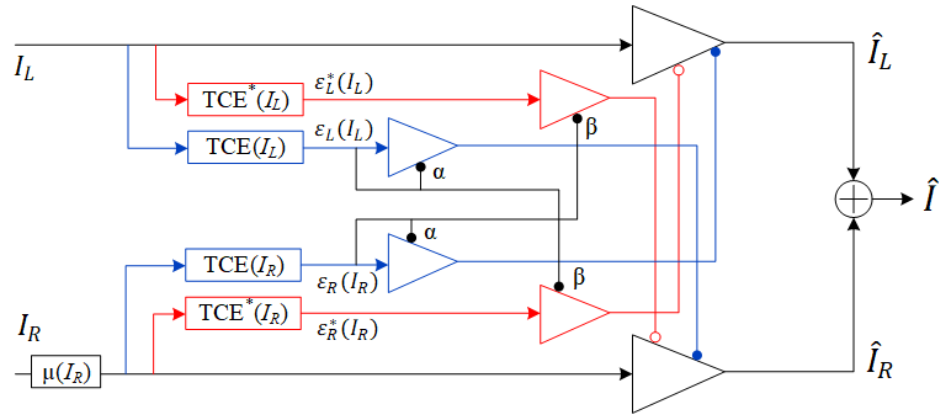


Figure 7.1: The diagram of Ding-Sperling-Klein-Levi (DSKL) model.  $I_L$  and  $I_R$  are the strength input to each eye, and each eye involves three distinct layers for vision processing. The selective signal layer (represented by black lines) processes the eye-specific input independently and incorporates both gain control (shown as black filled circles) and gain enhancement (shown as red open circles) signals from the opposite eye. The non-selective gain-control layer (illustrated with blue lines) gathers total contrast energy (TCE) to apply gain control ( $\epsilon_L$  and  $\epsilon_R$  represent contrast energy from each eye) to all layers, with varying gain-control efficiencies ( $1$ ,  $\alpha$ , and  $\beta$ ) to account for different inhibition strengths directed toward the opposite eye. The gain-enhancement layer (represented by red lines) is responsible for extracting image contrast energy (denoted as  $TCE^*$ ), providing gain enhancement exclusively to the selective signal layer of the opposite eye. By amplifying the weaker eye's input, gain enhancement works alongside gain control to help equalize the inputs from both eyes, facilitating a balanced binocular percept. Image adapted from Ding et al.(2013a)

### 7.2.1 The contribution of eye-position and retinal position information in binocular visual direction.

It is important to distinguish between relative and absolute visual direction. Relative direction is determined with reference to a fixed external point, such as another object in the visual field (Mapp, Ono, & Howard, 2002; Ono & Mapp, 1995), while absolute direction pertains to an object's position relative to bodily references (e.g., head, torso, visual axis). The head-centric frame, defined by the eyes' median and transverse planes, serves as the primary reference for assessing absolute direction (Khokhotva et al., 2005).

The integration of retinal (position of the retinal images) and oculomotor (position of the eyes in the head) signals constitutes a fundamental

requirement for accurate head-centric directional judgments (Mapp et al., 2002). Gregory's (1958, 1966) theoretical framework proposes that these signals from the eyes and head operate synergistically to establish egocentric visual direction. Swanson, Wade, and Ono (1990) further elaborated this concept, suggesting that retino-centric and eye movement signals undergo weighted integration for each eye, culminating in a unified egocentric representation. As illustrated in Figure 7.2, perceived egocentric direction results from combining signals from left and right eye positions ( $e'_L$  and  $e'_R$ , respectively) and retinal data ( $i'_L$  and  $i'_R$  for left and right retino-centric signals, respectively). The binocular retino-centric level ( $M'_{(rB)}$ ) is determined by the combination of left and right retino-centric signals, with weights ( $\alpha$ ) applied based on the relative strengths of stimulation in each eye and the similarity of contours on corresponding retinal areas. The egocentric signal ( $M'_{(s)}$ ) depends on the integration of binocular retino-centric information and binocular eye movements. The final egocentric representation results from combining these binocular signals.

Although Hering's law of visual direction assumes equal contribution from both eyes, individual differences—such as variations in contrast sensitivity or other ocular parameters—may influence the weighting applied to each eye. These individual differences, including contrast sensitivity imbalances, could explain why the weighting varies across individuals, leading to differences in perceived visual direction and egocentric alignment. Hering's assumption (1879/1942) of equal contributions from both eyes was challenged by Barbeito and Simpson (1991), who demonstrated that during asymmetric vergence (when one eye focuses on a closer object while the other eye remains fixated on a more distant point), the contributions from each eye are unequal. Their experiment involved participants pointing to a flashing target under different eye-position configurations with a change in the fixation distance of one eye. It was found that eye position and perceived egocentric direction were linearly related; however, the slopes of regression lines for

the two eyes unequal for some participants. The unequal slopes indicate that the two eyes are not equally weighted in the computation of egocentric direction, such differences may be attributed to an unequal weighting of the positional information from the two eyes. Their work suggests that such variability could be explained by differences in how retino-centric information, monocular eye-position signals, or their integration is weighted across individuals. In individuals who rely more heavily on one eye than the other, unequal weighting of positional information from each eye may cause shifts in the egocentre. Moreover, variability could result from noise in the retino-centric signals, differing accuracy or consistency of eye movement control, or a combination of these factors. Sridhar and Bedell (2011) compared the contribution of position information from each eye in determining the egocentric direction under asymmetric vergence condition, suggesting that the relative contribution of monocular eye position and retinal information do not contribute equally to all subjects, but they are similar in most of them. Specifically, they found that decreasing the visibility of one eye's retinal signal through blurring or reducing luminance reduced the contribution of that eye's position signal to perceived egocentric visual direction.

The integration of retinal and eye-position information exhibits remarkable consistency in establishing egocentric visual direction, despite individual variations. This consistency suggests the existence of a common neural locus for integration within the visual cortex. However, the systematic individual differences observed in egocentric localization in my work raise an important question: does monocular deprivation primarily affect the quality of retinal information (such as contrast sensitivity or spatial input), or influence the extra-retinal sense of eye position in the head? To test these possibilities, further tests could be designed to measure egocentre location under conditions where retinal and eye-position information are independently manipulated. For example, participants could undergo monocular deprivation, followed by tasks that separately assess retinal contributions (e.g., measuring changes in contrast sensitivity) and oculomotor contributions (e.g.,



evaluating changes in vergence dynamics). By correlating these manipulations with egocentric localization, it would help quantify the relative contribution of retinal and oculomotor signals to egocentric visual direction and determine whether the shift of egocentric localization observed following short-term monocular deprivation arises from changes in retinal information, eye-position information or an integration between them.

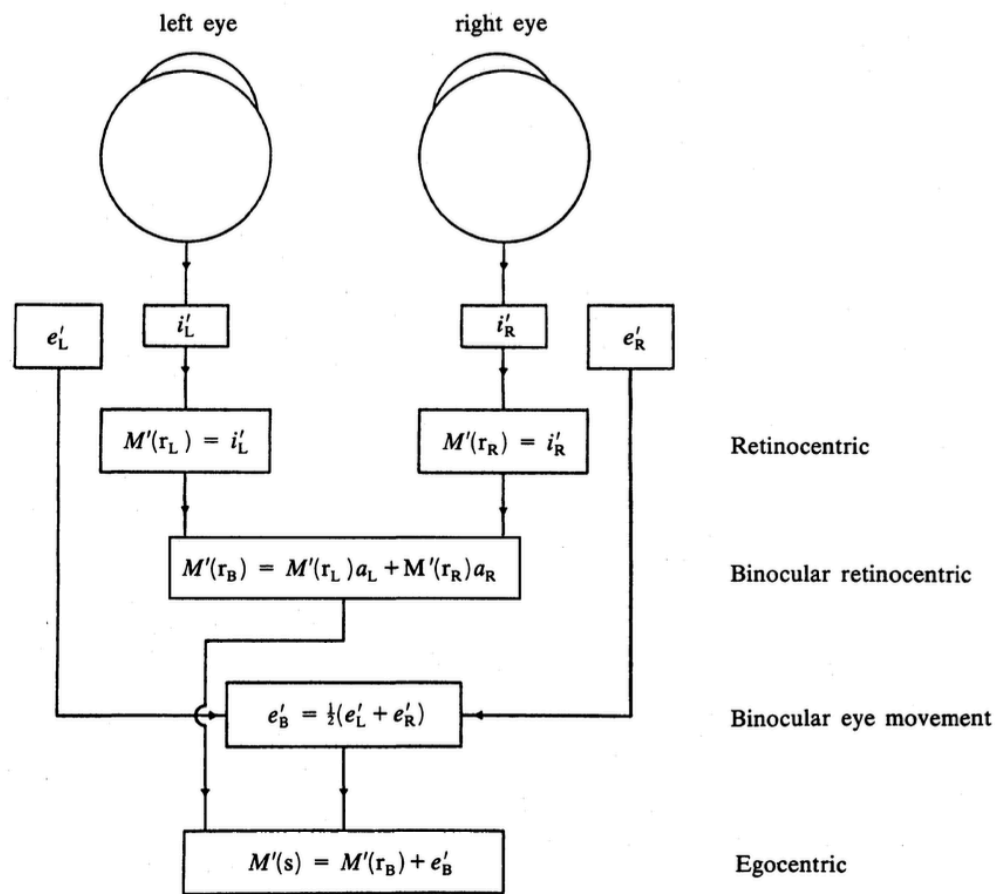


Figure 7.2: The diagram showing an integration of binocular retinocentric and eye-movement information to determine an egocentric direction. Information for displacements over retinæ ( $i'_L$  and  $i'_R$ ) represents the retinal signals from left and right eye, respectively. Combined with signals of eye movements ( $e'_L$  and  $e'_R$ ) and corresponding weighting factors ( $\alpha$ ) for each eye at the egocentric level to determine the egocentric representation ( $M'(s)$ ). If the values of weighting factors ( $\alpha_L$  and  $\alpha_R$ ) are equal, then the egocentre is located in the midway between the two eyes. However, any inequality shifts towards one eye. (Image from Swanston, Wade & Ono, 1990).

## 7.2.2 Factors contributing to individual variations in visual egocentre location

The visual egocentre is typically located on or around the median plane of the head and posterior to the corneal plane, although its precise location exhibits significant inter-individual variability (see Chapter 4). Empirical evidence indicates that individual variations in egocentre location correlate with differences in perceived direction (e.g., Barbeito & Ono, 1979). The egocentre location represents a complex perceptual construct influenced by multiple factors, including anatomical, neurological, experiential, and psychological variables. Church's (1966, 1970) research identified the "cyclops effect," wherein young children demonstrate a tendency to position viewing tubes between their eyes rather than viewing monocularly, suggesting an early developmental basis for cyclopean perception (Howard, 1982).

Several models have been provided to explain binocular combination (Baker & Wade, 2017; Ding et al., 2013a, 2013b; Ding & Sperling, 2006; Meese et al., 2006; Moradi & Heeger, 2009). Ding and Sperling (2006) introduced a two-layer gain-control model to explain how the brain weights input from each eye based on contrast. The first layer involves mutual inhibition of inputs from each eye, while the second layer involves mutual inhibition of the gain control in the first layer. This two-layer structure successfully predicts stable contrast perception, whether one or both eyes are open. Hou et al. (2013) extended this model with a multi-pathway contrast gain-control framework, incorporating disparity minimum threshold and cyclopean contrast perception of dynamic random dot stereograms (dRDS). Building on this, Ding and Levi (2021) later proposed a unified depth model that incorporates interocular contrast gain controls and enhancement before binocular combination. In this model, input from both eyes undergoes mutual inhibition and subsequent enhancement (Ding & Sperling, 2006; Ding, Klein, & Levi, 2013a; 2013b). The gain control process ultimately combines both eyes' outputs, resulting in a fused percept. Binocular energy is calculated by

normalizing monocular energy post-binocular combination, where images from each eye are first processed through multiple spatial-frequency filters to detect spatial features for identifying disparities. The images then pass through phase and position disparity detectors at each scale (large-, medium-, and small-scale detectors), yielding a sensory shift that minimizes misalignment. The combined disparity energies across scales are summed with appropriate weighting to achieve depth perception.

Variations in visual egocentre location observed in this dissertation may be attributable to individual differences in the weighting of eye position and retinal position information, providing a physiological basis for understanding how visual direction from two eyes merges to form a unified single direction. Therefore, to further develop this model to extract perceived visual direction, an additional layer can be added where retinal signals interact with information about eye position (eye movements). As illustrated in Figure 7.3, an enhanced model is developed to explain how retinal signals and eye position signals dynamically interact dynamic to achieve egocentric perception. Building on the DSKL mode, an additional retino-positional integration layer (represented by green lines) is introduced to integrate binocular eye position signals ( $\hat{e}$ ) (represented by yellow lines) from left and right eye positions ( $e_L$  and  $e_R$ , respectively) with binocular retinocentric integration ( $\hat{I}$ ) to compute an egocentric perception. A feedback loop from the egocentric perception to the retino-positional integration layer dynamically adjusts the integration between retinal inputs and eye position signals, maintaining accurate egocentric perception in response to changes induced by short-term monocular deprivation. during recalibration, the egocentric perception detects discrepancies between the perceived and expected egocentric position following monocular deprivation, generating a feedback signal to the retino-positional integration layer. This feedback induces a recalibration process where the gain of the deprived eye is gradually increased to compensate for its reduced input. Additionally, the feedback mechanism

adjusts positional offsets to account for changes in gaze direction, ensuring accurate egocentric perception despite the imbalance.

### 7.2.3 Eye dominance and its influence on egocentric visual direction

The findings in this thesis reveal varying degrees of eye dominance among individuals (see Chapters 5 and 6). In line with established literature, most individuals exhibit a preference for one eye across different tasks, demonstrating consistent ocular dominance (Miles, 1930; Crider, 1944; Walls, 1951; Coren & Kaplan, 1973; Porac & Coren, 1976; Osburn & Klingsporn, 1998). It has been reported that between 52% and 82% of the population favours the right eye, whereas 18% to 40% prefer the left (e.g. Li et al., 2011). However, these findings were obtained with participants maintaining a straight-ahead gaze. Research have increasingly link eye dominance to differences in cortex activity, particularly within the primary visual cortex (V1).

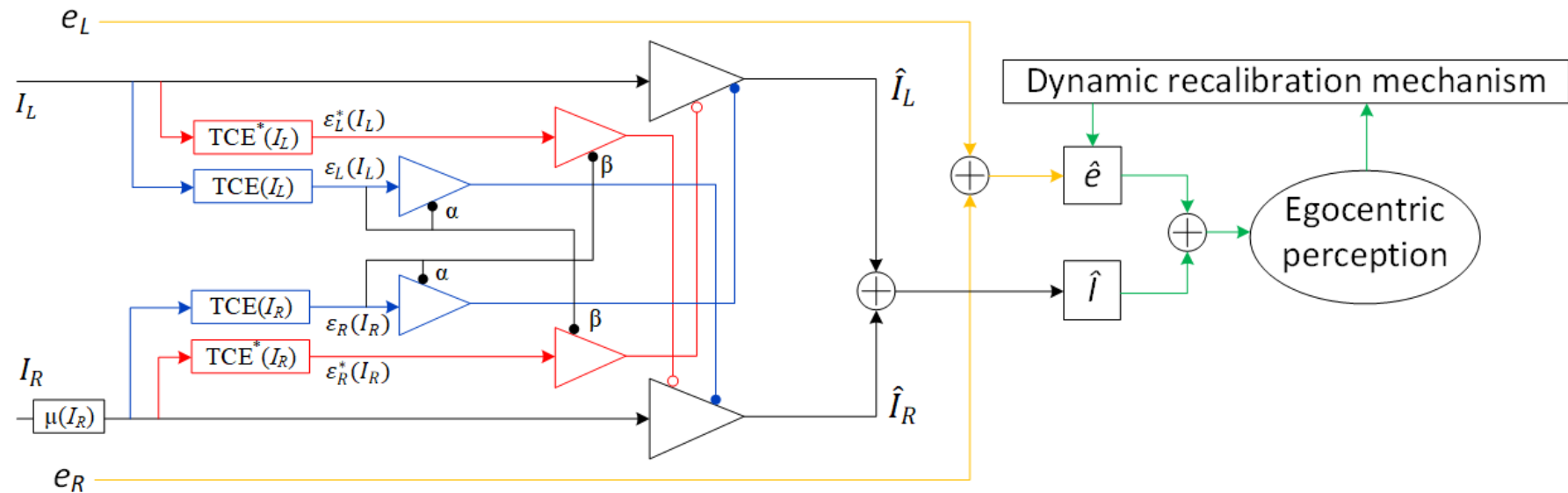


Figure 7.3: An enhanced model for incorporating retinal and eye position signals for achieving egocentric perception. An additional retino-positional integration layer (represented by green lines) is introduced to combine positional signals ( $\hat{e}$ ) (represented by yellow lines) from extraocular muscles or motor efferences with binocular retinocentric integration ( $\hat{I}$ ) to compute egocentric perception. A dynamic recalibration mechanism is introduced as a feedback loop to adjust the integration of retino-positional signals and maintain egocentric perception in response to the changes following short-term monocular deprivation

According to Hubel and Wiesel (1968), layer three of V1 is the first location of binocularity. Notably, Rombouts et al. (1996) discovered that, in right-eye dominant individuals, a larger portion of the primary visual cortex was activated by the dominant eye, a pattern further corroborated by Menon et al. (1997), who observed more right-eye dominant active voxels in fMRI scans of right-eyed observers. In recent studies on normal human vision, asymmetries have been observed in V1 activation: the dominant eye elicits a higher fMRI signal magnitude, and the non-dominant eye produces a lower signal, as determined by visual and grating acuity (Conner et al., 2007). Anatomically segregated inputs from both eyes to V1 have approximately equivalent reciprocal inhibition, which contributes to eye dominance, at least in part (Meese et al., 2006). Any asymmetry in this interocular inhibition is associated with eye dominance (Sengpiel et al., 1994; Huang et al., 2010). Individuals with stronger eye dominance tend to exhibit greater interocular differences in GABAergic inhibition in V1, suggesting a differential inhibitory influence of one eye during active viewing (Ip et al., 2021).

Coren and Kaplan (1973) identified three primary criteria for defining the dominant eye: (1) the eye with superior acuity, (2) the eye that consistently prevails during binocular rivalry, and (3) the eye used for sighting. Research has shown these factors to be largely independent, with little correlation among them. Asymmetries between the eyes are primarily attributed to variations in sighting dominance (Coons & Mathias, 1928; Cuff, 1931; Downey, 1933; Fink, 1938; Gahagan, 1933; Gronwall & Sampson, 1971; Hildreth, 1949; Merrell, 1957; Mills, 1925; Pointer, 2001; Porac & Coren, 1976; Walls, 1951; Warren & Clark, 1938; Washburn, Faison, & Scott, 1934; Friedlander, 1971; Money, 1972; Porac, Whitford, & Coren, 1976; Schoen & Scofield, 1935). Consistent with these earlier studies, our findings indicate a higher prevalence of right-eye dominance in sighting task. Neural responses may be associated with sighting dominance, as these were measured using binocular sighting tasks, with 53.85% participants favouring their right eyes. Additionally, our results indicate that eye dominance varies by task,

supporting the view that eye dominance is not a fixed attribute for most individuals. Khan and Crawford (2001) further observed that dynamic eye dominance could reverse depending on horizontal gaze angle, suggesting that the sighting dominant eye serves as a reference for directional judgments.

#### 7.2.4 The influence of short-term monocular deprivation on eye dominance plasticity

Unlike previously reported studies (e.g. Lunghi et al., 2011, 2013; Zhou et al., 2013; Wang et al., 2020, 2021), that reported a rivalry shift towards the previously deprived eye, my findings demonstrate that 60 minutes of monocular deprivation induced a significant shift in the egocentre location towards the median plane of the head (see Chapter 5). It is important to note that earlier studies did not measure shifts in the egocentre location, which differentiates our study in terms of focus and observed outcome. Our findings unequivocally reveal the residual plasticity of the adult visual system, consistent with previous studies (Gibert & Li, 2012; Lunghi et al., 2013; Wang et al., 2024), highlighting that the visual cortex retains some life-long, experience-dependant plasticity. Previous studies have shown that even brief periods of monocular deprivation (2–2.5 hours) induce a temporary shift in ocular dominance toward the deprived eye (Lunghi et al., 2011; Lunghi et al., 2013). This shift occurs at both perceptual (Lunghi et al., 2011, 2013) and neural levels (Binda et al., 2018; Binda & Lunghi, 2017; Lunghi et al., 2015a, 2015b), illustrating homeostatic plasticity in the adult visual cortex, which attempts to maintain a stable level of neural activity in response to sensory deprivation.

On a perceptual level, this shift manifests through both competitive and collaborative interocular interactions and can persist up to three hours after removing the eye patch (Lunghi et al., 2013). At the neural level, short-term monocular deprivation temporarily alters activity in the primary visual cortex (V1): visual evoked potentials (VEPs) for the deprived eye

(specifically the initial C1 component) increase, while activity of the non-deprived eye decreases (Lunghi et al., 2015a). Additionally, imaging studies demonstrate that blood-oxygen-level-dependent (BOLD) responses increase for the deprived eye, while they decrease for the non-deprived eye. This is accompanied by a neural tuning shift toward higher spatial frequencies specifically in the deprived eye, which is presumed to reflect the engagement of the parvocellular pathway and its role in compensatory processing following deprivation (Binda et al., 2018). This homeostatic mechanism helps prevent the brain from becoming overly active or underactive, thereby maintaining stability within the visual system (Turrigiano, 1999, 2011).

The findings of Barendregt et al. (2005) demonstrated that V1 primarily represents the monocular retinal image while beyond this (V2 to LO) seem to represent cycloptopy. This cycloptopic activity integrates information from both eyes to construct a single unified projection. Following monocular deprivation, adaptive plasticity may shift the peak cycloptopic activity, raising a question of whether the shifts align with the eye that has been deprived or recalibrate toward the median plane of the head. My findings that the egocentre location shift toward the median plane is consistent with the idea that cycloptopic activity in extrastriate areas play an important role in integrating and recalibrating binocular inputs following deprivation. Further study can extend my work by directly assessing changes in cycloptopic representations pre- and post-deprivation measured with functional Magnetic Resonance Imaging (fMRI) to have a better understanding of the neural basis of these perceptual shifts.

Aligned with Hering's perspective that the eyes operate as two halves of a unified visual organ (1868/1977), the brain integrates inputs from both eyes to maintain a cohesive perception of visual direction. Studies confirm that positional information from the occluded eye continues to influence egocentric visual direction, though less significantly than during binocular viewing (Khokhotva, Ono & Mapp, 2005; Ono & Gonda, 1978;



Ono, Mapp & Howard, 2002; Ono & Weber, 1981; Park & Shebilske, 1991; Simpson, 1992). This reciprocal inhibition, occurring before excitatory binocular integration, reflects a dynamic binocular interaction rather than a monocular adjustment to the occlusion. This normalization effect likely represents an underlying neural mechanism that stabilizes visual perception, even when one eye is temporarily deprived of sensory input.

Collectively, these findings highlight interocular suppression as an adaptive mechanism, crucial for maintaining perceptual coherence in binocular vision. Even during temporary deprivation of one eye, the brain compensates by shifting the visual egocentre closer to the median plane, balancing sensory input to support effective binocular coordination. This adjustment aligns with the theory of interocular contrast gain control (Ding, Klein & Levi, 2013a, 2013b; Ding & Sperling, 2006; Meese et al., 2006; Meese & Hess, 2004) and suggests that the visual system's capacity to adapt to sensory inputs. The findings of Exp.1 demonstrate that the perceived visual direction depends on the ratio of contrasts between the two eyes, revealing how the visual system compensate for inter-ocular contrast differences and maintain functional binocular vision even one eye is deprived. In the context of these findings, the compensatory shift in the egocentre could be modelled as a mechanism that adjusts contrast gain across the eyes to achieve equivalent perceived contrasts. This process may serve to restore perceptual balance, even when one eye is temporarily deprived, and offers valuable insights for therapeutic interventions targeting visual disorders like amblyopia, where interocular suppression and sensory discrepancies challenge binocular integration.

## 7.3 Limitations and further directions

A central focus of this dissertation was the measurement of the visual egocentre in individuals with normal vision. In Chapter 4, absolute directional tasks were employed, in which observers rotated a rod to point toward themselves. However, it is possible that observers unintentionally

relied on personal reference points (e.g., their face or the bridge of their nose), potentially influencing their perceived egocentre location. Furthermore, these internal reference frames may have shifted before and after monocular deprivation, raising the question of whether such shifts represent systematic errors or actual changes in the egocentre.

Eye movements and phoria (the misalignment of eye position when binocular vision is prevented) were not recorded in this study due to space constraints within the apparatus. However, efforts were made to minimize the impact of eye movements by emphasizing fixation markers, reducing the duration of stereo patch presentations in Chapter 3, and stabilizing head movement with a chin rest in Chapters 3, 4, 5, and 6. Phoria is particularly relevant to the patching experiments conducted in this study, as the prevention of binocular vision for an extended period may cause the covered eye to shift away from alignment with the viewing eye. This shift under cover could potentially contribute to subsequent changes in egocentre location. Given that phoria varies based on task type (Schroeder, Rainey, Goss, & Grosvenor, 1996), observer age (Freier & Pickwell, 1983), and fixation duration (Alvarez, Kim, Yaramothu, & Granger-Donetti, 2017), future research should investigate the relationship between phoria, cyclopean perception, and shifts in egocentre location to better understand their interplay in visual adaptation.

In relation to feature specificity (e.g. contrast, spatial frequency, motion) in eye dominance, inconsistencies in feature selectivity have been observed across different measurements (e.g., Holopigian, 1989; Ledgeway et al., 2013). Further research could work on investigating whether selective attention could be directed to one eye and whether this modifies perceived visual direction. Wang et al. (2021) research suggested that top-down attentional selection during monocular deprivation may enhance the contribution of the deprived eye during subsequent binocular perception. Zhang et al. (2012) demonstrated that top-down attention can be eye-specific, modulating visual input from

monocular channel even though when the target stimulus is suppressed from consciousness. In this case, attention could enhance the neural representation of one eye, thereby influencing our perception of visual direction. In future experiments, top-down attentional mechanisms could be explored to determine whether selective attention to the input from one eye alters the visual egocentre position. In this way, we could gain valuable insights into how voluntary attention modulates sensory dominance.

Our work supports the idea that the visual system defaults to a centrally aligned egocentre and that short-term deprivation may disrupt learned monocular preferences, resetting the egocentre to a more balanced state. This mechanism has potential implications for treating binocular vision disorders, such as amblyopia and strabismus, where interocular suppression and dominance imbalance challenge binocular integration. The idea of using measures of visual direction as a treatment outcome is promising, particularly when paired with assessments of suppression depth during eye dominance shifts. These measures could provide valuable insights into the relationship between suppression depth and recovery, which may vary across individuals.

Our findings can be contextualized by recent studies. The findings of Webber et al. (2020) indicated that suppression is the primary determinant of binocular function in amblyopia, rather than visual acuity loss. Hu et al. (2023) demonstrated that reverse masking significantly reduces binocular suppression and enhances neuroplasticity, especially in amblyopic patients resistant to conventional treatment. However, Bossi et al. (2017) found that binocular therapy for amblyopia improved vision without significantly reducing interocular suppression, challenging the findings that inter-ocular suppression may be linked with the degree of recovery of binocular function such as stereopsis. Our approach (using linear polarizers), which measures egocentric shifts with precision, could provide clinicians with a sensitive tool to evaluate treatment efficacy beyond traditional metrics like acuity or stereoacuity. This method can be

used to track how interventions like patching, dichoptic training, or perceptual learning recalibrate visual processing and restore binocular balance. Future research should explore how suppression depth and egocentric shifts interact, particularly in longitudinal studies, to determine whether repeated short-term deprivation sessions can induce lasting improvements in visual function. This approach could open new avenues for personalized treatment strategies for amblyopia and other binocular vision disorders.

## 7.4 Conclusion

In conclusion, this thesis provides a cohesive understanding of binocular vision as a dynamic and plastic system, capable of adapting to changes in input through weighted computations and neural recalibration. The insights have gained implications for both fundamental vision science and clinical applications. For instance, understanding how to manipulate sensory eye dominance could enhance interventions for binocular dysfunction and improve VR/AR technologies. Future research should continue to refine measurement techniques, explore the long-term effects of monocular deprivation, and investigate the links between sensory dominance, depth perception, and other aspects of binocular function. By bridging basic science with practical applications, this work paves the way for innovative strategies to enhance visual experiences and address clinical challenges in binocular vision.

## References

- Adams, D. L., Sincich, L. C., & Horton, J. C. (2007). Complete Pattern of Ocular Dominance Columns in Human Primary Visual Cortex. *The Journal of Neuroscience*, 27(39), 10391–10403. <https://doi.org/10.1523/JNEUROSCI.2923-07.2007>
- Adams, G.L. (1965). Effect of Eye Dominance on Baseball Batting. *Research Quarterly. American Association for Health, Physical Education and Recreation*, 36, 3-9.
- Aguilonius, F. (1613). *Opticorum Libri Sex. Antwerp: Plantin*.
- Alhazen, I. (1989). *Book of optics*. In A. I. Sabra (Trans.), *The optics of Ibn al-Haytham*. London: Warburg Institute. (Original work published 1083)
- Allard, R., & Faubert, J. (2008). The noisy-bit method for digital displays: Converting a 256 luminance resolution into a continuous resolution. *Behavior Research Methods*, 40(3), 735–743. <https://doi.org/10.3758/BRM.40.3.735>.
- Allard, T., Clark, S. A., Jenkins, W. M., & Merzenich, M. M. (1991). Reorganization of somatosensory area 3b representations in adult owl monkeys after digital syndactyly. *Journal of Neurophysiology*, 66(3), 1048–1058. <https://doi.org/10.1152/jn.1991.66.3.1048>
- Alvarez, T. L., Kim, E. H., Yaramothu, C., & Granger-Donetti, B. (2017). The influence of age on adaptation of disparity vergence and phoria. *Vision Research*, 133, 1–11. <https://doi.org/10.1016/j.visres.2017.01.002>
- Anderson, P. A., & Movshon, J. A. (1989). Binocular combination of contrast signals. *Vision Research*, 29(9), 1115–1132. [https://doi.org/10.1016/0042-6989\(89\)90060-6](https://doi.org/10.1016/0042-6989(89)90060-6)
- Antonini, A., Fagiolini, M., & Stryker, M. P. (1999). Anatomical correlates of functional plasticity in mouse visual cortex. *Journal of Neuroscience*, 19(11), 4388–4406. <https://doi.org/10.1523/JNEUROSCI.19-11-04388.1999>
- Artal, P. (2014). Optics of the eye and its impact in vision: A tutorial. *Advances in Optics and Photonics*, 6(3), 340-367.
- Auerbach, A., & Bennett, M. V. L. (1969). Chemical synaptic transmission. *The Journal of General Physiology*, 54(5), 517-548.
- Bai, J., Dong, X., He, S., & Bao, M. (2017). Monocular deprivation of Fourier phase information boosts the deprived eye's dominance during interocular competition but not interocular phase combination. *Neuroscience*, 352, 122–130. <https://doi.org/10.1016/j.neuroscience.2017.03.053>
- Baker, D. H., & Wade, A. R. (2017). Evidence for an optimal algorithm underlying signal combination in human visual cortex. *Cerebral Cortex*, 27(1), 254–264. <https://doi.org/10.1093/cercor/bhw395>
- Baker, D. H., Meese, T. S., Mansouri, B., & Hess, R. F. (2007). Binocular summation of contrast remains intact in strabismic amblyopia. *Investigative Ophthalmology & Visual Science*, 48(11), 5332–5338. <https://doi.org/10.1167/iovs.07-0194>

- Baker, F. H., Grigg, P., & von Noorden, G. K. (1974). Effects of visual deprivation and strabismus on the response of neurons in the visual cortex of the monkey, including studies on the striate and prestriate cortex in the normal animal. *Brain Research*, 66(2), 185–208. doi:10.1016/0006-8993(74)90140-1
- Baldwin, A. S., & Hess, R. F. (2018). The mechanism of short-term monocular deprivation is not simple: Separate effects on parallel and cross-oriented dichoptic masking. *Scientific Reports*, 8 (1), 1–8. doi:10.1038/s41598-018-24584-9
- Bang, J. W., Khalilzadeh, O., Hamalainen, M., Watanabe, T., & Sasaki, Y. (2014). Location-specific sleep spindle activity in the early visual areas and perceptual learning. *Vision Research*, 99, 162–171. <https://doi.org/10.1016/j.visres.2013.12.016>
- Bang, J. W., Sasaki, Y., Watanabe, T., & Rahnev, D. (2018). Feature-Specific Awake Reactivation in Human V1 after Visual Training. *The Journal of Neuroscience : The Official Journal of the Society for Neuroscience*, 38(45), 9648–9657. <https://doi.org/10.1523/JNEUROSCI.0884-18.2018>
- Banister, H. (1935). A study in eye dominance. *British Journal of Psychology*, 26, 32-48. <https://doi.org/10.1111/j.2044-8295.1935.tb00279.x>
- Banks, M. S., van Ee, R., & Backus, B. T. (1997). The computation of binocular visual direction: A re-examination of Mansfield and Legge (1996). *Vision Research*, 37, 1605–1610.
- Barbeito, R. (1981). Sighting dominance: An explanation based on the processing of visual direction in tests of sighting dominance. *Vision Research*, 21, 855–860. [https://doi.org/10.1016/0042-6989\(81\)90185-1](https://doi.org/10.1016/0042-6989(81)90185-1)
- Barbeito, R. (1983). Sighting from the cyclopean eye: The Cyclops effect in preschool children. *Perception & Psychophysics*, 33, 561-564. <https://doi.org/10.3758/BF03202937>.
- Barbeito, R., & Ono, H. (1979). Four methods of locating the egocenter: A comparison of their predictive validities and reliabilities. *Behavior Research Methods & Instrumentation*, 11(1), 31–36. <https://doi.org/10.3758/BF03205428>
- Barbeito, R., & Simpson, T. L. (1991). The relationship between eye position and egocentric visual direction. *Perception & Psychophysics*, 50(4), 373–382. <https://doi.org/10.3758/bf03212230>
- Barendregt, M., Harvey, B. M., Rokers, B., & Dumoulin, S. O. (2015). Transformation from a Retinal to a Cyclopean Representation in Human Visual Cortex. *Current Biology*, 25(15), 1982–1987. <https://doi.org/10.1016/j.cub.2015.06.003>
- Barlow, H. B., Blakemore, C., & Pettigrew, J. D. (1967). The neural mechanism of binocular depth discrimination. *The Journal of Physiology*, 193(2), 327–342. <https://doi.org/10.1113/jphysiol.1967.sp008360>
- Barrett, B. T., Bradley, A., & McGraw, P. V. (2004). Understanding the neural basis of amblyopia. *Neuroscientist*, 10(2), 106–117. <https://doi.org/10.1177/1073858403262153>

- Baskaran, A. A., Ramalingam, E., Britto, T., Thomas, P. A., & Muthusamy, P. (2023). Validity of TNO Cards as a Screening Test for Defects of Binocularity in Children. *The Journal of Ophthalmic Science and Research*, 61(2), 172-176.
- Bearse, M. A., Jr, & Freeman, R. D. (1994). Binocular summation in orientation discrimination depends on stimulus contrast and duration. *Vision Research*, 34(1), 19–29. [https://doi.org/10.1016/0042-6989\(94\)90253-4](https://doi.org/10.1016/0042-6989(94)90253-4)
- Berardi, N., Pizzorusso, T., & Maffei, L. (2000). Critical periods during sensory development. *Current Opinion in Neurobiology*, 10(1), 138–145. [https://doi.org/10.1016/s0959-4388\(99\)00047-1](https://doi.org/10.1016/s0959-4388(99)00047-1).
- Berner, G. E., & Berner, D. E. (1953). Relation of ocular dominance, handedness, and the controlling eye in binocular vision. *A.M.A. Archives of Ophthalmology*, 50, 603-608. <https://doi.org/10.1001/archophth.1953.00940090605003>
- Bian, Z., & Andersen, G. J. (2013). Aging and the perception of egocentric distance. *Psychology and Aging*, 28(3), 813–825. <https://doi.org/10.1037/a0030991>
- Binda, P., & Lunghi, C. (2017). Short-term monocular deprivation enhances physiological pupillary oscillations. *Neural Plasticity*. <https://doi.org/10.1155/2017/6724631>
- Binda, P., Kurzawski, J. W., Lunghi, C., Biagi, L., Tosetti, M., & Morrone, M. C. (2018). Response to short-term deprivation of the human adult visual cortex measured with 7T BOLD. *Elife*, 7. <https://doi.org/10.7554/eLife.40014>
- Birch E. E. (2013). Amblyopia and binocular vision. *Progress in Retinal and Eye Research*, 33, 67–84. <https://doi.org/10.1016/j.preteyeres.2012.11.001>
- Bishop, P. O., & Henry, G. H. (1971). Spatial vision. *Annual Review of Psychology*, 22, 119-160.
- Björk A. (1980). The variable angle-mirror, a new tool for the study of ocular dominance and eye fixation. *Acta Ophthalmologica*, 58(2), 202–209. <https://doi-org.nottingham.idm.oclc.org/10.1111/j.1755-3768.1980.tb05710.x>
- Black, J. M., Thompson, B., Maehara, G., & Hess, R. F. (2011). A compact clinical instrument for quantifying suppression. *Optometry and Vision Science: Official Publication of the American Academy of Optometry*, 88(2), E334–E343. <https://doi.org/10.1097/OPX.0b013e318205a162>
- Blake, R., & Boothroyd, K. (1985). The precedence of binocular fusion over binocular rivalry. *Perception & Psychophysics*, 37(2), 114–124. <https://doi.org/10.3758/BF03202845>
- Blake R. (1989). A neural theory of binocular rivalry. *Psychological review*, 96(1), 145–167. <https://doi-org.nottingham.idm.oclc.org/10.1037/0033-295x.96.1.145>
- Blake, R., & Sekuler, R. (2006). *Perception*. New York; London: McGraw-Hill.
- Blake, R., Yang, Y. D., & Wilson, H. R. (1991). On the coexistence of stereopsis and binocular rivalry. *Vision research*, 31(7-8), 1191–

1203. [https://doi-org.nottingham.idm.oclc.org/10.1016/0042-6989\(91\)90044-6](https://doi-org.nottingham.idm.oclc.org/10.1016/0042-6989(91)90044-6)
- Blakemore, C., Garey, L. J., & Vital-Durand, F. (1978). The physiological effects of monocular deprivation and their reversal in the monkey's visual cortex. *Journal of Physiology*, 283, 223–262.
- Blakemore, C., & van Sluyters, R. C. (1974). Reversal of the physiological effects of monocular deprivation in kittens: further evidence for a sensitive period. *The Journal of Physiology*, 237(1), 195–216. doi:10.1113/jphysiol.1974.sp010478
- Blasdel, G. G., & Fitzpatrick, D. (1984). Physiological organization of layer 4 in macaque striate cortex. *The Journal of Neuroscience: The Official Journal of the Society for Neuroscience*, 4(3), 880–895. <https://doi.org/10.1523/JNEUROSCI.04-03-00880.1984>
- Bliss, T. V., & Lomo, T. (1973). Long-lasting potentiation of synaptic transmission in the dentate area of the anaesthetized rabbit following stimulation of the perforant path. *The Journal of Physiology*, 232(2), 331–356. <https://doi.org/10.1113/jphysiol.1973.sp010273>.
- Bock, O., & Kommerell, G. (1986). Visual localization after strabismus surgery is compatible with the “outflow” theory. *Vision Research*, 26(11), 1825–1829. [https://doi.org/10.1016/0042-6989\(86\)90114-0](https://doi.org/10.1016/0042-6989(86)90114-0)
- Boff, K. R., Kaufman, L., & Thomas, J. P. (Eds.). (1986). *Handbook of Perception and Human Performance (Vol. 1)*. New York: Wiley.
- Bossi, M., Hamm, L. M., Dahlmann-Noor, A., & Dakin, S. C. (2018). A comparison of tests for quantifying sensory eye dominance. *Vision Research*, 153, 60–69. <https://doi.org/10.1016/j.visres.2018.09.006>
- Bossi, M., Taylor, V. K., Anderson, E. J., Bex, P. J., Greenwood, J. A., Dahlmann-Noor, A., & Dakin, S. C. (2017). Binocular Therapy for Childhood Amblyopia Improves Vision Without Breaking Interocular Suppression. *Investigative Ophthalmology & Visual Science*, 58(7), 3031. <https://doi.org/10.1167/iovs.16-20913>
- Bosten J. M., Goodbourn P. T., Lawrance-Owen A. J., Bargary G., Hogg R. E., Mollon J. D. (2015). A population study of binocular function. *Vision Research*, 110(Part A), 34–50, 10.1016/j.visres.2015.02.017.
- Braddick, O., & Atkinson, J. (2011). Development of human visual function. *Vision Research*, 51(13), 1588–1609. <https://doi.org/10.1016/j.visres.2011.02.018>
- Bridgeman, B., & Stark, L. (1991). Ocular proprioception and efference copy in registering visual direction. *Vision Research*, 31(11), 1903–1913. [https://doi.org/10.1016/0042-6989\(91\)90189-3](https://doi.org/10.1016/0042-6989(91)90189-3)
- Bruce, V., Green, P. R., & Georgeson, M. A. (1996). *Visual perception: Physiology, Psychology, and Ecology* (p. 433). Hove: Psychology Press.
- Cakir, G. B., Murray, J., Dulaney, C., & Ghasia, F. (2024). Multifaceted interactions of stereoacuity, inter-ocular suppression, and fixation eye movement abnormalities in amblyopia and strabismus.



- Investigative Ophthalmology & Visual Science*, 65(3), 19.  
<https://doi.org/10.1167/iov.65.3.19>
- Campos, E. (1995). Major Review: Amblyopia. *Survey of Ophthalmology*, 40(1), 23–39. doi:10.1016/S0039-6257(95)80044-1
- Casagrande, V. A., & Boyd, J. D. (1996). The neural architecture of binocular vision. *Eye*, 10(2), 153–160.  
<https://doi.org/10.1038/eye.1996.40>
- Castaldi, E., Lunghi, C., & Morrone, M. C. (2020). Neuroplasticity in adult human visual cortex. *Neuroscience and biobehavioral reviews*, 112, 542–552.  
<https://doi-org.nottingham.idm.oclc.org/10.1016/j.neubiorev.2020.02.028>
- Chadnova, E., Reynaud, A., Clavagnier, S., & Hess, R. F. (2017). Short-term monocular occlusion produces changes in ocular dominance by a reciprocal modulation of interocular inhibition. *Scientific Reports*, 7, 41747. <https://doi.org/10.1038/srep41747>
- Chamwood, J. R. B. (1949). Observations on ocular dominance. *The Optician*, 118, 85-88.
- Chan, A. Y., & Chang, D. H. (2022). Neural correlates of eye dominance in human visual white matter tracts. *eneuro*, 9(6).  
<https://doi.org/10.1523/ENEURO.0232-22.2022>.
- Chen, G., Lu, H. D., & Roe, A. W. (2008). A map for horizontal disparity in monkey V2. *Neuron*, 58(3), 442–450.  
<https://doi.org/10.1016/j.neuron.2008.02.032>
- Cheng, C. Y., Yen, M. Y., Lin, H. Y., Hsia, W. W., & Hsu, W. M. (2004). Association of ocular dominance and anisometropic myopia. *Investigative Ophthalmology & Visual Science*, 45(8), 2856–2860. <https://doi.org/10.1167/iov.03-0878>
- Chenkov, N., Sprekeler, H., & Kempter, R. (2017). Memory replay in balanced recurrent networks. *PLoS Computational Biology*, 13(1), e1005359. <https://doi.org/10.1371/journal.pcbi.1005359>
- Church, J. (1966). *Language and the discovery of reality*. New York, NY: Vintage Press.
- Church, J. (1970). Techniques for the differential study of cognition in early childhood. In K. Hellmuth (Ed.), *Cognitive Studies* (Vol. 1, pp. 1-23). New York: Brunner.
- Cogan A. I. (1987). Human binocular interaction: towards a neural model. *Vision Research*, 27(12), 2125–2139.  
[https://doi.org/10.1016/0042-6989\(87\)90127-1](https://doi.org/10.1016/0042-6989(87)90127-1)
- Cohen, J. (1952). Eye-dominance. *American Journal of Psychology*, 65, 634-636. <https://doi.org/10.2307/1420563>
- Cohn, T. E., & Lasley, D. J. (1976). Binocular vision: two possible central interactions between signals from two eyes. *Science (New York, N.Y.)*, 192(4239), 561–563.  
<https://doi.org/10.1126/science.1257791>
- Cole, J. (1957). Laterality in the use of the hand, foot and eye in monkeys. *Journal of Comparative and Physiological Psychology*, 50(3), 296–299. <https://doi-org.nottingham.idm.oclc.org/10.1037/h0046343>
- Coons, J. C., & Mathias, R. J. (1928). Eye and hand preference tendencies. *Journal of Genetic Psychology*, 35, 629–632.

- Coren, S., & Duckman, R. H. (1975). Ocular dominance and amblyopia. *Optometry and Vision Science*, 52(1), 47–50. doi:10.1097/00006324-197501000-00006
- Coren, S., & Kaplan, C. P. (1973). Patterns of ocular dominance. *American Journal of Optometry and Archives of American Academy of Optometry*, 50, 283–292.
- Coren, S., & Porac, C. (1976). Size accentuation in the dominant eye. *Nature*, 260, 527–528. <https://doi.org/10.1038/260527a0>
- Corso, J. F. (1981). *Aging sensory systems and perception*. Praeger Publishers.
- Cowey, A., & Ellis, C. M. (1967). Visual acuity of rhesus and squirrel monkeys. *Journal of Comparative and Physiological Psychology*, 64(1), 80–84. <https://doi.org/10.1037/h0024821>
- Crair, M. C., Ruthazer, E. S., Gillespie, D. C., & Stryker, M. P. (1997). *Journal of Neurophysiology*, 77(6), 3381–3385. <https://doi.org/10.1152/jn.1997.77.6.3381>
- Crawford, L. C. J., & Griffiths, H. J. (2015). The repeatability of the Sbisa bar for testing density of suppression. *British and Irish Orthoptic Journal*, 12, 35–40. <https://doi.org/10.22599/bioj.94>
- Crawford, M. L. J., & Harwerth, R. S. (2004). Ocular dominance column width and contrast sensitivity in monkeys reared with strabismus or anisometropia. *Investigative Ophthalmology and Visual Science*, 45(9), 3036–3042. <https://doi.org/10.1167/iov.04-0029>
- Crawford, M. L. J., Blake, R., Cool, S. J., & von Noorden, G. K. (1975). Physiological consequences of unilateral and bilateral eye closure in macaque monkeys: some further observations. *Brain Research*, 84 (1), 150–154. doi:10.1016/0006-8993(75)90809-4
- Crider, B. (1935). The relationship of eye muscle balance to the sighting eye. *Journal of Experimental Psychology*, 18(1), 152–154. <https://doi.org/10.1037/h0054478>
- Crider, B. (1935). The relationship of eye muscle balance to the sighting eye. *Journal of Experimental Psychology*, 18, 152–154.
- Crider, B. (1943). The importance of the dominant eye. *Journal of Psychology*, 16, 145–151. <https://doi.org/10.1080/00223980.1943.9917226>
- Crider, B. (1944). A battery of tests for the dominant eye. *Journal of General Psychology*, 31, 179–190.
- Crinella, F. M., Beck, F. W., & Robinson, J. W. (1971). Unilateral dominance is not related to neuropsychological integrity. *Child Development*, 42, 2033–2054. <https://doi.org/10.1111/j.1111.1971.00042.tb01111.x>
- Crone, R.A., Leuridan, O.M.A. Tolerance for aniseikonia. *Albrecht von Graefes Arch. Klin. Ophthalmol.* 188, 1–16 (1973). <https://doi.org/10.1007/BF00410860>
- Cuff, N. (1931). A study of eyedness and handedness. *Journal of Experimental Psychology*, 14, 164–175.
- Cui, Q. N., Razavi, B., O'Neill, W. E., & Paige, G. D. (2010). Perception of auditory, visual, and egocentric spatial alignment adapts differently to changes in eye position. *Journal of*

- neurophysiology*, 103(2), 1020–1035. <https://doi-org.nottingham.idm.oclc.org/10.1152/jn.00500.2009>
- Cumming, B. G., & DeAngelis, G. C. (2001). The physiology of stereopsis. *Annual Review of Neuroscience*, 24, 203–238. <https://doi.org/10.1146/annurev.neuro.24.1.203>
- Cumming, B. G., & Parker, A. J. (1997). Responses of primary visual cortical neurons to binocular disparity without depth perception. *Nature*, 389(6648), 280–283. <https://doi.org/10.1038/38487>
- Daw, N. W. (1995). *Visual development* (2nd ed.). Springer.
- Daw, N. W. (1998). Critical periods and amblyopia. *Archives of ophthalmology* (Chicago, Ill.: 1960), 116(4), 502–505. <https://doi.org/10.1001/archophth.116.4.502>
- de Valois, R. L., & Jacobs, G. H. (1968). Primate Color Vision. *Science*, 162(3853), 533–540. <http://www.jstor.org/stable/1724907>
- Dengis, C. A., Simpson, T. L., Steinbach, M. J., & Ono, H. (1998). The cyclops effect in adults: sighting without visual feedback. *Vision Research*, 38, 327–331.
- Dengis, C. A., Steinbach, M. J., Goltz, H., & Stager, C. (1993a). Visual alignment from the midline: a declining developmental trend in normal, strabismic, and monocularly enucleated children. *Journal of Pediatric Ophthalmology & Strabismus*, 30, 323–326.
- Dengis, C. A., Steinbach, M. J., Ono, H., Kraft, S. K., Smith, D. R., & Graham, J. E. (1993b). Egocenter location in strabismics is in the median plane and is unchanged by surgery. *Investigative Ophthalmology & Visual Science*, 34(10), 2990–2995.
- Dews, P. B., & Wiesel, T. N. (1970). Consequences of monocular deprivation on visual behaviour in kittens. *The Journal of Physiology*, 206(2), 437–455. doi:10.1113/jphysiol.1970.sp009023
- Dieter, K. C., Melnick, M. D., & Tadin, D. (2016). Perceptual training profoundly alters binocular rivalry through both sensory and attentional enhancements. *Proceedings of the National Academy of Sciences of the United States of America*, 113(45), 12874–12879. doi:10.1073/pnas.1602722113
- Dieter, K. C., Sy, J. L., & Blake, R. (2017). Individual differences in sensory eye dominance reflected in the dynamics of binocular rivalry. *Vision Research*, 141, 40–50. doi:10.1016/j.visres.2016.09.014
- Ding, J., & Sperling, G. (2006). A gain-control theory of binocular combination. *Proceedings of the National Academy of Sciences of the United States of America*, 103(4), 1141–1146.
- Ding, J., Klein, S. A., & Levi, D. M. (2013a). Binocular combination in abnormal binocular vision. *Journal of Vision*, 13(2), 11–31. <https://doi.org/10.1167/13.2.14>
- Ding, J., Klein, S. A., & Levi, D. M. (2013b). Binocular combination of phase and contrast explained by a gain-control and gain-enhancement model. *Journal of Vision*, 13(2), 11–37. <https://doi.org/10.1167/13.2.13>

- Dorman R., & van Ee R. (2017). 50 Years of stereoblindness: Reconciliation of a continuum of disparity detectors with blindness for disparity in near or far depth. *I-Perception*, 8(6), 1–13, 10.1177/2041669517738542.
- Dougherty, K., Carlson, B. M., Cox, M. A., Westerberg, J. A., Zinke, W., et al. (2021). Binocular suppression in the macaque lateral geniculate nucleus reveals early competitive interactions between the eyes. *eNeuro*, 8, ENEURO.0364-20.2020. <https://doi.org/10.1523/ENEURO.0364-20.2020>
- Dougherty, K., Schmid, M. C., & Maier, A. (2018). Binocular response modulation in the lateral geniculate nucleus. *Journal of Comparative Neurology*, 527(3), 522–534. <https://doi.org/10.1002/cne.24565>
- Douglas, R. M., Alam, N. M., & Prusky, G. T. (2004). Enhancement of spatial vision in adult mice induced by monocular deprivation. *Abstract Viewer/Itinerary Planner*, Program no. 866.15. Society for Neuroscience, Washington, DC.
- Downey, J. E. (1933). Laterality of function. *Psychological Bulletin*, 30, 109–142.
- Duke-Elder, W. S. (1952). *Textbook of Ophthalmology (Vol. 4)*. London: Henry Kimpton.
- Duménieu, M., Marquèze-Pouey, B., Russier, M., & Debanne, D. (2021). Mechanisms of Plasticity in Subcortical Visual Areas. *Cells*, 10(11), 3162. <https://doi.org/10.3390/cells10113162>
- Eadie, A. S., & Carlin, P. J. (1995). Evolution of control system models of ocular accommodation, vergence and their interaction. *Medical & Biological Engineering & Computing*, 33(4), 517–524. <https://doi.org/10.1007/BF02522508>
- Ehrenstein, W. H., Arnold-Schulz-Gahmen, B. E., & Jaschinski, W. (2005). Eye preference within the context of binocular functions. *Graefes Archive for Clinical and Experimental Ophthalmology*, 243(9), 926–932, <https://doi.org/10.1007/s00417-005-1128-7>.
- Elbaum, T., Wagner, M., & Botzer, A. (2017). Cyclopean, Dominant, and Non-dominant Gaze Tracking for Smooth Pursuit Gaze Interaction. *Journal of Eye Movement Research*, 10(1), 10.16910/jemr.10.1.2. <https://doi.org/10.16910/jemr.10.1.2>
- Epelbaum, M., Milleret, C., Buisseret, P., & Duffer, J. L. (1993). The Sensitive Period for Strabismic Amblyopia in Humans. *Ophthalmology*, 100(3), 323–327. doi:10.1016/S0161-6420(13)32170-8
- Erkelens, C. J. (2000). Perceived direction during monocular viewing is based on signals of the viewing eye only. *Vision Research*, 40(18), 2411–2419.
- Erkelens, C. J., & van de Grind, W. A. (1994). Binocular visual direction. *Vision Research*, 34(22), 2963–2969. [https://doi.org/10.1016/0042-6989\(94\)90268-2](https://doi.org/10.1016/0042-6989(94)90268-2)
- Erkelens, C. J., & van Ee, R. (2002). The role of the cyclopean eye in vision: sometimes inappropriate, always irrelevant. *Vision Research*, 42(9), 1157–1163. [https://doi.org/10.1016/s0042-6989\(01\)00280-2](https://doi.org/10.1016/s0042-6989(01)00280-2)

- Erkelens, C. J., Muijs, A. J., & van Ee, R. (1996). Binocular alignment in different depth planes. *Vision Research*, 36(14), 2141–2147. [https://doi.org/10.1016/0042-6989\(95\)00268-5](https://doi.org/10.1016/0042-6989(95)00268-5)
- Evans, B. J. W. (2001). *Binocular vision and orthoptics: Investigation and management* (p. 69). London: Butterworth-Heinemann.
- Farrer, D. N., & Graham, E. S. (1967). Visual acuity in monkeys: A monocular and binocular subjective technique. *Vision Research*, 7(9), 743–747. [https://doi.org/10.1016/0042-6989\(67\)90036-3](https://doi.org/10.1016/0042-6989(67)90036-3)
- Fechner G.T. (1860/1966) *Elemente der Psychophysik*. Breitkopf & Härtel, Leipzig (reprinted in 1964 by Bonset, Amsterdam); English translation by HE Adler (1966): *Elements of psychophysics*. Holt, Rinehart & Winston, New York
- Fender, D., & Julesz, B. (1967). Extension of Panum, P. L. (1858). *Physiologische Untersuchungen über das Sehen mit zwei Augen [Physiological studies on seeing with two eyes]*. Schwes. Retrieved from <https://archive.org/details/physiologischeun00panu>'s fusional area in binocularly stabilized vision. *Journal of the Optical Society of America*, 57(6), 819-830.
- Fink, W. H. (1938). The dominant eye: Its clinical significance. *Archives of Ophthalmology*, 19, 555–582.
- Fischer, Q. S., Graves, A., Evans, S., Lickey, M. E., & Pham, T. A. (2007). Monocular deprivation in adult mice alters visual acuity and single-unit activity. *Learning & Memory*, 14(4), 277–286. <https://doi.org/10.1101/lm.392107>
- Francis, J. L. & Harwood, K. A. (1951). The variation of the projection centre with differential stimulus and its relation to ocular dominance. In *Transactions of the International Congress* (pp. 75-87). London: British Optical Association.
- Freier, B. E., & Pickwell, L. D. (1983). Physiological exophoria. *Ophthalmic and Physiological Optics*, 3, 267–272. <https://doi.org/10.1111/j.1475-1313.1983.tb00613.x>
- Frenkel, M. Y., & Bear, M. F. (2004). How monocular deprivation shifts ocular dominance in visual cortex of young mice. *Neuron*, 44 (6), 917– 923. doi:10.1016/j.neuron.2004.12.003
- Friedlander, W. J. (1971). Some aspects of eyedness. *Cortex*, 7, 357–371.
- Fronius, M., Cirina, L., Ackermann, H., Kohnen, T., & Diehl, C. M. (2014). Efficiency of electronically monitored amblyopia treatment between 5 and 16 years of age: New insight into declining susceptibility of the visual system. *Vision Research*, 103, 11–19. <https://doi.org/10.1016/j.visres.2014.06.007>
- Fry, G. A. (1950). Visual perception of space. *American Journal of Optometry*. doi: 10.1097/00006324-195011000-00001
- Funaishi, S. (1926). Weiteres über das Zentrum der Sehrichtungen. *Albrecht von Graefes Archiv für Ophthalmologie*, 117, 296-303.
- Furmanski, C. S., Schluppeck, D., & Engel, S. A. (2004). Learning strengthens the response of primary visual cortex to simple patterns. *Current Biology*, 14(7), 573–578. <https://doi.org/10.1016/j.cub.2004.03.032>



- Gahagan, L. (1933). Visual dominance-acuity relationships. *Journal of General Psychology*, 9, 455-459.
- Gazova, I., Laczo, J., Rubinova, E., Mokrisova, I., Hyncicova, E., Andel, R., Vyhnaek, M., Sheardova, K., Coulson, E. J., & Hort, J. (2013). Spatial navigation in young versus older adults. *Frontiers in Aging Neuroscience*, 5, 94. <https://doi.org/10.3389/fnagi.2013.00094>
- Gilbert, C. D., & Li, W. (2012). Adult visual cortical plasticity. *Neuron*, 75(2), 250-264.
- Gilbert, C. D., & Wiesel, T. N. (1989). Columnar specificity of intrinsic horizontal connections in cat visual cortex. *Journal of Neuroscience*, 9(8), 2432-2442.
- Gockeln R. (1996). Der Einfluss der Interpupillardistanz auf die Tiefensehschärfe Effect of interpupillary distance on acuity of depth perception. *Klinische Monatsblätter für Augenheilkunde*, 209(4), 205-210. <https://doi.org/10.1055/s-2008-1035303>
- González, E. G., Steinbach, M. J., Gallie, B. L., & Ono, H. (1999). Egocentric localization: visually directed alignment to projected head landmarks in binocular and monocular observers. *Binocular vision & strabismus quarterly*, 14(2), 127-136.
- Gonzalez, F., & Perez, R. (1998). Neural mechanisms underlying stereoscopic vision. *Progress in Neurobiology*, 55(3), 191-224. [https://doi.org/10.1016/S0301-0082\(98\)00012-4](https://doi.org/10.1016/S0301-0082(98)00012-4)
- Goodale, M. A. & Milner, A. D. (1992). Separate visual pathways for perception and action. *Trends in Neurosciences*, 15(1), pp.20-25.
- Goodyear, B. G., Nicolle, D. A., & Menon, R. S. (2002). High resolution fMRI of ocular dominance columns within the visual cortex of human amblyopes. *Strabismus*, 10(2), 129-136. doi:10.1076/stra.10.2.129. 8140
- Gordon, J. A., & Stryker, M. P. (1996). Experience-dependent plasticity of binocular responses in the primary visual cortex of the mouse. *Journal of Neuroscience*, 16(10), 3274-3286. <https://doi.org/10.1523/JNEUROSCI.16-10-03274.1996>
- Gould G (1910). A method of determining ocular dominance. *JAMA*, 55:369 -370.
- Gregory, R. (1958). Eye movements and the stability of the visual world. *Nature*, 182, 1214. doi.org/10.1038/1821214a0
- Gregory, R. (1966). *Eye and Brain*. New York: McGraw Hill.
- Gregory, R. L. (1958). Eye movements and the stability of the visual world. *Nature*, 182(4644), 1214-1216. <https://doi.org/10.1038/1821214a0>
- Gronwall, D. M. A., & Sampson, H. (1971). Ocular dominance: A test of two hypotheses. *British Journal of Psychology*, 62, 175-185. <https://doi.org/10.1111/j.2044-8295.1971.tb01416.x>
- Grünert, U., & Martin, P. R. (2020). Cell types and cell circuits in human and non-human primate retina. *Progress in Retinal and Eye Research*, 78, 100844. <https://doi.org/10.1016/j.preteyeres.2020.100844>
- Guillery, R. W., & Colonnier, M. (1970). Synaptic patterns in the dorsal lateral geniculate nucleus of the monkey. *Zeitschrift für*

- Zellforschung und mikroskopische Anatomie (Vienna, Austria : 1948), 103(1), 90–108.  
<https://doi.org/nottingham.idm.oclc.org/10.1007/BF00335403>.
- Hall, K. R., & Mayer, B. (1966). Hand preferences and dexterities of captive patas monkeys. *Folia Primatologica*, 4, 169–185.  
<https://doi.org/10.1159/000155025>
- Hamm, L., Chen, Z., Li, J., Black, J., Dai, S., Yuan, J., Yu, M., & Thompson, B. (2017). Interocular suppression in children with deprivation amblyopia. *Vision Research*, 133, 112–120.  
<https://doi.org/10.1016/j.visres.2017.01.004>
- Handa, T., Mukuno, K., Uozato, H., Niida, T., Shoji, N., & Shimizu, K. (2004). Effects of dominant and nondominant eyes in binocular rivalry. *Optometry and Vision Science*, 81, 377–382.  
<https://doi.org/10.1097/01.OPX.0000133295.04923.E0>
- Handa, T., Shimizu, K., Uozato, H., Shoji, N., & Ishikawa, H. (2012). A new method for quantifying ocular dominance using the balancing technique. *The American Orthoptic Journal*, 62, 77–86, doi:10.3368/aoj.62.1.77.
- Harrad, R. A., Sengpiel, F., & Blakemore, C. (1996). Physiology of suppression in strabismic amblyopia. *British Journal of Ophthalmology*, 80(4), 373–377.  
<https://doi.org/10.1136/bjo.80.4.373>
- Harris, J. M. (2004). Binocular vision: moving closer to reality. *Philosophical Transactions of the Royal Society of London A: Mathematical, Physical and Engineering Sciences*, 362(1825), 2721–2739. doi:[10.1098/rsta.2004.1464](https://doi.org/10.1098/rsta.2004.1464).
- Harwerth, R. S., Smith, E. L., & Siderov, J. (1995). Behavioral studies of local stereopsis and disparity vergence in monkeys. *Vision Research*, 35(12), 1755–1770. [https://doi.org/10.1016/0042-6989\(94\)00256-L](https://doi.org/10.1016/0042-6989(94)00256-L)
- Hashemi, H., KhabazKhoob, M., Yazdani, K., Mehravaran, S., Jafarzadehpur, E., & Fotouhi, A. (2010). Distribution of angle kappa measurements with Orbscan II in a population-based survey. *Journal of refractive surgery (Thorofare, N.J.: 1995)*, 26(12), 966–971. <https://doi.org/10.3928/1081597X-20100114-06>
- Hawken, M. J., Parker, A. J. & Simmons, D. R. (1987). Human thresholds for a stereoscopic depth-discrimination task are no higher than those for simple monocular detection. *Journal of Physiology*, London, 396, 137P.
- Hayashi, T., & Bryden, M. P. Ocular dominance and perceptual asymmetry. *Perceptual and Motor Skills*, 1967, 25, 605–612.
- Hebb, D. O., Martinez, J. L., & Glickman, S. E. (1994). The organization of behavior: A neuropsychological theory. *Contemporary Psychology*, 39(11), 1018–1020.
- Hensch, T. K. (2004). Critical period regulation. *Annual Review of Neuroscience*, 27, 549–579.  
<https://doi.org/10.1146/annurev.neuro.27.070203.144327>

- Hensch, T. K. (2005). Critical period plasticity in local cortical circuits. *Nature Reviews Neuroscience*, 6(11), 877–888. <https://doi.org/10.1038/nrn1787>
- Hensch, T. K., & Quinlan, E. M. (2018). Critical periods in amblyopia. *Visual Neuroscience*, 35, E014. <https://doi.org/10.1017/S0952523817000219>
- Hensch, T. K., Fagiolini, M., Mataga, N., Stryker, M. P., Baekkeskov, S., & Kash, S. F. (1998). Local GABA circuit control of experience-dependent plasticity in developing visual cortex. *Science (New York, N.Y.)*, 282(5393), 1504–1508. [https://doi-org.nottingham.idm.oclc.org/10.1126/science.282.5393.1504](https://doi.org/doi-nottingham.idm.oclc.org/10.1126/science.282.5393.1504)
- Hering, E. (1868/1977). *The theory of binocular vision* (B. Bridgeman, Trans.; Eds. B. Bridgeman & L. Stark). New York: Plenum Press.
- Hering, E. (1942). *Spatial sense and movements of the eye* (A. Raddle, Trans.). Baltimore, MD: American Academy of Optometry. (Original work published 1879).
- Hess, R. F., Ding, R., Clavagnier, S., Liu, C., Guo, C., Viner, C., Barrett, B. T., Radia, K., & Zhou, J. (2016). A Robust and Reliable Test to Measure Stereopsis in the Clinic. *Investigative Ophthalmology & Visual Science*, 57(3), 798–804. <https://doi.org/10.1167/iovs.15-18690>
- Hess, R. F., Hutchinson, C. V., Ledgeway, T., & Mansouri, B. (2007). Binocular influences on global motion processing in the human visual system. *Vision Research*, 47(12), 1682–1692. <https://doi.org/10.1016/j.visres.2007.02.005>
- Hess, R. F., To, L., Zhou, J., Wang, G., & Cooperstock, J. R. (2015). Stereo Vision: The Haves and Have-Nots. *i-Perception*, 6(3), 2041669515593028.
- Hibbard, P. B., Haines, A. E., & Hornsey, R. L. (2017). Magnitude, precision, and realism of depth perception in stereoscopic vision. *Cognitive Research: Principles and Implications*, 2(1), 25. <https://doi.org/10.1186/s41235-017-0062-7>
- Hildreth, G. J. (1949). The development and training of hand dominance. *Journal of Genetic Psychology*, 75, 221–275.
- Holopigian, K. (1989). Clinical suppression and binocular rivalry suppression: The effects of stimulus strength on the depth of suppression. *Vision Research*, 29(10), 1325–1333. [https://doi.org/10.1016/0042-6989\(89\)90189-2](https://doi.org/10.1016/0042-6989(89)90189-2)
- Hou, F., Huang, C.-B., Liang, J., Zhou, Y., & Lu, Z.-L. (2013). Contrast gain-control in stereo depth and cyclopean contrast perception. *Journal of Vision*, 13(8), Article 3. <https://doi.org/10.1167/13.8.3>
- Howard, I. P. (1982). *Human visual orientation*. Chichester: Wiley.
- Howard, I. P. (2002). *Seeing in Depth: Vol. 1. Basic mechanisms*. Toronto: I. Porteous.
- Howard, I. P., & Rogers, B. J. (1995). *Binocular Vision and Stereopsis*. Oxford University Press, USA.
- Howard, I. P., & Rogers, B. J. (2012). *Perceiving in depth, volume 1: Basic mechanisms*. Oxford University Press.
- Howard, I. P., & Templeton, W. B. (1966). *Human Spatial Orientation*. John Wiley & Sons.



- Howard, I. P., & Wade, N. J. (1996). Ptolemy's contributions to the geometry of binocular vision. *Perception*, 25(11), 1189-1201. <https://doi.org/10.1068/p251189>
- Hu, J., Chen, J., Ku, Y., & Yu, M. (2023). Reduced interocular suppression after inverse patching in anisometropic amblyopia. *Frontiers in Neuroscience*, 17, 1280436. <https://doi.org/10.3389/fnins.2023.1280436>
- Huang, C. B., Zhou, J., Lu, Z. L., Feng, L., & Zhou, Y. (2009). Binocular combination in anisometropic amblyopia. *Journal of Vision*, 9(3), 1–16. <https://doi.org/10.1167/9.3.17>
- Huang, C. B., Zhou, J., Zhou, Y. F., & Lu, Z. L. (2010). Contrast and phase combination in binocular vision. *PLoS One*, 5(12), e15075.
- Hubel, D. H., & Wiesel, T. N. (1959). Receptive fields of single neurones in the cat's striate cortex. *The Journal of Physiology*, 148(3), 574–591. <https://doi.org/10.1113/jphysiol.1959.sp006308>.
- Hubel, D. H., & Wiesel, T. N. (1962). Receptive fields, binocular interaction and functional architecture in the cat's visual cortex. *The Journal of Physiology*, 160(1), 106–154. <https://doi.org/10.1113/jphysiol.1962.sp006837>
- Hubel, D. H., & Wiesel, T. N. (1968). Receptive fields and functional architecture of monkey striate cortex. *Journal of Physiology*, 195: 215-243.
- Hubel, D. H., & Wiesel, T. N. (1969). Anatomical demonstration of columns in the monkey striate cortex. *Nature*, 221(5182), 747–750. <https://doi.org/10.1038/221747a0>.
- Hubel, D. H., & Wiesel, T. N. (1972). Laminar and columnar distribution of geniculo-cortical fibers in the macaque monkey. *Journal of Comparative Neurology*, 146(4), 421–450.
- Hubel, D. H., Wiesel, T. N., & LeVay, S. (1977). Plasticity of ocular dominance columns in monkey striate cortex. *Philosophical transactions of the Royal Society of London. Series B, Biological Sciences*, 278(961), 377–409. doi:10.1098/rstb.1977.0050
- Hueck, A. (1840). Von den Gränzen des Sehvermögens. *Archiv für Anatomie, Physiologie und wissenschaftliche Medizin*, 82-97.
- Humphiss, D. (1969). The measurement of sensory ocular dominance and its relation to personality. *American Journal of Optometry and Archives of American Academy of Optometry*, 46(8), 603–616. <https://doi.org/10.1097/00006324-196908000-00007>
- Iny, K., Heynen, A. J., Sklar, E., & Bear, M. F. (2006). Bidirectional modifications of visual acuity induced by monocular deprivation in juvenile and adult rats. *Journal of Neuroscience*, 26(28), 7368–7374. <https://doi.org/10.1523/JNEUROSCI.0124-06.2006>
- Ip, I. B., Emir, U. E., Lunghi, C., Parker, A. J., & Bridge, H. (2021). GABAergic inhibition in the human visual cortex relates to eye dominance. *Scientific reports*, 11(1), 17022. <https://doi.org/10.1038/s41598-021-95685-1>
- Jasper, H. H., & Raney, E. T. (1937). The phi test of lateral dominance. *The American Journal of Psychology*, 49, 450–457. <https://doi.org/10.2307/1415779>

- Jiang, F., Chen, Z., Bi, H., Ekure, E., Su, B., Wu, H., Huang, Y., Zhang, B., & Jiang, J. (2015). Association between ocular sensory dominance and refractive error asymmetry. *PLoS ONE*, 10(8), e0136222. <https://doi.org/10.1371/journal.pone.0136222>
- Julesz, B. (1971). *Foundations of Cyclopean Perception*. Chicago: University of Chicago Press
- Julesz, B., Kropfl, W., & Petrig, B. (1980). Large evoked potentials to dynamic random-dot correlograms and stereograms permit quick determination of stereopsis. *Proceedings of the National Academy of Sciences of the United States of America*, 77(4), 2348–2351. <https://doi.org/10.1073/pnas.77.4.2348>
- Kam, K. Y. & Chang, D. H. F. (2023). Eye dominance plasticity in the human adult visual cortex. *Frontiers in neuroscience*, 17, 1250493. <https://doi.org/10.3389/fnins.2023.1250493>
- Kameyama, K., Sohya, K., Ebina, T., Fukuda, A., Yanagawa, Y., & Tsumoto, T. (2010). Difference in binocularity and ocular dominance plasticity between GABAergic and excitatory cortical neurons. *Journal of Neuroscience*, 30(4), 1551–1559. <https://doi.org/10.1523/JNEUROSCI.4883-09.2010>
- Kandel, E. R., Dudai, Y., & Mayford, M. R. (2014). The molecular and systems biology of memory. *Cell*, 157(1), 163–186. <https://doi.org/10.1016/j.cell.2014.03.001>
- Kandel, E. R., Schwartz, J. H., Jessell, T. M., Siegelbaum, S. A., Hudspeth, A. J., & Mack, S. (Eds.). (2014). *Principles of neural science* (5th ed.). McGraw-Hill Education.
- Karmarkar, U. R., & Dan, Y. (2006). Experience-Dependent Plasticity in Adult Visual Cortex. *Neuron*, 52(4), 577–585. <https://doi.org/10.1016/j.neuron.2006.11.001>
- Keck, T., Toyozumi, T., Chen, L., Doiron, B., Feldman, D. E., Fox, K., Gerstner, W., Haydon, P. G., Hübner, M., Lee, H. K., Lisman, J. E., Rose, T., Sengpiel, F., Stellwagen, D., Stryker, M. P., Turrigiano, G. G., & van Rossum, M. C. (2017). Integrating Hebbian and homeostatic plasticity: the current state of the field and future research directions. *Philosophical transactions of the Royal Society of London. Series B, Biological Sciences*, 372(1715), 20160158. <https://doi.org/10.1098/rstb.2016.0158>
- Kehrein, S., Kohnen, T., & Fronius, M. (2016). Dynamics of Interocular Suppression in Amblyopic Children during Electronically Monitored Occlusion Therapy: First Insight. *Strabismus*, 24(2), 51–62. <https://doi.org/10.3109/09273972.2016.1170047>
- Kephart, N. C., & Revesman, S. (1933). Measuring differences in speed performance. *Optometric Weekly*, 44, 1965–1967.
- Khan, A. Z., & Crawford, J. D. (2001). Ocular dominance reverses as a function of horizontal gaze angle. *Vision Research*, 41(14), 1743–1748. [https://doi.org/10.1016/s0042-6989\(01\)00079-7](https://doi.org/10.1016/s0042-6989(01)00079-7)
- Khokhotva, M., Ono, H., & Mapp, A. P. (2005). The cyclopean eye is relevant for predicting visual direction. *Vision Research*, 45(18), 2339–2345. <https://doi.org/10.1016/j.visres.2005.04.007>

- Kim, H.-W., Kim, C.-Y., & Blake, R. (2017). Monocular perceptual deprivation from interocular suppression temporarily imbalances ocular dominance. *Current Biology*, 27(6), 884–889. <https://doi.org/10.1016/j.cub.2017.01.063>
- Knox, P. J., Simmers, A. J., Gray, L. S., & Cleary, M. (2012). An exploratory study: Prolonged periods of binocular stimulation can provide an effective treatment for childhood amblyopia. *Investigative Ophthalmology & Visual Science*, 53(2), 817. <https://doi.org/10.1167/iovs.11-8219>
- Kounin, J. S. (1938). Laterality in monkeys. *Journal of Genetic Psychology*, 52, 375. <https://doi.org/10.1080/00221325.1938.10533177>
- Kruper, D. C., Boyle, B., & Fatten, R. (1967). Eye preference in hemisectomized monkeys. *Psychonomic Science*, 7, 105–106. <https://doi.org/10.3758/BF03331949>
- Kruper, D. C., Patton, R. A., & Koskoff, Y. D. (1971). Hand and eye preference in unilaterally brain ablated monkeys. *Physiology and Behavior*, 7, 181–185. [https://doi.org/10.1016/0031-9384\(71\)90276-3](https://doi.org/10.1016/0031-9384(71)90276-3)
- Kwon, M., Lu, Z. L., Miller, A., Kazlas, M., Hunter, D. G., & Bex, P. J. (2014). Assessing binocular interaction in amblyopia and its clinical feasibility. *Plos One*, 9(6), e100156. <https://doi.org/10.1371/journal.pone.0100156>
- Kwon, M., Wiecek, E., Dakin, S. C., & Bex, P. J. (2015). Spatial-frequency dependent binocular imbalance in amblyopia. *Scientific Reports*, 5, 17181.
- Lavery, F. S. (1944). *Ocular Dominance*. Transactions of the Ophthalmological Society of the United Kingdom, 63, 409–435.
- Le Conte, J. (1871). On some phenomena of binocular vision: The mode of representing the position of double images. *American Journal of Science*, 1, 33–44.
- Le Conte, J. (1881). *Sight: An exposition of the principles of monocular and binocular vision*. New York: Appleton.
- Lederer, J. (1961). Ocular dominance. *Australian Journal of Optometry*, 44, 531–574.
- Ledgeway, T., McGraw, P. V., & Thompson, B. (2013). What determines the depth of interocular suppression during continuous flash suppression? *Journal of Vision*, 13(9), 541. <https://doi.org/10.1167/13.9.541>
- Legge G. E. (1984a). Binocular contrast summation--I. Detection and discrimination. *Vision Research*, 24(4), 373–383. [https://doi.org/10.1016/0042-6989\(84\)90063-4](https://doi.org/10.1016/0042-6989(84)90063-4)
- Legge G. E. (1984b). Binocular contrast summation--II. Quadratic summation. *Vision Research*, 24(4), 385–394. [https://doi.org/10.1016/0042-6989\(84\)90064-6](https://doi.org/10.1016/0042-6989(84)90064-6)
- Legge, G. E. & Gu, Y. (1989). Stereopsis and contrast. *Vision Research*, 29, 989–1004.
- Legge, G. E., & Rubin, G. S. (1981). Binocular interactions in suprathreshold contrast perception. *Perception & Psychophysics*, 30(1), 49–61. <https://doi.org/10.3758/bf03206136>

- Lehmann, K., & Löwel, S. (2008). Age-dependent ocular dominance plasticity in adult mice. *PLoS ONE*, 3(10), e3120. <https://doi.org/10.1371/journal.pone.0003120>
- Lennie, P., Haake, P. W., & Williams, D. R. (1991). The design of chromatically opponent receptive fields. In M. S. Landy & J. A. Movshon (Eds.), *Computational Models of Visual Processing* (pp. 71–82). The MIT Press.
- Le Vay, S., Wiesel, T. N., & Hubel, D. H. (1980). The development of ocular dominance columns in normal and visually deprived monkeys. *Journal of Comparative Neurology*, 191(1), 1–51. doi:10.1002/cne.901910102
- Levelt, W. J. M. (1965). *On Binocular Rivalry*. <https://doi.org/10.4249/scholarpedia.1578>
- Levy, W. B., & Steward, O. (1983). Temporal contiguity requirements for long-term associative potentiation/depression in the hippocampus. *Neuroscience*, 8(4), 791–797. [https://doi.org/10.1016/0306-4522\(83\)90010-6](https://doi.org/10.1016/0306-4522(83)90010-6)
- Li, J., Lam, C. S., Yu, M., Hess, R. F., Chan, L. Y., Maehara, G., Woo, G. C., & Thompson, B. (2010). Quantifying sensory eye dominance in the normal visual system: a new technique and insights into variation across traditional tests. *Investigative Ophthalmology & Visual Science*, 51(12), 6875–6881. <https://doi.org/10.1167/iovs.10-5549>
- Li, J., Thompson, B., Yang, E., Blake, R., & McDonald, J. E. (2010). A new interocular suppression technique for measuring sensory eye dominance. *Investigative Ophthalmology & Visual Science*, 51(2), 588–593. <https://doi.org/10.1167/iovs.08-3076>
- Li, S. L., Jost, R. M., Morale, S. E., Stager, D. R., Dao, L., Stager, D., & Birch, E. E. (2014). A binocular iPad treatment for amblyopic children. *Eye*, 28(10), 1246–1253. <https://doi.org/10.1038/eye.2014.165>
- Longo, M. R., Rajapakse, S. S., Alsmith, A. J. T., & Ferrè, E. R. (2020). Shared contributions of the head and torso to spatial reference frames across spatial judgments. *Cognition*, 204, 104349. <https://doi.org/10.1016/j.cognition.2020.104349>
- Lunghi, C., Berchicci, M., Morrone, M. C., & Di Russo, F. (2015). Short-term monocular deprivation alters early components of visual evoked potentials. *Journal of Physiology*, 593, 4361–4372. <https://doi.org/10.1113/JP270297>
- Lunghi, C., Burr, D. C., & Morrone, C. (2011). Brief periods of monocular deprivation disrupt ocular balance in human adult visual cortex. *Current Biology*, 21(14), R538–R539. <https://doi.org/10.1016/j.cub.2011.06.004>
- Lunghi, C., Burr, D. C., & Morrone, M. C. (2013). Long-term effects of monocular deprivation revealed with binocular rivalry gratings modulated in luminance and in color. *Journal of Vision*, 13(6), 1. <https://doi.org/10.1167/13.6.1>
- Lunghi, C., Emir, U. E., Morrone, M. C., & Bridge, H. (2015). Short-term monocular deprivation alters GABA in the adult human visual cortex. *Current Biology*, 25(11), 1496–1501. <https://doi.org/10.1016/j.cub.2015.04.021>

- Lunghi, C., Morrone, M. C., Secci, J., & Caputo, R. (2016). Binocular rivalry measured 2 hours after occlusion therapy predicts the recovery rate of the amblyopic eye in anisometropic children. *Investigative Ophthalmology and Visual Science*, 57 (4), 1537–1546. doi:10.1167/iovs.15-18419
- Lunghi, C., & Sale, A. (2015). A cycling lane for brain rewiring. *Current Biology*, 25(23), R1122–R1123. <https://doi.org/10.1016/j.cub.2015.10.025>
- Lunghi, C., Sframeli, A. T., Lepri, A., Lepri, M., Lisi, D., Sale, A., & Morrone, M. C. (2019). A new counterintuitive training for adult amblyopia. *Annals of Clinical and Translational Neurology*, 6(2), 274–284. doi:10.1002/acn3.698
- Mach, E., & Dvorak, V. (1872). Über Analoga der persönlichen Differenz zwischen beiden Augen und den Netzhautstellen desselben Auges. *Sitzungsberichte der königlichen böhmischen Gesellschaft der Wissenschaft*, 65-74. Prague.
- Maehara, G., Thompson, B., Mansouri, B., Farivar, R., & Hess, R. F. (2011). The perceptual consequences of interocular suppression in amblyopia. *Investigative Ophthalmology & Visual Science*, 52(12), 9011-9017. <https://doi.org/10.1167/iovs.11-7748>
- Magee, J. C., & Grienberger, C. (2020). Synaptic Plasticity Forms and Functions. *Annual Review of Neuroscience*, 43, 95–117. <https://doi.org/10.1146/annurev-neuro-090919-022842>.
- Maier, A., Cox, M. A., Westerberg, J. A., & Dougherty, K. (2022). Binocular Integration in the Primate Primary Visual Cortex. *Annual Review of Vision Science*, 8, 345–360. <https://doi.org/10.1146/annurev-vision-100720-112922>
- Malenka, R. C., & Bear, M. F. (2004). LTP and LTD: an embarrassment of riches. *Neuron*, 44(1), 5–21. <https://doi.org/10.1016/j.neuron.2004.09.012>.
- Malus, É.-L. (1809). *Mémoires de physique et de chimie de la Société d'Arcueil*, 2, 254.
- Mansfield, J. S. & Legge, G. E. (1995). Is there more than one cyclopean eye for visual direction? *Investigative Ophthalmology and Visual Science*, 36, S813.
- Mansfield, J. S., & Legge, G. E. (1996). The binocular computation of visual direction. *Vision Research*, 36(1), 27–41. [https://doi.org/10.1016/0042-6989\(95\)00095-H](https://doi.org/10.1016/0042-6989(95)00095-H)
- Mansfield, J. S., & Legge, G. E. (1997). Binocular visual direction, the cyclopean eye, and vergence: Reply to Banks, van Ee and Backus (1997). *Vision Research*, 37(12), 1610-1613.
- Mapp, A. P., & Ono, H. (1999). Wondering about the wandering cyclopean eye. *Vision Research*, 39, 2381-2386. doi:10.1016/S0042-6989(98)00278-8
- Mapp, A. P., Ono, H., & Barbeito, R. (2003). What does the dominant eye dominate? A brief and somewhat contentious review. *Perception & Psychophysics*, 65(2), 310–317. <https://doi.org/10.3758/BF03194802>



- Mapp, A. P., Ono, H., & Howard, I. P. (2002). Binocular visual direction. In I. P. Howard & B. J. Rogers (Eds.), *Seeing in depth: Vol. 2. Depth perception* (pp. 85–99). Toronto: I. Porteous.
- Marr, D. (1982). *Vision: A computational investigation into the human representation and processing of visual information*. San Francisco, CA: W.H. Freeman.
- Matin, L. (1986). Visual localization and eye movements. In K. R. Boff, L. Kaufman, & J. P. Thomas (Eds.), *Handbook of perception and human performance: Volume 1. Sensory processes and perception* (pp. 20-41). New York: Wiley.
- McCormick, A., Bhola, R., Brown, L., Squirrel, D., Giles, J., & Pepper, I. (2002). Quantifying relative afferent pupillary defects using a Sbisabar. *The British Journal of Ophthalmology*, 86(9), 985–987. <https://doi.org/10.1136/bjo.86.9.985>
- McGee, A. W., Yang, Y., Fischer, Q. S., Daw, N. W., & Strittmatter, S. M. (2005). Experience-driven plasticity of visual cortex limited by myelin and Nogo receptor. *Science*, 309(5734), 2222–2226. <https://doi.org/10.1126/science.1113694>
- McIntyre, A., Viana, R., Janzen, S., Mehta, S., Pereira, S., & Teasell, R. (2012). Systematic review and meta-analysis of constraint-induced movement therapy in the hemiparetic upper extremity more than six months post stroke. *Topics in stroke rehabilitation*, 19(6), 499–513. <https://doi-org.nottingham.idm.oclc.org/10.1310/tsr1906-499>
- McKee S. P. (1983). The spatial requirements for fine stereoacuity. *Vision Research*, 23(2), 191–198. [https://doi.org/10.1016/0042-6989\(83\)90142-6](https://doi.org/10.1016/0042-6989(83)90142-6)
- McKee S. P., Welch L., Taylor D. G., & Bowne S. F. (1990). Finding the common bond: Stereoacuity and the other hyperacuities. *Vision Research*, 30(6), 879–891, 10.1016/0042-6989(90)90056-Q.
- Meese, T. S., & Hess, R. F. (2004). Low spatial frequencies are suppressively masked across spatial scale, orientation, field position, and eye of origin. *Journal of Vision*, 4(10), 843–859. <https://doi.org/10.1167/4.10.2>
- Meese, T. S., Georgeson, M. A., & Baker, D. H. (2006). Binocular contrast vision at and above threshold. *Journal of Vision*, 6(11), 1224–1243. <https://doi.org/10.1167/6.11.7>
- Mefferd, R. B. J., & Wieland, B. A. (1969). Influence of eye dominance on the apparent centers of simple horizontal lines. *Perceptual and Motor Skills*, 28, 847–850. <https://doi.org/10.2466/pms.1969.28.3.847>
- Meier, K., & Giaschi, D. (2017). Unilateral amblyopia affects two eyes: Fellow eye deficits in amblyopia. *Investigative Ophthalmology & Visual Science*, 58(3), 1779–1800. <https://doi.org/10.1167/iovs.16-20964>
- Menon, R. S., Ogawa, S., Strupp, J. P., & Ugurbil, K. (1997). Ocular dominance in human V1 demonstrated by functional magnetic resonance imaging. *Journal of Neurophysiology*, 77, 2780–2787.
- Merrell, D. J. (1957). Dominance of eye and hand. *Human Biology*, 29, 314–328.

- Miles, W. R. (1929). Ocular dominance demonstrated by unconscious sighting. *Journal of Experimental Psychology*, 12, 113-126. <https://doi.org/10.1037/h0070522>
- Miles, W. R. (1930). Ocular dominance in human adults. *Journal of General Psychology*, 3, 412-420. <https://doi.org/10.1080/00221309.1930.9918218>
- Mills, L. (1925). Eyedness and handedness. *American Journal of Ophthalmology*, 8 (Series 3), 933-941.
- Min, S. H., Baldwin, A. S., & Hess, R. F. (2019). Ocular dominance plasticity: A binocular combination task finds no cumulative effect with repeated patching. *Vision Research*, 161, 36-42. <https://doi.org/10.1016/j.visres.2019.05.007>.
- Min, S. H., Baldwin, A. S., Reynaud, A., & Hess, R. F. (2018). The shift in ocular dominance from short-term monocular deprivation exhibits no dependence on duration of deprivation. *Scientific Reports*, 8(1), 17083. <https://doi.org/10.1038/s41598-018-35084-1>
- Minucci, P. K., & Connors, M. M. (1964). Reaction time under three viewing conditions: Binocular, dominant eye, and nondominant eye. *Journal of Experimental Psychology*, 67, 268-275. <https://doi.org/10.1037/h0042475>
- Mitchell D. E. (1966a). Retinal disparity and diplopia. *Vision Research*, 6(7), 441-451. [https://doi.org/10.1016/0042-6989\(66\)90052-6](https://doi.org/10.1016/0042-6989(66)90052-6)
- Mitchell D. E. (1966b). A review of the concept of "Panum's fusional areas". *American journal of optometry and archives of American Academy of Optometry*, 43(6), 387-401.
- Mitchell, D. E., & MacKinnon, S. (2002). The present and potential impact of research on animal models for clinical treatment of stimulus deprivation amblyopia. *Clinical & Experimental Optometry*, 85(1), 5-18. <https://doi.org/10.1111/j.1444-0938.2002.tb03067.x>
- Mitson, G. L., Ono, H., & Barbeito, R. (1976). Three methods of measuring the location of the egocentre: Their reliability, comparative locations and intercorrelations. *Canadian Journal of Psychology*, 30, 1-8.
- Mitzdorf, U. (1985). Current source-density method and application in cat cerebral cortex: Investigation of evoked potentials and EEG phenomena. *Physiological Reviews*, 65(1), 37-100.
- Moidell, B. G., & Bedell, H. E. (1988). Changes in oculocentric visual direction induced by the recalibration of saccades. *Vision Research*, 28(2), 329-336. [https://doi.org/10.1016/0042-6989\(88\)90174-1](https://doi.org/10.1016/0042-6989(88)90174-1)
- Mollon, J. D., Bosten, J. M., Peterzell, D. H., & Webster, M. A. (2017). Individual differences in visual science: What can be learned and what is good experimental practice? *Vision Research*, 141, 4-15. <https://doi.org/10.1016/j.visres.2017.11.001>
- Money, J. (1972). Studies on the functioning of sighting dominance. *Quarterly Journal of Experimental Psychology*, 24, 454-464.

- Moradi, F., & Heeger, D. J. (2009). Inter-ocular contrast normalization in human visual cortex. *Journal of Vision*, 9(3), 1–22. <https://doi.org/10.1167/9.3.13>
- Morus, I. R. (2005). *When Physics Became King*. The University of Chicago Press.
- Norman, J. F., Clayton, A. M., Shular, C. F., & Thompson, S. R. (2004). Aging and the perception of depth and 3-D shape from motion parallax. *Psychology and Aging*, 19(3), 506–514. <https://doi.org/10.1037/0882-7974.19.3.506>
- O'Connor, A. R., Birch, E. E., Anderson, S., Draper, H., & FSOS Research Group (2010). The functional significance of stereopsis. *Investigative Ophthalmology & Visual Science*, 51(4), 2019–2023. <https://doi.org/10.1167/iov.09-4434>
- O'Neill, J., Pleydell-Bouverie, B., Dupret, D., & Csicsvari, J. (2010). Play it again: Reactivation of waking experience and memory. *Trends in Neurosciences*, 33(5), 220–229. <https://doi.org/10.1016/j.tins.2010.02.006>
- Ogle, K. N. (1950) *Research in Binocular Vision*. Saunders: Philadelphia.
- Ogle, K. N. (1952). On the limits of stereoscopic vision. *Journal of Experimental Psychology*, 44(4), 253. doi:10.1037/h0057643
- Ogle, K. N. (1962a). Spatial localization through binocular vision. In H. Davson (Ed.), *The Eye* (Vol. 4, pp. 271-320). New York, NY: Academic Press.
- Ogle, K. N. (1964). *Researches in Binocular Vision*. New York: Hafner.
- Ogle, K. N., & de Prangen, A. (1953). Observations on vertical divergences and hyperphorias. *A.M.A. Archives of Ophthalmology*, 49(3), 313–334. <https://doi.org/10.1001/archopht.1953.00920020322009>
- Ogle, K. N., & Weil, M. P. (1958). Stereoscopic vision and the duration of the stimulus. *A.M.A. Archives of Ophthalmology*, 59(1), 4–17. <https://doi.org/10.1001/archopht.1958.00940020028002>
- Oishi, A., Tobimatsu, S., Arakawa, K., Taniwaki, T., & Kira, J. (2005). Ocular dominance in conjugate eye movements at reading distance. *Neuroscience Research*, 52(3), 263–268, doi:10.1016/j.neures.2005.03.013.
- Olson, C. R., & Freeman, R. D. (1980). Profile of the sensitive period for monocular deprivation in kittens. *Experimental Brain Research*, 39(1), 17–21. doi:10.1007/BF00237065
- Ong, J., & Rodman, T. (1972). Sex and eye-hand preferential difference in star-tracing performance. *American Journal of Optometry and Archives of the American Academy of Optometry*, 49, 436-438.
- Ono, H. (1979). Axiomatic summary and deductions from Hering's principles of visual direction. *Perception and Psychophysics*, 25, 473-477.
- Ono, H. (1981). On Wells's (1792) law of visual direction. *Perception & Psychophysics*, 30(4), 403–406. <https://doi.org/10.3758/BF03206159>
- Ono, H. (1991). Binocular visual directions of an object when seen as single or double. In D. Regan (Ed.), *Vision and Visual Dysfunction*, Vol. 9, *Binocular Vision* (pp. 1-18). London: Macmillan.



- Ono, H., & Barbeito, R. (1982). The cyclopean eye vs. The sighting-dominant eye as the center of visual direction. *Perception & Psychophysics*, 32(3), 201–210. <https://doi.org/10.3758/BF03206224>
- Ono, H., & Gonda, G. (1978). Apparent movement, eye movement, and phoria when the viewing eyes alternate in viewing a stimulus. *Perception*, 7, 75–83.
- Ono, H., & Mapp, A. P. (1995). A restatement and modification of Wells-Hering's laws of visual direction. *Perception*, 24(2), 237–252. <https://doi.org/10.1068/p240237>
- Ono, H., & Weber, E. U. (1981). Nonveridical visual direction produced by monocular viewing. *Journal of Experimental Psychology: Human Perception & Performance*, 7(5), 937–947. <https://doi.org/10.1037/0096-1523.7.5.937>
- Ono, H., Angus, R., & Gregor, P. (1977). Binocular single vision achieved by fusion and suppression. *Perception & Psychophysics*, 21(6), 513–521. <https://doi.org/10.3758/BF03198731>
- Ono, H., Mapp, A. P., & Howard, I. P. (2002). The cyclopean eye in vision: the new and old data continue to hit you right between the eyes. *Vision Research*, 42(10), 1307–1324. [https://doi.org/10.1016/s0042-6989\(01\)00281-4](https://doi.org/10.1016/s0042-6989(01)00281-4)
- Ono, H., Wilkinson, A., Muter, P., & Mitson, L. (1972). Apparent movement and change in perceived location of a stimulus produced by a change in accommodative vergence. *Perception & Psychophysics*, 12(3), 187–192. <https://doi.org/10.3758/BF03212825>
- Ooi, T. L., & He, Z. J. (2001). Sensory eye dominance. *Optometry (St. Louis, Mo.)*, 72(3), 168–178.
- Ooi, T. L., & He, Z. J. (2020). Sensory Eye Dominance: Relationship Between Eye and Brain. *Eye and Brain*, 12, 25–31. <https://doi.org/10.2147/EB.S176931>
- Ooi, T. L., Su, Y. R., Natale, D. M., & He, Z. J. (2013). A push-pull treatment for strengthening the 'lazy eye' in amblyopia. *Current Biology*, 23(8), R309–R310. <https://doi.org/10.1016/j.cub.2013.03.004>
- Osburn, D. M., & Klingsporn, M. J. (1998). Consistency of performance on eyedness tasks. *British Journal of Psychology*, 89, 27–37.
- Osuoben, E. P., & al-Fahdi, M. (1994). Differences between anatomical and physiological interpupillary distance. *Journal of the American Optometric Association*, 65(4), 265–271.
- Owsley, C., Sekuler, R., & Siemsen, D. (1983). Contrast sensitivity throughout adulthood. *Vision Research*, 23, 689–699. [https://doi.org/10.1016/0042-6989\(83\)90210-9](https://doi.org/10.1016/0042-6989(83)90210-9)
- Owsley, C., & Sloane, M. E. (1990). Vision and aging. In F. Bolter & J. Grafman (Eds.), *Handbook of Neuropsychology* (Vol. 4, pp. 229–249). Elsevier.
- Palmisano, S., Gillam, B., Govan, D. G., Allison, R. S., & Harris, J. M. (2010). Stereoscopic perception of real depths at large distances. *Journal of Vision*, 10(6), 19. <https://doi.org/10.1167/10.6.19>

- Panum, P. L. (1858). *Physiologische Untersuchungen über das Sehen mit zwei Augen [Physiological studies on seeing with two eyes]*. Schwes.
- Park, K., & Shebilske, W. L. (1991). Phoria, Hering's laws, and monocular perception of direction. *Journal of Experimental Psychology: Human Perception and Performance*, 17(1), 219–231. <https://doi.org/10.1037/0096-1523.17.1.219>
- Parson, B. S. (1924). *Lefthandedness*. New York: Macmillan.
- Perry, N. W., Jr, & Childers, D. G. (1972). Monocular contribution to binocular vision in normals and amblyopes. *Advances in Experimental Medicine and Biology*, 24(0), 213–222. [https://doi.org/10.1007/978-1-4684-8231-7\\_21](https://doi.org/10.1007/978-1-4684-8231-7_21)
- Pfeiffer, B. E. (2020). The content of hippocampal “replay”. *Hippocampus*, 30(1), 6–18. <https://doi.org/10.1002/hipo.23150>
- Pham, T. A., Graham, S. J., Suzuki, S., Barco, A., Kandel, E. R., Gordon, B., & Lickey, M. E. (2004). A semi-persistent adult ocular dominance plasticity in visual cortex is stabilized by activated CREB. *Learning and Memory*, 11(6), 738–747. doi:10.1101/lm.75304
- Pickwell, L. D. (1972). Hering's law of equal innervation and the position of the binoculus. *Vision Research*, 12(10), 1499–1507. [https://doi.org/10.1016/0042-6989\(72\)90180-9](https://doi.org/10.1016/0042-6989(72)90180-9)
- Pointer, J. S. (2001). Sighting dominance, handedness, and visual acuity preference: Three mutually exclusive modalities? *Ophthalmic & Physiological Optics*, 21, 117–126.
- Porac, C. (1974). *Ocular Dominance and Suppressive Processes in Binocular Vision* (Doctoral dissertation, Graduate Faculty of the New School for Social Research). Dissertation Abstracts International, 35, 4229B. (University Microfilms No. 75-2323).
- Porac, C., & Coren, S. (1975a). Is eye dominance a part of generalized laterality? *Perceptual and Motor Skills*, 40(3), 763–769. <https://doi.org/10.2466/pms.1975.40.3.763>
- Porac, C., & Coren, S. (1975b). Suppressive processes in binocular vision. *Ocular Dominance and Amblyopia*. doi:10.1097/00006324-197510000-00001
- Porac, C., & Coren, S. (1976). The dominant eye. *Psychological Bulletin*, 83(5), 880–897. <https://doi.org/10.1037/h0077958>
- Porac, C., & Coren, S. (1981). *Lateral preferences and human behavior*. New York: Springer-Verlag.
- Porac, C., & Coren, S. (1986). Sighting dominance and egocentric localization. *Vision Research*, 26(10), 1709–1713. [https://doi.org/10.1016/0042-6989\(86\)90057-x](https://doi.org/10.1016/0042-6989(86)90057-x)
- Porac, C., Whitford, F. W., & Coren, S. (1976). The relationship between eye dominance and monocular acuity: An additional consideration. *American Journal of Optometry & Physiological Optics*, 53, 803–806.
- Porta, I. B. (1593). De refractione. Optics Parte: Libri Novem. Ex Officina Horatij Salvania. Naples: Apud Io Iacobum Carlinum & Antonium Pacem.

- Prince, S. J., & Eagle, R. A. (2000). Stereo correspondence in one-dimensional Gabor stimuli. *Vision Research*, 40, 913-924. [https://doi.org/10.1016/S0042-6989\(99\)00242-4](https://doi.org/10.1016/S0042-6989(99)00242-4)
- Prusky, G. T., Alam, N. M., & Douglas, R. M. (2006). Enhancement of Vision by Monocular Deprivation in Adult Mice. *Journal of Neuroscience*, 26 (45), 11554–11561. doi:10.1523/JNEUROSCI.3396-06.2006
- Pulfrich, C. (1922). Die Stereoscopie im Dienste der isochromem und heterochromen Photometrie. *Naturwissenschaften*, 10, 553-564.
- Purves, D., & White, L. E. (1994). Monocular preferences in binocular viewing. *Proceedings of the National Academy of Sciences of the United States of America*, 91(18), 8339-8342 <https://doi.org/10.1073/pnas.91.18.8339>.
- Purves, D., Augustine, G. J., Fitzpatrick, D., Katz, L. C., LaMantia, A.-S., McNamara, J. O., & Williams, S. M. (2001). Thalamocortical interactions. In D. Purves, G. J. Augustine, D. Fitzpatrick, L. C. Katz, A.-S. LaMantia, J. O. McNamara, & S. M. Williams (Eds.), *Neuroscience* (2nd ed., pp. 618). Sinauer Associates.
- Quinan, C. (1931). The handedness and eyedness of speeders and of reckless drivers. *Archives of Neurology and Psychiatry*, 25, 829-837.
- Ramamurthy, M., & Blaser, E. (2018). Assessing the kaleidoscope of monocular deprivation effects. *Journal of Vision*, 18(13), 14. <https://doi.org/10.1167/18.13.14>.
- Ranson, A., Cheetham, C. E., Fox, K., & Sengpiel, F. (2012). Homeostatic plasticity mechanisms are required for juvenile, but not adult, ocular dominance plasticity. *Proceedings of the National Academy of Sciences of the United States of America*, 109, 1311–1316. <https://doi.org/10.1073/pnas.1112204109>
- Read, J. (2015). Stereo vision and strabismus. *Eye*, 29, 214–224 <https://doi.org/10.1038/eye.2014.279>
- Read, J. C. A. (2021). Binocular Vision and Stereopsis Across the Animal Kingdom. *Annual Review of Vision Science*, 7(1), 389–415. <https://doi.org/10.1146/annurev-vision-093019-113212>
- Regan, D., & Beverley, K. I. (1973). Some dynamic features of depth perception. *Vision Research*, 13(12), 2369–2379. [https://doi.org/10.1016/0042-6989\(73\)90236-8](https://doi.org/10.1016/0042-6989(73)90236-8)
- Regan, D., & Spekreijse, H. (1970). Electrophysiological Correlate of Binocular Depth Perception in Man. *Nature*, 225(5227), 92–94. <https://doi.org/10.1038/225092a0>
- Repérant, J., Miceli, D., Vesselkin, N., & Molotchnikoff, S. (1989). The centrifugal visual system of vertebrates: A century-old search reviewed. *International Review of Cytology*, 118, 115–171.
- Reynaud, A., et al. (2018). Interocular normalization in monkey primary visual cortex. *Journal of Vision*, 18(10), 534. <https://doi.org/10.1167/18.10.534>.
- Rodriguez-Lopez, V., Barcala, X., Zaytouny, A., Dorronsoro, C., Peli, E., & Marcos, S. (2023). Monovision correction preference and eye dominance measurements. *Translational Vision Science & Technology*, 12(3), 18. <https://doi.org/10.1167/tvst.12.3.18>

- Roelofs, C. O. (1959). Considerations on the visual egocentre. *Acta Psychologica*, 16, 226-234.
- Rogers, B. J., & Bradshaw, M. F. (1993). Vertical disparities, differential perspective and binocular stereopsis. *Nature*, 361(6409), 253-255. <https://doi-org.nottingham.idm.oclc.org/10.1038/361253a0>
- Rogers, B., & Graham, M. (1979). Motion parallax as an independent cue for depth perception. *Perception*, 8(2), 125-134. <https://doi.org/10.1068/p080125>
- Rombouts, S. A., Barkhof, F., Sprenger, M., Valk, J., & Scheltens, P. (1996). The functional basis of ocular dominance: Functional MRI (fMRI) findings. *Neuroscience Letters*, 221, 1-4.
- Rönne, H. (1915). Zur Theorie und Technik der Bjerrumschen Gesichtsfelduntersuchung. *Archiv für Augenheilkunde*, 78(4), 284-301.
- Roska, B., & Meister, M. (2014). The retina dissects the visual scene. In J. S. Werner & L. M. Chalupa (Eds.), *The New Visual Neurosciences* (pp. 163-182). MIT Press.
- Roth, H. L., Lora, A. N., & Heilman, K. M. (2002). Effects of monocular viewing and eye dominance on spatial attention. *Brain: a Journal of Neurology*, 125(Pt 9), 2023-2035. <https://doi.org/10.1093/brain/awf210>
- Rubin, M. L., & Walls, G. L. (1969). *Fundamentals of Visual Science*. Springfield, IL: Charles C. Thomas.
- Ruggiero, G., D'Errico, O., & Iachini, T. (2016). Development of egocentric and allocentric spatial representations from childhood to elderly age. *Psychological Research*, 80(2), 259-272. <https://doi.org/10.1007/s00426-015-0658-9>
- Sanderson, K. J., Bishop, P. O., & Darian-Smith, I. (1971). The properties of the binocular receptive fields of lateral geniculate neurons. *Experimental Brain Research*, 13(2), 178-207. doi:10.1007/BF00234085
- Sanderson, K. J., Darian-Smith, I., & Bishop, P. O. (1969). Binocular corresponding receptive fields of single units in the cat dorsal lateral geniculate nucleus. *Vision Research*, 9(10), 1297-1303. doi:10.1016/0042-6989(69)90117-5
- Sato, M., & Stryker, M. P. (2008). Distinctive features of adult ocular dominance plasticity. *Journal of Neuroscience*, 28(41), 10278-10286. doi:10.1523/JNEUROSCI.2451-08.2008
- Sawtell, N. B., Frenkel, M. Y., Philpot, B. D., Nakazawa, K., Tonegawa, S., & Bear, M. F. (2003). NMDA receptor-dependent ocular dominance plasticity in adult visual cortex. *Neuron*, 38(6), 977-985. [https://doi.org/10.1016/S0896-6273\(03\)00323-4](https://doi.org/10.1016/S0896-6273(03)00323-4)
- Schoen, Z. J., & Scofield, C. F. (1935). A study of the relative neuromuscular efficiency of the dominant and non-dominant eye in binocular vision. *Journal of General Psychology*, 11, 156-181.
- Schor C. M. (1992). A dynamic model of cross-coupling between accommodation and convergence: simulations of step and frequency responses. *Optometry and vision science: official publication of the American Academy of Optometry*, 69(4), 258-269. <https://doi.org/10.1097/00006324-199204000-00002>

- Schor, C. M., Edwards, M., & Pope, D. R. (1998). Spatial-frequency and contrast tuning of the transient-stereopsis system. *Vision research*, 38(20), 3057-3068.
- Schor, C. M., Wood, I. C., & Ogawa, J. (1984). Spatial tuning of static and dynamic local stereopsis. *Vision Research*, 24(6), 573–578. [https://doi.org/10.1016/0042-6989\(84\)90111-1](https://doi.org/10.1016/0042-6989(84)90111-1)
- Schrader, C. W. (1971). The effect of visual differences on hand-eye coordinated performance. *Western Carolina University Journal of Education*, 2, 28-33.
- Schröder, J. H., Fries, P., Roelfsema, P. R., Singer, W., & Engel, A. K. (2002). Ocular dominance in extrastriate cortex of strabismic amblyopic cats. *Vision Research*, 42(1), 29–39. doi:10.1016/S0042-6989(01) 00263-2
- Schroeder, C. E., Mehta, A. D., & Givre, S. J. (1998). A spatiotemporal profile of visual system activation revealed by current source density analysis in the awake macaque. *Cerebral Cortex*, 8(7), 575–592.
- Schroeder, C. E., Tenke, C. E., Arezzo, J. C., & Vaughan, H. G. (1990). Binocularity in the lateral geniculate nucleus of the alert macaque. *Brain Research*, 521(1-2), 303–310. doi:10.1016/0006-8993(90)91556- V
- Schwartz, R., & Yatziv, Y. (2015). The effect of cataract surgery on ocular dominance. *Clinical Ophthalmology*, 2329–2333.
- Seijas, O., Gómez de Liaño, P., Gómez de Liaño, R., Roberts, C. J., Piedrahita, E., & Diaz, E. (2007). Ocular dominance diagnosis and its influence in monovision. *American Journal of Ophthalmology*, 144(2), 209–216. <https://doi.org/10.1016/j.ajo.2007.03.053>
- Sekuler, R., & Ball, K. (1986). Visual localization: Age and practice. *Journal of the Optical Society of America A*, 3(5), 864–867. <https://doi.org/10.1364/josaa.3.000864>
- Sengpiel, F., Blakemore, C., & Harrad, R. A. (1995). Interocular suppression in the primary visual cortex: a possible neural basis of binocular rivalry. *Vision Research*, 35(2), 179–195. doi:10.1016/0042-6989(94) 00125-6
- Sengpiel, F., Blakemore, C., Kind, P. C., & Harrad, R. (1994). Interocular suppression in the visual cortex of strabismic cats. *The Journal of neuroscience : the official journal of the Society for Neuroscience*, 14(11 Pt 2), 6855–6871. <https://doi-org.nottingham.idm.oclc.org/10.1523/JNEUROSCI.14-11-06855.1994>
- Shadmehr, R., Smith, M. A., & Krakauer, J. W. (2010). Error correction, sensory prediction, and adaptation in motor control. *Annual Review of Neuroscience*, 33(1), 89–108. <https://doi.org/10.1146/annurev-neuro-060909-153135>
- Sheard, C. (1926). Unilateral sighting and ocular dominance. *American Journal of Physiological Optics*, 7, 558-567.
- Sheedy, J. E., Bailey, I. L., Buri, M., & Bass, E. (1986). *Binocular vs. Monocular Task Performance*. *American Journal of Optometry and Physiological Optics*, 63(10), 839–846.



- Shibata, K., Sasaki, Y., Bang, J. W., Walsh, E. G., Machizawa, M. G., Tamaki, M., & others. (2017). Overlearning hyperstabilizes a skill by rapidly making neurochemical processing inhibitory-dominant. *Nature Neuroscience*, 20(3), 470–475. <https://doi.org/10.1038/nn.4490>
- Shick J. (1971). Relationship between depth perception and hand-eye dominance and free-throw shooting in college women. *Perceptual and Motor Skills*, 33(2), 539–542. <https://doi.org/10.2466/pms.1971.33.2.539>
- Shimono, K., & Wade, N. J. (2002). Monocular alignment in different depth planes. *Vision Research*, 42(9), 1127–1135. [https://doi.org/10.1016/s0042-6989\(02\)00051-2](https://doi.org/10.1016/s0042-6989(02)00051-2)
- Shonkoff, J. P., & Phillips, D. A. (Eds.). (2000). *From neurons to neighborhoods: The science of early childhood development*. Washington, DC: National Academies Press.
- Simmons, D. R. (1992). *Spatiotemporal properties of stereoscopic mechanisms*. D. Phil thesis, University of Oxford, England.
- Simmons, D. R. & Kingdom, F. A. A. (1994). Contrast thresholds for stereoscopic depth identification with isoluminant and isochromatic stimuli. *Vision Research*, 34, 2971–2982.
- Simons, K. (2005). Amblyopia characterization, treatment, and prophylaxis. *Survey of Ophthalmology*, 50(2), 123–166. <https://doi.org/10.1016/j.survophthal.2004.12.005>
- Simpson, T. L. (1992). The vergence components and observer-relative direction. (Doctoral dissertation, University of Houston).
- Singer, W. [Wolf]. (1970). Inhibitory binocular interaction in the lateral geniculate body of the cat. *Brain Research*, 18(1), 165–170. doi:10.1016/0006-8993(70)90463-4
- Sireteanu, R., & Fronius, M. (1981). Naso-temporal asymmetries in human amblyopia: Consequence of long-term interocular suppression. *Vision Research*, 21(7), 1055–1063. [https://doi.org/10.1016/0042-6989\(81\)90010-9](https://doi.org/10.1016/0042-6989(81)90010-9)
- Smallman, H. S., & McKee, S. P. (1995). A contrast ratio constraint on stereo matching. *Proceedings of the Royal Society of London. Series B: Biological Sciences*, 260(1359), 265–271.
- Smith, A. M. (1996). *Ptolemy's theory of visual perception: An English translation of the optics with introduction and commentary*. Philadelphia, PA: The American Philosophical Society.
- Smith, L. (1970). Eye dominance in a monkey. *Perceptual and Motor Skills*, 31, 657–658. <https://doi.org/10.2466/pms.1970.31.2.657>
- Spector, R. H. (1990). Visual fields. In *Clinical methods: The history, physical, and laboratory examinations* (3rd ed.). Butterworths. ISBN 9780409900774.
- Spiegel, D. P., Baldwin, A. S., & Hess, R. F. (2017). Ocular dominance plasticity: Inhibitory interactions and contrast equivalence. *Scientific Reports*, 7(November 2016), 1–9. DOI:[10.1038/srep39913](https://doi.org/10.1038/srep39913).
- Spolidoro, M., Sale, A., Berardi, N., & Maffei, L. (2009). Plasticity in the adult brain: Lessons from the visual system. *Experimental Brain*

- Research*, 192(3), 335–341. <https://doi.org/10.1007/s00221-008-1509-3>
- Spreen, O., Miller, C. G., & Benton, A. L. (1966). The phitest and measures of laterality in children and adults. *Cortex*, 2, 308–321.
- Toch, H. H. Can eye dominance be trained? *Perceptual and Motor Skills*, 1960, 11, 31–34.
- Sridhar, D., & Bedell, H. E. (2011). Relative contributions of the two eyes to perceived egocentric visual direction in normal binocular vision. *Vision Research*, 51(9), 1075–1085. <https://doi.org/10.1016/j.visres.2011.02.023>
- Sterken, Y., Postma, A., De Haan, E. H. F., & Dingemans, A. (1999). Egocentric and Exocentric Spatial Judgements of Visual Displacement. *The Quarterly Journal of Experimental Psychology Section A*, 52(4), 1047–1055. <https://doi.org/10.1080/713755862>
- Stettler, D. D., Das, A., Bennett, J., & Gilbert, C. D. (2002). Lateral connectivity and contextual interactions in macaque primary visual cortex. *Neuron*, 36(4), 739–750. [https://doi-org.nottingham.idm.oclc.org/10.1016/s0896-6273\(02\)01029-2](https://doi-org.nottingham.idm.oclc.org/10.1016/s0896-6273(02)01029-2)
- Stevenson, S. B., Cormack, L. K., & Schor, C. M. (1989). Hyperacuity, superresolution and gap resolution in human stereopsis. *Vision Research*, 29(11), 1597–1605. [https://doi.org/10.1016/0042-6989\(89\)90141-7](https://doi.org/10.1016/0042-6989(89)90141-7)
- Strettoi, E., Di Marco, B., Orsini, N., & Napoli, D. (2022). Retinal Plasticity. *International Journal of Molecular Sciences*, 23(3), 1138. <https://doi.org/10.3390/ijms23031138>
- Su, Y., He, Z. J., & Ooi, T. L. (2009). Coexistence of binocular integration and suppression determined by surface border information. *Proceedings of the National Academy of Sciences of the United States of America*, 106, 15990–15995. <https://doi.org/10.1073/pnas.0906460106>
- Swanston, M. T., Wade, N. J., & Ono, H. (1990). The Binocular Representation of Uniform Motion. *Perception*, 19(1), 29–34. <https://doi.org/10.1068/p190029>
- Swindale, N. V., Vital-Durand, F., & Blakemore, C. (1981). Recovery from monocular deprivation in the monkey. II. Reversal of morphological effects in the lateral geniculate nucleus. *Proceedings of the Royal Society of London - Biological Sciences*, 213 (1193), 425–433. doi:10.1098/rspb.1981.0073
- Tagawa, Y., Kanold, P. O., Majdan, M., & Shatz, C. J. (2005). Multiple periods of functional ocular dominance plasticity in mouse visual cortex. *Nature Neuroscience*, 8(3), 380–388. <https://doi.org/10.1038/nn1410>
- Techentin, C., Voyer, D., & Voyer, S. D. (2014). Spatial abilities and aging: A meta-analysis. *Experimental Aging Research*, 40(4), 395–425. <https://doi.org/10.1080/0361073X.2014.926776>
- Tong, F., Meng, M., & Blake, R. (2006). Neural bases of binocular rivalry. *Trends in Cognitive Sciences*, 10(11), 502–511. <https://doi.org/10.1016/j.tics.2006.09.003>
- Towne, J. (1866). Contributions to the physiology of binocular vision—Section VII. *Guy's Hospital Reports*, 12, 285–301.

- Traquair, H. M. (1938). *An Introduction to Clinical Perimetry* (Chapter 1). London: Henry Kimpton.
- Tso, D., Miller, R., & Begum, M. (2017). Neuronal responses underlying shifts in interocular balance induced by short-term deprivation in adult macaque visual cortex. *Journal of Vision*, 17(10), 576. <https://doi.org/10.1167/17.10.576>.
- Turrigiano, G. (2011). Too many cooks? Intrinsic and synaptic homeostatic mechanisms in cortical circuit refinement. *Annual Review of Neuroscience*, 34, 89–103. <https://doi.org/10.1146/annurev-neuro-060909-153238>
- Turrigiano G. (2012). Homeostatic synaptic plasticity: local and global mechanisms for stabilizing neuronal function. *Cold Spring Harbor perspectives in biology*, 4(1), a005736. <https://doi.org/10.1101/cshperspect.a005736>
- Turrigiano, G. G. (1999). Homeostatic plasticity in neuronal networks: The more things change, the more they stay the same. *Trends in Neurosciences*, 22, 221–227. [https://doi.org/10.1016/s0166-2236\(98\)01341-1](https://doi.org/10.1016/s0166-2236(98)01341-1)
- Turrigiano, G. G., & Nelson, S. B. (2000). Hebb and homeostasis in neuronal plasticity. *Current Opinion in Neurobiology*, 10(3), 358–364. [https://doi.org/10.1016/s0959-4388\(00\)00091-x](https://doi.org/10.1016/s0959-4388(00)00091-x)
- Tyler, C. W. (1997). On Ptolemy's geometry of binocular vision. *Perception*, 26(11), 1579-1581. <https://doi.org/10.1068/p261579>
- Valle-Inclán, F., Blanco, M. J., Soto, D., & Leirós, L. (2008). A new method to assess eye dominance. *Psicológica*, 29(1), 55–64.
- van de Grind, W. A., Erkelens, C. J., & Laan, A. C. (1995). Binocular correspondence and visual direction. *Perception*, 24(2), 215–235. <https://doi.org/10.1068/p240215>
- Vergilino-Perez, D., Fayel, A., Lemoine, C., Senot, P., Vergne, J., & Doré-Mazars, K. (2012). Are there any left-right asymmetries in saccade parameters? Examination of latency, gain, and peak velocity. *Investigative Ophthalmology & Visual Science*, 53(7), 3340–3348. <https://doi.org/10.1167/iovs.11-9273>
- Verhoef, P. C., Kannan, P. K., & Inman, J. J. (2015). From multi-channel retailing to omni-channel retailing: Introduction to the special issue on multi-channel retailing. *Journal of Retailing*, 91(2), 174-181. <https://doi.org/10.1016/j.jretai.2015.02.005>
- Verhoeff, F. H. (1933). Effect on stereopsis produced by disparate retinal images of different luminosities. *Archives of Ophthalmology*, 10, 640–644.
- Verhoeff, F. H. (1935). A new theory of binocular vision. *Archives of Ophthalmology*, 13, 152-175.
- Vishwanath, D. (2014). Toward a new theory of stereopsis. *Psychological Review*, 121(2), 151.
- Vishwanath, D., & Hibbard, P. B. (2013). Seeing in 3-D with just one eye: Stereopsis without binocular vision. *Psychological Science*, 24(9), 1673-1685.



- von Noorden, G. K. (1973). Histological studies of the visual system in monkeys with experimental amblyopia. *Investigative Ophthalmology & Visual Science*, 12(10), 727–738.
- von Noorden, G. K., Dowling, J. E., & Ferguson, D. C. (1970). Experimental Amblyopia in Monkeys: I. Behavioral Studies of Stimulus Deprivation Amblyopia. *Archives of Ophthalmology*, 84(2), 206–214. doi:10.1001/archophth.1970.00990040208014
- Wade, N. J., & Swanston, M. T. (1996). A general model for the perception of space and motion. *Perception*, 25(2), 187–194. <https://doi.org/10.1068/p250187>
- Wagemans, J., Elder, J. H., Kubovy, M., Palmer, S. E., Peterson, M. A., Singh, M., & von der Heydt, R. (2012). A century of Gestalt psychology in visual perception: I. Perceptual grouping and figure-ground organization. *Psychological Bulletin*, 138(6), 1172–1217. <https://doi.org/10.1037/a0029333>
- Walls, G. L. (1951). A theory of ocular dominance. *AMA Archives of Ophthalmology*, 45(4), 387–412. <https://doi.org/10.1001/archophth.1951.01700010395007>
- Wandell, B. A. (1995). *Foundations of vision*. Sinauer Associates.
- Wang, M., McGraw, P., & Ledgeway, T. (2020). Short-term monocular deprivation reduces inter-ocular suppression of the deprived eye. *Vision Research*, 173, 29–40. <https://doi.org/10.1016/j.visres.2020.05.001>
- Wang, M., McGraw, P., & Ledgeway, T. (2021). Attentional eye selection modulates sensory eye dominance. *Vision Research*, 188, 10–25. <https://doi.org/10.1016/j.visres.2021.06.006>
- Wang, M., McGraw, P. V., & Ledgeway, T. (2024). Collective plasticity of binocular interactions in the adult visual system. *Scientific Reports*, 14(1), 10494. <https://doi.org/10.1038/s41598-024-57276-8>
- Wang, P., & Nikolić, D. (2011). An LCD monitor with sufficiently precise timing for research in vision. *Frontiers in Human Neuroscience*, 5, 85.
- Warren, N., & Clark, B. (1938). A consideration of the use of the term ocular dominance. *Psychological Bulletin*, 35, 298–304.
- Washburn, M. F., Faison, C., & Scott, R. (1934). A Comparison between the Miles A-B-C Method and Retinal Rivalry as Tests of Ocular Dominance. *The American Journal of Psychology*, 46(4), 633–636. <https://doi.org/10.2307/1415504>
- Webber, A. L. (2007). Amblyopia treatment: An evidence-based approach to maximising treatment outcome. *Clinical and Experimental Optometry*, 90(4), 250–257. doi:10.1111/j.1444-0938.2007.00164.x
- Webber, A. L., & Wood, J. (2005). Amblyopia: Prevalence, natural history, functional effects, and treatment. *Clinical and Experimental Optometry*, 88(6), 365–375. <https://doi.org/10.1111/j.1444-0938.2005.tb05102.x>
- Webber, A. L., Schmid, K. L., Baldwin, A. S., & Hess, R. F. (2020). Suppression Rather Than Visual Acuity Loss Limits Stereoacuity in Amblyopia. *Investigative Ophthalmology & Visual Science*, 61(6), 50. <https://doi.org/10.1167/iovs.61.6.50>

- Webster M. A. (2015). Visual Adaptation. *Annual review of vision science*, 1, 547–567. <https://doi.org/10.1146/annurev-vision-082114-035509>
- Webster, M. A., Georgeson, M. A., & Webster, S. M. (2002). Neural adjustments to image blur. *Nature Neuroscience*, 5(9), 839–840. <https://doi.org/10.1038/nn906>
- Wells, W. C. (1792). *An essay upon single vision with two eyes; together with experiments and observations on several other subjects in optics*. T. Cadell.
- Wertheim, A. H. (1994). Motion perception during self-motion: The direct versus inferential controversy revisited. *Behavioral and Brain Sciences*, 17(2), 293–355. <https://doi.org/10.1017/S0140525X00034721>
- Wheatstone, C. (1838). On some remarkable, and hitherto unobserved phenomena of binocular vision. *Philosophical Transactions of the Royal Society of London*, 128, 371–394.
- Wiecek, E., Lashkari, K., Dakin, S. C., & Bex, P. (2015). Metamorphopsia and interocular suppression in monocular and binocular maculopathy. *Acta ophthalmologica*, 93(4), e318–e320. <https://doi.org/10.1111/aos.12559>
- Wiesel, T. N. (1982). Postnatal development of the visual cortex and the influence of environment. *Nature*, 299, 583–591. <https://doi.org/10.1038/299583a0>
- Wiesel, T. N., & Hubel, D. H. (1963a). Single-cell responses in striate cortex of kittens deprived of vision in one eye. *Journal of Neurophysiology*, 26(6), 1003–1017. <https://doi.org/10.1152/jn.1963.26.6.1003>
- Wiesel, T. N., & Hubel, D. H. (1963b). Effects of visual deprivation on morphology and physiology of cells in the cat's lateral geniculate body. *Journal of Neurophysiology*, 26(6), 978–993. <https://doi.org/10.1152/jn.1963.26.6.978>
- Wilke, M., Mueller, K.-M., Leopold, D. A., & Jones, E. G. (2009). Neural activity in the visual thalamus reflects perceptual suppression. *Proceedings of the National Academy of Sciences of the United States of America*, 106(23), 9465–9470. <https://doi.org/10.1073/pnas.0900714106>
- Wolpert, D. M., Diedrichsen, J., & Flanagan, J. R. (2011). Principles of sensorimotor learning. *Nature Reviews Neuroscience*, 12(12), 739–751. <https://doi.org/10.1038/nrn3112>
- Woo, T. L., & Pearson, K. (1927). Dextrality and sinistrality of hand and eye. *Biometrika*, 19(1 & 2), 165–199. <https://doi.org/10.1093/biomet/19.1-2.165>
- Woodhouse, R. (2009). *A Changing View of Eye Dominance* [PhD's thesis, Cardiff University].
- Worth, C. (1921). *Squint: Its Causes, Pathology and Treatment*. C. Blakiston's Son.
- Wright, M. J., & Johnston, A. (1983). Spatiotemporal contrast sensitivity and visual field locus. *Vision Research*, 23(10), 983–989.

- Xu, J. P., He, Z. J., & Ooi, T. L. (2011). A binocular perimetry study of the causes and implications of sensory eye dominance. *Vision Research*,
- Yang, E., Blake, R., & McDonald, J. E. (2010). A new interocular suppression technique for measuring sensory eye dominance. *Investigative Ophthalmology & Visual Science*, 51(2), 588–593. <https://doi.org/10.1167/iovs.08-3076>
- Zaroff, C. M., Knutelska, M., & Frumkes, T. E. (2003). Variation in stereoacuity: Normative description, fixation disparity, and the roles of aging and gender. *Investigative Ophthalmology & Visual Science*, 44(2), [https://doi.org/891–900](https://doi.org/891-900), 10.1167/iovs.02-0361.
- Zeater, N., Cheong, S. K., Solomon, S. G., Dreher, B., & Martin, P. R. (2015). Binocular Visual Responses in the Primate Lateral Geniculate Nucleus. *Current biology : CB*, 25(24), 3190–3195. <https://doi-org.nottingham.idm.oclc.org/10.1016/j.cub.2015.10.033>
- Zeri, F., De Luca, M., Spinelli, D., & Zoccolotti, P. (2011). Ocular dominance stability and reading skill: a controversial relationship. *Optometry and Vision Science: Official Publication of the American Academy of Optometry*, 88(11), 1353–1362. <https://doi.org/10.1097/OPX.0b013e318229635a>.
- Zhang, P., Bao, M., Kwon, M., He, S., & Engel, S. A. (2009). Effects of orientation-specific visual deprivation induced with altered reality. *Current Biology*, 19(22), 1956–1960. <https://doi.org/10.1016/j.cub.2009.09.066>
- Zhang, P., Bobier, W., Thompson, B., & Hess, R. F. (2011). Binocular balance in normal vision and its modulation by mean luminance. *Optometry and Vision Science: Official Publication of the American Academy of Optometry*, 88(9), 1072–1079. <https://doi.org/10.1097/OPX.0b013e3182217295>.
- Zhang, P., Jiang, Y., & He, S. (2012). Voluntary attention modulates processing of eyespecific visual information. *Psychological Science*, 23(3), 254–260. <https://doi.org/10.1177/0956797611424289>.
- Zhou, J., Baker, D. H., Simard, M., Saint-Amour, D., & Hess, R. F. (2015). Short-term monocular patching boosts the patched eye's response in visual cortex. *Restorative Neurology and Neuroscience*, 33, 381–387.
- Zhou, J., Clavagnier, S., & Hess, R. F. (2013). Short-term monocular deprivation strengthens the patched eye's contribution to binocular combination. *Journal of Vision*, 13(5), 12–12. <https://doi.org/10.1167/13.5.12>.
- Zhou, J., Huang, P. C., & Hess, R. F. (2013). Interocular suppression in amblyopia for global orientation processing. *Journal of Vision*, 13(5), 19. <https://doi.org/10.1167/13.5.19>.
- Zhou, J., Reynaud, A., & Hess, R. F. (2014). Real-time modulation of perceptual eye dominance in humans. *Proceedings of the Royal Society B: Biological Sciences*, 281(1795), 20141717. <https://doi.org/10.1098/rspb.2014.1717>

- Zhou, J., Reynaud, A., Kim, Y. J., Mullen, K. T., & Hess, R. F. (2017). Chromatic and achromatic monocular deprivation produce separable changes of eye dominance in adults. *Proceedings of the Royal Society B: Biological Sciences*, 284(1867), 20171669. <https://doi.org/10.1098/rspb.2017.1669>
- Zhou, J., Thompson, B., & Hess, R. F. (2013). A new form of rapid binocular plasticity in adult with amblyopia. *Scientific Reports*, 3, 2638. doi:10. 1038/srep02638